Investigating Cancer Cell Sensitivity to Anticancer Drugs in Relation to Heat Shock Factor 1 Expression

Candidate's Name: Canh Vinh Ngoc Nguyen

University ID: 4527316

Supervisors: Professor John Price and Dr Craig Goodman

ABSTRACT

Breast cancer (BrCa) is the most common cancer diagnosed in women, with many patients progressing to advanced stages where prognosis is poor and morbidity more likely. Ninety per cent of patients will succumb to their disease primarily due to metastasis. Metastatic cancer cells are invasive, migratory and highly resistant to standard chemotherapies. Therefore, greater knowledge is needed to characterize mechanisms by which cancer cells become resistant to anticancer agents. A mechanism by which cancer cells may develop resistance is through stimulating stress response pathways such as the heat shock response (HSR). This pathway is regulated by heat shock factor 1 (HSF1), which transcriptionally regulates transcription of heat shock proteins (HSP) as well as many non-HSPs. HSPs protect normal cells during exposure to proteotoxic stresses; however, HSF1 has also been found to facilitate pro-metastatic pathways in cancer, distinct from the canonical HSR. HSF1 expression is known to be significantly increased in multiple cancers and significantly correlates with poor clinical outcomes; yet little is known regarding the role of HSF1 in the resistance/sensitivity of cancer cells towards anticancer therapeutics. To address this, the aim of this project was to examine whether HSF1 may have a direct role in mediating anticancer drug sensitivity in cancer cells and whether anticancer drugs stimulate HSF1 activation. To achieve this, a series of doxycycline-inducible HSF1 knockdown (KD) BrCa cell lines, T47D and MDA-MB-231, were generated. From previous bioinformatic studies, HSF1 was identified as potentially mediating the sensitivity of cancer cells to several anticancer drugs. A number of these drugs were screened in both the T47D and MDA-MB-231 series of doxycycline-inducible HSF1 KD cells. From these screens, it was identified that loss of HSF1 resulted in a significant decrease in the sensitivity of MDA-MB-231 cells towards the EGFR inhibitor, Lapatinib, but this was not evident in the less advanced T47D BrCa cells.

However, the T47D cells were found to be increased in their sensitivity to doxorubicin with HSF1 knockdown. To determine whether anticancer drugs stimulated the HSR, T47D and MDA-MB-231 heat shock element (HSE) bioluminescent reporter cells were generated. Cells were successfully generated to express firefly luciferase under the control of HSE, indicative of HSF1 activity and the quantitative assessment of anticancer drug induced-stress. However, these reporter cell models revealed the previously undetermined impact of drug vehicles (DMSO, EtOH) upon HSE activation indicative of the potential for false positives within drug screens if not properly controlled. This work has identified that HSF1 plays a role in mediating the sensitivity of aggressive BrCa cells to the EGFR inhibitor, Lapatinib. Conversely, HSF1 mediates resistance to doxorubicin in the less aggressive T47D BrCa cells. Moreover, the use of HSE reporter cells to determine HSR activation by anticancer drugs needs stringent controls in relation to drug vehicles due to the potential for these vehicles to activate the HSR leading to false positives within anticancer drug screens.

DECLARATION

"I, Canh Vinh Ngoc Nguyen, declare that the Master of Research thesis entitled **"Investigating Cancer Cell Sensitivity to Anticancer Drugs in Relation to Heat shock factor 1 Expression"** is no more than 50,000 words in length including quotes and exclusive of tables, figures, appendices, bibliography, references and footnotes. This thesis contains no material that has been submitted previously, in whole or in part, for the award of any other academic degree or diploma. Except where otherwise indicated, this thesis is my own work".

"I have conducted my research in alignment with the Australian Code for the Responsible Conduct of Research and Victoria University's Higher Degree by Research Policy and Procedures".

Signatur	Date
	21/08/2021

COVID-19 IMPACT STATEMENT

This thesis was completed under the limitations of the COVID-19 pandemic.

In March 2020, in response to the pandemic, Melbourne went into lockdown. This has affected the progression of my work enormously as all candidates, like myself, lost access to laboratories, offices and study spaces due to university restrictions, access to the laboratory at Western Centre for Health Research and Education (WCHRE), Sunshine Hospital, St Albans 3021 was severely impacted for at least 6-months.

By late May, working permits could be applied for, this allowed candidates only limited access to campus for the purpose of continuing research projects. Alongside, the Victorian Government also instituted a series of regulations limiting the contact between people which impacted training, specialist callouts, equipment access and data collection. These measures remained in place and was followed by multiple lockdowns into 2021 because of the delta variant outbreaks. In addition to these restrictions, I also was required to self-isolate when someone at the laboratory was reported as close contact to a positive case. Events like these and the repeated disruptions were very challenging for cell culturing which requires continual maintenance. With each episode, new cultures were required to be started again with weeks lost for each lockdown, at the time of writing I am currently entering Lockdown 6.0. In addition, the restrictions and lockdowns were also limiting for experiments that are often carried out over several time points spreading over days to weeks.

Therefore, despite the working permit becoming available after months of lockdown during my project and all my efforts to make up for the time lost, inevitably my work was affected

by continuing loss of afterhours access, resources (training, supplies, orders) and general consumables that had to be put on back order.

ACKNOWLEDGEMENTS

"A long road tests a horse's strength, and a long task reveals a person's heart.", and boy has it been what feels like an eternity trapped in lockdown after lockdown. Melbourne had six during this thesis, with some lasting months at a time. When I first committed to the idea of this research thesis, I had never even heard of COVID-19, I think very few had, but halfway into my research the world was aware, with it quickly becoming a pandemic of a generation. Stress, fear and uncertainty became a regular emotion. Stress evoked by the situation and people, fear whether I could finish my research and uncertain how the pandemic will affect all our lives. I could not have done this alone. Making it out on this side I certainly feel more resilient, tougher, and optimistic but I would not have learnt this without the support of every single person that has supported me, believed in me, and backed me up.

The submission of this thesis marks the end of what has been a triumphant yet turbulent journey for me. It represents too many long days in the laboratory – from the crack of dawn to late nights, skipped meals, experiment schedules so tight that there was not even time for restroom breaks, dinner at the office, a very sore back from crouching over the work bench, sacrifices and, definitely, a desire to perfect, learn and succeed. I did all this both during times when the laboratory and offices felt like a scene from the 'Bees' movies where lots of busy bees moved studiously around and in isolation when this was our only option to keep one another safe.

Firstly, I must thank my primary supervisor, Professor John T. Price and co-supervisor, Dr Craig A. Goodman who have contributed greatly to my project. Thank you, Professor Price, for offering me the opportunity to work on this project and supported me throughout all stages of this thesis, offering me your patience, guidance, extensive knowledge, while

allowing me the freedom to direct my research. I would not have been able to complete this thesis if it was not for you. Thank you so much. Every time I was challenged in my research or had felt defeated, speaking to you, my love for science would be reborn, your passion for research is so great that I could feel it transferred via passive diffusion when you spoke. Besides this, you and the team have set my standards for professional relationships, how to work effectively in a team and supporting one another just because you are able to. As a supervisor and research group leader, you have made sure that our team's research practice was strict, ethical and that we worked inclusively, collaboratively and to always look out for one another. I could not have been luckier than to have met you and the team so early in my professional career. I also want to thank Dr Goodman for being available on-site when I was learning about molecular biology and for his remote help, as well. I remember when I had to facetime you from two different devices at once during lockdown. Without your help and expertise of reporter assays I would not have understood it so easily and clearly. It has been amazing to witness how you could explain something that could have been so complex in the most logical manner and so succinct that the ending comes naturally. Thank you for your support in this project, your validation and constructive feedback.

Next, I cannot go forward without thanking the members of the Price lab (Cancer biology and metastasis), my colleagues who are now also my valuable friends. I would have been lost without the intellectual discussions, jokes, laughter, significant-life events and the many culinary experiences we shared. To the senior PhD who helped me when I started, Charlett, Tabitha and Joseph (Joe). Thank you for teaching me science from growing my first flask of cancer cells to running my first westerns and all its mysteries. To Joe, thank you for being at many of my progress meetings and thank you for always making sure I am okay, that I have no issues and that I am really at peace with what I understand. Thank you to the girls

who started their research journey with me, Asha and Natasha. Without you girls I do not think anyone would ever understand what I went through. Venturing this journey together with you two has been a blessing, when we cried, we cried together and when we succeeded, we all celebrated. I also want to thank Sarrabeth, who later joined our group as a research fellow. Thank you for your support while you were with us and for your research insight. You were the glue to our group during the lockdown periods, you listened, and you protected us. All in all, the highlight of my time in our lab came from the darkest experiences but like John said, 'it takes the bad times to know a person' and you are all truly the most amazing people I have met. Thank you to the time we united as a lab in support of me, for taking my concerns seriously and being my good Samaritan. Thank you everyone for listening to me when I am so tired that I speak nonsense and empathising with me when it was a bad day. You are my second family.

Furthermore, I would also like to thank many people at the Western Centre for Health Research and Education (WCHRE). Thank you to Professor Gustavo Duque, Associate Professor Damien Myers and Dr Ahmed Al Saedi from Melbourne University for my first exposure at WCHRE during my third-year project for which I had no idea would then become my second home considering the hours I have spent here. Thank you Dr Elizabeth Verghese who introduced me to Professor John Price. Thank you, Valentina, for being the sweetest person and making sure there was support and training for all of us. Thank you to my dear friends, Lauren, Dean, Nicholas (Nick), Hannah, Bo and many more who motivated me and was my voice of reason when I needed to hear it. Thank you to Professor Alan Hayes, our Assistant Dean at WCHRE, in being my point of contact for all things course and administration related. Thank you to the university and Western Health for providing the resources and facility where I could feel safe to do my research.

Finally, last but certainly not least is the fact that I am deeply indebted to my family and best of friends. Thank you for sticking with me during my good and bad times. The times when I am in euphoria because I was able to do something at the lab even though you have no clue what it means but still celebrated with me or the times, I felt busted. Your unconditional and never-ending love and support has kept me going, for which I am forever grateful. Thank you for being so patient with me and treating me delicately when I am at my worst. Thank you, dear friends who did long hours alongside me, thank you family, my mum and my dad, my brother who all made sure I got home safe and fed. It is such a special feeling to know you have a support system that even when they do not understand what you do but is always there to listen and love you unconditionally. I give them my most warm and great gratitude knowing that I am and will forever be grateful for their limitless support that is not confined within these years but always has been and I know, without taking it for granted, will always be.

From all my heart, my deepest gratitude, thank you all for where your hearts lie, and I cannot wait for what the future holds.

TABLE OF CONTENTS

LIST OF FIGURES

LIST OF TABLES

ABBREVIATIONS

17-AAG	17-N-allylamino-17-demethoxygeldanamycin (Tanespimycin)
ABC	ATP binding cassette transporters
AIHW	Australian Institute of Health and Welfare
AKT	Also called protein kinase B
ANOVA	Analysis of variance
ATCC	American Type Culture Collection
AUY922	Luminespib
AZD8055	A potent, selective ATP-competitive mTOR kinase inhibitor
BCA	Bicinchoninic acid assay
bp	Base pair
BrCa	Breast cancer
BSA	Bovine serum albumin
$CaCl_2$	Calcium chloride
CIC	Cancer initiating cell
CIP2A	Cancerous inhibitor of protein phosphatase 2A
CMV	Cytomegalovirus major
DDR	DNA damage response
DDT	DNA damage tolerance
DLR	Dual-Luciferase® Reporter
DMEM	Dulbecco's Modified Eagle Medium (Gibco)
DMSO	Dimethyl sulfoxide
DN	Dominant negative

DNA	Deoxyribonucleic acid
E. coli	*Escherichia coli*
ECL	Enhanced chemiluminescence
EDTA	Ethylenediaminetetraacetic acid
EGF	Epidermal growth factor
EGFR	Epidermal growth factor receptor
ER	Oestrogen receptor
ErbB-2	Erb-B2 Receptor Tyrosine Kinase 2. Also called HER2
ERK	Extracellular signal-regulated kinase
FBS	Foetal bovine serum
FM3A/M	Multi-drug resistant mouse mammary carcinoma cells overexpressing p-glycoprotein
G148	Geneticin, an analog of neomycin sulphate
GDP	Guanosine diphosphate
GMO	Genetically modified organism
GTP	Guanosine triphosphate
HEPES	4-(2-hydroxyethyl)-1-piperazineethanesulfonic acid (zwitterionic sulfonic acid buffering agent)
HER2	Human epidermal growth factor receptor 2
HIF	Hypoxia inducible factor
HIF-1α	Hypoxia inducible factor 1α
HSE	Heat shock element
HSF1	Heat shock factor 1
HSP	Heat shock protein
HSP105	Heat shock protein 105

HSP70	Heat shock protein 70
HSP90	Heat shock protein 90
HSR	Heat shock response
HuR	Human antigen R
IC50	Half maximal inhibitory concentration
IGF-IIR	Insulin-like growth factor receptor II
IL6/8	Interleukin-6/-8
KD	Knockdown
LB	Lysogeny broth
luc2P	*Photinus pyralis* (firefly)
MAPK	Mitogen-activated protein kinase
MDR-1	Multidrug resistance gene
MES	2-(N-morpholino) ethanesulfonic acid buffer
MICS	Metastasis initiating cells
MK-2206	Highly selective inhibitor of AKT1, AKT2 and AKT3
MOPS	3-(N-morpholino) propanesulfonic acid buffer
MRP-1	Multidrug resistance-associated protein 1
mTOR	Mammalian target of rapamycin
NaCl	Sodium chloride
OD	Optical density
OHS	Occupational health safety
P388/M	Leukemia cells
P53/ PT53	Tumour protein 53
p95^{ErbB-2}	Truncated erbb-2 receptor (constitutively active form of HER2)
PARP	Poly-ADP ribose polymerase

PBS	Phosphate-buffered saline buffer
pcDNA-RLuc8	Plasmid containing the coding sequence for renilla luciferase
PDK1	Phosphoinositide-dependent kinase-1
PFA	Paraformaldehyde
PI3K	Phosphoinositide 3-kinase
PICC	Peripherally inserted central catheter
PIP3	Phosphatidylinositol (3,4,5)-trisphosphate
PP2A	Cellular protein phosphatase 2A (tumour suppressor)
PR	Progesterone receptor
RAS	A small GTPase and is a member of the G protein (guanine nucleotide binding protein) family
RFP	Red fluorescent protein
RLU	Relative light unit (luminescence measurement)
RNA	Ribonucleic acid
RNAi	RNA interference
ROS	Reactive oxygen species
rpm	Rotation per minute
RPMI	Roswell Park Memorial Institute
RT/ RTx/ RTy	Room temperature / room temperature (x)/ room temperature (y)
rtTA3	Reverse tetracycline-transactivator 3 for tetracyclinedependent induction of the TRE promoter
SD	Standard deviation
shRNA	Short hairpin RNA
SOD	Superoxide dismutase
TBS	Tris-buffered saline

TBS-T	Tris-buffered saline (TBS) and Polysorbate 20 (also known as Tween 20)
TET	Tetracycline (TET-ON: tetracycline activated/ 'turn on' dependent)
TGF-α	Transforming growth factor alpha
TKI	Tyrosine kinase inhibitor
TNBC	Triple negative breast cancer
TNFα	Tumour Necrosis Factor alpha
TRE	Tetracycline-inducible promoter
tRFP	TurboRFP reporter for visual tracking of transduction and shRNA expression
TRIPZ	Inducible Lentiviral shRNA vector
Tris	Trisaminomethane
UBC	Human ubiquitin C promoter for constitutive expression of rtTA3 and puromycin resistance genes
UV	Ultra-violet (light)
VC	Vehicle control
WCHRE	Western Centre for Health Research and Education
WHO	World health organisation
WNT7B	WNT Family Member 7B
WT	Wildtype

CHAPTER 1: INTRODUCTION

1.1. The Burden of Cancer

Cancer is a major cause of mortality worldwide and can significantly diminish the length and quality of life for afflicted individuals. According to the World Health Organisation (WHO), in 2020, cancer accounted for an estimated 10 million deaths and breast cancer (BrCa) is the most common cancer in the world recorded at 2.26 million cases (World Health, 2020). The Australian Institute of Health and Welfare (AIHW) also expects BrCa to be the most commonly diagnosed cancer in Australia and estimates that in 2021 20,825 Australians will be diagnosed (Health and Welfare, 2021). While the number of people being diagnosed in Australia is increasing, the number of deaths from BrCa is decreasing.

Cancers are caused by accumulated genetic mutations in the genome that interfere with the highly conserved regulatory pathways responsible for protecting the normal cell (Khalid et al., 2017). Cancer is characterised by neoplastic growth (abnormal cell division) and eventual metastasis (tumours spreading to distant parts of the body) (Guan, 2015). Tumorous growths can compromise vital organ functions; while undesirable, the location of the tumour can have a vast effect on its prognosis (Hanahan and Weinberg, 2011). Tumours are distinguished between the primary and secondary/ metastatic site (Hanahan and Weinberg, 2011, Valastyan and Weinberg, 2011). The five-year-survival statistics for most primary tumours have improved due to targeted treatments, surgery and chemotherapy regimens (Lu and Chao, 2012). However, patients diagnosed with metastatic cancers still have a significantly reduced survival rates as their cancers are broadly resistant to available treatment options (Guan, 2015). Complete surgical

removal is limited due to the nature of these tumours, i.e., poorly defined borders, numerous sites and undetectable tumours (related to size) (Guan, 2015).

Overall, metastasis accounts for at least two thirds of cancer deaths in solid tumours (Dillekås et al., 2019) or about 90% of cancer deaths (Guan, 2015, Carpenter et al., 2017), and remains an enormous burden to the patients, their families and the healthcare system. An example that highlights the fundamental challenges of metastasis and its contribution to poor prognosis is the five-year survival rate of BrCa patients after metastasis (Stage IV) compared to Stage I (Table 1) (Saunders et al., 2018).

Table 1 Five-year survival rates for Breast Cancer

Cancer Stage	Five-year survival rate (2018)	Reference
Stage I	>95%	(Saunders et al., 2018)
Stage II	95%	(Saunders et al., 2018)
Stage III	75%	(Saunders et al., 2018)
Stage IV	25%	(Saunders et al., 2018)

1.2. Metastatic Breast Cancer is Resistant to Treatment

1.2.1. Breast Cancer Subtypes

There are five different BrCa subtypes, and these are classified according to their gene expression patterns. The subtypes are Luminal A, normal-like breast tumours (ER and PR positive, HER2 negative), Luminal B, HER2/ neu over-expressing and triple-

negative BrCa (TNBC), in order of worsening prognosis (refer to Table 2) (Liu et al., 2014, Goldstein et al., 2007). Each subtype possesses distinctly different histological and clinical features, including patient outcome, response to treatment and likelihood of progressing to secondary/ metastatic tumours (Sørlie, 2004).

Table 2 Molecular Sub-types for Breast Cancer

Subtype	Characteristic Receptor Status			Aggressive	Prognosis
	ER	**PR**	**HER2**		
Luminal A	+++	+++	−	1	4
Luminal B	++/+	+/−	−	2	3
HER2/ neu overexpressing	−	−	+++	3	2
Triple Negative	−	−	−	4	1

+++ High positive expression
++ Moderate positive expression
+ Low positive expression[†]
− Negative expression
Score: 1 (Least/ Better) → 4 (More/ Worse)

[†] *Characteristic but not defining expression pattern. Low-level expression could be considered negative.* [Adapted from (Goldstein et al., 2007)].

In terms of expression profiles, Luminal A and B have more similar profiles to normal breast tissue, with the expression of both estrogen (ER) and progesterone (PR) receptors (Yau and Benz, 2008). Luminal A has the best overall survival rate of the different subtypes because of its responsiveness to hormone therapy due to the presence of these receptors (Sørlie, 2004). Luminal B tumours have an increased proliferation rate due to the overexpression of cell cycle promoters and thus have a poorer prognosis (Dai et al., 2017).

HER2/ neu overexpressing tumours have a poor clinical outcome as the cells lack ER and PR receptors, and therefore, do not respond to hormone therapy (Dai et al., 2017). However, they have increased expression of the HER2 oncogene; hence they are highly responsive to HER2-targeted drugs and the combination with other anticancer agents and treatments (Goldstein et al., 2007).

The TNBC tumours lack expression of all three receptors, thus are generally less responsive to treatments (Han et al., 2019). TNBC is also the most aggressive of the different subtypes and highly resistant to most current therapies (Han et al., 2019). TNBC are also metastatic, characterized by a willingness to invade, migrate and proliferate at preferential secondary sites such as the lungs and brain (Proia et al., 2014).

Regardless of the subtype, when tumours become metastatic, cells are more likely to develop drug resistance making them harder to treat, thereby decreasing a good prognosis for the patient. Thus, there is a general need for better therapeutics or new ways to sensitize highly metastatic BrCa to current therapeutics, thereby, developing more effective treatments in hard-to-treat cancers for improved patient outcomes.

1.2.2. Potential Treatment for Metastatic Breast Cancer

It is postulated that to survive the stresses encountered during cancer progression and metastasis, cancer cells engage highly conserved stress response pathways, such as the Heat Shock Response (HSR), to survive. It is also postulated that this pathway may also reduce the efficacy of chemotherapy (Valastyan and Weinberg, 2011, Lu and Chao, 2012). Thus, patients with metastatic cancer face resistance to chemotherapeutics leading to increased morbidity and death, which further reiterates the necessity of novel and effective therapeutics. Blocking the cancer cells' adaption to stress remains a viable treatment option. There is the potential to reduce the cells' adaptive stress response through interference with these stress pathways. Research into the effect that 'overloading' the stress response has in cancer treatment is currently being tested in the clinical setting with combinations of chemotherapy and proteasome inhibitors (drugs that block the breakdown of proteins) (Park et al., 2019, Au et al., 2009). Despite our knowledge of the stresses in cancer, much remains unknown about its effect on cancer cell sensitivity to anticancer therapies.

1.3. Types of Stressors in Cancer

Cancer cells are exposed to numerous stress insults that can directly or indirectly influence their phenotype and progression (Solimini et al., 2007b, Tiligada, 2006, Spisek and Dhodapkar, 2007). Stresses in the microenvironment include marked fluctuation in oxygen, pH, glucose, free radicals, DNA damage, inflammation and competition for space (Zhang et al., 2018, Klaunig and Wang, 2018). As a result, cancer cells are often referred to as being in a sustained stress state (Yeldag et al., 2018, Mosser and Morimoto, 2004). Exposure to stress often leads to the activation of signal

transduction pathways and gene expression that supports cancer cell survival and advances cancer progression (Fitzgerald et al., 2017). Previous studies have shown that nutrient deprivation, acidosis, heat shock and hypoxia are associated with diminished therapeutic response and increased malignant progression (Zhang et al., 2018, Klaunig and Wang, 2018, Fitzgerald et al., 2017, Dairkee et al., 2007, Baghban et al., 2020). These studies also suggest that these conditions may support cancer recurrence and metastasis.

It has been proposed that stress can mediate metastasis through three potential mechanisms; genomic instability, alteration in stress signalling pathways and/ or selection of tumour cells that can sustain these stresses (Hanahan and Weinberg, 2011). The first, genomic instability, is the result of genotoxic stress, a hallmark of cancer which is defined as DNA damage from environmental stress (Bartek et al., 2007). In normal cells genome stability is critical and is protected by DNA repair mechanisms facilitated by the DNA damage response (DDR) signalling, the DNA damage tolerance (DDT) pathway, and checkpoint pathways (Ghosal and Chen, 2013). Cancer cells are characteristically known to have altered or impaired DNA repair mechanisms, thus leading to genome instability as mutations in the genome accumulate. In cancer, the DNA damage can potentially affect genes encoding for tumour suppression and/ or oncogenes. Undetected, genome stability is compromised leading to tumour formation (Zingoni et al., 2017). Furthermore, mutations in the DNA promotes uncontrolled proliferation and has been shown to enhance carcinogenesis (Widschwendter and Jones, 2002).

Several stress events such as hypoxia, inflammation or oxidative stress can instigate cellular signal transduction cascades, tumour-promoting factors and gene expression to aid cancer cell survival (Valko et al., 2006, Fitzgerald et al., 2017, Tiligada, 2006, Federico et al., 2007, Finger and Giaccia, 2010). In brief, as the tumour proliferates, its vasculature may become inadequate to supply enough oxygen and nutrients for its growth, even after increased angiogenesis. This effect can be explained by the Warburg effect that suggests some cancer cell's preference of anaerobic energy production over aerobic despite oxygen availability (Khalid et al., 2017, Liberti and Locasale, 2016). Consequently, hypoxia and glucose-deprivation has been shown to support a more aggressive phenotype. Furthermore, cancer cells under hypoxic environments often switch to anaerobic metabolism (inefficient process of energy conversion in the absence of oxygen) and increase acidic metabolites, such as hydrogen ions, leading to lower extracellular pH (Finger and Giaccia, 2010, Rankin and Giaccia, 2016). Cumulatively, both hypoxic and acidic conditions act as selective pressures directing towards cancer cell survival and proliferation while normal cells would die (Estrella et al., 2013). One molecular pathway that has been described to facilitate this increased survival is the transcription factor, hypoxia inducible factor 1α (HIF-1α), which has been shown to promote cancer metastasis due to its regulation of glycolysis, tissue remodelling, angiogenesis, cell growth and survival (Kimbro and Simons, 2006, Rankin and Giaccia, 2016, Semenza, 2010, Finger and Giaccia, 2010). In addition, hypoxia also generates an inflammatory response, and its recruitment of macrophages promotes the development of cancer-related inflammation at the primary site. These macrophages are localised at the invasive front of advanced tumours and facilitate cancer cell invasion through the secretion of proteases that induce extracellular matrix degradation and tissue remodelling (Avraamides et al., 2008, Hildenbrand and Schaaf, 2009, Jodele et al.,

2005). This is exacerbated by cytokine release from macrophages into the stroma which further enhances the cells' migratory and growth phenotype (Lewis et al., 2000).

A clinical study by *Tsutsui et al. (2005)* supports the association between inflammation and poor cancer outcome, where it was demonstrated that in BrCa patients, elevated tumour-associated macrophages densities correlates with worse survival (Tsutsui et al., 2005). Furthermore, chronic inflammation, glucose deprivation and hypoxia can induce oxidative damage and contribute to tumour progression and metastasis through factors and cytokines, such as TNFα, IL6/8, or reactive oxygen species (ROS) such as superoxide and hydrogen peroxide (Federico et al., 2007, Lee et al., 1997, Aggarwal et al., 2019). Interestingly, while these oxidative stresses are a product of other stresses as mentioned, they also induce cancer cell survival, proliferation, increased invasiveness and angiogenesis, all associated with poor clinical prognosis in BrCa patients (Dairkee et al., 2007, Dolado et al., 2007, Lander, 1997, Yau and Benz, 2008, Aggarwal et al., 2019). Oxidative stress further promotes DNA damage and this damage often affects the activation of transcription factors and proto-oncogenes, whilst inactivating tumour suppressor genes (Valko et al., 2006, Aggarwal et al., 2019).

Overall, stress can expose cancer cells to pro-tumourigenesis factors and promote pro-metastatic transcriptional cascades that enable gene expression that is unfavourable for patient outcome. Of these stress pathways, one that is yet to be discussed is that of the heat shock stress pathway. Heat shock stress is another well-defined pathway that is critical in normal cell homeostasis but is correlated to poor patient survival in cancer and is regulated by the master transcriptional regulator, Heat Shock Factor 1 (HSF1).

1.4. HSF1 is a Master Regulator of the Heat Stress Response in the Cell

1.4.1. The Heat Shock Response

Many different types of stresses upregulate and activate HSF1 as a result of the protein misfolding and damage that they elicit. HSF1 is known to play a major role in regulating the heat shock response (HSR). It is a transcription factor that responds to proteotoxic stress by initiating the transcription of heat shock proteins (HSPs) (Triandafillou and Drummond, 2016). HSPs are involved in protein folding and protection upon proteotoxic stress in normal and cancer cells alike. Misfolded proteins and protein damage are a consequence of induced stress, such as heat shock, hypoxia, acidosis and many others as mentioned in section 1.3 (Desai et al., 2013, Hanahan and Weinberg, 2011). Therefore, the HSF1 adaptive response is essential for proteostatsis (homeostasis of proteins) and overall cell survival (Desai et al., 2013).

1.4.2. Activation of HSF1 And HSF1 Normal Function

During homeostasis, HSF1 monomers are bound to chaperones in the cytoplasm that prevent trimerization of HSF1 (activation) and stop monomeric HSF1 from degradation (Desai et al., 2013). These chaperones include the Heat Shock Protein 90 (HSP90)-p23 complex and Heat Shock Protein 70 (HSP70) (McConnell et al., 2015). When the cells undergo stress this causes an accumulation of protein damage which induces HSP90 to dissociate from HSF1, allowing HSP90 to assist in protecting cells by facilitating protein folding, trafficking and ubiquitination (Anckar and Sistonen, 2011). As a result, HSF1 monomers either degrade or trimerise and enter the nucleus. In the nucleus, trimeric HSF1 is subjected to either stimulatory or inhibitory phosphorylation (Cigliano et al.,

2017) events. Specifically, stimulatory phosphorylation occurs at sites Ser230 and Ser326, whilst, inhibitory phosphorylation is at sites Ser303, Ser307 and Ser363 (Vihervaara and Sistonen, 2014). This cascade of modification to HSF1 will either inhibit its function or enable transcription of its target genes, HSPs, which are important in protein folding and recovery after stress. Overall, HSF1 is protective in normal cell biology and helps cells maintain homeostasis (Vihervaara and Sistonen, 2014). However, in advanced cancer, cells are constantly stressed, and HSF1 expression is typically elevated compared to normal cells. Significantly, in cancer cells, HSF1 has also been shown to facilitate pro-metastatic pathways, separate from the typical HSR (Triandafillou and Drummond, 2016, Mendillo et al., 2012).

1.5. HSF1 Alters Expression of Other Genes Besides the HSR In Cancer

In multiple cancers, including BrCa, HSF1 protein expression is increased and correlated with poor clinical outcomes (Powell et al., 2016, Santagata et al., 2011b). As established by *Mendillo et al. (2012)*, HSF1 gains a broader function as a multifaceted modifier of carcinogenesis for growth and metastasis (Mendillo et al., 2012). This study compared transformed cells ('normal' cells made cancerous) with normal mammary epithelial cells and found that instead of regulating a normal HSR, HSF1 regulated the transcription of genes that encouraged the metastatic phenotype. More specifically, in transformed cells, HSF1 upregulates genes associated with energy metabolism, cell cycle, stress response and translation, while downregulating genes associated with adhesion, the extracellular matrix, apoptosis, immune processes and development (Mendillo et al., 2012). These alternative genes that HSF1 regulates may contribute to the distinct differences between the highly malignant and the primary tumour cells, including changes in cell shape, expression of epithelial markers and survivability in

stressed microenvironments (Mendillo et al., 2012, Nguyen et al., 2013a, Vihervaara and Sistonen, 2014, Jiang et al., 2015, Vydra et al., 2014).

Cancer is the consequence of damaged key regulatory checkpoints within the cell cycle. Although cancer cells may 'thrive' in this dysregulation, HSF1 is an essential mediator of survival in these circumstances (Dai et al., 2018). Another difficulty is some cancer cells may become resistant to the anticancer drugs prescribed. As a result, patients' conditions may worsen with treatment as cells become adapted to the stresses from treatment. Furthermore, cells are exposed to dramatic environmental changes and inevitable alterations in signal transduction, energy production, and the metabolism of nucleic acids and proteins with cellular transformation. High cellular demands, resulting from hypoxia, acidosis, nutrient deprivation, and an adverse immune response within the patient, increase the stress on these cells, and to survive cancer cells need to adapt effectively (Valastyan and Weinberg, 2011). One way of overcoming the initial oncogenic and malignant stress is through the targeting of HSF1 (Tchénio et al., 2006, Desai et al., 2013). Indeed, some studies have shown that HSF1 depletion can reverse the metastatic and more aggressive phenotype of cancers in functional assays and *in-vivo* studies (Mendillo et al., 2012, Cigliano et al., 2017). However, yet to be explored is the effect that HSF1 inhibition/ depletion has on cancer cell sensitivity to anticancer therapeutics. The potential for HSF1 knockdown to increase the sensitivity of cancer cells to anticancer agents is an attractive avenue to explore and may result in developing novel combination therapies.

1.6. The Biology of Resistant Cells to Anticancer Therapies

Unlike normal cells, cancer cells have lost the ability to stop dividing when they come into contact with like cells, meaning they no longer undergo 'contact inhibition' (Pavel et al., 2018). Thus, existing hallmarks that control normal cell differentiation and limit cell division are no longer active (Pavel et al., 2018).

Generally, several types of chemotherapies are available, including alkylating agents, plant alkaloids, antitumour antibiotics, antimetabolites, topoisomerase inhibitors, and miscellaneous antineoplastics (Cleveland, 2021b). Ultimately, chemotherapy is toxic, its purpose is to stop cells from dividing and kill cells to prevent tumour growth. Alkylating agents are cell-cycle non-specific and act on cells during their resting phase. Some examples are Carboplatin, Cisplatin and Oxaliplatin (Michael Colvin, 2003). Plant alkaloids are cell-cycle specific that target cells during various division phases (Matsuura and Fett-Neto, 2017), and examples of these are Paclitaxel and Docetaxel (Matsuura and Fett-Neto, 2017). Antitumour antibiotics are produced by the soil fungus Streptomyces and are also cell-cycle specific; some examples are anthracyclines like Doxorubicin, Epirubicin and Mitomycin (Tenconi and Rigali, 2018). Antimetabolites are cell-cycle specific; they are similar to the naturally found small molecules in cells. Therefore, they can stop cellular division when incorporated by the cell into the cellular metabolism (Lansiaux, 2011), examples of antimetabolites are 5-Fluorouracil and Gemcitabine. Topoisomerase inhibitors prevent the activity of topoisomerase enzymes (topoisomerase I and II) which interferes with cell structural manipulation of DNA necessary for cell replication (Bethesda, 2012). In addition to chemotherapy treatments, there have been great strides in targeted therapy for cancers. These include monoclonal antibodies and tyrosine kinase inhibitors towards cancer cell receptors and cell

signalling pathways upon which the cancer cell is dependent. Examples of targeted cancer therapies include signal transduction inhibitors like Gefitinib which target the EGF receptor, while others include monoclonal antibodies such as Trastuzumab which targets HER-2 (Cleveland, 2021b). Overall, treatment effectiveness is measured in terms of 'response', a series of tests similar to those used to diagnose cancer (Cleveland, 2021a). The response can be complete, partial, stable or disease progression. A complete response is when the tumour disappears; a partial response is when the cancer has shrunk, while a stable response is when the cancer has not changed, and disease progression is when the cancer has grown (Cleveland, 2021a).

When cancer has been responding to treatment but becomes 'disease progressed', this is known as chemotherapy resistance (Yeldag et al., 2018). There are several reasons why cancers become resistant; some cells that were not killed by the treatment mutate and become resistant to the drug. As they continue to multiply, this population of cells is less sensitive to the drug (Daisuke et al., 2016). Gene amplification by the cancer cell could also cause an overproduction of proteins that change the way the anticancer drugs interact inside the cell, or cancer cells may pump the drug out of the cells via p-glycoproteins at equilibrium to the drug coming in (Callaghan et al., 2014). Alternatively, if the transporter for the drug into the cell becomes ineffective, this could also impede the drug's effect. Cancer cells may also gain the ability to repair DNA breaks caused by some-anticancer drugs, which would otherwise kill the cells or develop a mechanism that disables the drug (Harris, 1985). The development of drug resistance is one reason that treatments are often given in combination and why there is a growing need for sensitizers to enhance cancer cells' response to anticancer drugs, such as the use of HSF1 inhibitors for its potential benefits (Chen et al., 2013).

1.7. HSF1 Can Promote Resistance to Anticancer Drugs

A major concern for cancer patients and oncologists is cancer cell metastasis, because this is an indication of the disease worsening. Metastasis is more likely to lead to reoccurrence of the disease. It is linked to a significantly reduced patient survival and is partly due to the development of drug resistance in the cancer cells (Valastyan and Weinberg, 2011, Proia et al., 2014, Dai et al., 2018).

In clinical trials, the use of chemotherapeutics in conjunction with proteasome and HSP90 inhibitors was hoped to improve patient outcomes, however, it was found that these combinations were of limited effect due to the activation of cytoprotective responses in the tumour cells, in particular, that of HSF1 activation (Grimmig et al., 2017).

In cancer, one HSF1-activated gene is the multidrug resistance gene (MDR-1), responsible for multidrug resistance. The overexpression of MDR-1, and its product, p-glycoprotein has been shown to promote the multi-drug resistance phenotype in cancer cells (Kioka et al., 1992). Further evidence for the association of HSF1 in drug resistance was provided by *Kim et al. (1998)* who demonstrated that the cell lines FM3A/M and P388/M, which display a multidrug resistance phenotype, exhibit constitutively activated HSF1 (Kim et al., 1998). Moreover, *Kim et al. (1998)* showed that the inhibition of HSF1 using quercetin downregulated MDR-1 expression and sensitized the cancer cells to anticancer drugs (Kim et al., 1998). Furthermore, these investigations identified that there were two heat shock elements upstream of the MDR-1 promoter (Kim et al., 1998). However, this specific relationship between HSF1 and MDR-1 has not been extensively followed up, although one further study did demonstrate HSF1

regulation of MDR-1/ p-glycoprotein expression and drug transport activity due to its binding to the HSE in the MDR-1 gene promoter (Vilaboa et al., 2000). Another study in 2006 showed that HSF1 induced the multidrug resistance phenotype mediated by MDR-1 independently of heat shock or cellular stress at both the mRNA and protein level (Tchénio et al., 2006, Mendillo et al., 2012). As already discussed, (refer to section 1.5), it was later proven that HSF1 also has functions that are broader than the HSR. Consistent with a role in anticancer drug resistance *Tchénio et al. (2006)* showed that the inhibition of HSF1 can enhance the anticancer drug efficacy in tumour cells, in both *in-vitro* and *in-vivo* models of different cancer types (Tchénio et al., 2006, Mendillo et al., 2012).

Of note, although these studies point towards an involvement of HSF1 in multidrug resistance, further studies are still needed. Delineating the role of HSF1 in anticancer resistance may lead to novel combination treatments with the inclusion of HSF1 inhibition as a key element, in conjunction with anticancer drugs. However, it is still to be determined whether HSF1 acts broadly to provide multi-drug resistance or in a more defined and specific manner.

1.8. Compounds That Activate HSF1

The HSR begins with HSF1 transcription of genes encoding for molecular chaperones, proteases and many proteins essential for proteostasis (Dai, 2018). This process can be activated by mutations or environmental conditions, either acute or chronic (Westerheide and Morimoto, 2005). Examples include inflammation, cancer, neurodegenerative diseases, ischemia, tissue wound healing/ repair or heat, heavy metals, small molecule chemical toxicants, infections and oxidative stress (Westerheide

and Morimoto, 2005). While HSF1 activation can promote cancer progression, the activation of HSF1 can also be beneficial for the treatment of diseases where protein homeostasis is disrupted, and misfolded proteins then accumulate (Jiang et al., 2015, Dai and Sampson, 2016, Mendillo et al., 2012, Kim et al., 1999, Nguyen et al., 2013a).

HSF1 is known to be activated by different classes of compounds such as protein synthesis inhibitors, proteosome inhibitors, serine protease inhibitors, HSP90 inhibitors, inflammatory mediators and triterpenoids (Westerheide and Morimoto, 2005) (refer to Table 3). There is a potential benefit of using HSF1-activating compounds in the treatment of cancer due to the sustained stressed phenotype. Activators of HSF1 may push cancer cell protein homeostasis to levels that may be beyond the buffering capacity in cancer cells, thus leading to cell death. Consistent with this, compounds like HSP90 inhibitors are known to increase stress within tumour cells, inducing HSF1. However, these have been tested in clinical trials for cancer treatment but have not proven successful (Santagata et al., 2012, Shimomura et al., 2019, Kryeziu et al., 2019, Kijima et al., 2018b). A reason that has been provided is that activation of HSF1, rather than causing cancer cells to overload their stress buffering capacity, in fact provided them with a more resistant phenotype. Therefore, rather than stimulating HSF1 for better anticancer drug efficacy, removal of HSF1 activity may be a better approach. Moreover, anticancer drugs that activate HSF1, thereby utilising its survival signalling, may be made more efficacious if HSF1 activity is removed.

Table 3 HSF1 Activating Compounds

	Class	Compound	Reference
Activators	Protein Synthesis Inhibitors	Puromycin	(Hightower, 1980, Lee and Dewey, 1987)
		Azetidine	(Hightower, 1980)
	Proteasome Inhibitors	Carbobenzoxy-l-leucyl-l-leucyl-l-leucinal	(Holmberg et al., 2000)
		Lactacystin	
	Serine Protease Inhibitors	3,4-dichloroisocoumarin	(Rossi et al., 1998)
		tosyl-L-phenylalanine chloromethyl ketone	
		tosyl-L-lysine chloromethyl ketone	
	HSP90 Inhibitors	Radicicol	(Bagatell et al., 2000, Hay et al., 2004)
		Geldanamycin	(Bagatell et al., 2000, Kim et al., 1999, Sittler et al., 2001, Hay et al., 2004)
		17-AAG	(Bagatell et al., 2000)
		AUY922	(K. Rochani et al., 2020)
	Inflammatory Mediators	Cyclopentenone Prostaglandins	(Ohno et al., 1988, Amici et al., 1992)
		Arachidonate	(Jurivich et al., 1994)
		Phospholipase A_2	(Jurivich et al., 1996)
	Triterpenoids	Celastrol	(Westerheide et al., 2004)
		Withaferin A	(Xu et al., 2009)
Co-inducers	Nonsteroidal anti-inflammatory drug	Sodium salicylate *(by inducing HSF1 trimerisation)*	(Jurivich et al., 1992)
		Indomethacin *(by inducing HSF1 binding and hyperphosphorylation)*	(Lee et al., 1995, Jurivich et al., 1992)
	Hydroxylamine derivatives	Bimoclomol *(by decreasing temperature threshold and altering cell membrane fluidity)*	(Vígh et al., 1997, Hargitai et al., 2003)
		Arimoclomol *(by decreasing temperature threshold and altering cell membrane fluidity)*	(Kieran et al., 2004)

(Table adapted from (Westerheide and Morimoto, 2005, Chau Hoang, 2017)

1.9. Project Rationale

HSF1 orchestrates the heat shock response (HSR) in normal cells but is also central to several pathological conditions, including cancer, where it has been shown to be involved in facilitating cancer initiation, progression, metastasis and potentially drug resistance. Consistent with this, the level of HSF1 is elevated in cancer and its activation is directly correlated to cancer progression and prognosis (Santagata et al., 2011b). Moreover, studies have demonstrated that the absence of HSF1 reduces the growth and metastatic phenotype, improving the overall survival rates in animal cancer models (Sharma and Seo, 2018, Cigliano et al., 2017, Nakamura et al., 2010, Zou et al., 1998). This evidence indicates that inhibition of HSF1 may provide a potential strategy for advanced cancer treatment. In addition, HSF1 is a key regulator of many genes that promote the metastatic phenotype some of which are involved in drug resistance (Mendillo et al., 2012), and inhibiting HSF1 activity may result in preventing or reversing a drug resistant phenotype or sensitising cancer cells to certain types of anticancer drugs (Vydra et al., 2014).

Despite this, studies which examine HSF1 in relation to resistance/sensitivity to anticancer therapeutics are currently limited. Thus, this project seeks to provide a comprehensive investigation into the relationship between HSF1 and its role in chemotherapeutic and targeted drug sensitivity in a series of BrCa cell lines. The study will investigate which therapeutics activate the HSR with a view of identifying anticancer drugs that may be more effective with HSF1 inhibition. In addition, the study will examine the impact of HSF1 loss in sensitising BrCa cells to a panel of anticancer drugs that have been previously identified by the Price lab using gene expression arrays and a bioinformatics approach.

It is hoped that the findings from this study will contribute to the rationale for the continued development of HSF1 inhibitors that would be used in combination with current and future anticancer agents with a view to enhance cancer cell sensitivity to these agents.

1.10. Hypothesis and Aims

<u>Hypothesis</u>

The effectiveness of anticancer therapeutics used in the treatment of metastatic BrCa is dependent on the levels and activity of HSF1, and a number of anticancer therapeutics are also potent activators of HSF1.

<u>Overall Aim</u>

To determine whether HSF1 knockdown in cancer cells will sensitise them to anticancer drugs and whether there is a direct link between chemotherapeutic and targeted agents that induce a HSR and their requirement for HSF1 to enable resistance.

To achieve the overall aim, the following two specific aims will be undertaken:

Aim 1: To screen a series of targeted and chemotherapeutic agents in HSF1 knockdown BrCa cells to determine whether loss of HSF1 will make these BrCa cells more sensitive to these anticancer agents.

Aim 2: To identify chemotherapeutic agents that cause an HSR in cancer cell lines.

CHAPTER 2: MATERIALS AND METHODS

2.1. Molecular Cloning and Generation of Expression Constructs

2.1.1. Bacterial Transformation

Competent bacteria were prepared using the calcium chloride ($CaCl_2$) method (Nakata et al., 1997). Briefly, TOP10B *Escherichia coli (E. coli)* were grown overnight in 5 ml Lysogeny broth (LB). Two ml of this cell culture were transferred to 100 ml of fresh LB, and the culture was grown at 37°C at 225rpm until the optical density (OD) reached 0.4-0.6 (approximately two-three hours). The culture was incubated on ice for twenty minutes. The cells were centrifuged at 5000rpm for five minutes. The supernatant was discarded, and the pellet resuspended in 50 ml ice-cold 100mM $CaCl_2$ and incubated on ice for thirty minutes. After the incubation, the cells were pelleted and resuspended in another 50 ml of ice-cold 100mM $CaCl_2$, followed by incubation on ice for one hour. The cells were centrifuged again, and the pellet was resuspended into 5 ml sterile ice-cold storage solution (100mM $CaCl_2$ and 15% v/v glycerol). The competent bacteria were stored in 100μL aliquots at -80°C for up to three months.

To transform bacterial cells with plasmids, 100 ng of plasmid was added to 100μL of the $CaCl_2$ competent TOP10B bacterial cells and incubated on ice for ten minutes. The cells were heat-shocked for 45 seconds at 42°C and immediately cooled on ice. Two hundred microliters of LB were added to dilute the bacteria cells, and 100μL of the diluted transformed bacterial solution was streak-plated onto an LB agar plate containing appropriate antibiotics for selection. Appropriate antibiotics to a final

concentration of 100μg/ ml for ampicillin and 50μg/ ml kanamycin. The plate was inverted and incubated at 37°C overnight with visible colonies by the morning.

2.1.2. Bacterial Liquid Cultures

The LB was sterilized by autoclaving at 121°C for twenty minutes. When ready, in a sterile environment and using aseptic technique, a single colony from the LB agar plate (refer to section 2.1.1) was picked using a pipette tip and dropped into the sterile LB (1% w/v tryptone, 0.5% w/v yeast extract and 1% w/v NaCl) containing appropriate antibiotics. Liquid bacteria cultures were grown at 37°C with shaking at 225rpm for approximately eighteen hours.

2.1.3. Bacterial Glycerol Stocks

To prepare bacterial glycerol stocks for the plasmid transformed bacteria, a colony from the bacterial plate culture was picked and inoculated into 5 ml of LB broth containing appropriate antibiotics and grown overnight at 37°C with agitation (225 rpm). Eight hundred microliters of that culture were mixed with 200μL of 80% v/v sterile glycerol in a 2 ml cryotube and stored at -80°C.

2.1.4. Plasmid Extraction and DNA Purification

PureLink™ HiPure Plasmid Maxiprep Kit (Invitrogen, California, USA, Catalog number: K210006) was utilised to extract plasmids as per manufacturer's instructions and ready to use for transfection. In brief, the overnight bacterial liquid cultures (section 2.1.2.) were harvested by centrifugation at 16,000 x g for ten minutes and the pellet was resuspended in resuspension buffer with RNase A. Cells were lysed using lysis buffer

and precipitation buffer was added before another centrifugation step at >12,000 x g for ten minutes. Next, the supernatant was loaded into the kit's equilibrated column, washed, and drained before the purified DNA was eluted off the column per Invitrogen's kit instruction. The final DNA was suspended in 200μl TE buffer (included in the kit) and stored at -20ºC.

2.1.5. DNA Quantitation

The quantity and purity of DNA after purification was tested using two methods: [1] Restriction enzyme digestion (section 2.1.6.), followed by agarose gel electrophoresis (section 2.1.7.) and [2] by absorbance at 260/280 using Nanodrop Spectrophotometer 2000 set to nucleic acid (μg/ ml) (Thermofisher Scientific, California, USA).

2.1.6. Double Restriction Enzyme Digestion

Restriction enzyme digestion was used for diagnosis or for size-reduction purposes. For diagnostic digestions that confirmed the identity of the plasmid, 1μg DNA was used in a reaction of 10μl (total volume). For size-reduction, 10μg DNA was used in a total 50μl reaction. The final DNA samples were subjected to agarose electrophoresis as described in section 2.1.7. and section 2.1.8. for DNA extraction. Enzyme digestion followed protocols as outlined by the manufacturer of the enzymes, New England Biolabs (Ipswich, MA, US).

2.1.6.1. Digesting specification of the Reporter Vector Expressing HSE (pGL4.41)

The pGL4.41 vector (Promega Corporation, Madison, WI 53711 USA) contains a destabilised luciferase under the control of a minimal promoter and HSE and has 6,045 base pairs (bp), (Figure 1). To reduce its size, the plasmid was cut at two single cutting sites, BsmAI [cut site 55, GTCTC (4nt 5' extension)] and PciI [cut site 4336, ACATGT (4nt 5' extension)]. These cuts separate the ampicillin resistance domain that is no longer needed for transfection in the cells. The new sequence of interest is 4,281 bp long and has reduced the sequence by 1,764 bp from original size, 6,045 bp.
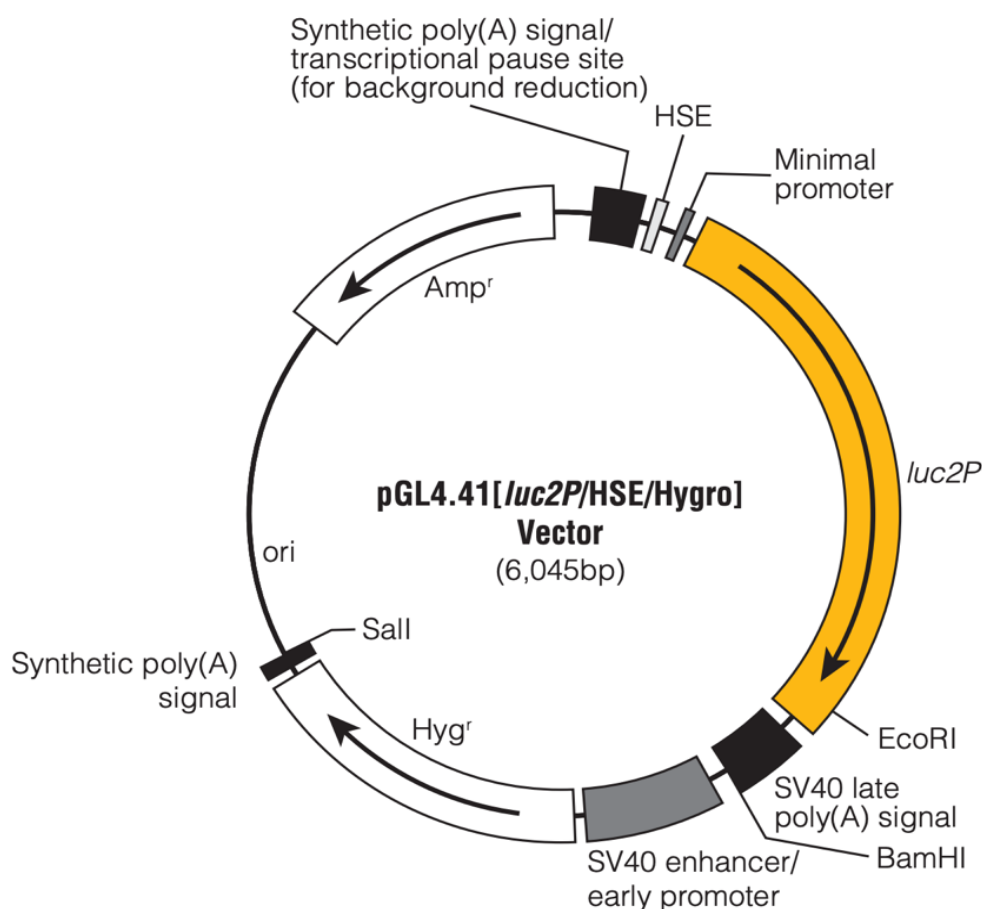
Figure 1 pGL4.41[luc2P/HSE/Hygro] Vector Map from 'Promega'

2.1.6.2. Digesting specification of the Reporter Vector Expressing Renilla Luciferase

The pcDNA-RLuc8 vector (Sanjiv Sam Gambhir Addgene plasmid #87121; http://n2t.net/addgene:87121; RRID: Addgene_87121) has 6,361 bp, (Figure 2). To reduce its size, the plasmid was cut at two single cutting sites, BgIII (cut site 5469) and PciI (cut site 3641). These cuts separate the ampicillin resistance domain that is no longer needed for transfection in the cells. The new sequence of interest is 4,533 bp, removing 1,828 bp from the original 6,361 bp long sequence.
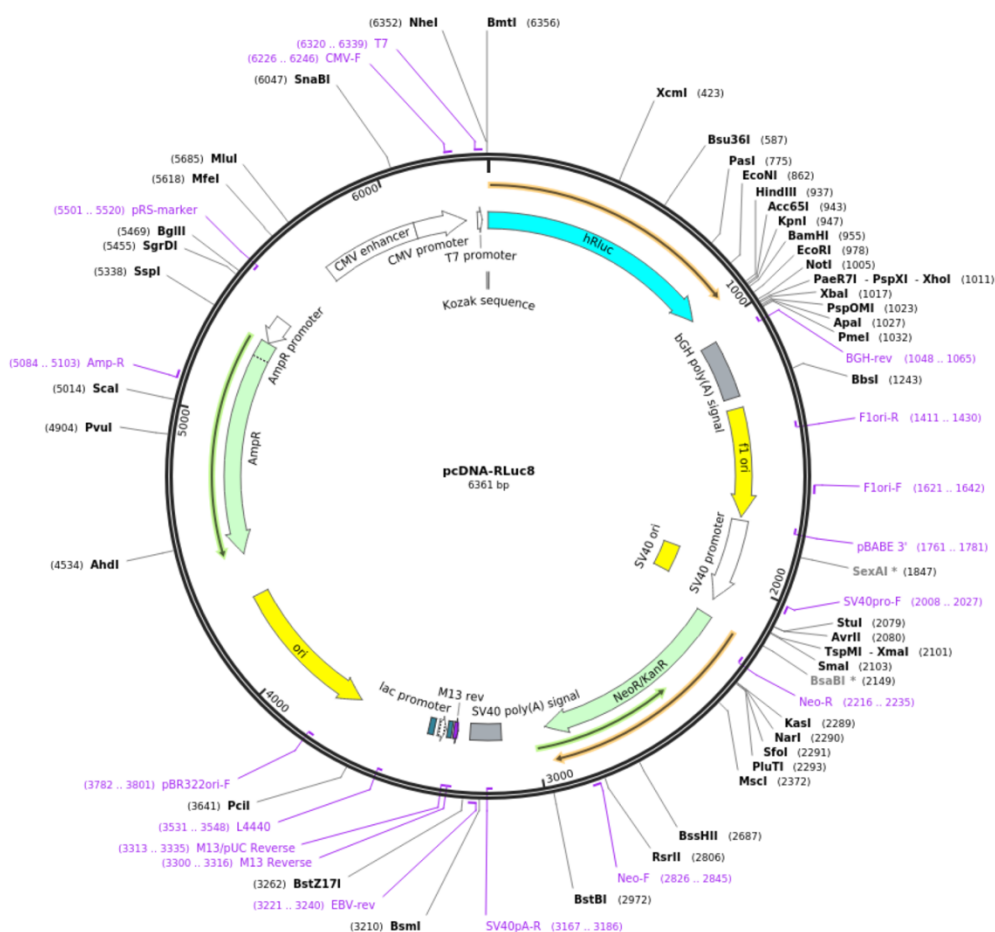
Figure 2 pcDNA-RLuc8 Vector Map from 'Addgene'

2.1.7. Agarose Gel Electrophoresis

One percent agarose gel was prepared in 1x TAE buffer (40mM Tris-acetate, 1mM EDTA, pH 8.3) with 0.0001% v/v Sybr Safe DNA gel stain (Invitrogen, California, USA) for DNA visualisation. The recommendation for DNA larger than 500 bp is 1% w/v gel. Before loading, DNA samples were prepared with 5x loading buffer (0.125% w/v xylene cyanol, 0.125% w/v bromophenol phenol blue, 15% v/v glycerol) and HyperLadder™ 1 kb (Bioline, London, UK) was loaded for size estimation of the DNA samples. The gel was voltage at 100V for eighty minutes and visualized using the UV transilluminator.

2.1.8. Purifying DNA from an Agarose Gel

DNA was electrophoresed after double restriction enzyme digest for the purpose of size-reduction. The DNA was excised from the agarose gel at the appropriate band with reference to the bp length and extracted using QIAquick® Gel Extraction Kit (Qiagen, California, USA), following manufacturer's manual. The DNA retrieved was ready to use for transfection in the cell.

2.2. Cell Culture

2.2.1. Routine Cell Culturing

MDA-MB-231 (ATCC HTB-26) and T47D (ATCC HTB-133) cell lines were obtained from the American Type Culture Collection (ATCC) and were routinely cultured, subculture as per the ATCC (Gaithersburg, Maryland, USA) instructions. It was also important that all cells used were mycoplasma free and were regularly tested to ensure

they remained mycoplasma free (section 2.2.1.1). All cells were grown in a 5% CO_2 humidified incubator at 37°C. MDA-MB-231 was maintained in Dulbecco's modified Eagle Medium (DMEM) medium and T47D was maintained in Roswell Park Memorial Institute (RPMI) medium (Gibco Invitrogen, California, USA) and supplemented with 10% v/v foetal bovine serum (FBS) (Invitrogen, California, USA), 1% v/v HEPES (Gibco Invitrogen, California, USA), 1% v/v GlutaMAX (Gibco Invitrogen, California, USA), 1% v/v Sodium Pyruvate (Gibco Invitrogen, California, USA) and 1% v/v antibiotic/ antimycotic (Gibco Invitrogen, California, USA). The cell lines were maintained in monolayer culture and cells grown in T75 flasks were passaged every 3-4 days once confluent. For passaging, growth medium was removed, and the cell monolayer was washed twice with 10 ml PBS. One millilitre of TryplE express (Gibco Invitrogen, California, USA) was added to cover the cells and the cells were incubated at 37°C for 15-20 minutes to detach. Once detached, cells were resuspended in 10 ml (total) of appropriate medium. Cells were either plated or passaged at 1:10 into a new T75 flask of cell suspension in fresh medium.

2.2.1.1.   Mycoplasma testing

Regular mycoplasma testing was performed to ensure that cells were free of contamination. Aliquots of cell culture medium was centrifuged at 2000 x g for 5 minutes before 100μL supernatants were added in triplicates to white 96 well plates and mixed with reagent (100μL) from MycoAlert Mycoplasma Detection Kit (Lonza, Basel, Switzerland) as per the manufacturer's instructions. The mixture was left to equilibrate for 5 minutes at room temperature before luminescence signal intensity was measured using Varioskan Flash Multimode Plate Reader (ThermoFisher Scientific). MycoAlert substrate (100μL) was added to each sample and after 10 minutes a second luminescence

signal was measured using the plate reader. A ratio was calculated by dividing the first signal from the results of the second signal. Ratios less than 0.9 is negative for mycoplasma. Borderline mycoplasma contaminated cultures with a ratio between 0.9 and 1.2 would be retested in 24 hours and ratios greater than 1.2 is positive for mycoplasma contamination. The kit also included positive and negative mycoplasma control samples to run alongside test samples.

2.2.2. Cryopreservation of Cell Lines

All cell lines in this study were cryopreserved in liquid nitrogen at low passages. Low passages are no more than 10-12 number of times the culture has been subcultured. Cells were cultured in T75 flasks to 80-90% confluence and then lifted as described in 2.2.1., and pelleted at 1500rpm for three minutes. The cell pellet was resuspended in 4 ml of ice-cold freezing medium [90% v/v FBS and 10% v/v dimethyl sulfoxide (DMSO)]. Cell suspension was transferred as 1 ml aliquots into cryotubes and incubated on ice for 5-10 minutes. The cryotubes were packed in a Mr Frosty Cryo 1° freezing container filled with isopropanol at -80°C overnight before being transferred into towers for long term storage in liquid nitrogen. Cell viability following this slow freeze method is well maintained.

2.2.3. Cell Transfections

2.2.3.1.   Cell lines stably transduced with inducible shRNA targeting HSF1

HSF1 vectors were previously designed by our lab group (Nguyen et al., 2013b). Five retroviral MSCV-LMP vectors were used to produce retroviruses expressing HSF1

shRNAmir1-5 (Paddison et al., 2004). In brief, the viruses were prepared by delivering the DNA to HEK293T cells using Lipofectamine LTX (Invitrogen, California, USA) using the manufacturers' instructions. Fifteen to sixteen hours after the transfection medium was replaced with harvesting medium. The harvesting medium was ready for collection by 48/96 hours following addition of harvesting medium and was filtered through 0.45μM size filter and stored at -80°C, ready for transfection. Five hundred microlitres of virus containing supernatant expressing HSF1 shRNAmir1 and shRNAmir4 were selected and used to transfect MDA-MB-231 and T47D in the presence of 10μg / ml polybrene. After twenty-four hours incubation, the virus-containing medium was replaced with fresh medium and transfected cells were left to recover for twenty-four hours. Stably transfected cells were selected using Puromycin (2μg/ ml). Cells that were successfully transfected survived the treatment of Puromycin (Sigma-Aldrich, Missouri, USA), resistance is induced by an enzyme that permits its breakdown a part of the design with the construct, while parental cells died. The expression of the shRNA in the stably transfected cells were activated with doxycycline (Sigma-Aldrich, Missouri, USA). Live cell reporter, a red fluorescent protein (RFP), was visualised under a TRITC filter and western blot analysis for Recombinant Anti-HSF1 antibody (ab52757) (Abcam, Cambridge, MA, USA) was performed to determine the knockdown efficiency of each HSF1 shRNA mir in the MDA-MB-231 and T47D cell lines. As a control, a non-targeting shRNA was also transfected alongside the HSF1 shRNA mirs to ensure that the introduction of a vector did not have an unexpected effect on behaviour of the cells subjected to transfection.

2.2.3.2. Developed Dual-reporting Heat Shock Response Model

The two cell lines, T47D and MDA-MB-231 were stably transfected with the two vectors, pGL4.41[luc2P/HSE/Hygro] and pcDNA-RLuc8. The vectors were delivered using Lipofectamine® 3000 (Invitrogen, California, USA) following the manufacturers' prescribed lipofection technique. In brief, plasmid DNA-lipid complexes were prepared and added to wells of a 6-well plate at 1.25μg DNA per pGL4.41 and pcDNA-RLuc8 or combined 2.5μg total DNA. The stock concentration of pGL4.41[luc2P/HSE/Hygro] and pcDNA-RLuc8 used were 0.23μg/μL and 0.145 μg/μL, respectively, with an A260/280 ration of 1.86. To prepare the DNA-lipid complexes, in one tube, the optimised amount of DNA was added to P3000 reagent and medium. This was then mixed with a second tube containing the lipofectamine 3000 reagent and medium and incubated for fifteen minutes at room temperature.

2.3. Expression Analysis

2.3.1. Protein Extraction and Quantitation

Cells were grown in 6-well plates to appropriate (>60%) confluency, then washed once with ice-cold PBS and incubated in a modified RIPA buffer (50mM Tris- HCl pH 7.4, 150mM NaCl, 0.1% v/v SDS, 0.5 % w/v Sodium Deoxycholate, 1% v/v NP40, 5mM EDTA) containing a mixture of protease (Sigma-Aldrich, Missouri, USA) and phosphatase inhibitors at 1:100 (Sigma-Aldrich, Missouri, USA) at 4°C for 30-60 minutes to lyse. Cell lysates were harvested with cell scraper and pipetted into 1.5 ml Eppendorf tubes to continue lysis before centrifugation at 13,000rpm for thirty minutes at 4°C. After centrifugation, the supernatant was transferred into fresh Eppendorf tubes for storage at -80°C and the protein collection was complete.

Following protein extraction, protein concentrations were quantified using the bicinchoninic acid (BCA) assay kit as per manufacturer's instructions (Pierce Biotechnology, Illinois, USA). Briefly, to generate a standard curve, Pierce™ Bovine Serum Albumin Standard Ampules were serially diluted with water to produce final standard concentrations of 2, 1, 0.5, 0.25, 0.125, 0.0625 and 0.03125mg/ ml. Sixteen microlitres of the standards and four microlitres of the protein samples were loaded into a 96 well plate in triplicate and 150μL of BCA reagents A and B (50:1, respectively) were added to each well. The plate was incubated at 37°C for thirty minutes before the absorbance of each sample was determined at 540nM using a Varioskan Flash Spectral Scanning Multimode Reader (Thermofisher Scientific, Massachusetts, USA). Protein concentrations of the samples were determined by referencing to the standard curve.

2.3.2. Western Blot: Gel Electrophoresis

Equal amount of protein (10-30μg) was combined with NuPAGE™ LDS Sample Buffer (4X) (Invitrogen, California, USA) and NuPAGE™ Sample Reducing Agent (10X) (Invitrogen, California, USA) before denaturation at 95°C for 5 minutes. Then, the protein samples were cooled and loaded into a 20 well NuPAGE 4-12% Bis-Tris pre-cast gel (Invitrogen, California, USA) with Novex™ Sharp Pre-stained Protein Standard (Invitrogen, California, USA) for size determination. The gel was electrophoresed at 110V for eighty minutes in NuPAGE MOPS or MES SDS running buffer containing antioxidants (Invitrogen, California, USA). The proteins from the completed run were transferred using iBlot 2 dry blotting system (Invitrogen, California, USA). Briefly, the gel after electrophoresis was submerged in 20% v/v ethanol for fifteen minutes before ten minutes in Milli-Q water then stacked between the iBlot regular transfer stack (Invitrogen, California, USA) and transferred for seven minutes on 20V.

For immunoblotting, membranes were blocked in Tris buffered saline (TBST, 50mM Tris-HCl, 150mM NaCl, 0.1% v/v Tween-20, pH 7.4) containing 5% skim milk for one hour at room temperature, followed by overnight incubation with primary antibodies diluted in 1x TBST with 3% w/v skim milk at 4°C with rotation. The next morning, membranes were washed for three times for nine minutes each wash with 1x TBST and incubated at room temperature in the appropriate horseradish-conjugated secondary antibodies diluted at $1:1 \times 10^4$ for one hour. This was followed by three, nine-minute washes in TBST. To develop luminescence, membranes were soaked in chemiluminescent ECL western blotting substrate (Pierce, Illinois, USA). The detection reagents I and II were mixed in a 1:1 ratio and added to the blot for one minute before visualisation using Fusion FX Spectra (Vilber Lourmat, ZAC de Lamirault, Collegien. France).

2.3.3. Western Blot Analysis

The imaged western blot was analysed using Fusion FX Spectra analysing program (Vilber Lourmat, ZAC de Lamirault, Collegien. France) and the densitometry of the individual bands were normalised to the respective loading control, ß-actin, unless specified otherwise as appropriate.

2.3.4. Stripping and Reprobing Western Blot Membranes

When necessary, membranes were stripped using Restore Western Blot Stripping Buffer (Thermo Scientific, Massachusetts, USA). Following the product instructions, the blots were stripped for 30 minutes at 37°C, then washed with TBST and blocked. Before the

blot was reprobed with a new primary antibody per usual, the blot was first probed with an appropriate secondary antibody and visualised using Fusion FX Spectra (Vilber Lourmat, ZAC de Lamirault, Collegien. France) (as previously described in section 2.3.2.) to ensure sufficient removal of the previous primary antibody.

2.4. *In-vitro* Assays

2.4.1. Cytotoxicity Assay

Drugs were prepared freshly from stock solutions in DMSO and diluted with the appropriate volumes of the growth medium. After cell seeding with medium containing +/- doxycycline 0.5μg/ ml (to activate inducible HSF1 knockdown in modified T47D and MDA-MB-231 cell lines, refer to section 2.2.3.1.) in 96-well plates at 1×10^4 cells/well, cells were left to adhere overnight. The next morning, the medium was replaced with the medium containing the anticancer drug of interest. To keep this mass screen consistent, the drug concentration range was kept the same. The drugs were serially diluted for concentrations of 100pM, 1nM, 10nM, 100nM, 1μM, 10μM, 100μM in medium with or without +/- Doxycycline 0.5μg/ ml. Vehicle control cells were cultured in the medium containing the same concentration of DMSO as the highest experimental cultures (100μM) for 0-, 24-, 48- and/ or 72- hours. Earlier observations showed that DMSO at these concentrations were not toxic to the cells.

2.4.2. Alamar Blue Assay

The Alamar Blue stock was stored in a light sensitive container at 4°C. Cells were grown in a 96-well plate (refer to section 2.4.1., for experimental conditions) and once ready, 100μL of the diluted Alamar Blue was added to each well and re-incubated for two

hours at 37°C avoiding exposure to light. The Alamar Blue stock was diluted at 1:10 with the appropriate cell culture medium. After incubation, the Alamar Blue was transferred to a white plate for fluorescence to be measured in the Varioskan Flash Spectral Scanning Multimode Reader (Thermofisher Scientific, Massachusetts, USA) with excitation at 550nm and emission at 590nm. The IC50 values were calculated from the fluorescence value in GraphPad after they were normalised to their relative DMSO vehicle controls (set as 100% viability) for each cell line.

The plate with the live cells was fixed for two minutes with Methanol and followed with Quik Dip reagents I and II for one and two minutes, respectively (Fronine Lab Supplies, New South Wales, Australia).

2.4.3. Dual-Luciferase Reporter Assay

Once cells were ready from their experiments, lysates were prepared using Passive Lysis Buffer supplied in the Dual-Luciferase® Reporter (DLR) Assay System (Promega Corporation, Madison, WI 53711 USA). The lysates were collected at 200μL from each well of plate sized 24 wells and 20μL was aliquoted in triplicate per group into an opaque white 96-well plate. Plates was assayed using freshly prepared substrates and buffers that were correctly stored per the DLR Assay System (Promega Corporation, Madison, WI 53711 USA) manufacturer's instructions. The signals were recorded using Varioskan Flash Spectral Scanning Multimode Reader with automatic injectors (Thermofisher Scientific, Massachusetts, USA) and an optimised protocol.

2.5. Statistical Analysis

Assays were performed at least n=3 and presented as mean ± standard deviation (SD). All n values refer to biological repeats. Where appropriate, a two-way-ANOVA was performed with a Tukey's multiple comparison test unless otherwise specified. P-value format is set to GraphPad style which reports four digits after the decimal point with a leading zero and represented as ns (0.1234), * (0.0332), ** (0.0020), *** (0.0002) and **** (<0.0001).

2.6. Materials

2.6.1. Plasmid Constructs

Table 4 List of Plasmids

Plasmids	Source
Scrambled non-targeting control shRNAmir (renilla)	Price Lab Group
pMSCV-LMP HSF1 shRNAmir1 Target site on HSF1 mRNA: 1292-1312	Price Lab Group
pMSCV-LMP HSF1 shRNAmir4 Target site on HSF1 mRNA: 2010-2030 (3'UTR)	Price Lab Group
cDNA-RLuc8	Sanjiv Sam Gambhir Addgene plasmid # 87121; http://n2t.net/addgene:87121; RRID: Addgene_87121
pGL4.41[luc2P/HSE/Hygro]	Promega Corporation, Madison, WI 53711 USA
pEGFP-N1	Clontech Laboratories, Inc., USA

2.6.2. Reagents used in the Cloning and Generation of Vectors

Table 5 List of Reagents for Cloning and Generation of Vectors

Item	Cat. No.	Supplier
Ampicillin	A-2804	Sigma-Aldrich, Missouri, USA
HyperLadder™ 1kb	BIO-33025	Bioline, London, UK
Kanamycin	BP861	Sigma-Aldrich, Missouri, USA
LB Agar	71752-5	Merck, New Jersey, USA
Restriction Enzymes (and buffer): BsmAI, PciI, BgIII		New England Biolabs, Massachusetts, USA
SYBR Safe DNA Gel Stain	S33102	Invitrogen, California, USA

2.6.3. Reagents used in Cell Culture and *in-vitro* assays

Table 6 List of Reagents for Cell Culture and *in-vitro* Assays

Item	Cat. No.	Supplier
100X Antibiotic/Antimycotic	15240062	Gibco Invitrogen, California, USA
alamarBlue™ Cell Viability Reagent	DAL1100	Invitrogen, California, USA
Crizotinib	PZ0191	Sigma-Aldrich, Missouri, USA
DMSO (Dimethyl Sulfoxide)	276855	Sigma-Aldrich, Missouri, USA
Doxorubicin	D-4000	Selleck, USA
Doxycycline	D3447	Sigma-Aldrich, Missouri, USA
Dulbecco's modified Eagle Medium (DMEM)	11995-073	Gibco Invitrogen, California, USA
Foetal Bovine Serum (FBS)	15-010.02	Thermo Scientific, California, USA
G-418 (Neomycin)	S3028	Selleck, USA
GlutaMAX	35050079	Gibco Invitrogen, California, USA
HEPES	15630106	Gibco Invitrogen, California, USA
HSP90 Inhibitors: Luminespib (NVP-AUY-922)	S1069	Selleck, USA
Tanespimycin (17-AAG)	S1141	Selleck, USA
Hygromycin	H3274-250MG	Sigma-Aldrich, Missouri, USA
Lipofectamine® 3000	L3000008	Invitrogen, California, USA
Methanol	106009	Merck, New Jersey, USA
Puromycin	P8833	Sigma-Aldrich, Missouri, USA
RPMI Medium	11875-119	Gibco Invitrogen, California, USA
Sodium Pyruvate	11360070	Gibco Invitrogen, California, USA
TrypLE Express	12604-039	Gibco Invitrogen, California, USA

2.6.4. General Reagents and Materials

Table 7 List of General Reagents

Item	Supplier
Acetic Acid	BDH AnalaR, Poole, England
Disodium Phosphate (Na_2HPO_4)	Astral Scientific, New South Wales, Australia
DMSO (Dimethyl Sulfoxide)	Sigma-Aldrich, Missouri, USA
EDTA (Ethylenediaminetetra Acetic Acid Disodium Salt)	BDH AnalaR, Poole, England
Ethanol	Merck, New Jersey, USA
Isopropanol Alcohol	Merck, New Jersey, USA
Methanol	Merck, New Jersey, USA
Paraformaldehyde (PFA)	BDH AnalaR, Poole, England
Potassium Chloride (KCl)	Astral Scientific, New South Wales, Australia
Potassium Dihydrogenphosphate (KH_2PO_4)	Astral Scientific, New South Wales, Australia
Sodium Chloride (NaCl)	Astral Scientific, New South Wales, Australia
Sodium Dioxycholate	Sigma-Aldrich, Missouri, USA
Sodium dodecyl sulfate (SDS)	Thermo Scientific, California, USA
Tris-HCl (Tris aminomethane) (hydroxymethyl)	Astral Scientific, New South Wales, Australia
Triton-X100 (t-octylphenoxypoly-ethoxyethanol)	Sigma-Aldrich, Missouri, USA
Tween-20 (Polyoxyethylene sorbitanmonolaurate)	Sigma-Aldrich, Missouri, USA

Table 8 List of Reagents and Materials for Protein Expression Analysis

Item	Supplier
iBlot™ 2 Transfer Stacks, PVDF	Invitrogen, California, USA
MES Buffer	Invitrogen, California, USA
Novex™ Sharp Pre-stained Protein Standard	Invitrogen, California, USA
NUPAGE Bis-Tris 20-well Gel	Invitrogen, California, USA
NuPAGE™ Antioxidant	Invitrogen, California, USA
NuPAGE™ LDS Sample Buffer (4X)	Invitrogen, California, USA
NuPAGE™ MOPS SDS Running Buffer (20X)	Invitrogen, California, USA
NuPAGE™ Sample Reducing Agent (10X)	Invitrogen, California, USA
Phosphatase Inhibitor	Sigma-Aldrich, Missouri, USA
Protease Inhibitor	Sigma-Aldrich, Missouri, USA
Restore Western Blot Stripping Buffer	Thermo Scientific, Massachusetts, USA
Skim Milk Powder	Coles, Victoria, Australia

2.6.5. Commercial Kits

Table 9 List of Commercial Kits

Item	Cat. No.	Supplier
BCA Protein Assay Kit	23227	Pierce Biotechnology, Illinois, USA
Chemiluminescence Luminol	34080	Pierce Biotechnology, Illinois, USA
Diff Quik Dyes		Fronine Lab Supplies, New South Wales, Australia
Dual-Luciferase® Reporter Assay System	E1980	Promega Corporation, Madison, WI 53711 USA
MycoAlert Mycoplasma Detection Kit	LT07-218	Lonza, Basel, Switzerland
PureLink™ HiPure Plasmid Maxiprep Kit	K210006	Invitrogen, California, USA,
QIAquick DNA Purification Kit	28704	Qiagen, California, USA

2.6.6. Chemotherapeutic and Targeted Therapeutic Drugs

Table 10 List of Chemotherapeutic and Targeted Therapeutic Drugs

	Item	Main Target	Induces	Cat. No.	Supplier
HSP90 Inhibitors	17-AAG	Heat shock protein 90	▪ Apoptosis ▪ Necrosis ▪ Autophagy ▪ Mitophagy	S1141	Selleck, USA
	AUY-922	Heat shock protein 90α/β	▪ Growth inhibition ▪ Autophagy ▪ Apoptosis	S1069	Selleck, USA
mTOR Inhibitor	AZD8055	ATP-competitive mTOR	▪ Caspase-dependent apoptosis ▪ Autophagy	S1555	Selleck, USA
Chemotherapeutic	Doxorubicin/ Adriamycin	DNA topoisomerase II (also, reduces basal phosphorylation of AMPK)	▪ DNA damage ▪ Mitophagy ▪ Apoptosis	D-4000	Selleck, USA
Tyrosine Kinase Inhibitor (TKI)	Crizotinib	c-Met ALK ROS1	Via inhibition of the STAT3 pathway Autophagy	PZ0191	Sigma-Aldrich, Missouri, USA
	Gefitinib	EGFR (Tyr1173, Tyr992 and Tyr992)	Via blockade of the PI3K/AKT/mTOR pathway ▪ Autophagy ▪ Apoptosis	SML1657	Sigma-Aldrich, Missouri, USA
	Lapatinib	Receptor autophosphorylation: EGFR ErbB-2 (p95^{ErbB-2})	▪ Ferroptosis ▪ Autophagic cell death Associated with inhibition of AKT phosphorylation (Rusnak et al., 2001): ▪ G1 arrest ▪ Apoptosis	SML2259	Sigma-Aldrich, Missouri, USA (Xia et al., 2004)

				S1078	
AKT Inhibitor	MK-2206	AKT1/2/3	▪ Autophagy ▪ Apoptosis		Selleck, USA
PI3K Inhibitors	Pictilisib	PI3K (p110α/δ)	▪ Autophagy ▪ Apoptosis	S1065	Sigma-Aldrich, Missouri, USA
	Idelalisib	PI3K (p110δ)	Autophagy	S2226	Sigma-Aldrich, Missouri, USA

2.6.7. Antibodies

Table 11 List of Antibodies

Item	Dilutions for Western Blot Analysis	Specie of Origin	Supplier
AKT (pan)	1:2,000	Rabbit	Cell Signalling, Massachusetts, USA
Anti-HSF1 (phospho Ser326) (ab115702)	1:4,000	Rabbit	Abcam, Cambridge, MA USA
Beta Actin	1:5,000	Mouse	Cell Signalling, Massachusetts, USA
Goat Anti-Mouse IgG+IgM, (H+L), Peroxidase conjugated	1:10,000	Goat	Pierce Biotechnology, Illinois, USA
Goat Anti-Rabbit IgG, (H+L), Peroxidase conjugated	1:10,000	Goat	Pierce Biotechnology, Illinois, USA
GSK-3β (D5C5Z)	1:1,000	Rabbit	Cell Signalling, Massachusetts, USA
HSP105	1:5,000	Mouse	Abcam, Cambridge, MA USA
HSP70	1:2,000	Rabbit	Abcam, Cambridge, MA USA
HSP90 α	1:10,000	Mouse	Santa Cruz Biotechnology, Dallas, Texas, USA
HSP90β	1:5,000	Rabbit	Abcam, Cambridge, MA USA
p-PDK1	1:1,000	Rabbit	Cell Signalling, Massachusetts, USA
P70s6 kinase	1:1,000	Rabbit	Cell Signalling, Massachusetts, USA
PDK1	1:1,000	Rabbit	Cell Signalling, Massachusetts, USA
Phospho-AKT (s473)	1:3,000	Rabbit	Cell Signalling, Massachusetts, USA
Phospho-AKT (t308)	1:2,000	Rabbit	Cell Signalling, Massachusetts, USA
Phospho-GSK-3β (ser9) (D85E12)	1:1,000	Rabbit	Cell Signalling, Massachusetts, USA
Phospho-p70s6 kinase T389)	1:1,000	Rabbit	Cell Signalling, Massachusetts, USA
Recombinant Anti-HSF1 antibody (ab52757)	1:4,000	Rabbit	Abcam, Cambridge, MA USA
Recombinant Anti-renilla Luciferase antibody [EPR17791] (ab185925)	1:1,000	Rabbit	Abcam, Cambridge, MA USA

CHAPTER 3: THE ROLE OF HSF1 IN CANCER CELL SENSITIVITY TO ANTICANCER DRUGS

3.1. Introduction

HSF1 regulates the HSR and several other important biological processes including tumour development, cancer progression and potentially drug resistance (Santagata et al., 2011b). Despite its essential role in normal cells, accumulating evidence has revealed its role in advanced cancers supporting the view that HSF1 constitutes an anticancer therapeutic target and by inhibiting this transcription factor this may provide an effective treatment strategy for advanced cancers in the future (Mendillo et al., 2012). Furthermore, HSF1 may also have defined roles in mediating drug resistance and inhibition of HSF1 may act to sensitise cancers to anticancer drugs (Chen et al., 2013, Carpenter et al., 2017, Cigliano et al., 2017, Desai et al., 2013). Previously in the Price laboratory, Oncomine™ analysis of gene expression alterations when HSF1 was overexpressed in Ras^{v12} Transformed MCF10A cells identified a list of anticancer drugs that may have altered sensitivity in advanced cancer cells with HSF1 loss. The primary anticancer drugs that were identified through this bioinformatic approach targeted EGFR, HER2, mTOR, AKT, PI3Kinase and HSP90 and included Gefitinib, Lapatinib, Pictilisib, Idelalisib, Crizotinib, AZD8055, MK-2206, 17-AAG, and AUY922. For a full list of these anticancer drugs and their targets refer to section 2.6.6 Table 10. This list of anticancer drugs was used to determine whether cancer cells with HSF1 knockdown would have an altered sensitivity to any of these agents. However, some of the results are not presented in the main body of the thesis but are relocated to Appendix 1 as a

result of intentional premature termination of the investigation, reasons are discussed later in the chapter.

To investigate HSF1's contribution to cancer sensitivity to anticancer drugs, an inducible model of HSF1 knockdown was generated. A stable inducible HSF1 knockdown model was done in two cell lines, the T47D and the MDA-MB-231, this was to examine any variations between cancer cells with low- and high- metastatic cell biology, respectively (Figure 4).

The TRIPZ inducible lentiviral shRNA system was used which combines the advantages of microRNA lentiviral vector design with Tet-inducibility to produce reversible, controlled gene silencing. As seen in Figure 3, there are five main components to this vector. The UBC is the constitutive promoter for the expression of rtTA3 which, when doxycycline is added to the cell cultures, enables it to bind to the TRE (tetracycline-inducible) promoter. Upon activation of the TRE, turbo-RFP (tRFP) is expressed to identify cells that are actively expressing the shRNA which lies downstream and is a surrogate marker for HSF1 knockdown (Figure 3). Such an inducible model of knockdown has previously been shown in the Price lab to have differences to that of a constitutively expressed shRNA in cancer cells and more comparable to the acute inhibition of therapeutic targets by anticancer drugs (refer to Figure 5-8).
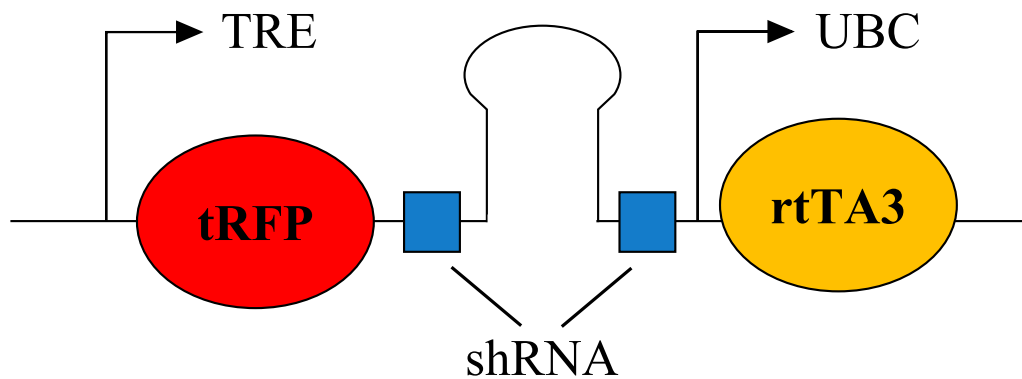
Figure 3 Functional segment of the TRIPZ inducible lentivirus shRNA system

There are five main components of the TRIPZ inducible lentivirus shRNA system. TRE is the tetracycline-inducible promoter. The turbo-RFP (tRFP) is for visual tracking of shRNA. The shRNA is the microRNA coding the HSF1 gene enabling knockdown when transcription is activated. The UBC is the constitutive promoter for expression of rtTA3, the tetracycline-transactivator 3.

Overall, the aims of this chapter are:

1. To successfully generate stable models of inducible HSF1 knockdown in two BrCa cell lines with differing metastatic phenotypes.

2. To test how HSF1 knockdown impacts cancer cell sensitivity towards a series of anticancer drugs.

It is hypothesised that knockdown of HSF1 in cancer cells will increase the cells sensitivity to anticancer drugs as this important regulator of cancer cell survival is removed.

3.2. Results:

3.2.1. Generation of stable inducible HSF1 knockdown BrCa cell lines

T47D and MDA-MB-231 were chosen due to their differing metastatic phenotypes (Figure 4). The T47D cell line was selected for its low metastatic potential, and less aggressive phenotype, while MDA-MB-231 was selected for its high metastatic potential and more aggressive phenotype (refer to Table 12). Additionally, while levels of HSF1 are elevated in cancers, more aggressive BrCa cells have been reported to express even higher levels (Powell et al., 2016, Santagata et al., 2011b, Prince et al., 2020). This is consistent with previous studies done in our lab examining levels and activation status of HSF1 in a panel of BrCa cell lines which showed BrCa cells with increased aggressiveness, such as the MDA-MB-231 cells, correlated with higher and more active levels of HSF1.

Table 12 Breast Cancer Sub-types & Cancer Progression Specific to T47D and MDA-MB-231

Cell Line	Gene Expression Profile				Sub-type	Patient Prognosis	Cancer Aggressiveness
	ER	PR	HER2	EGFR			
T47D	+	+	–	–	Luminal A	High	Low
MDA-MB-231	–	–	–	+	Triple Negative	Low	High

ER: Oestrogen Receptor, PR: Progesterone Receptor, HER2: Human Epithelial Growth Factor 2, EGFR: Epidermal Growth Factor Receptor (Kumaraswamy et al., 2015)

+ Expressing
– Not expressing

To knockdown HSF1, two HSF1 shRNAmir TRIPZ inducible lentivirus constructs, shRNAmir1 and shRNAmir4, were selected from previously designed and established constructs by our lab (refer to Table 4). Cells were transduced with either the HSF1 shRNAmir constructs or a non-silencing control (renilla). The non-silencing shRNAmir sequence that was used as a negative control targeted renilla and could not bind any known vertebrate genes. These constructs were designed with resistance genes for selection by antibiotics.
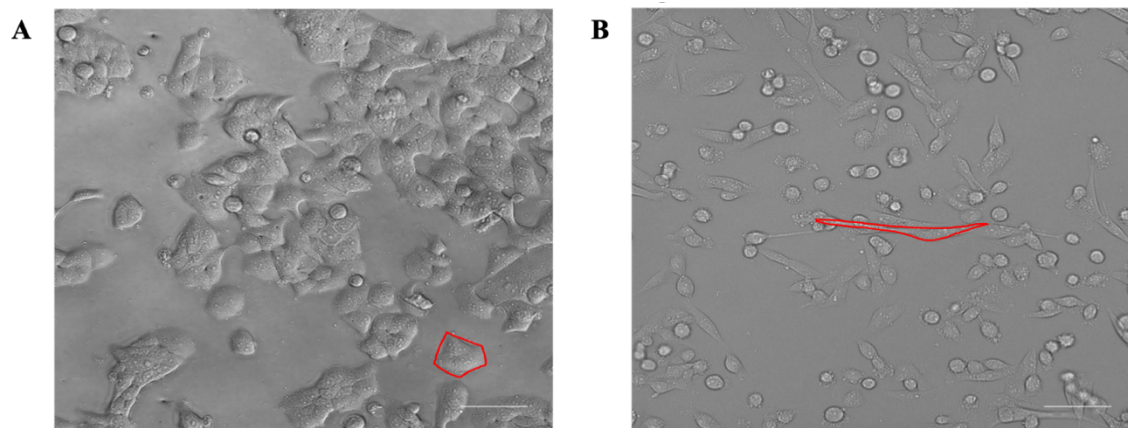
Figure 4 Morphology of low/ high-metastatic potential breast cancer cell lines

Micrograph of cells highlighting morphological differences (outlined in red) between metastatic potentials. Low metastatic potential cancer cells have shapes that are more cuboidal like seen here of the T47D **(A)**. While cancer cells with higher metastatic potential like the MDA-MB-231, seen here, are more mesenchymal, is a phenotype favouring migration and are generally more aggressive **(B)** (refer to Table 12). Scale bar = 50μm

A

| | Non-silencing (Renilla) | | shRNA HSF1 (Mir1) | | shRNA HSF1 (Mir4) | |
| | BF | TRITC | BF | TRITC | BF | TRITC |

Doxycycline: 0 µg/mL, 0.5 µg/mL, 2 µg/mL

B

Doxycycline: 0 µg/mL, 0.25 µg/mL, 0.5 µg/mL, 1 µg/mL, 1.5 µg/mL, 2 µg/mL

HSF1

Beta actin
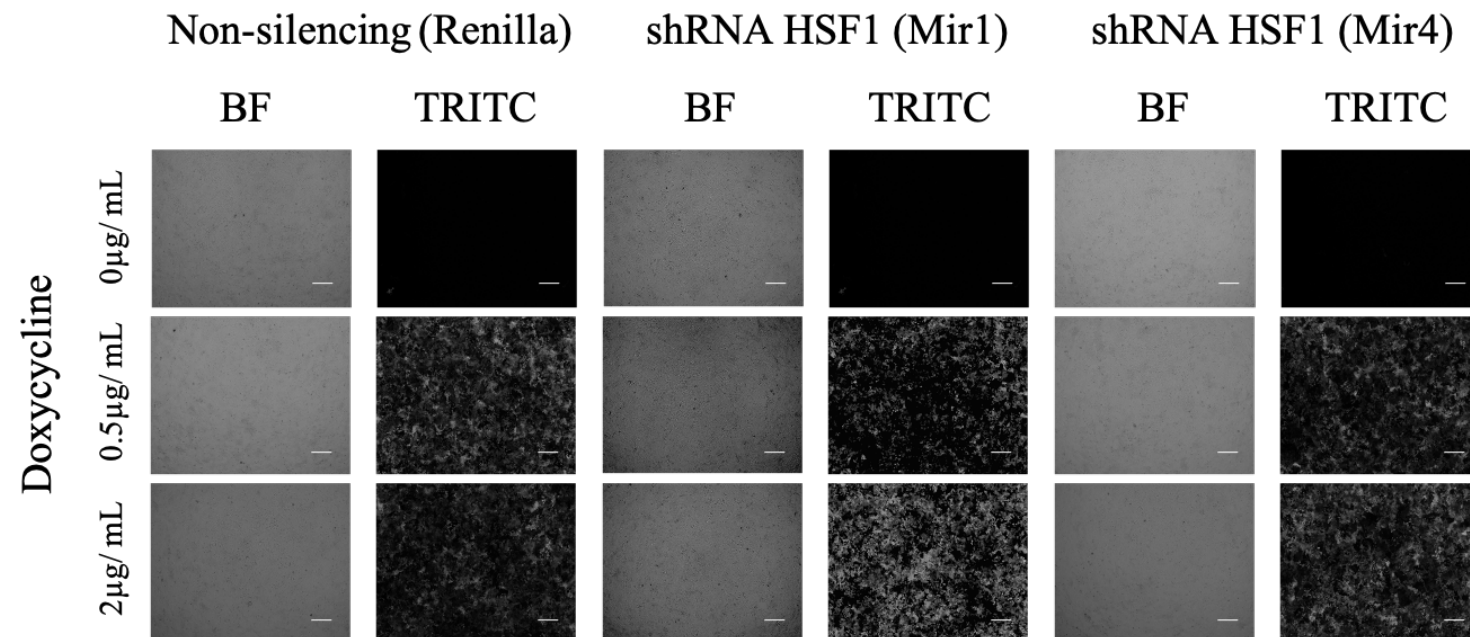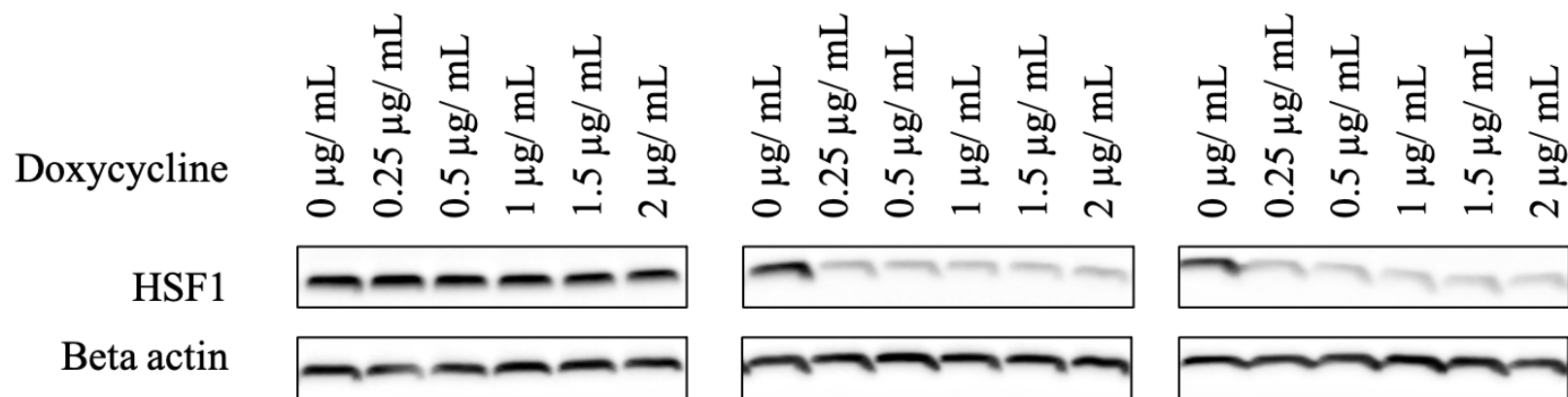
Figure 5 Induced HSF1 knockdown in T47D using different concentrations of Doxycycline

Doxycycline was titrated for concentrations 0, 0.25, 0.5, 1.0, 1.5 and 2.0μg/ ml. Addition of doxycycline to transduced T47D cells shows that when the tetracycline induced pathway is activated, tRFP is expressed and cells fluoresce under a TRITC filter **(A)**. Western blots analysis for cells with the knockdown construct, shRNA HSF1 Mir1 and Mir4, identified that levels of HSF1 were consistently reduced with the addition of all concentrations of doxycycline compared to the 0μg/ ml and non-silencing controls, where HSF1 levels did not decrease **(B)**. Scale bar = 200μm
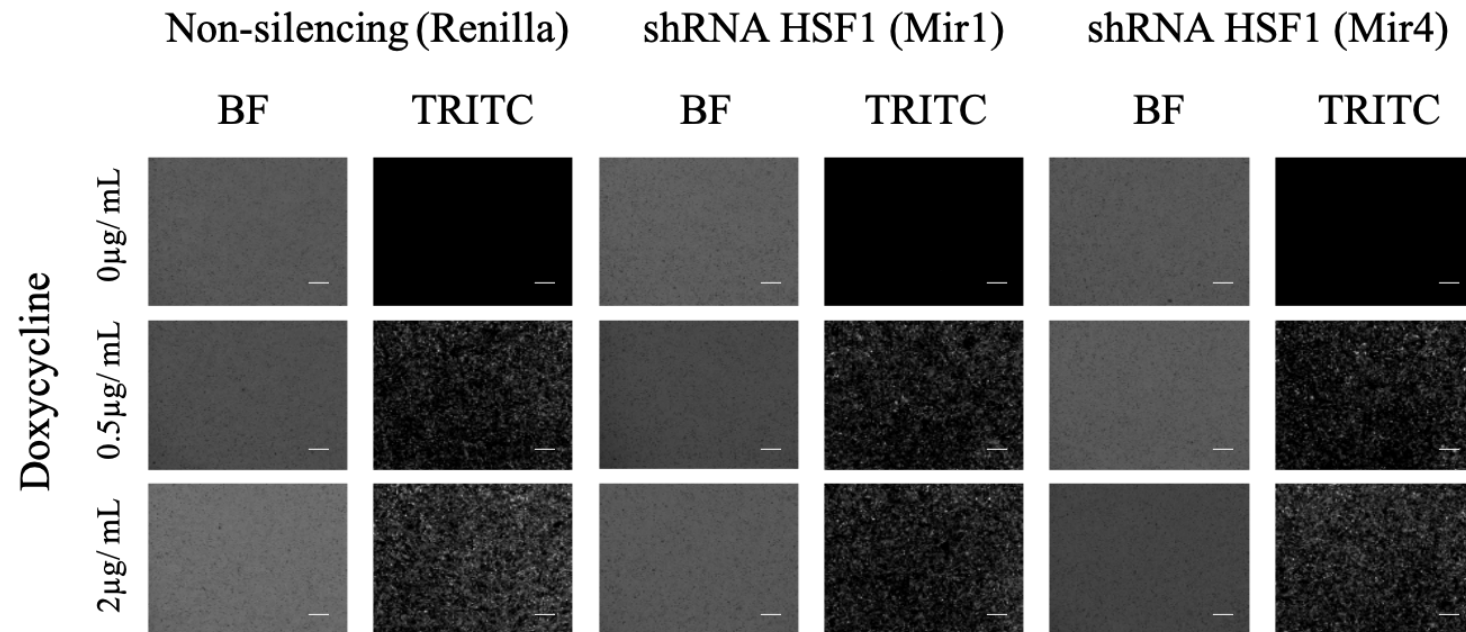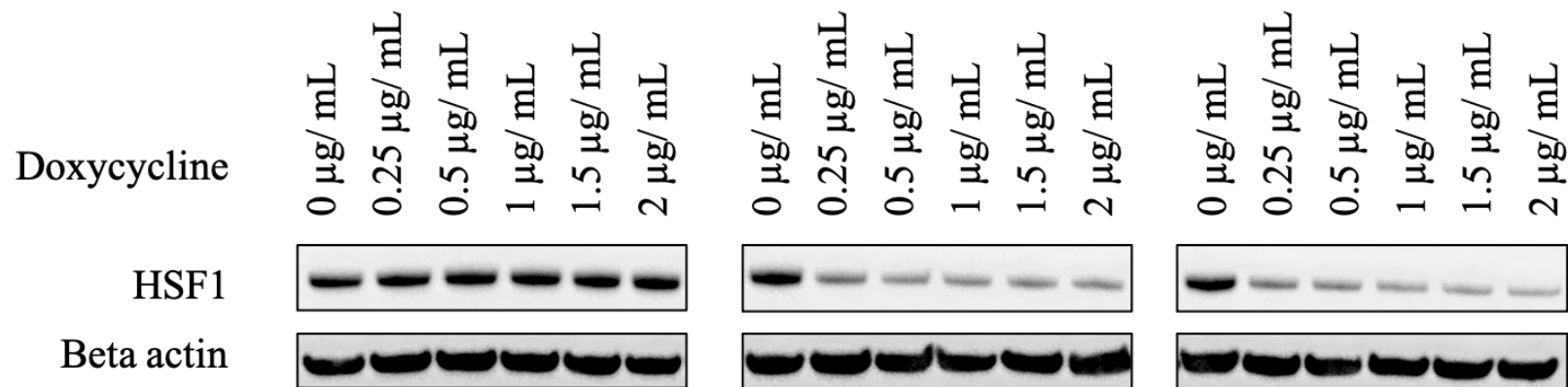
Figure 6 Induced HSF1 knockdown in MDA-MB-231 using different concentrations of Doxycycline

Doxycycline was titrated for concentrations 0, 0.25, 0.5, 1.0, 1.5 and 2.0µg/ ml. Addition of doxycycline to transduced MDA-MB-231 cells shows that when the tetracycline induced pathway is activated, tRFP is expressed and cells fluoresce under a TRITC filter **(A)**. Western blots analysis for cells with the knockdown construct, shRNA HSF1 Mir1 and Mir4, identified that levels of HSF1 were consistently reduced with the addition of all concentrations of doxycycline compared to the 0µg/ ml and non-silencing controls, where HSF1 levels did not decrease **(B)**. Scale bar = 200µm

A

		Bright Field	TRITC
Non-silencing (Renilla)	−		
	+		
shRNA HSF1 Mir1	−		
	+		
shRNA HSF1 Mir4	−		
	+		

B

Confirmation of HSF1 Knockdown in T47D

** P=0.0020

HSF1 (/Beta actin)

Non-silencing (Renilla)   shRNA HSF1 Mir 1   shRNA HSF1 Mir 4

− Control

+ 0.5µg/mL Doxycycline

HSF1

Beta actin
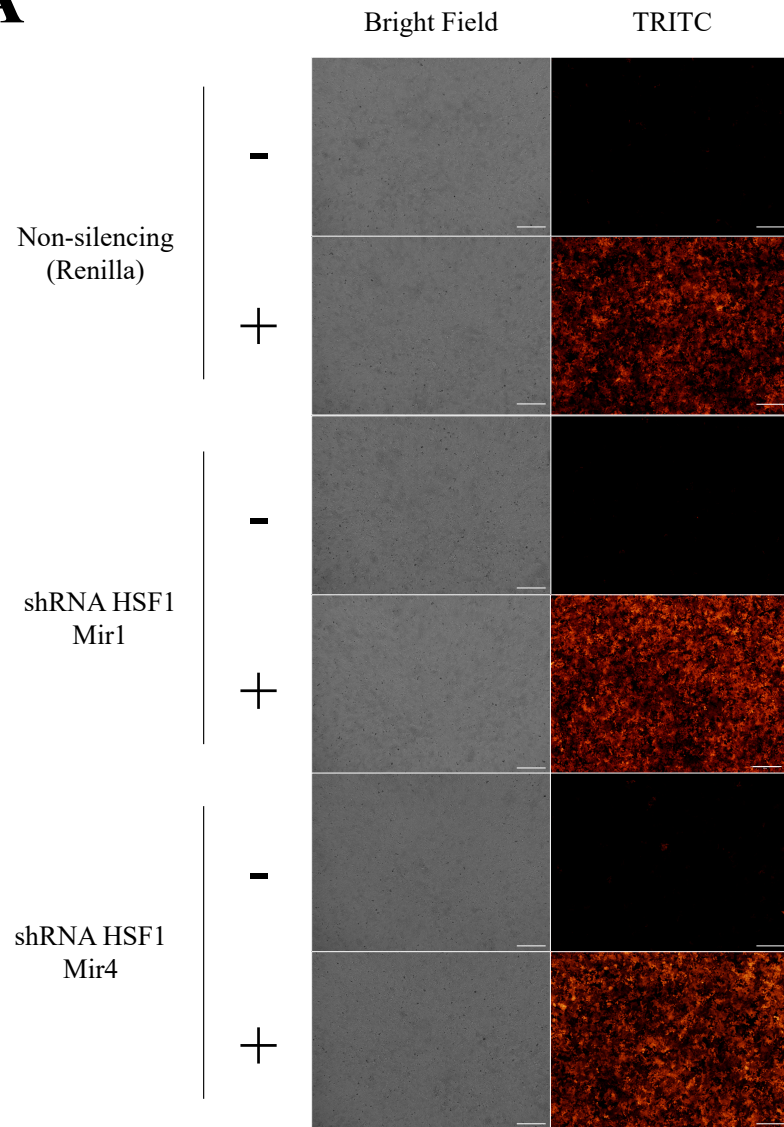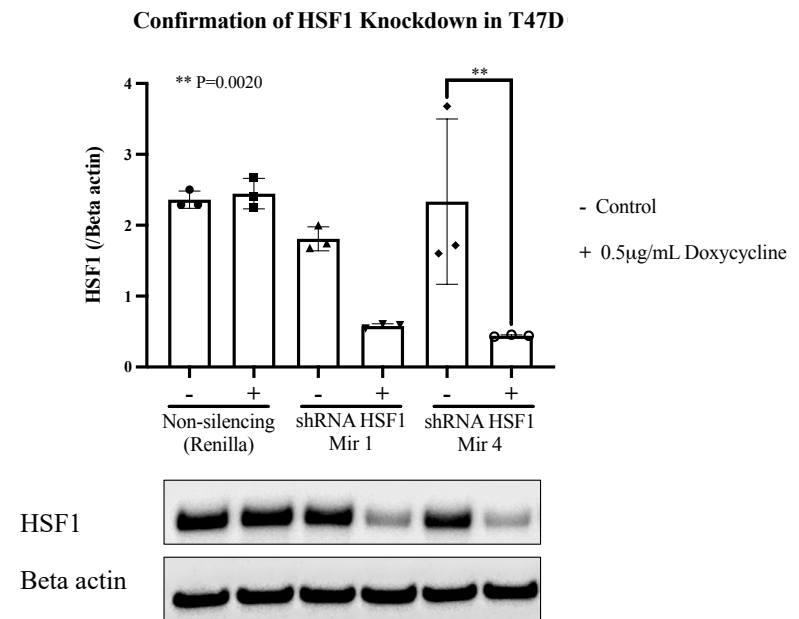
Figure 7 Confirmation of HSF1 knockdown in T47D BrCa Cells

Bright field and TRITC microscope images of T47D inducible HSF1 knockdown cells at 72 hours. x40 magnification **(A)**. Western blot analysis and respective quantitative graphs confirming HSF1 knockdown in inducible cells treated with 0.5μg/ ml doxycycline **(B)**. Results are expressed as mean ± SD, n=3. P-value are represented as ns (0.1234), * (0.0332), ** (0.0020), *** (0.0002) and **** (<0.0001). Scale bar = 200μm

A

		Bright Field	TRITC
Non-silencing (Renilla)	−		
	+		
shRNA HSF1 Mir1	−		
	+		
shRNA HSF1 Mir4	−		
	+		

B

Confirmation of HSF1 Knockdown in MDA-MB-231

** P=0.0020

HSF1 (/Beta actin)

- Control
+ 0.5µg/mL Doxycycline
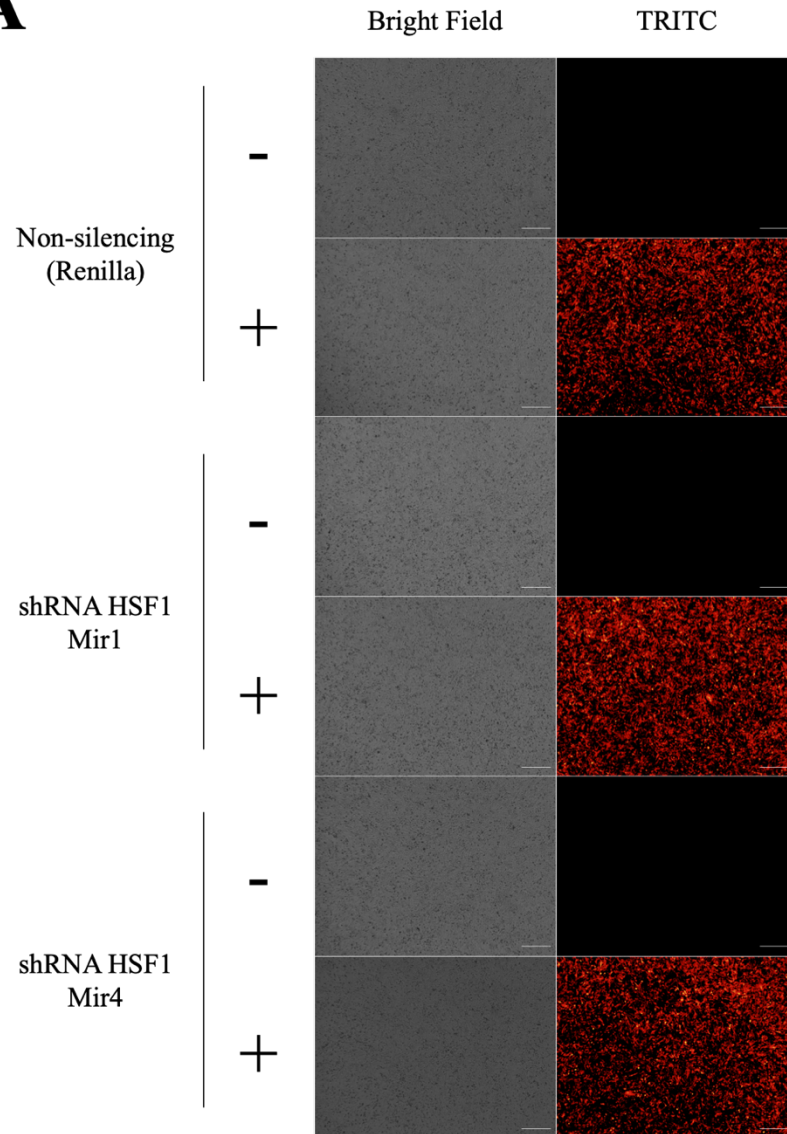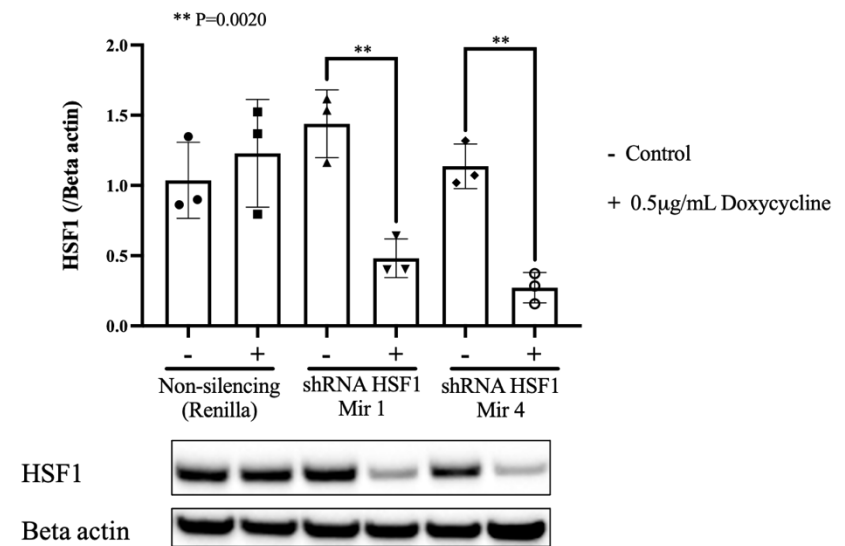
HSF1
Beta actin

Figure 8 Confirmation of HSF1 knockdown in MDA-MB-231 BrCa Cells

Bright field and TRITC microscope images of MDA-MB-231 HSF1 inducible knockdown cells at 72 hours. x40 magnification **(A)**. Western blots and respective graph confirming HSF1 knockdown in inducible cells with the addition of 0.5μg/ ml doxycycline **(B)**. Results are expressed as mean ± SD, n=3. P-values were represented as ns (0.1234), * (0.0332), ** (0.0020), *** (0.0002) and **** (<0.0001). Scale bar = 200μm

3.2.2. Impact of HSF1 knockdown upon BrCa cell sensitivity to different categories of anticancer drugs

High expression of HSF1 is significantly correlated with cancer aggressiveness (Santagata et al., 2011b). Previous studies have shown that decreased HSF1 expression can decrease cancers' metastatic potential by influencing biological processes such as cell proliferation, migration and invasion, hallmarks of cancer progression. Some work has been done in liver cancer to compare the differences between cell viability and death when HSF1 is overexpressed and knocked down (Zhang et al., 2017). However, little work has been done to look at this in relation to HSF1's effect on breast cancer cells in response to anticancer drugs. Chapter 3 examines the IC50 of two different BrCa cell lines with different metastatic potential in response to ten anticancer drugs with knockdown of HSF1. Cells were seeded at ten-thousand cells per well in 96-well plates and left to adhere overnight before respective drugs were added. For more information about other time points recorded, no treatment controls and statistical analysis, refer to Appendix 1 and 2.

3.2.2.1. Impact of HSF1 knockdown upon BrCa cell sensitivity to Tyrosine Kinase Inhibitors

Lapatinib is a potent dual inhibitor of epidermal growth factor receptor (EGFR) and human epidermal growth factor 2 (HER2) (also called, ErbB-2, a transmembrane receptor tyrosine kinase) activity (Liu et al., 2011b). Inhibiting EGFR has been shown to cause a reversible growth arrest and apoptosis (Moyer et al., 1997, Modjtahedi et al., 1998, Busse et al., 2000, Fan and Mendelsohn, 1998). Activation of EGFR and ErbB-2 are associated with the PI3K/AKT cell survival pathway (Rusnak et al., 2001), and thus

inhibition of EGFR or ErbB-2 catalytic activity should induce cell death in cancer cells. Further, *Yallowitz et al. (2018)* reported that pharmacological inhibition of HSF1 using KRIBB11 (385570, Calbiochem, Billerica, MA, USA) downregulated ErbB-2, mutant TP53 and its combination with lapatinib avoided development of lapatinib resistance *in-vitro* (Yallowitz et al., 2018).

Interestingly, in this study, Lapatinib treatment coupled with HSF1 knockdown in T47D cells had no significant impact on the cells' sensitivity to Lapatinib (Figure 9), yet HSF1 knockdown in the MDA-MB-231 cells significantly increased cell resistance to Lapatinib (Figure 10). The IC50 for MDA-MB-231 for both the shRNA- Mir1 and Mir4 cells plus doxycycline cells were significantly increased when compared to their non-induced controls (Figure 10C). Thus, MDA-MB-231 cells with HSF1 knockdown have a decreased sensitivity to Lapatinib.

A
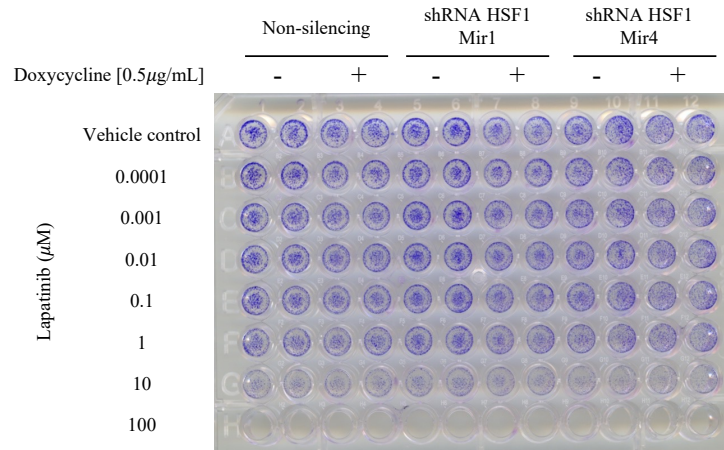
B

C
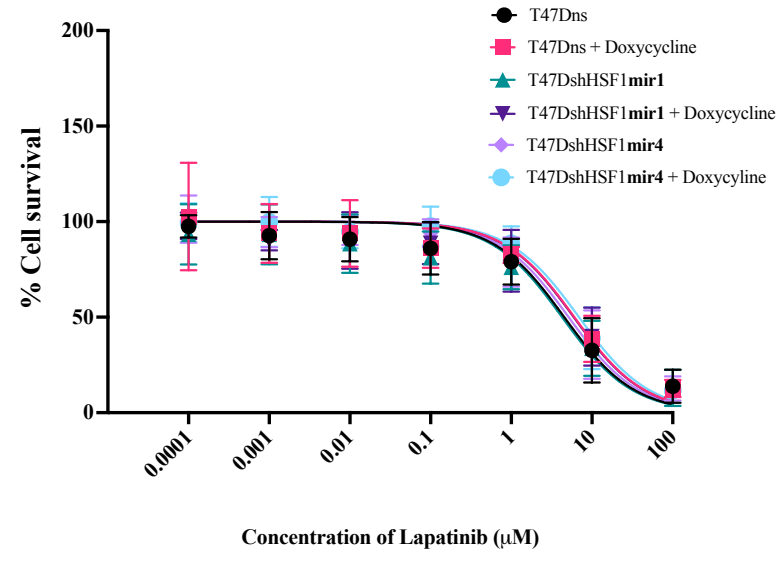
IC$_{50}$ Cell Survival (μM)	
	T47D
Cell Line	
Time (Hours)	**72**
Non-silencing	5
Non-silencing + Doxycycline	6
shRNA HSF1 Mir1	4
shRNA HSF1 Mir1 + Doxycycline	6
shRNA HSF1 Mir4	5
shRNA HSF1 Mir4 + Doxycycline	7

Figure 9 T47D cells with HSF1 knockdown tested for sensitivity to Lapatinib

T47D BrCa cells with HSF1 inducible knockdown treated with Lapatinib over 72 hours. Photograph of 96-well plate stained with Diff-Quik after Alamar Blue assay **(A)**. Vehicle control is 0.2% v/v DMSO. Cell survival graphed as log10 drug concentration from Alamar Blue assay **(B)**. IC50 values are represented in table according to cell conditions: non-silencing (ns), ns + Doxycycline [0.5μg/ ml], shRNA HSF1 Mir1, shRNA HSF1 Mir1 + Doxycycline [0.5μg/ ml], shRNA HSF1 Mir4 and shRNA HSF1 Mir4 + Doxycycline [0.5μg/ ml] **(C)**. Expressed as mean ± SD. n=6

A

	Non-silencing	shRNA HSF1 Mir1	shRNA HSF1 Mir4
Doxycycline [0.5μg/mL]	− +	− +	− +

Lapatinib (μM)

Vehicle control
0.0001
0.001
0.01
0.1
1
10
100

B

- MDA-MB-231ns
- MDA-MB-231ns + Doxycycline
- MDA-MB-231shHSF1**mir1**
- MDA-MB-231shHSF1**mir1** + Doxycycline
- MDA-MB-231shHSF1**mir4**
- MDA-MB-231shHSF1**mir4** + Doxycycline

% Cell survival

Concentration of Lapatinib (μM)

C
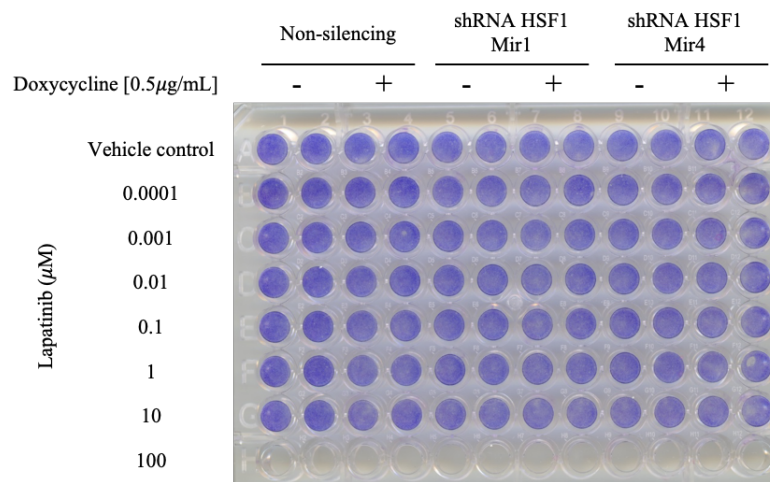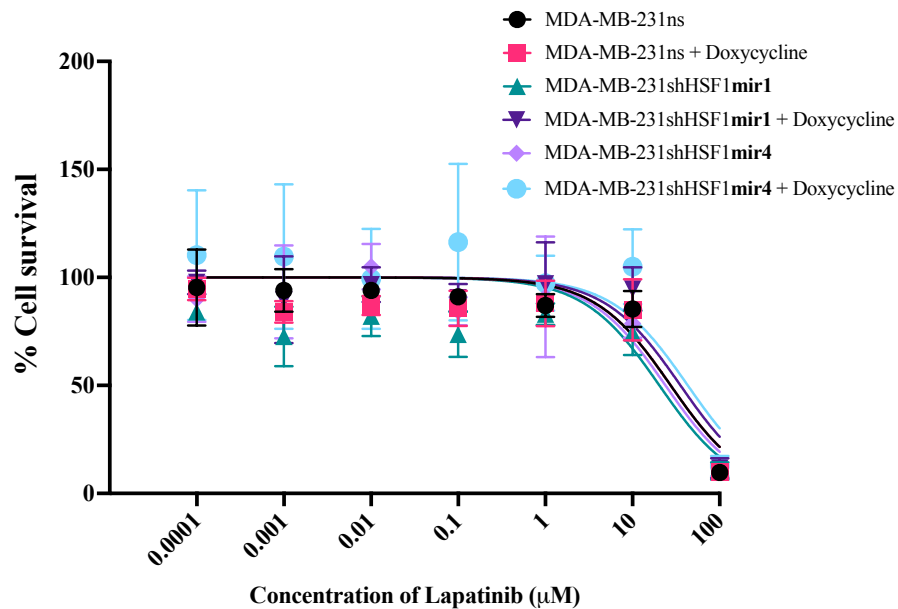
IC_{50} Cell Survival (μM)	
Cell Line	**MDA-MB-231**
Time (Hours)	**72**
Non-silencing	27
Non-silencing + Doxycycline	27
shRNA HSF1 Mir1	20
shRNA HSF1 Mir1 + Doxycycline	36
shRNA HSF1 Mir4	24
shRNA HSF1 Mir4 + Doxycycline	43

shRNA HSF1 Mir1 / shRNA HSF1 Mir1 + Doxycycline: *

shRNA HSF1 Mir4 / shRNA HSF1 Mir4 + Doxycycline: *

Figure 10 MDA-MB-231 cells with HSF1 knockdown tested for sensitivity to Lapatinib

MDA-MB-231 BrCa cells with HSF1 inducible knockdown treated with Lapatinib over 72 hours. Photograph of 96-well plate stained with Diff-Quik after Alamar Blue assay **(A)**. Vehicle control is 0.2% DMSO. Cell survival graphed as log10 drug concentration from Alamar Blue assay **(B)**. IC50 values are represented in table according to cell conditions: non-silencing (ns), ns + Doxycycline [$0.5\mu g/$ ml], shRNA HSF1 Mir1, shRNA HSF1 Mir1 + Doxycycline [$0.5\mu g/$ ml], shRNA HSF1 Mir4 and shRNA HSF1 Mir4 + Doxycycline [$0.5\mu g/$ ml] **(C)**. Expressed as mean ± SD. n=3

Gefitinib is a specific and sensitive inhibitor of only the EGFR tyrosine kinase (Tyr1068 and Tyr1086) and has been shown to prevent the growth, proliferation, survival and invasion of tumour cells overexpressing EGFR (Pedersen et al., 2005, Arteaga and Johnson, 2001). However, clinical response to Gefitinib in relation to EGFR levels and activity has failed suggesting that other molecular mechanisms such as downstream signalling and mutations could significantly effect clinical response (Pedersen et al., 2005).

The type III EGFR mutation is the most common mutation in the EGFR gene in cancer that causes deletion of exons 2-7 and impairs the mutant receptor from binding to any known ligands (Pedersen et al., 2001, Gan et al., 2013). This mutated form has a constitutively active receptor tyrosine kinase responsible for transformed fibroblasts and influences tumorigenicity (Huang et al., 1997, Pedersen et al., 2004). Interestingly *Learn et al. (2004)*, found that cells expressing the type III EGFR mutation were more resistant to treatment with Gefitinib as a result of a deficiency in receptor dephosphorylation and constitutive AKT activity (Learn et al., 2004). The levels of Gefitinib sufficient to suppress wild-type EGFR phosphorylation were not enough to target the type III EGFR phosphorylation, with Tyr1148 and Tyr1173 being the more resistant sites (Pedersen et al., 2005). In fact, Tyr1173 have been shown to play an important role in the activation of MAPK possibly for pro-proliferative and anti-apoptotic affect (Sturla et al., 2005, Yue and López, 2020). Thus, the ability via HSF1 knockdown to sensitise cancer cells to drugs and induce efficacy on type III EGFR could assist in more specific treatments as overwhelming evidence has indicated type III EGFR is a tumour-specific receptor and many published studies showing that normal tissues are without it (Jungbluth et al., 2003, Wikstrand et al., 1995, Humphrey et al., 1988, Lu et al., 2009, Ge et al., 2002,

Aldape et al., 2004, Saikali et al., 2007, Feldkamp et al., 1999, Arjona et al., 2005, Biernat et al., 2004, Ekstrand et al., 1992, Gupta et al., 2010, Heimberger et al., 2005, Moscatello et al., 1995, Olapade-Olaopa et al., 2000, Shinojima et al., 2003, Sugawa et al., 1990, Wong et al., 1992, Yamazaki et al., 1988, Sonnweber et al., 2006, Viana-Pereira et al., 2008, Gan et al., 2013). Additionally, in a study by *Tang et al. (2015)* revealed that the RAS/ MAPK signalling pathway also regulates HSF1 activation (Ser326) (Tang et al., 2015). Therefore, together it is hypothesised that maybe through the activation of HSF1 via resistant type III EGFR, clinical response is decreased with Gefitinib treatment and HSF1 knockdown may mitigate this limitation.

In this study, the sensitising effect to Gefitinib expected from HSF1 knockdown was not observed in either the T47D or the MDA-MB-231 BrCa cells lines (Figure 11, 12).

A

B

	IC$_{50}$ Cell Survival (μM)
	T47D
Cell Line	
Time (Hours)	**72**
Non-silencing	33
Non-silencing + Doxycycline	64
shRNA HSF1 Mir1	48
shRNA HSF1 Mir1 + Doxycycline	67
shRNA HSF1 Mir4	23
shRNA HSF1 Mir4 + Doxycycline	39
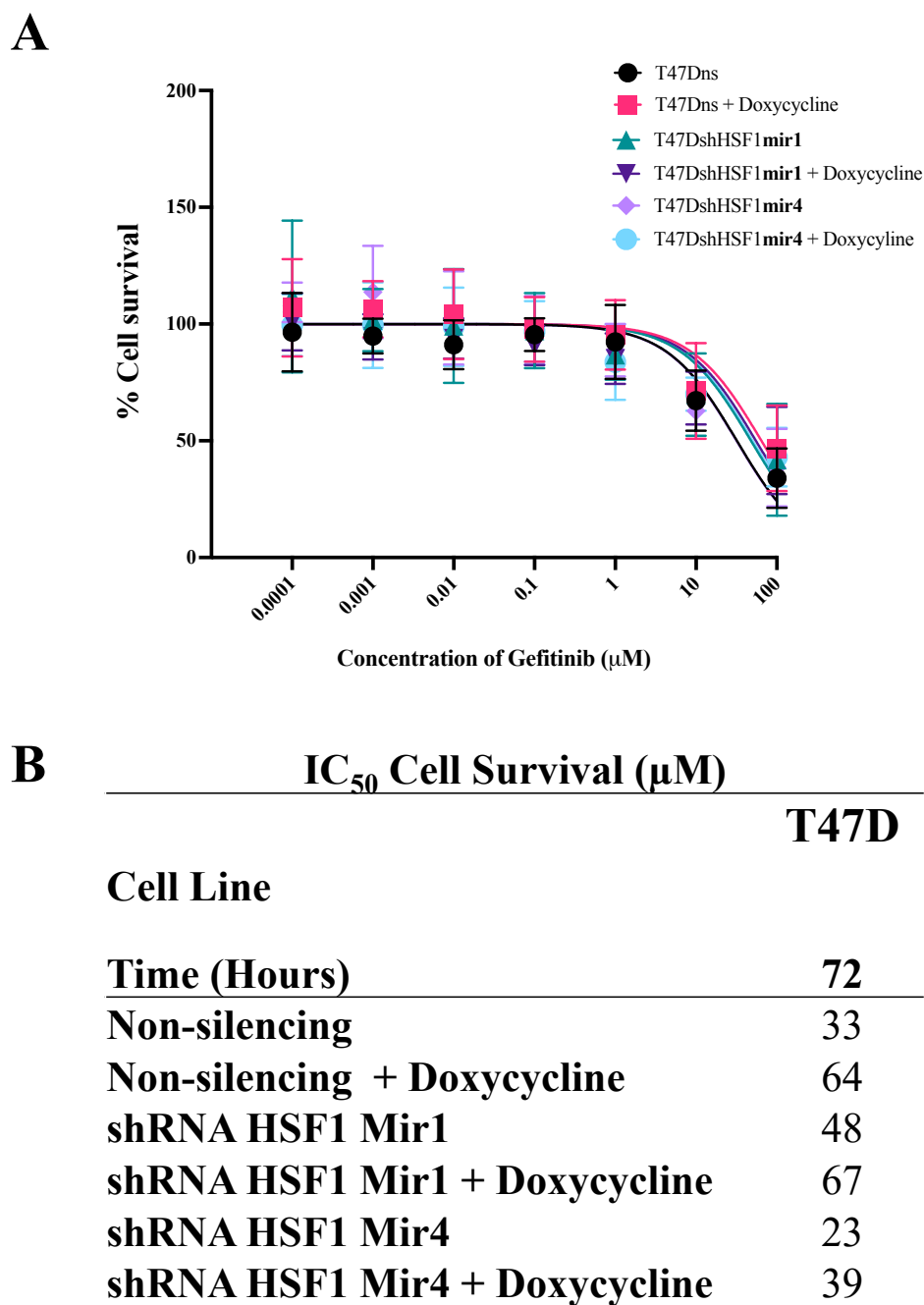
Figure 11 T47D cells with HSF1 knockdown tested for sensitivity to Gefitinib

T47D BrCa cells with HSF1 inducible knockdown treated with Gefitinib over 72 hours. Cell survivability graphed as log10 drug concentration from Alamar Blue assay **(A)**. IC50 values are represented in table according to cell conditions: non-silencing (ns), ns + Doxycycline [0.5μg/ ml], shRNA HSF1 Mir1, shRNA HSF1 Mir1 + Doxycycline [0.5μg/ ml], shRNA HSF1 Mir4 and shRNA HSF1 Mir4 + Doxycycline [0.5μg/ ml] **(B)**. Expressed as mean ± SD. n=6

A

B
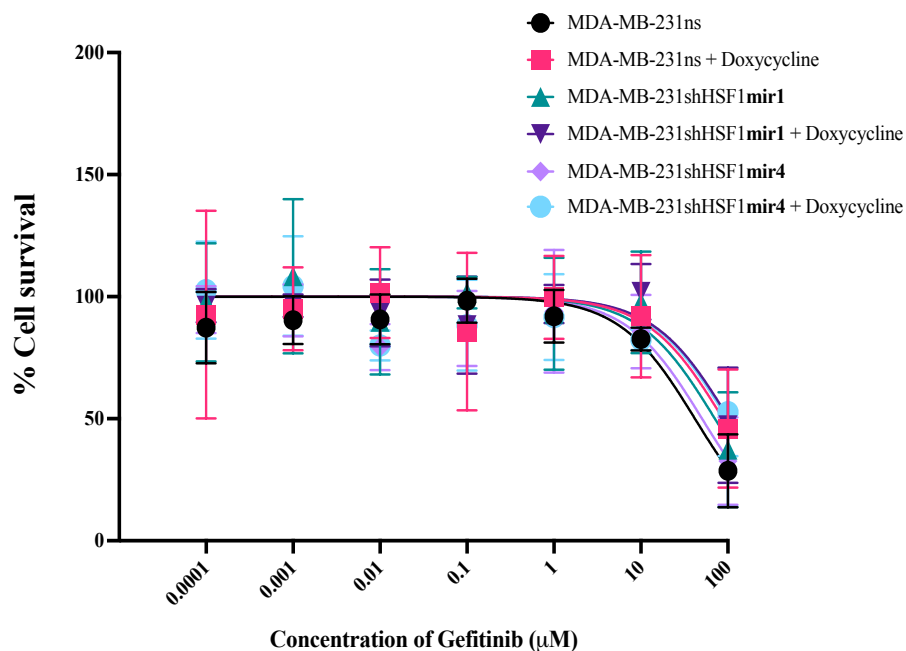
IC$_{50}$ Cell Survival (μM)	
Cell Line	**MDA-MB-231**
Time (Hours)	**72**
Non-silencing	42
Non-silencing + Doxycycline	88
shRNA HSF1 Mir1	71
shRNA HSF1 Mir1 + Doxycycline	103
shRNA HSF1 Mir4	50
shRNA HSF1 Mir4 + Doxycycline	98

Figure 12 MDA-MB-231 cells with HSF1 knockdown tested for sensitivity to Gefitinib

MDA-MB-231 BrCa cells with HSF1 inducible knockdown treated with Gefitinib over 72 hours. Cell survivability graphed as log10 drug concentration from Alamar Blue assay **(A)**. IC50 values are represented in table according to cell conditions: non-silencing (ns), ns + Doxycycline [0.5μg/ ml], shRNA HSF1 Mir1, shRNA HSF1 Mir1 + Doxycycline [0.5μg/ ml], shRNA HSF1 Mir4 and shRNA HSF1 Mir4 + Doxycycline [0.5μg/ ml] **(B)**. Expressed as mean ± SD. n=3

Crizotinib is a tyrosine kinase inhibitor targeting the MET/ALK/ROS1 with clinical evidence suggesting developed resistance in patients can be acquired via secondary point mutations in the ROS1 kinase (Zou et al., 2015). Long-term exposure to MET targeting TKI *in-vitro* also leads to acquired resistance and addiction to MET inhibitors (Funakoshi et al., 2013, Qi et al., 2011). Interestingly, HSP90 inhibition can partially restore Crizotinib sensitivity to two TKI-resistant MET mutants (Miyajima et al., 2013). HSP90 inhibition suppresses EGFR activity and suppresses ALK activity and signalling via MET sensitivity to TKI in cells expressing Crizotinib-resistant (Zou et al., 2015). Thus, dual targeting with HSP90 inhibitor and Crizotinib severely inhibited MET signalling, colony growth, cell invasion, and xenograft growth *in-vivo* (Katayama et al., 2011). The synergistic effect of this combination also highlights the complex influence of HSP90 activity on kinase conformation.

Naturally, HSP90 acts as a molecular chaperone important in the maintenance of functional conformation and stability of cellular proteins, including oncoproteins (Dai et al., 2012a). Some particularly reliant client proteins and mutant driver oncoproteins of HSP90 include ErbB-2, c-MET, AKT and mutant TP53 (Dai et al., 2012a, Workman and van Montfort, 2014). HSF1 regulates a number of HSP90 isoforms and depletion of HSF1 diminishes oncoproteins in cancer cells, including EGFR, mutant TP53, and AKT (Vihervaara and Sistonen, 2014, Dai et al., 2012b, Li et al., 2014, Fujimoto et al., 2012). Therefore, HSF1 facilitates oncogenesis not only through enhancement of general protein synthesis but possibly through stabilization of targets like MET via regulation of HSP90 (Dai and Sampson, 2016, Katayama et al., 2011). Thus, HSF1 knockdown in BrCa cell lines may sensitise cells to Crizotinib.

Again, in this study, contrary to our hypothesis, knockdown of HSF1, a regulator of HSP90, in the T47D and the MDA-MB-231 HSF1 knockdown BrCa cells did not sensitise them to Crizotinib (Figure 13, 14).

A

B
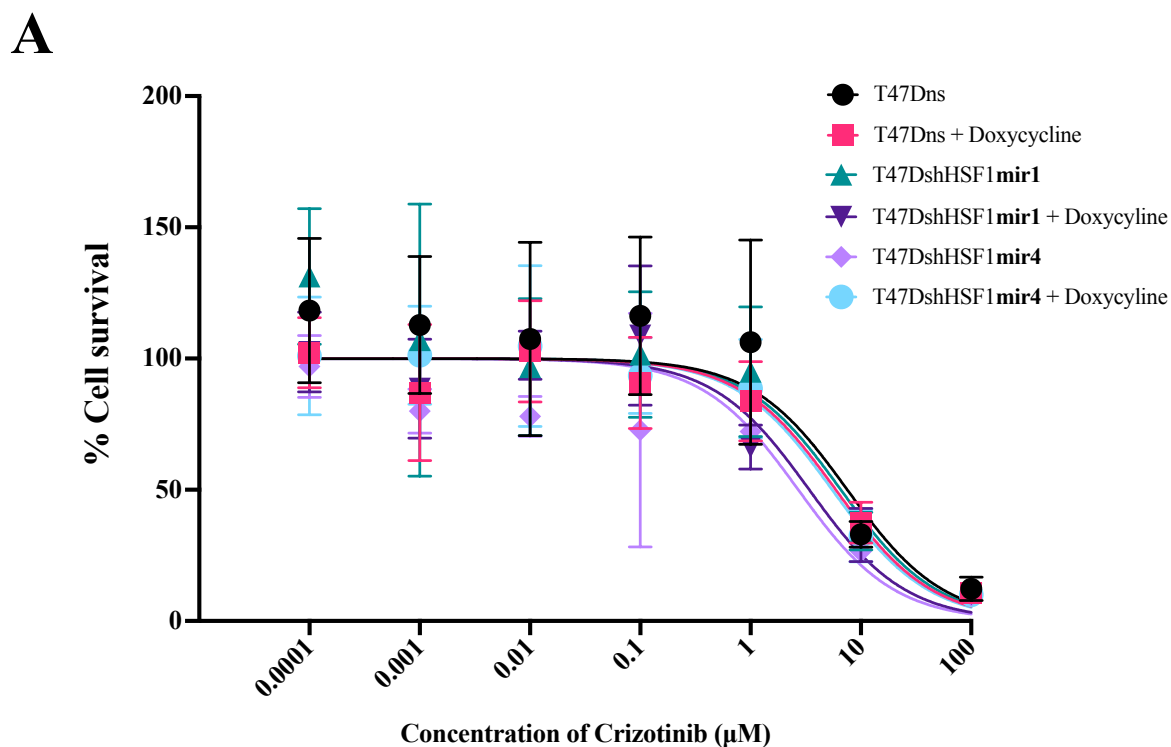
IC$_{50}$ Cell Survival (μM)	
Cell Line	**T47D**
Time (Hours)	**72**
Non-silencing	8
Non-silencing + Doxycycline	6
shRNA HSF1 Mir1	7
shRNA HSF1 Mir1 + Doxycycline	3
shRNA HSF1 Mir4	3
shRNA HSF1 Mir4 + Doxycycline	5

Figure 13 T47D cells with HSF1 knockdown tested for sensitivity to Crizotinib

T47D BrCa cells with HSF1 inducible knockdown treated with Crizotinib over 72 hours. Cell survival graphed as log10 drug concentration from Alamar Blue assay **(A)**. IC50 values are represented in table according to cell conditions: non-silencing (ns), ns + Doxycycline [0.5μg/ ml], shRNA HSF1 Mir1, shRNA HSF1 Mir1 + Doxycycline [0.5μg/ ml], shRNA HSF1 Mir4 and shRNA HSF1 Mir4 + Doxycycline [0.5μg/ ml] **(B)**. Expressed as mean ± SD. n=4

A

B
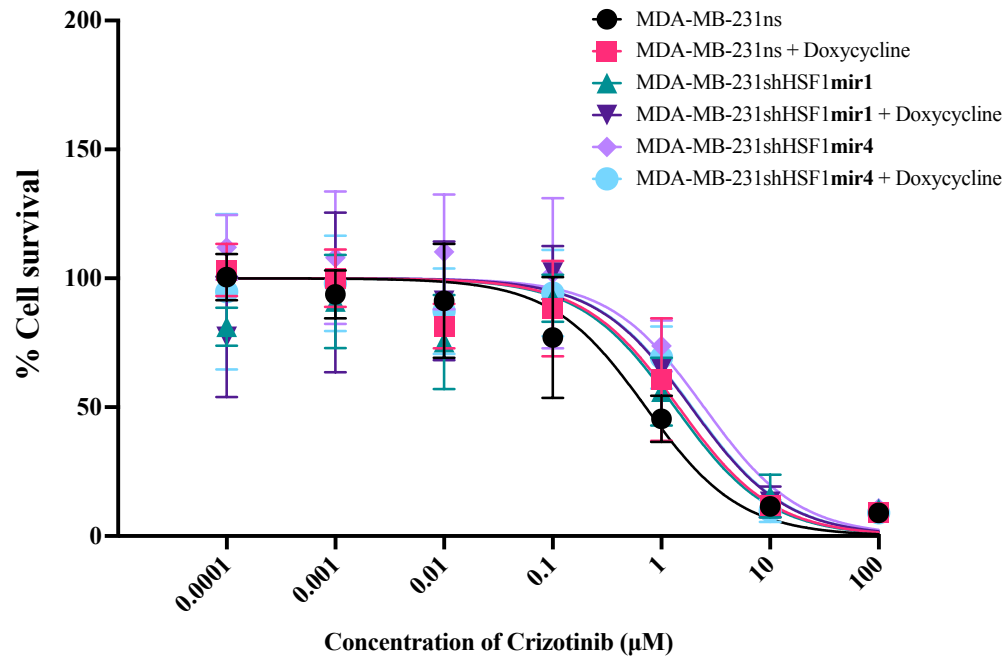
IC$_{50}$ Cell Survival (µM)	
Cell Line	**MDA-MB-231**
Time (Hours)	**72**
Non-silencing	1
Non-silencing + Doxycycline	1
shRNA HSF1 Mir1	1
shRNA HSF1 Mir1 + Doxycycline	2
shRNA HSF1 Mir4	2
shRNA HSF1 Mir4 + Doxycycline	2

Figure 14 MDA-MB-231 cells with HSF1 knockdown tested for sensitivity to Crizotinib

MDA-MB-231 BrCa cells with HSF1 inducible knockdown treated with Crizotinib over 72 hours. Cell survival graphed as log10 drug concentration from Alamar Blue assay **(A)**. IC50 values are represented in table according to cell conditions: non-silencing (ns), ns + Doxycycline [0.5µg/ ml], shRNA HSF1 Mir1, shRNA HSF1 Mir1 + Doxycycline [0.5µg/ ml], shRNA HSF1 Mir4 and shRNA HSF1 Mir4 + Doxycycline [0.5µg/ ml] **(B)**. Expressed as mean ± SD. n=4

3.2.2.2. Impact of HSF1 knockdown upon BrCa cell sensitivity to PI3K Inhibitors

The PI3K/AKT pathway has a major role in cell survival and is commonly constitutively activated in cancer (Kohno and Pouyssegur, 2006). There are 4 class I PI3K isozymes, PI3K α, PI3K β, PI3K γ, and PI3K δ responsible for regulation of a variety of cellular functions through activation of the downstream serine/threonine kinase, AKT and the mTOR, both of which promote cell survival, proliferation, growth, and metabolism (Engelman et al., 2006, Hay, 2005). Pictilisib and Idelalisib are PI3K (p110) inhibitors specifically targeting the α/δ and δ isoforms, respectively (Meadows et al., 2012). HSF1 is known to be post-translationally altered downstream of the PI3K/AKT signal transduction pathway as well as *by* several other RAS-dependent pathways (Frezzato et al., 2019, Tang, 2018). HSF1 mediates HSP70 expression not only in normal cells but also in cancer cells such as in B-cell chronic lymphocytic leukaemia (Frezzato et al., 2019). High levels of HSP70 have been associated with a lowered response towards treatment (Yang et al., 2012). Like HSF1, HSP70 is also a major attenuator of HSF1 activity and mediates a protective role for cancer cells, supporting their adaptation to changes in the microenvironment typically as a result of anticancer drugs (Yang et al., 2012, Nitika et al., 2020). Inhibition of PI3K has been shown to reduce the expression of both HSP70 and HSF1 (Frezzato et al., 2019). Interestingly, GSK3 a/b in the PI3K/AKT cascade phosphorylates HSF1 and inhibits its action. Overexpression of AKT (Serine 473), the inhibited form, inhibits GSK3 a/b and prevents HSF1 inhibition. Inability to inhibit HSF1 activity leads to overexpression of HSP70 and induced apoptosis in leukemia B cells (Frezzato et al., 2019). Thus, this interdependency of the PI3K/AKT pathway with HSF1 activity may suggest that by blocking both, cancer cells become more responsive.

To test this hypothesis, that combined with HSF1 knockdown, PI3K inhibitors would sensitise the BrCa cell lines to Idelalisib (Frezzato et al., 2019) and Pictilisib, thus, induce apoptosis or cell death. However, despite this was not seen experimentally. Knockdown of HSF1 in the T47D or the MDA-MB-231 did not make them more sensitive to either Pictilisib or Idelalisib (Figure 15-18).

A

B
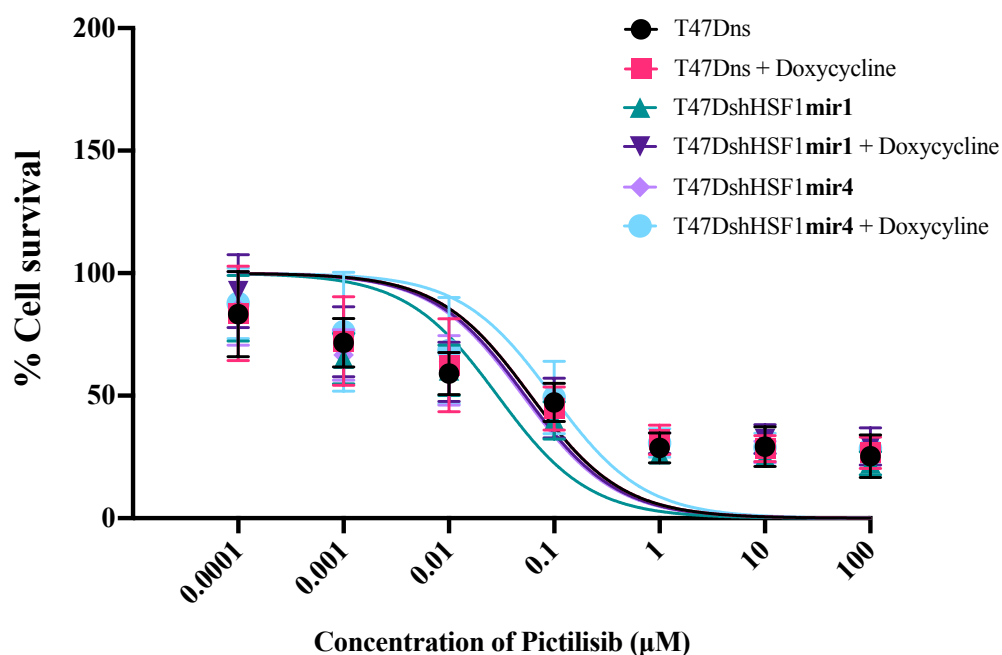
IC$_{50}$ Cell Survival (µM)	
Cell Line	**T47D**
Time (Hours)	**72**
Non-silencing	0.06
Non-silencing + Doxycycline	0.06
shRNA HSF1 Mir1	0.03
shRNA HSF1 Mir1 + Doxycycline	0.05
shRNA HSF1 Mir4	0.05
shRNA HSF1 Mir4 + Doxycycline	0.10

Figure 15 T47D cells with HSF1 knockdown tested for sensitivity to Pictilisib

T47D BrCa cells with HSF1 inducible knockdown treated with Pictilisib over 72 hours. Cell survivability graphed as log10 drug concentration from Alamar Blue assay **(A)**. IC50 values are represented in table according to cell conditions: non-silencing (ns), ns + Doxycycline [0.5µg/ ml], shRNA HSF1 Mir1, shRNA HSF1 Mir1 + Doxycycline [0.5µg/ ml], shRNA HSF1 Mir4 and shRNA HSF1 Mir4 + Doxycycline [0.5µg/ ml] **(B)**. Expressed as mean ± SD. n=7

A

B
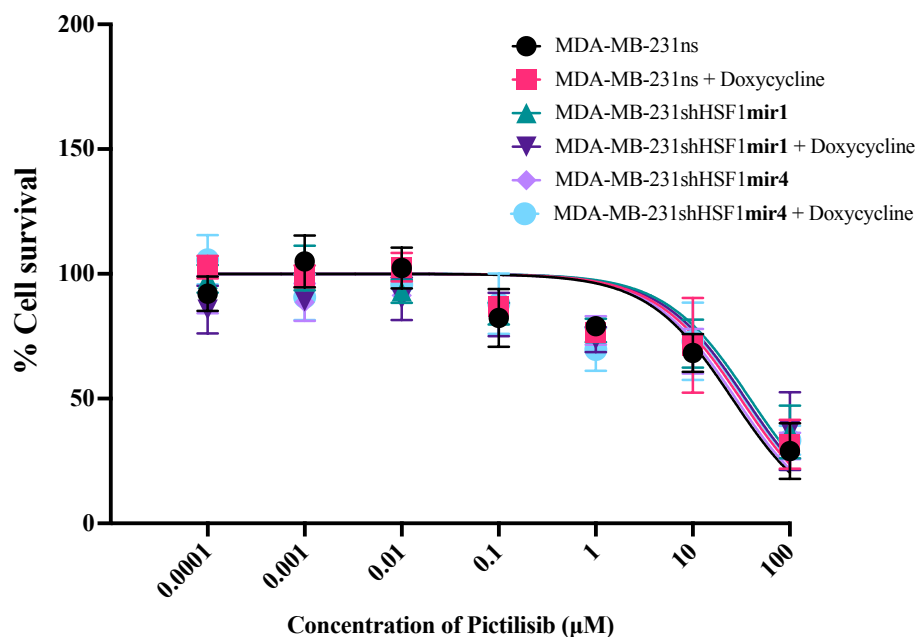
IC$_{50}$ Cell Survival (µM)	
Cell Line	**MDA-MB-231**
Time (Hours)	**72**
Non-silencing	25.53
Non-silencing + Doxycycline	31.03
shRNA HSF1 Mir1	38.76
shRNA HSF1 Mir1 + Doxycycline	34.85
shRNA HSF1 Mir4	27.76
shRNA HSF1 Mir4 + Doxycycline	33.71

Figure 16 MDA-MB-231 cells with HSF1 knockdown tested for sensitivity to Pictilisib

MDA-MB-231 BrCa cells with HSF1 inducible knockdown treated with Pictilisib over 72 hours. Cell survival graphed as log10 drug concentration from Alamar Blue assay **(A)**. IC50 values are represented in table according to cell conditions: non-silencing (ns), ns + Doxycycline [0.5μg/ ml], shRNA HSF1 Mir1, shRNA HSF1 Mir1 + Doxycycline [0.5μg/ ml], shRNA HSF1 Mir4 and shRNA HSF1 Mir4 + Doxycycline [0.5μg/ ml] **(B)**. Expressed as mean ± SD. n=3

A

B

IC$_{50}$ Cell Survival (μM)	
	T47D
Cell Line	
Time (Hours)	**72**
Non-silencing	46
Non-silencing + Doxycycline	53
shRNA HSF1 Mir1	57
shRNA HSF1 Mir1 + Doxycycline	49
shRNA HSF1 Mir4	53
shRNA HSF1 Mir4 + Doxycycline	68

Figure 17 T47D cells with HSF1 knockdown tested for sensitivity to Idelalisib

T47D BrCa cells with HSF1 inducible knockdown treated with Idelalisib over 72 hours. Cell survival graphed as log10 drug concentration from Alamar Blue assay **(A)**. IC50 values are represented in table according to cell conditions: non-silencing (ns), ns + Doxycycline [0.5μg/ ml], shRNA HSF1 Mir1, shRNA HSF1 Mir1 + Doxycycline [0.5μg/ ml], shRNA HSF1 Mir4 and shRNA HSF1 Mir4 + Doxycycline [0.5μg/ ml] **(B)**. Expressed as mean ± SD. n=5

A

B
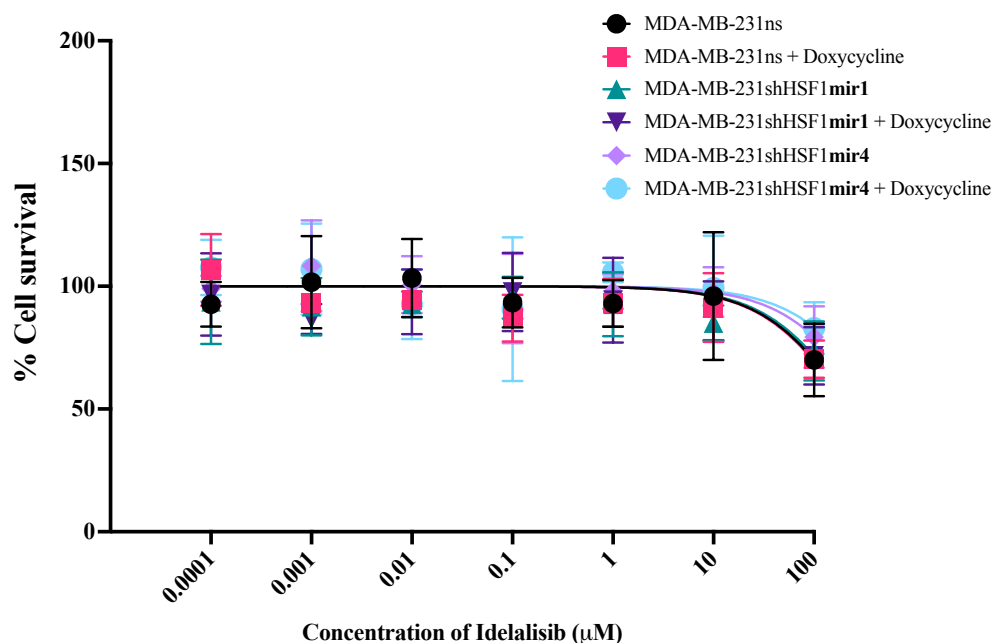
IC$_{50}$ Cell Survival (µM)	
Cell Line	**MDA-MB-231**
Time (Hours)	**72**
Non-silencing	232
Non-silencing + Doxycycline	226
shRNA HSF1 Mir1	251
shRNA HSF1 Mir1 + Doxycycline	238
shRNA HSF1 Mir4	384
shRNA HSF1 Mir4 + Doxycycline	497

Figure 18 MDA-MB-231 cells with HSF1 knockdown tested for sensitivity to Idelalisib

MDA-MB-231 BrCa cells with HSF1 inducible knockdown treated with Idelalisib over 72 hours. Cell survival graphed as log10 drug concentration from Alamar Blue assay **(A)**. IC50 values are represented in table according to cell conditions: non-silencing (ns), ns + Doxycycline [0.5μg/ ml], shRNA HSF1 Mir1, shRNA HSF1 Mir1 + Doxycycline [0.5μg/ ml], shRNA HSF1 Mir4 and shRNA HSF1 Mir4 + Doxycycline [0.5μg/ ml] **(B)**. Expressed as mean ± SD. n=3

3.2.2.3. Impact of HSF1 knockdown upon BrCa cell sensitivity to Chemotherapeutics

Chemotherapeutics are used extensively in the treatment of cancer and are especially effective at managing the growth of chemosensitive tumours. However, advanced cancers are often chemoresistant, developing resistance through multiple pathways. Cancer cells may develop an adaptive and protective phenotype through the influence of HSF1 activity, such as the upregulation of HSPs which is especially true when cancer cells are subjected to anticancer drug treatment (Prince et al., 2020, Vydra et al., 2013).

Several studies have shown that elevated HSP90 isoforms, HSPA1 or HSPB1 levels are associated with cell resistance to cisplatin or doxorubicin (Krawczyk et al., 2018, Liu et al., 2011a, Yang et al., 2012, Lee et al., 2007, Fortin et al., 2000). Also, in a study by *Nadin et al. (2003)*, it was observed that the damage post-doxorubicin treatment is better repaired following heat shock and this correlated with the nuclear translocation of HSPB1 and HSPA1 (Nadin et al., 2003). Moreover, a study by *Sharma et al. (2010)*, reported that HSPA1 mediated a heat-induced carboplatin resistance in a p53-dependent hepatoma (Sharma et al., 2010). However, there is also conflicting evidence indicating that upregulation of HSPs does not enhance cancer cell survival along with some anticancer treatments including, cisplatin, colchicine, 5-fluorouracil, actinomycin D or methotrexate. Even when HSF1 was silenced, thereby reducing levels of HSPs, this was not sufficient to reduce the resistance of cervix carcinoma HeLa cells to cisplatin (Hettinga et al., 1996, Richards et al., 1996, Kimura and Howell, 1993, Ciocca et al., 1992, Rossi et al., 2006). Therefore, the influence of HSPs may be secondary to HSF1 activity and HSF1-dependent resistance of cancer cells to drugs could be associated with

HSF1's broader role in cancer such as regulation of non-HSPs genes (Dai and Sampson, 2016, Mendillo et al., 2012, Vydra et al., 2013).

To test this hypothesis, the T47D and the MDA-MB-231 cells with inducible HSF1 knockdown were treated with doxorubicin. The T47D cells with HSF1 knockdown were found to be significantly increased in their sensitivity to doxorubicin after 72 hours (Figure 19). Moreover, the MDA-MB-231 cells with HSF1 knockdown appeared to make the cells slightly more sensitive to Doxorubicin, however, this result did not reach statistical significance (Figure 20).

A

B
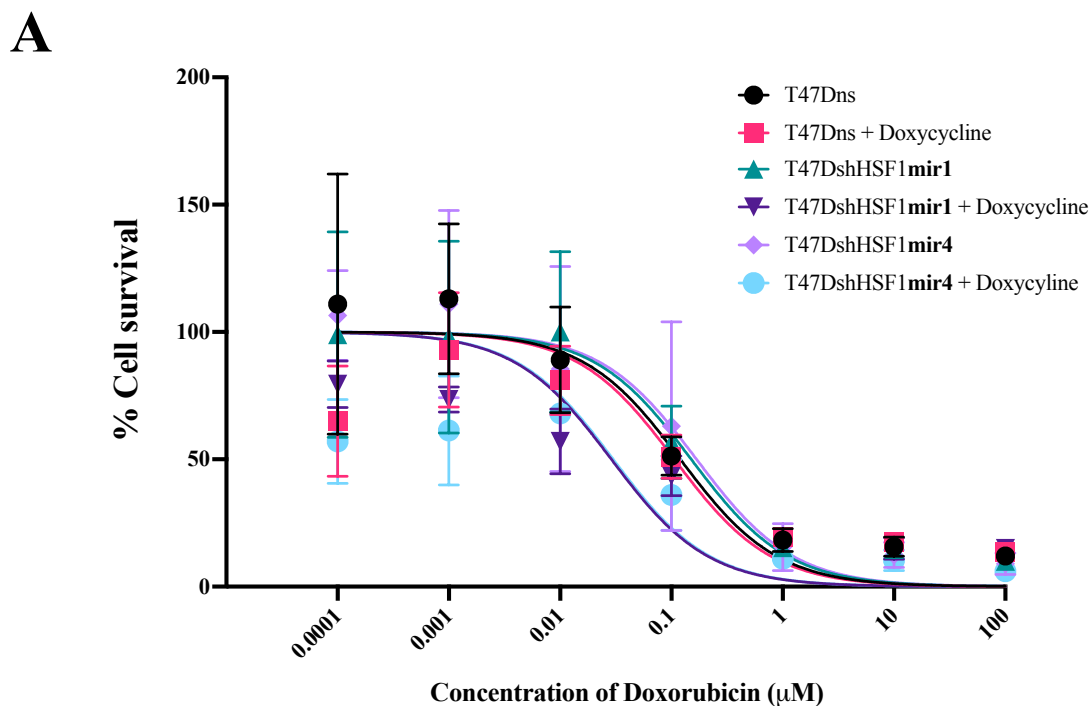
	IC$_{50}$ Cell Survival (µM)
	T47D
Cell Line	
Time (Hours)	**72**
Non-silencing	0.12
Non-silencing + Doxycycline	0.11
shRNA HSF1 Mir1	0.15
shRNA HSF1 Mir1 + Doxycycline	0.03
shRNA HSF1 Mir4	0.17 ⎤
shRNA HSF1 Mir4 + Doxycycline	0.03 ⎦ *

Figure 19 T47D cells with HSF1 knockdown tested for sensitivity to Doxorubicin

T47D BrCa cells with HSF1 inducible knockdown treated with doxorubicin over 72 hours. Cell survival graphed as log10 drug concentration from Alamar Blue assay **(A)**. IC50 values are represented in table according to cell conditions: non-silencing (ns), ns + Doxycycline [0.5µg/ ml], shRNA HSF1 Mir1, shRNA HSF1 Mir1 + Doxycycline [0.5µg/ ml], shRNA HSF1 Mir4 and shRNA HSF1 Mir4 + Doxycycline [0.5µg/ ml] **(B)**. Expressed as mean ± SD. n=3
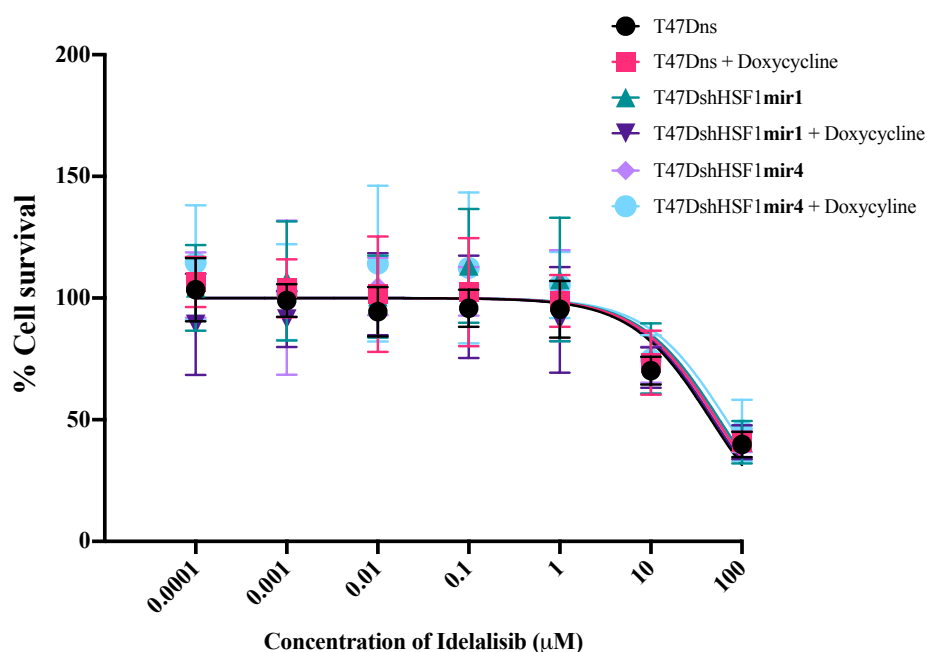
A

B
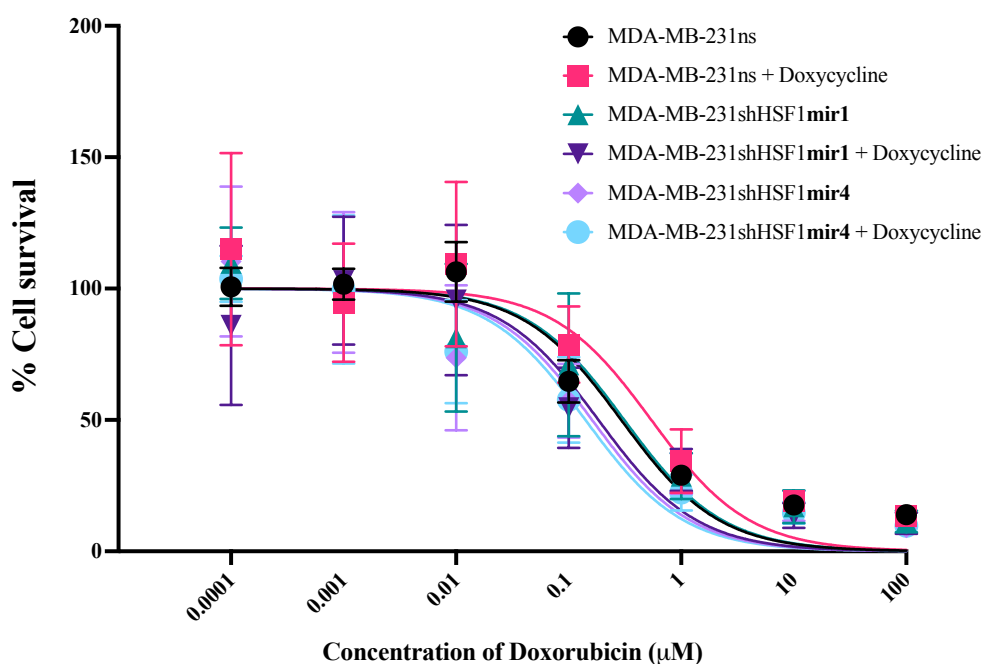
IC$_{50}$ Cell Survival (µM)	
Cell Line	**MDA-MB-231**
Time (Hours)	**72**
Non-silencing	0.29
Non-silencing + Doxycycline	0.54
shRNA HSF1 Mir1	0.31
shRNA HSF1 Mir1 + Doxycycline	0.18
shRNA HSF1 Mir4	0.16
shRNA HSF1 Mir4 + Doxycycline	0.14

Figure 20 MDA-MB-231 cells with HSF1 knockdown tested for sensitivity to Doxorubicin

MDA-MB-231 BrCa cells with HSF1 inducible knockdown treated with doxorubicin over 72 hours. Cell survivability graphed as log10 drug concentration from Alamar Blue assay **(A)**. IC50 values are represented in table according to cell conditions: non-silencing (ns), ns + Doxycycline [0.5μg/ ml], shRNA HSF1 Mir1, shRNA HSF1 Mir1 + Doxycycline [0.5μg/ ml], shRNA HSF1 Mir4 and shRNA HSF1 Mir4 + Doxycycline [0.5μg/ ml] **(B)**. Expressed as mean ± SD. n=3

3.3. Discussion

HSF1 is a transcription factor that protects normal cells from environmental insults (stress) but has also been shown to be exploited by cancer cells to drive proliferation, survival, invasion and metastasis (Jiang et al., 2015). Active HSF1 undergoes trimerization in the cytoplasm and translocates to the nucleus, where its levels are a prognostic indicator for cancer severity, potential resistance to therapy and shortened patient survival (Dai and Sampson, 2016). Thus, HSF1 has long been identified as an excellent therapeutic target demonstrated through previous studies of HSF1 inhibition studies, knockout and knockdown models (Cigliano et al., 2017, Vilaboa et al., 2017, Sharma and Seo, 2018, Velayutham et al., 2018, Kim et al., 1998). This chapter presents work that examined the effect of HSF1 knockdown on the sensitivity of two BrCa cell lines to anticancer drugs in a widescale screen. The current study successfully established an inducible HSF1 knockdown model in the two breast cancer cell lines that were chosen due to their differing metastatic cancer cell biology, the T47D and the MDA-MB-231 that have low- and high-metastatic potential, respectively. Our lab has previously shown that the inducible model of knockdown is more representative of an acute inhibition of HSF1 as would occur with therapeutic inhibition of a target rather than a constitutive knockdown or knockout model previously used.

3.3.1. Generated inducible model of HSF1 knockdown

Prior to the development of lentiviral knockdown, knockout technology was important and widely used for gene function studies, however, its limitation includes the inability to revert gene inactivation and replicability in other species (Glaser et al., 2005, Herold et al., 2008). The complete loss of a gene product can also impact on developmental processes, allow the potential of compensation mechanisms overtime and even induce severe malformations or lethality (Heitz et al., 2014). In contrast, lentiviral vectors with inducible expression can be used as a powerful tool to accurately manipulate gene expression which is also reversible. The advantages of such an inducible model includes a pool of shRNA clones that can lower off target effects compared to sustained gene loss, selectable puromycin marker, tRFP expression active-reporter in the live cell, available non-silencing control and convenience of a Tet-on induction (Herold et al., 2008). Furthermore, with withdrawal of doxycycline after transient induction, cells can completely recover expression of the target gene. Therefore, the doxycycline-dependent inducible model is a compelling model for the transient and tuneable knockdown of cancer targets.

T47D and MDA-MB-231 cells were transduced and then selected with puromycin to provide a population of stable cell lines. Selection with this antibiotic was extended to establish stable models of inducible HSF1 knockdown in both cell lines. Puromycin was only used for the purpose of selecting stably transduced cells and taken off after. To test the efficiency of the knockdown, a titration of doxycycline, a member of the tetracycline family and inducer of the inducible knockdown, was performed. Induction of tRFP in live cell imaging was observed and knockdown of HSF1 was confirmed at the protein level by western blot to confirm reduced protein levels of HSF1 (Figure 5, 6). There was

no difference seen in the ability of varying concentrations of doxycycline to induce knockdown between 0.25µg/ ml and 2µg/ ml. Even at low concentrations of doxycycline, tRFP expression was reflective of the activity of constructs being induced. At the concentration of 0.5µg/ ml doxycycline, successful models of stable HSF1 knockdown were confirmed in both cell lines via western blotting, (Figure 7, 8). As anticipated, expression of HSF1 was significantly reduced in both shRNAmir1 and shRNAmir4 expressing T47D and MDA-MB-231 cell lines.

3.3.2. HSF1 inhibition and sensitivity to anticancer drugs

Previous gene array work from our lab looking at HSF1 activity identified patterns of modulation in genes associated with multiple oncogenic signalling pathways downstream of growth factor receptors including Mammalian target of rapamycin (mTOR) and AKT pathways. To investigate this, we used the BrCa cell lines with HSF1 knockdown generated to screen a panel of drugs targeting multiple targets within these pathways (refer to Figure 21).
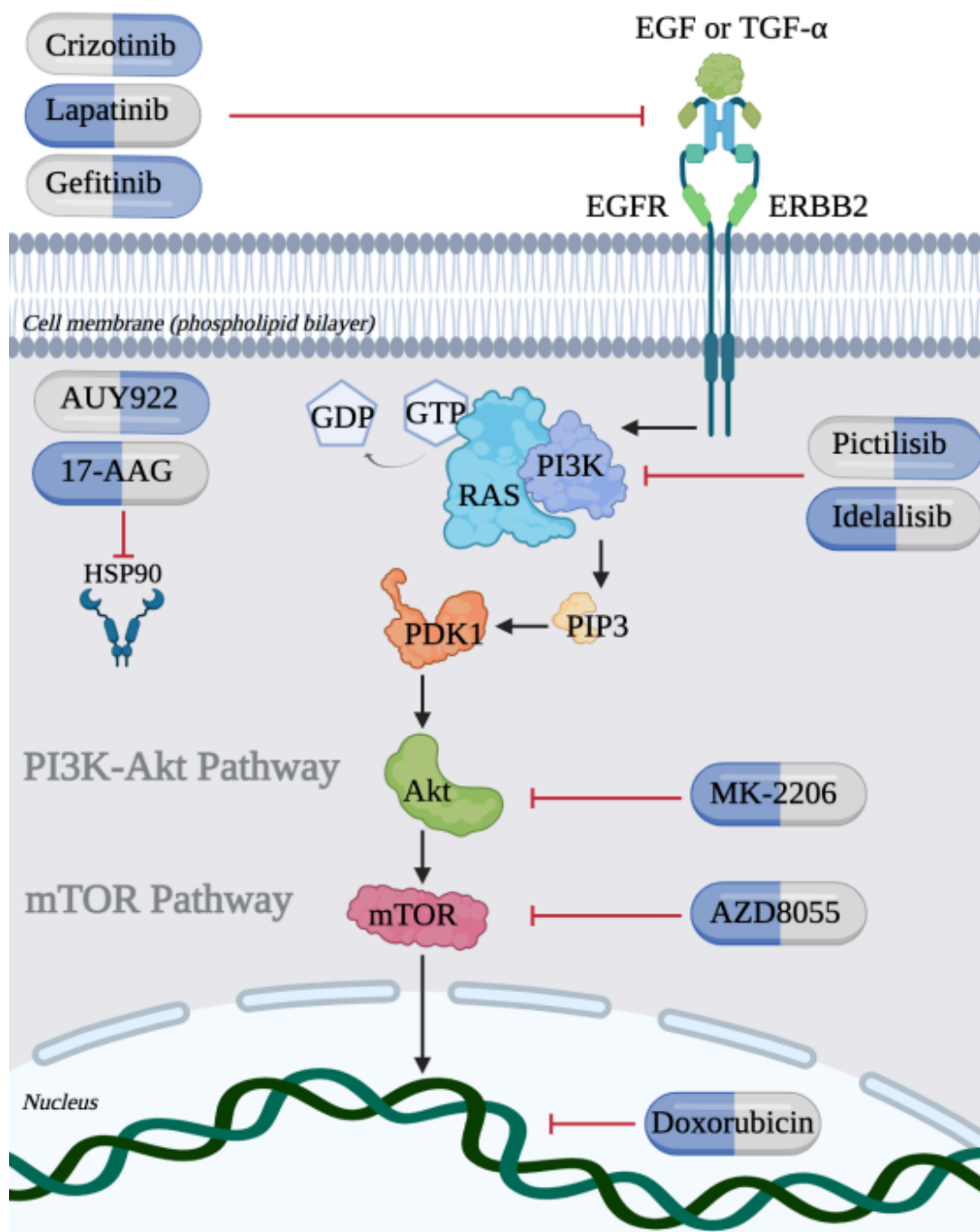
Figure 21 Targeting AKT/mTOR pathways with anticancer drugs

Simplified schematic of AKT/mTOR pathways illustrating interaction of the tested anticancer compounds and broadly the compounds' site of action. The drugs tested include: Lapatinib, Gefitinib [targets: Epidermal growth factor receptor (EGFR)] and Crizotinib (targets: MET/ALK) (Pedersen et al., 2005, Zou et al., 2015, Rusnak et al., 2001); Pictilisib and Idelalisib (targets: PI3K) (Haagensen et al., 2012, Meadows et al., 2012), MK-2206 (targets: Akt) (Cheng et al., 2011), AZD8055 (targets: mTOR) (Houghton et al., 2012), 17-AAG and AUY922 (targets: HSP90) (Lee et al., 2011, Kamal et al., 2003), doxorubicin (targets: intercalate DNA base pairs). Created with BioRender.com

3.3.2.1. Targeting HSF1 and EGFR in TNBC May Increase Resistance

The EGFR is a tyrosine kinase receptor in the HER family and plays a key role in cancer cell proliferation, survival, angiogenesis, invasion and metastasis (Hashmi et al., 2019, Brand et al., 2011, Song et al., 2020). Expression of EGFR is more common in BrCa with lower hormone receptor levels and HER-2/neu overexpression (Rimawi et al., 2010). Generally, TNBC lack expression of hormonal and HER2 receptors, thus conventional targeted therapies are ineffective but a study by *Changavi et al. (2015)* also demonstrated strong EGFR presence in some TNBC, especially in the basal-like molecular profile (Rimawi et al., 2010, Changavi et al., 2015, Hashmi et al., 2019). In our current study, we looked at three TKI: Gefitinib, Lapatinib and Crizotinib. Gefitinib and Lapatinib target EGFR, while Crizotinib is also a TKI, but it targets c-MET. Gefitinib selectively inhibits autophosphorylation of EGFR, while Lapatinib targets both the activated and inhibited forms of the EGFR and ErbB-2 (Dratkiewicz et al., 2018, Wood et al., 2004). Crizotinib targets include anaplastic lymphoma kinase (ALK), c-Met/hepatocyte growth factor receptor and c-ros oncogene 1 (Frampton, 2013). In the Luminal A cells, T47D, expressing hormone receptors but not ErbB-2 responded to Lapatinib but there was no change to its response when combined with HSF1 knockdown. Interestingly, in the basal-like TNBC, MDA-MB-231, lacking both hormone receptors expression and ErbB-2, but with high EGFR expression, became significantly resistant to Lapatinib with HSF1 knockdown (Figure 9, 10) (Chavez et al., 2011).

Targeting PI3K/AKT signalling has been disappointing in clinical trials to date, therefore, combinatorial treatment has become an attractive approach (Yang et al., 2019). PI3K activity can activate the serine-threonine kinase AKT (Carpenter et al.,

2017). Both PI3K and AKT have enhanced activity in BrCa and are associated with poor clinical outcomes (Panigrahi et al., 2004). PI3K can be activated by many receptor tyrosine kinases, including the epidermal growth factor receptor (EGFR) family of receptors (Carpenter et al., 2017). EGFR and erythroblastic oncogene B 2/ HER2 (ErbB-2) activation have been linked to the PI3K/AKT cell survival pathway, therefore inhibiting their catalytic activity can induce cell death (Rusnak et al., 2001). Lapatinib is a small-molecule tyrosine kinase inhibitor that suppresses the activity of EGFR and ErbB-2, which leads to a block to the autophosphorylation cascade of the PI3K/AKT pathway, which has important roles in cell proliferation and survival (Ciardiello et al., 2000). Thus, Lapatinib can be used to inhibit the growth of both EGFR- and ErbB-2-overexpressing cancers (Matsumoto et al., 2018).

Lapatinib is FDA-approved in combination with other anticancer drugs for the treatment of ErbB-2-positive breast cancer (Ryan et al., 2008). In addition to its inhibiting effect of the tyrosine kinases, Lapatinib is observed to also inhibit the function of ATP binding cassette (ABC) transporters to alter pharmacokinetics and decrease resistance (Beretta et al., 2017). The ABC transporters are glycoproteins principally located in the plasma membrane (Chen et al., 2014). In normal physiology, ABC transporters are important for protection against the accumulation of toxic compounds in a variety of cells and tissues with expression often enhanced in malignant cells (Sharom, 2007). Overexpression of ABC transporters is a major contributing factor to multiple drug resistance (MDR) (Zajdel et al., 2021). MDR refers to cancer cells resistance to structurally and mechanistically unrelated drugs that can significantly reduce therapeutic efficacy and lead to failed treatment (Zheng et al., 2021). ABC transporters can be problematic because they can facilitate the efflux of diverse drugs from cancer

cells causing decreased intracellular drug concentration (Wu and Fu, 2018). Increasing evidence suggests combining Lapatinib and Paclitaxel for treatment of MDR tumours including BrCa because the simultaneous delivery of two or more anticancer agents often resulted in increased toxicity compared to monotherapy (Dehghankelishadi et al., 2017, Zajdel et al., 2019, Wang et al., 2020, Gote et al., 2021). This could overcome unsuccessful attempts of Lapatinib as a monotherapy and introduce a novel role in ErbB-2-negative or TNBC cancers (Liu et al., 2016). Furthermore, a study by *Abo-Zeid et al. (2019)*, supports Lapatinib as a monotherapy as it reduced EGFR expression and induced cytotoxicity in the MDA-MB-231 cells (Abo-Zeid et al., 2019).

Another important consideration is the quiescent state of cancer cells in tumour recurrence, quiescence can protect cancer cells from chemotherapy. In a study by *Kwon et al. (2015)* using quiescent MDA-MB-231 tumoursphere cultures, they found that Lapatinib sensitizes MDA-MB-231 to doxorubicin by inhibiting doxorubicin-induced multidrug resistance-associated protein 1 (MRP-1) expression via PI3K/AKT and p38 mitogen-activated protein kinase (MAPK) signalling pathways (Kwon et al., 2015). They suggested that the synergistic effect of Lapatinib and Doxorubicin may be from the inhibition of both MRP-1 and EGFR-mediated survival signalling (Kwon et al., 2015). Taken together, Lapatinib is specific to inhibit tyrosine kinases overexpressing cells and there is evidence to suggest that use in combination with anti-mitotic drugs may be a suitable method for recurrent cancers to improve patient response by eliminating the quiescent cancer cell population (Kwon et al., 2015).

Contrary to my hypothesis that knockdown of HSF1 may sensitise BrCa cells to anticancer drugs and increase cell death, HSF1 knockdown in the EGFR expressing cells

MDA-MB-231 combined with Lapatinib significantly decreased cell death, thus increased drug resistance (Figure 10). In a study *by Liu et al. (2016)* that looked at the role that Lapatinib had in killing MDA-MB-231, they illustrated that Lapatinib initiated apoptosis by disturbing the binding of ELK1 to the cancerous inhibitor of protein phosphatase 2A (CIP2A) promoter and by inhibiting AKT protein levels in MDA-MB-231 (Liu et al., 2016). Moreover, this validates that Lapatinib has an ErbB-2-independent anticancer property as mentioned earlier. Furthermore, CIP2A has been shown to control oncogenic cellular signals by suppressing the tumour suppressor cellular protein phosphatase 2A (PP2A), while CIP2A overexpression is associated with several human malignancies including BrCa, hepatocellular carcinoma, gastric cancer, head and neck cancer, colon cancer, prostate cancer and non-small cell lung cancer (De et al., 2014, Niemelä et al., 2012, He et al., 2012, Lin et al., 2012, Li et al., 2008, Teng et al., 2012, Vaarala et al., 2010, Dong et al., 2011). CIP2A can activate oncogenic proteins such as c-Myc, extracellular signal-regulated kinase (ERK), and Akt (De et al., 2014). Interestingly, a study by *Lei et al. (2014)* showed CIP2A regulation of AKT phosphorylation at S473 and may recognize specific AKT targets that could promote cell proliferation through the AKT signalling pathway (Lei et al., 2014). Additionally, ErbB-2 activation can lead to AKT-mediated phosphorylation and the activation of HSF1 (serine326), whereas AKT inhibition reduces HSF1 activity and consistent with this, Lapatinib inhibits the transcriptional activation of HSF1 by suppressing its serine326 phosphorylation status (Carpenter et al., 2015). Taken together, Lapatinib may result in the inhibition of CIP2A activity and the AKT pathway, ultimately reducing HSF1 activation and increasing apoptosis (Figure 22). However, contrary to this, the current study has shown that a combined treatment of Lapatinib and HSF1 knockdown does not increase apoptosis but rather, increases MDA-MB-231 resistance to Lapatinib.

Furthermore, with consideration of HSF1 orchestrating a role in cancer; HSF1 could be targeted in two ways. The first may be to restore normal levels of HSF1 from its upregulation in cancer while still maintaining the regular HSR. The second could be to further overexpress HSF1, in doing so this may push the stress response to levels beyond adaptable even for the highly stressed cancer cells and induce apoptosis (Im et al., 2017, Salmand et al., 2008). A study by *Janus et al. (2020)* elucidated a dual role for HSF1 in response to stress which can be either pro-survival or pro-death, that is to, either induce cytoprotection or apoptosis (Janus et al., 2020). Lapatinib has been shown to reduce HSF1 levels via mediated mutant p53 destabilisation (Li and Marchenko, 2017). Use of both lapatinib and HSF1 knockdown can reduce HSF1 levels in cells. MDA-MB-231 increased resistance to this combination may suggest that the double loss approach was insufficient to deplete the stress response from the already elevated HSF1 levels that are too high in cancer cell and instead, the attempt to reduce it may have encouraged pro-survival through a stress response induced by attempt to remove HSF1. Alternatively, too low HSF1 levels could lead to a decrease cell response to Lapatinib and this is consistent with *Carpenter et al. (2017)* discussion of 'balanced' inhibition, where they observed that the efficacy of treatment is concentration-dependent (Carpenter et al., 2017). Additionally, this observation may also be attributable to depletion of the drug target, thus a reduction in the drug's efficacy. Despite HSF1 having a broad role in the cancer environment and being exploited by cancer cells, inevitably, in the non-diseased environment, HSF1 still has an important role in homeostasis. Therefore, future targeting of HSF1 may need to focus on balancing between normal levels of HSF1 and elevated levels in the disease conditions.

In cancer:

| ⇑ CIP2A | Lapatinib |
| | ⇓ CIP2A |

In cancer: Lapatinib

⇑ CIP2A   ⇓ CIP2A

↓   ↓

⇑ AKT   ⇓ AKT

↓   ↓

⇑ HSF1   ⇓ HSF1

↓   ↓

⇓ **Patient Survival**   ⇑ **Apoptosis**
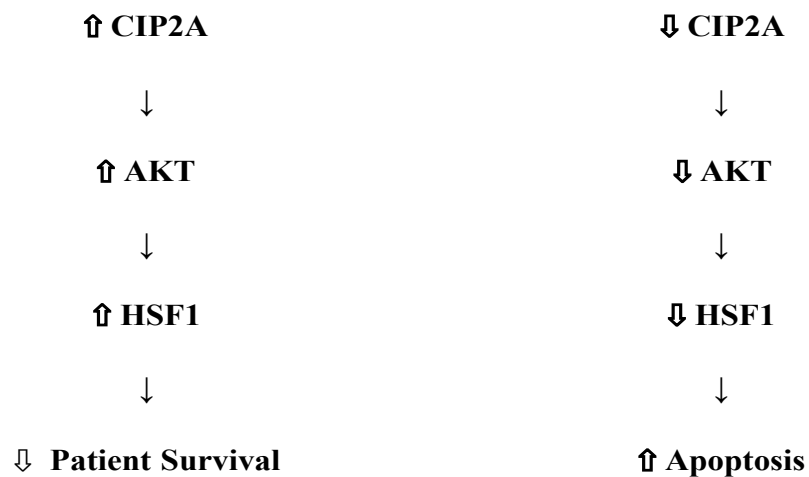
Figure 22 Schematic representing an alternative mechanism of Lapatinib in cancer cells

There is a potential that Lapatinib by some mechanism can inhibit CIP2A activity, AKT pathway and ultimately reduce HSF1 activation thus increasing apoptosis (Lei et al., 2014, Lin et al., 2012, Liu et al., 2016).

The relationship between HSF1 and EGFR may also be related to HSF1 involvement in EGFR recycling via autophagy mediated lysosomal mechanisms. A study by *Fraser et al. (2019)*, demonstrated that removal of autophagy-essential players like ATG7 or ATG16L1 is indirectly associated with stalling of EGFR recycling back to the plasma membrane (Fraser et al., 2019, Sigismund et al., 2008). Thus, preventing autophagy homeostatic regulation, reduces EGFR recycling to the plasma membrane and compromises downstream signalling, thus, cell survival. This is because autophagy is known to deliver cellular cargoes to lysosomes for degradation and relaying cues from the extracellular environment. This function is tied to HSF1's role in regulating autophagy and autophagy receptor SQSTM1/p62-associated proteostasis, whereby, targeting HSF1 impaired induction of autophagosome formation and elimination of protein aggregates (Watanabe et al., 2017, Dokladny et al., 2013, Dokladny et al., 2015). Furthermore, in a BrCa patient sample study by *Desai et al. (2013)*, revealed that a higher ATG7 expression level is also linked with poor patient survival and that HSF1 has a role in controlling cytoprotective autophagy through the regulation of ATG7 (Desai et al., 2013). This interplay between the two stress inducible processes, HSR and autophagy may increase cells ability to cope with stress and to improve survival and proteostasis (Kumsta et al., 2017). Additionally, a subset of receptor tyrosine kinases has been identified to employ autophagic signalling platforms thus regulating pro-growth signalling independent of autophagy proteins degradative function further supporting the fact that many tyrosine kinases like the EGFR activity is associated various cancers (Barrow-McGee et al., 2016, Lampada et al., 2017, Martinez-Lopez et al., 2013, Fraser et al., 2019).

In relation to what we observed in this chapter, HSF1 may be needed to aid cell death via autophagic pathways, therefore, a decrease in HSF1 did not increase cancer

sensitivity to EGFR inhibitors. This disproved our original hypothesis that knockdown of HSF1 will make cells more susceptible to TKI. In fact, it is postulated that knockdown of HSF1 may have hindered EGFR availability at the plasma membrane via downregulation of autophagy-mediated EGFR recycling (Figure 23). An interesting future investigation would be to investigate EGFR localisation in HSF1 knockdown cells and determine the role of HSF1 involvement in BrCa EGFR processing through the lysosome.

Thus, it maybe that rather than HSF1 inhibition, HSF1 activation may provide enhanced efficacy of lapatinib in BrCa. Consistent with this, others have shown synergistic activity between lapatinib and certain types of HSP90 inhibitors will activate HSF1, resulting in overcoming intrinsic and acquired lapatinib-resistance (Park et al., 2018, Lee et al., 2020, Ye et al., 2021, Brady et al., 2015). Moreover, hyperthermia or thermal therapy is another way which can activate HSF1 and this has been used to good effect to increase chemotherapy cancer efficacy (Bull et al., 2008). Overall, this supports the view that overexpression of HSF1 may stimulate TKI to EGFR and enhance drug efficacy via non canonical pathways such as autophagy.
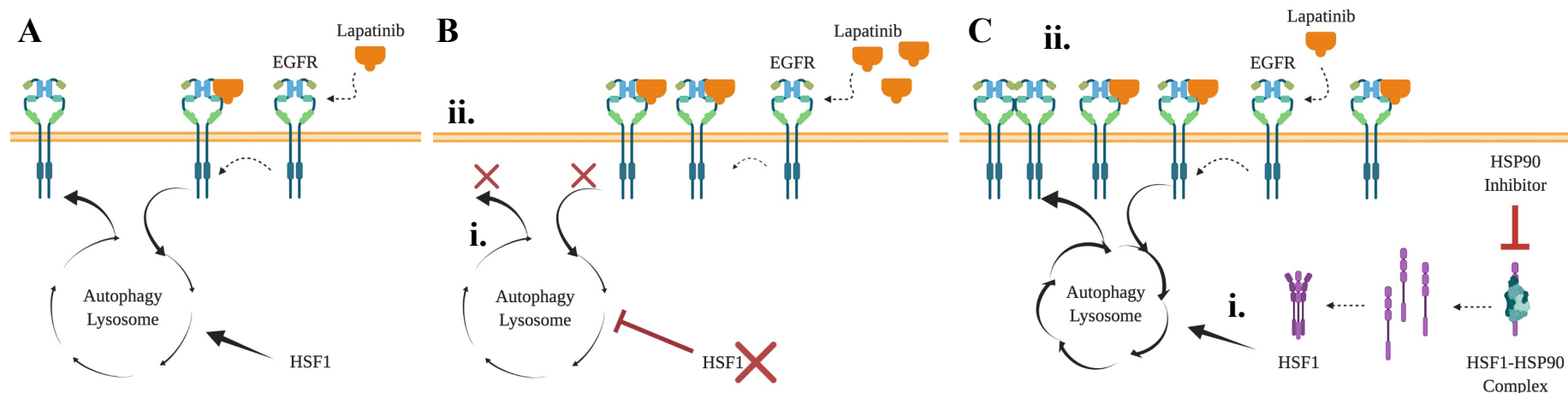
Figure 23 Diagram of hypothesised effect that HSF1 has on EGFR recycling and Tyrosine Kinase Inhibitor

Targeting HSF1 may affect EGFR recycling via autophagy-mediated lysosomal mechanisms, thus, when combined with TKI it is hypothesised that this could reduce TKI efficacy and make cells more resistant to treatment. Typically, when cells are treated with Lapatinib, Lapatinib will bind to its target EGFR **(A)**. However, when MDA-MB-231 cells were treated with both Lapatinib and HSF1 knockdown, cells became more resistant to Lapatinib. Potentially the inhibition of HSF1 will impair its modulation of autophagy-mediated lysosomal recycling of EGFR **(Bi)** preventing EGFR recycling to the plasma membrane **(Bii)**. Therefore, we hypothesise that using drugs like HSP90 inhibitors could enhance activation of HSF1 and upregulate lysosomal recycling of EGFR **(Ci)**. Thus, the result of this will be increased levels of EGFR at the plasma membrane that is available for Lapatinib binding **(Cii)**. We expect that activators of HSF1 would increase cell sensitivity to TKI that target the EGFR.

3.3.2.2. BrCa cells with HSF1 knockdown response to mTOR inhibitors

The serine/ threonine kinase mTOR is composed of two protein complexes within a cell, mTORC1 and mTORC2 (Chou et al., 2012). mTORC1 is activated by signals from cell surface receptors to induce Phosphoinositide 3-kinases (PI3K)/ AKT signalling, important for cell growth. mTORC1 has the adapter protein RAPTOR that is needed in substrate phosphorylation, while mTORC2 does not, mTORC2 functions independently of the growth factors upstream of mTORC1 and AKT signalling (Chou et al., 2012). Interestingly, mTOR also has been shown to directly phosphorylate HSF1 on Ser326, which is important for transcriptional activation and supported by mTOR knockdown studies *in-vivo* which led to an inhibition of stress-induced HSF1-Ser326 (Chou et al., 2012).

To look at the direct effect of mTOR inhibition in combination with HSF1 knockdown, AZD8055 was tested, unfortunately, we could not see any significant affect and dismissed further investigating this drug due to a noticeable effect that the vehicle control had on cell death compared to the lowest concentration of this drug (refer to Appendix 1 Figure A13). This may have been a limitation of the assay due to the drug concentration required in the screen and the solubility of this drug. Additionally, HSF1 knockdown may sensitise cells to DMSO. This postulation is supported by the fact that Rapamycin, a mTOR inhibitor, has been shown to enhance DMSO-mediated growth arrest in human myelogenous leukemia cells (Lalic et al., 2012, Guo et al., 2020). In addition, a previous study demonstrated that targeting mTOR and AKT enhanced overall efficacy, suggesting mTOR is a potential co-target with PI3K/AKT (Holler et al., 2016, Xu et al., 2013). Therefore, it is possible that knockdown of HSF1 may make

cells more sensitive to DMSO, however, there is not enough evidence to confirm this and will need to be investigated in the future.

3.3.2.3. BrCa cells with HSF1 knockdown response to PI3K/ AKT inhibitors

Most HSF1 phosphorylating molecules belong to the PI3K/ AKT/ mTOR and the RAF/ MEK/ ERK pathways (Frezzato et al., 2019). Under heat stress, AKT phosphorylates HSF1 (S230) to activate the transcription factor (Tang, 2018). In cancer, HSF1 activation by AKT also leads to epithelial to mesenchymal transition in ErbB-2-positive BrCa (Carpenter et al., 2017). Additionally, activated AKT (S473) and HSF1 (S326) are strongly associated with shortened time to metastasis (Carpenter et al., 2017). HSF1 binding to DNA is important for HSF1 activity and PI3K/ AKT signalling also regulates HSF1 ability to bind to DNA. AKT inhibitors MK-2206 and RG7440 decreased HSF1's ability to bind to HSP72 promoter (Tang, 2018, Morimoto, 2014). In combination, AKT and HSF1 inhibitors, MK-2206 and KRIBB11, respectively, lead to synergistic killing of BrCa cells and BrCa stem cells across different BrCa subtypes (Carpenter et al., 2017). *Carpenter et al. (2017)* observation in orthotopic xenograft mouse model saw that targeting AKT and HSF1 significantly reduced tumour growth, induced tumour apoptosis, delayed time to metastasis, and prolonged host survival (Carpenter et al., 2017). Noteworthy was another observation that the balance of AKT and HSF1 inhibition appears to be important to discern the enhanced efficacy accompanying a synergistic response. Therefore, in this thesis, MK-2206, an AKT inhibitor was used to block AKT phosphorylation (Figure 21). However, the vehicle control (0.1% v/v DMSO) was impacting on cell death more than the lowest concentration of MK-2206 (100pM), thus, the experiment was terminated before reaching an n=3 (refer to

Appendix 1 and 2). An explanation for MK-2206 insensitivity could be accounted for by the purity of the drug or alternatively, but not yet explored, is BrCa cell sensitivity to DMSO. Targeting HSF1 may sensitise cells to DMSO, given that the concentration of 0.1% DMSO is widely accepted as tolerable by cells without eliciting an effect.

Overall, inhibition of PI3K/AKT signalling blocks positive regulation of HSF1 (S230) DNA binding under heat shock but does not affect HSF1 nuclear translocation (Carpenter et al., 2017). In a mouse model of human megalencephaly, expression of a constitutively active PI3KCA promoted brain overgrowth, AKT-mediated HSF1 activation supported robust growth via balancing both protein quantity and quality while HSF1 deletion reduced brain size (Tang, 2018). *Tang (2018)* also revealed that HSF1 prevents HSP60 aggregation and maintains mitochondrial proteome homeostasis that encourages the overgrowth driven by PI3K/AKT signalling. HSF1 also suppressed amyloidogenesis-induced cell death (Tang, 2018). Therefore, HSF1 has a function in guarding mitochondrial proteostasis and protecting cells from the toxicity induced by amyloids attacking HSP60 in the mitochondria which would culminate in aggregation of both HSP60 and other mitochondrial proteins. In cancer, without HSF1 activity, enough mitochondrial damage can induce apoptosis (Tang, 2018). Thus, targeting PI3K and HSF1 remains an alluring combination to investigate.

3.3.2.4. Loss of HSF1 in Metastatic BrCa may make cells more Sensitive to Doxorubicin

HSF1 orchestrates a broad network beyond the HSR in tumourigenesis that protects cancer cells from apoptosis, overrides cell cycle checkpoints and facilitates metastasis (Khaleque et al., 2005, O'Callaghan-Sunol and Sherman, 2006, Kim et al., 2009, Dai et

al., 2007). Additionally, activation of the HSF1-dependent stress response can elevate the expression of HSPs which has been linked to cancer resistance induced by chemotherapeutic agents in several human malignancies (Mosser and Morimoto, 2004, Sreedhar and Csermely, 2004). To test this in our BrCa cells with HSF1 knockdown, we treated both T47D and MDA-MB-231 with doxorubicin. Doxorubicin is a type of anthracycline and is used as a chemotherapy drug to kill cancer cells by inhibiting the enzyme topoisomerase II, inducing DNA damage, mitophagy and apoptosis (Thorn et al., 2011).

In this thesis, we showed that the T47D cells with HSF1 knockdown were significantly sensitive to treatment with doxorubicin (Figure 19). Similarly, although not significant, the T47D shRNAMir1 the MDA-MB-231 cells also appeared to be more sensitive to doxorubicin with HSF1 knockdown, maybe with increased biological replicates and with tightened error bars the results would favour significance (Figure 19, 20). This may be because the variability of the assay is quite large. Nonetheless, several studies have reported that upregulation of HSP90, HSPA1 and HSPB1 are correlated with cell resistance to cisplatin or doxorubicin (Liu et al., 2011a, Yang et al., 2012, Lee et al., 2007, Fortin et al., 2000). It has also been demonstrated that cancer cells overexpressing HSF1 are more resistant to doxorubicin, independent of HSPs, but more dependent on a HSF1-mediated drug efflux via ABC transporters mechanism (Vydra et al., 2013). Furthermore, both *Vydra et al. (2013)* and *Tchénio et al. (2006)* have shown that the multidrug resistance phenotype was mediated by HSF1-dependent expression of the *ABCB1* gene, but not by HSP expression (Tchénio et al., 2006, Vydra et al., 2013, Vilaboa et al., 2000). *Tchénio et al. (2006)* also hypothesied that HSF1 overexpression could effect postranscriptional mechanisms of the ABCB1 mRNA (Tchénio et al.,

2006). This is plausible as HSF1 has been reported to incorporate into nuclear stress bodies at RNA splicing sites and is involved in the regulation of mRNA-binding protein HuR, responsible for mRNA stability and/or translation of many proteins in cancer (Cotto et al., 1997, Gabai et al., 2012).

Furthermore, in a study by *Huang et al. (2016)* they identified that through proteasome-mediated HSF1 degradation, the insulin-like growth factor receptor II (IGF-IIR) apoptotic signalling pathway was responsible for doxorubicin-induced cardiotoxicity (Huang et al., 2016). IGF-IIR has a vital role in the regulation of cardiac development, growth and survival but it has also been shown to be involved in pathological processes of heart failure, such as hypertrophy, cardiomyocyte apoptosis and end-stage heart failure (Chen et al., 2004, Chang et al., 2008, Wang et al., 2011, Wang et al., 2012a, Wang et al., 2012b, Wei et al., 2012, Chen et al., 2009, Chu et al., 2009). *Huang et al. (2016)* even proposed that administration of an HSF1 activator may be protective against doxorubicin-related cardiomyocyte toxicity.

Overall, in cancer HSF1 facilitates a pro-survival pathway and it has been shown to encourage drug efflux via regulation of ABC transporters, thus reducing doxorubicin efficacy (Krishnamurthy et al., 2012, Choi, 2005, Vydra et al., 2013). We show that in two BrCa cells that HSF1 knockdown and doxorubicin could be a potential combination for treatment of cancer cells, however, there have been other studies to suggest HSF1 activation may be protective against cardiotoxicity. This goes to highlight the complexity of anticancer treatments. One potential combination is with HSP90 inhibitors. During homeostasis, HSP90 belongs to a multichaperone complex believed to repress HSF1 monomers and keeping it in its inactivated form (Leach et al., 2012).

However, in cancer HSP90 facilitates folding of various oncogenic proteins and is necessary for the survival of some cancer cells (Park et al., 2019). Previously, studies suggested that HSF1 transcriptional activity is upregulated by HSP90 inhibition (Powers et al., 2008). Treatment with selected HSP90 inhibitor will dissociate HSP90-HSF1 relationship and increase released unbound HSF1 monomers. This favours HSF1 trimerisation that is necessary for HSF1 activities. Therefore, HSP90 inhibitors treated separately or as a combination with HSF1 shRNA have been shown to reduce HSP70, p-ERK, and HER2 levels, while, increasing cleaved poly-ADP ribose polymerase (PARP) that can be responsible for resistance mechanisms through upregulating the HSR (Chen et al., 2013). Furthermore, HSP90 inhibition to induce HSF1 activity can be supported in relation to the HSF1 mediated autophagy activity discussed earlier where induced autophagy can facilitate pro-growth and cell survival pathways (Mimnaugh et al., 1996, Xu et al., 2001, Fraser et al., 2019). Moreover, *Chen et al. (2013)* had identified that knockdown of HSF1 sensitises cells to HSP90 inhibitors and proposes targeting HSF1 to enhance HSP90 inhibitors efficacy and also to mitigate other side effects such skeletal complications for patients when dosed high concentrations of 17-AAG, a HSP90 inhibitor (Powers et al., 2008, Price et al., 2005, Chen et al., 2013). For this reason, we hypothesis that combining HSF1 inhibitor and a HSP90 inhibitor with a drug like doxorubicin will sensitise BrCa cells to doxorubicin and improve patient outcomes. Unlike other alternatives such as KRIBB11, an indirect inhibitor of HSF1 that acts to prevent HSF1 activation as it may be ineffective in the already HSF1 knockdown cells and in wild-type cells it is expected to have a similar impact as the HSF1 knockdown cells, thus may only impact some pathways of HSF1 and not others and consequently this could confound some results.

3.4. Conclusion

In conclusion, targeting HSF1 in BrCa cells may be context dependent. Combining HSF1 inhibitors with treatments that either influence or activate HSF1 could mitigate the stress response, that would otherwise salvage cell survival and enhance their synergistic effect. Cancer cells may become more sensitive to anticancer drugs that activate HSF1 if HSF1 is removed. Therefore, additional research in this area remains a necessity to fully understand its clinical implications, especially the identification of drugs that can activate HSF1.

CHAPTER 4: DEVELOPMENT OF A DUAL-REPORTER ASSAY TO MEASURE THE HEAT SHOCK RESPONSE IN BREAST CANCER CELL LINES

4.1. Introduction

In the normal, nonstressed condition, HSF1 monomers are inactive and are bound to chaperone complexes (Mendillo et al., 2012). During stress where HSF1 is activated, the HSF1 monomers are released from the chaperone complexes, spontaneously form trimers and relocate from the cytoplasm to the nucleus (Dai and Sampson, 2016). It is in this trimeric conformation, localised within the nucleus that HSF1 can bind to HSE sequences within the promoter region of target genes, thereby impacting upon the expression of these genes (Dai and Sampson, 2016, Anckar and Sistonen, 2011).

With the underlying hypothesis that anticancer drugs that activate the HSR via HSF1 may be less effective in killing advanced cancer cells due to their initiation of this potent survival pathway, the aim was to develop a cell-based, dual reporter system. This would then be utilised to screen anticancer compounds to identify activators of HSF1 with the view of then determining whether these anticancer agents are increased in efficacy in HSF1 knockdown BrCa cells.

Within the cell, HSF1 binds to cis-acting elements that are composed of inverted nGAAn pentamers termed HSEs (Amin et al., 1988). Therefore, tracking HSE activity directly represents binding of HSF1 and thus its activity. The ability to analyse this will help identify anticancer drugs that trigger the HSR and enables an efficient way to screen

activators of HSF1. The current study strived to develop two stable heat shock element (HSE) reporters in the T47D and MDA-MB-231 BrCa cell lines. Choosing the T47D and MDA-MB-231 cells as the host cell was to observe whether there are different stress responses in BrCa cells with different metastatic potential, thus, levels of HSF1 and degree of aggressiveness.

Specifically, the dual-luciferase reporter is possible due to the renilla and firefly luciferases having differing enzyme structures and substrate requirements, making it possible to selectively discriminate between their bioluminescent reactions (see Figure 24). Additionally, another advantage is that in an automated injector system, the firefly signal can be quenched while simultaneously activating the renilla catalyst reaction.
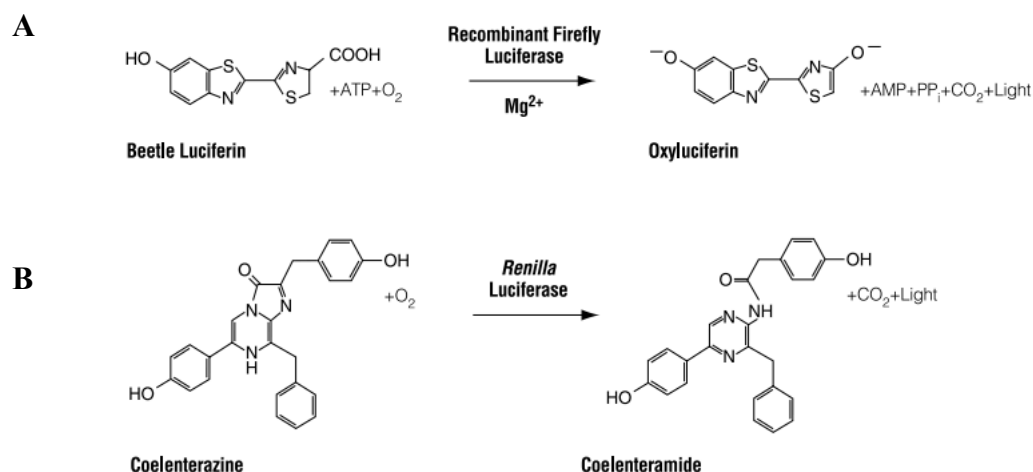
Figure 24 Firefly and Renilla Luciferases Bioluminescent reactions (Dual-Luciferase Reporter Assay System, Instructions for use [Promega Corp., MA)]

Luciferase bioluminescent chemical reaction for Firefly and Renilla. In the presence of recombinant firefly luciferase, beetle luciferin is converted to luminescence product, oxyluciferin **(A)** and renilla luciferase converts coelenterazine to luminescence product, coelenteramide **(B).**

Overall, the aims of this chapter are:

1. To successfully generate stable HSE reporter cell lines in T47D and MDA-MB-231.

2. To develop an optimised assay for HSE activity reporting, thereby generating a measure of HSF1 activation in BrCa cell lines.

Achieving these aims will provide a quantitative method that will efficiently screen and identify drugs which activate HSF1 and the HSR pathway. These will identify potential drugs whereby HSF1 inhibition would sensitise cancer cells to these anticancer agents.

4.2. Results

4.2.1. Plasmid Preparation and Generation of HSE Dual-Luciferase Reporter Model in BrCa Cell Lines

Before the reporter cell lines could be generated, the two plasmids, pGL4.41 (Promega Corporation, Madison, WI 53711 USA) and pcDNA-RLuc8 (CMV promoter) (RRID: Addgene_87121) underwent double restriction digestion at sites described in Figure 25 (refer to Figure 1 and 2 for plasmid maps). DNA purification was performed using Qiagen kit (Qiagen, California, USA), see section, 2.6.5., Table 9. Additionally, a section of the plasmids containing the ampicillin gene was removed after the bacterial work as it was no longer required in the next step. This cut also helped to reduce the size of the vector before delivery into the cell. The DNA was left linear for better transfection and to better enable stable incorporation into the genome. DNA transfection was achieved using Lipofectamine® 3000 (Invitrogen, California, USA), as outlined in section 2.2.3.2.

A

Plasmid	Digestive Enzyme	Cut Site (bp)	Cut size (bp)
HSE Reporter	BsmAI	55	4281
	PciI	4336	1764
Renilla	BgIII	5469	4533
	PciI	3641	1828

B
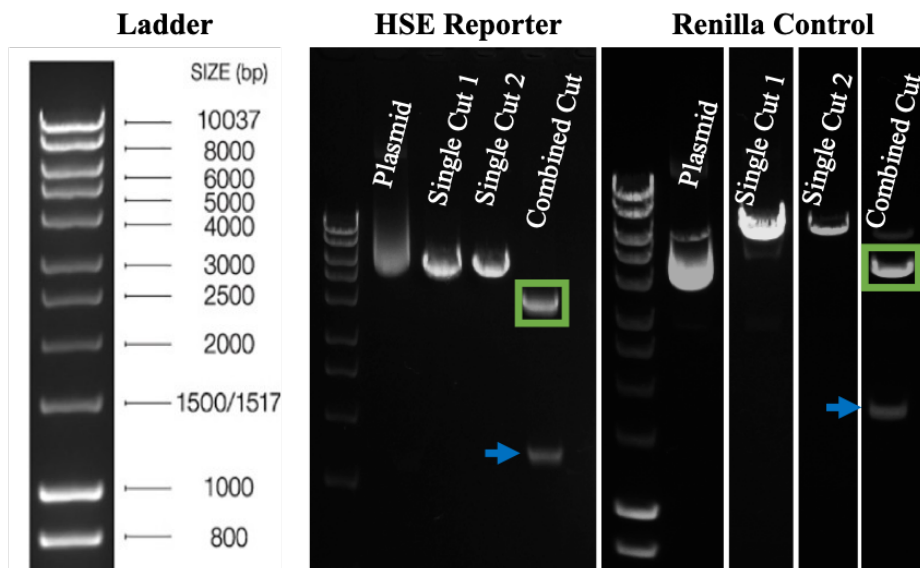
C
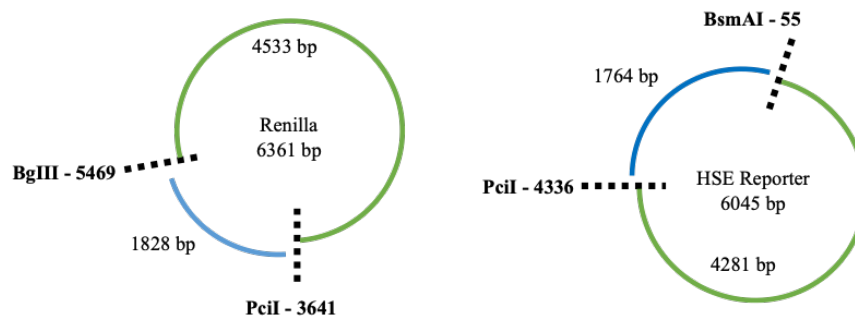
Figure 25 Heat Shock Element Reporter Plasmid

A double restriction digestion cut the DNA at two sites. For this experiment, both the HSE reporter (pGL4.41) and renilla (pcDNA-RLuc8) were cut at two sites for diagnostic confirmation and to reduce the size of the DNA to increase transfection efficiency. Specifies the restriction sites at which each plasmid was cut (including cut site) and the size of the resulting two fragments in base pair (bp) **(A)**. Image of the agarose gel after the plasmid DNA is cut and separated with respect to HyperLadder™ 1kb (Bioline, London, UK) for size determination. Green box: The section of DNA of interest to cut and purify for use. Blue arrow: The section of DNA removed from the original plasmid and discarded. **(B)**. Illustrates the molecular biology of each plasmid, visualising the cutting sites and resulting fragments **(C)**.

Once cells were successfully co-transfected with both plasmids simultaneously, they were selected with the appropriate antibiotics and stable HSE reporter cell lines in T47D and MDA-MB-231 were established. These cells were used to optimise a HSE reporter assay with the Promega Dual-Luciferase® Reporter Assay System (Promega Corporation, Madison, WI 53711 USA).

To optimise a protocol to enable screening of putative activators of HSF1 using the Varioskan reader (Thermofisher Scientific, Massachusetts, USA) and the newly generated reporter cells, appropriate cell numbers to seed in a 24-well plate were determined through a cell number titration. Increasing concentrations of cells were assayed for firefly and renilla signals to determine linearity and sensitivity of the assay. The firefly signal in this assay represents the baseline level for HSF1 activity in the BrCa cells while the renilla signal acts as an internal control and shows constitutive transcription and translation activity within the cells. From the results both T47D and MDA-MB-231 cell signals increased proportionately with increased cell number, respectively (Figure 26). It was observed that the renilla signal which is under a constitutively active promoter is linear across all cell densities. That is, with the doubling of cell number the signal intensity of renilla is doubled. This is also generally true of the firefly signal, however, linearity of the signal is lost between 80,000 and 160,000 cells for both T47D and MDA-MB-231 (Figure 26). That is, the doubling of cell number at this point does not result in a doubling of signal. This may represent a blunting of signal at these higher levels therefore 40,000 cells were chosen for plating for each cell line in the twenty-four well plates.

To determine the optimal time to read the signal outputs, a signal curve was plotted using twenty-four different readings recorded during one assay for both the firefly and renilla signals. This was done to determine the most constant reading for each luciferase signal once the activating reagents were added by the automated injectors in the Varioskan. The first reading cycle revealed that firefly signal reaches a maximal level quickly and is relatively stable upon addition of the first reagent (Figure 27). Once the second reagent is injected to block the firefly signal and activate the renilla signal, there is a significant delay until renilla reaches a maximal level and plateau. Therefore, it was determined that the reading for the firefly signal was to be recorded at reading 6 from the first reading cycle and the renilla signal was to be recorded at reading number twenty-four from the second reading cycle (Figure 27).

A

**T47D Cell Number Titration for
Firefly and Renilla Luciferase**

B

**MDA-MB-231 Cell Number Titration
for Firefly and Renilla Luciferase**
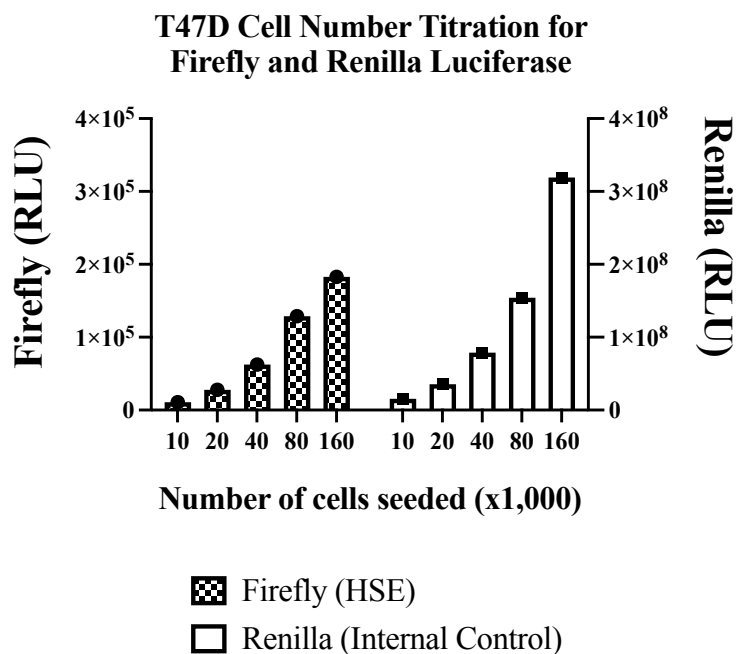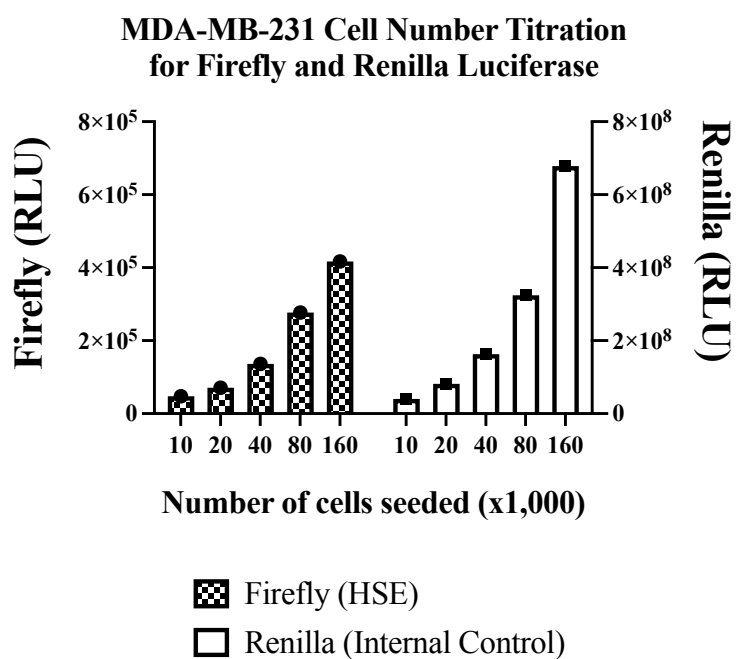
**Figure 26 Cell number titration in 24-well plate of Dual Luciferase HSE
Reporter Cell Lines**

Graphical representation of T47D cell number titration comparing firefly and renilla luminescence signal **(A)**. Graphical representation of MDA-MB-231 cell number titration comparing firefly and renilla luminescence signal **(B)**.
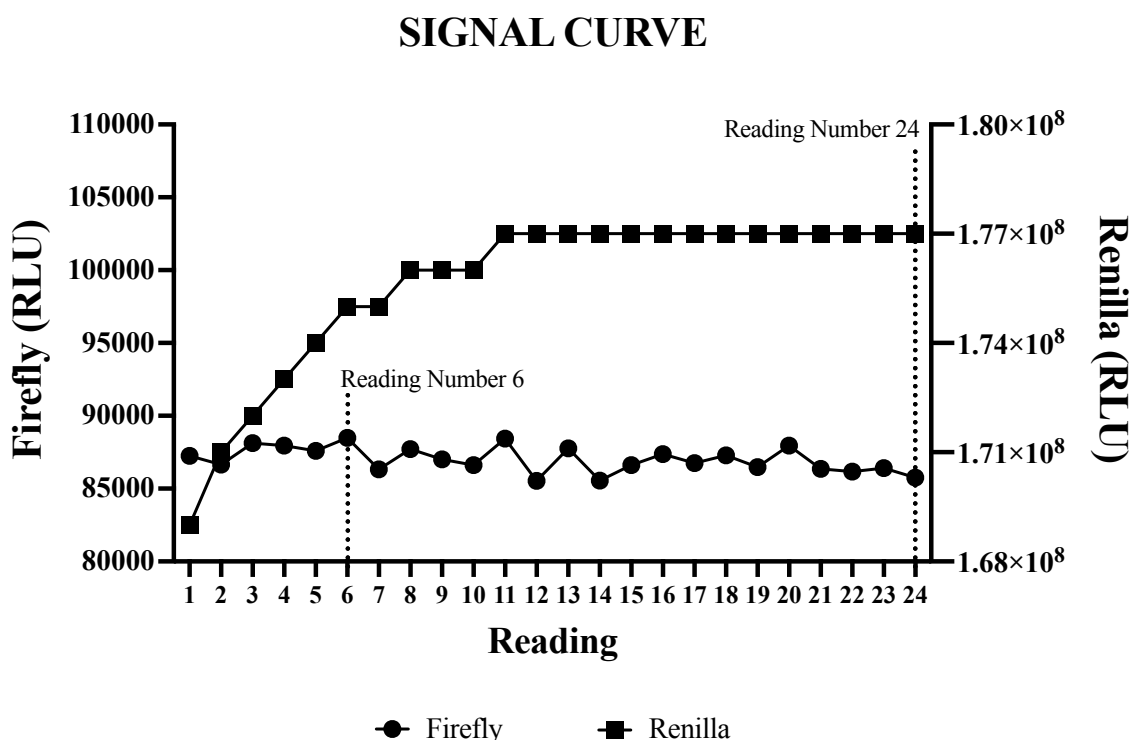
SIGNAL CURVE

Figure 27 Determining the optimal reading time for the Dual-Luciferase reporters

Representative display of the signal curve showing the luminescent power of the firefly and renilla luminescence over time (one reading per second, over twenty-four seconds). In the first reading cycle, the firefly signal (linear-like shape) was more consistent towards the start after the addition of the first reagent (LARII). The chosen reading number for analysis is reading number 6. In the second reading cycle (after the addition of second reagent STOP&GLO), the renilla signal (log-like shape) peaks later and this signal is more consistent towards the end of the reading where it plateaus. The reading number chosen for the renilla signal is reading number 24 as the signal appeared consistent up to this point.

4.2.2. Screening for activators of HSF1 using BrCa cells

A study by *Power et al. (2008)*, suggested that HSF1 transcriptional activity is upregulated by HSP90 inhibition and was later supported by *Chen et al. (2013)* demonstrating that through a feedback mechanism, HSF1 activity can be responsible for resistance and limiting drug efficacy (Powers et al., 2008, Chen et al., 2013). The relevance of this reporter model was to use two different BrCa cell lines expressing different levels of elevated HSF1 to screen for activators of the HSR.

The dual luciferase HSE reporter BrCa cells were first treated with the HSP90 inhibitors, AUY922 and 17-AAG to serve as positive controls for the anticancer drug screen (Powers et al., 2008, Koay et al., 2014, Kijima et al., 2018b). Previously in the Price lab we have demonstrated that AUY922 and 17-AAG are excellent activators of HSF1 through western blot analyses (Chai et al., 2014). Therefore, it was not surprising to identify that treating the reporter cell lines with these HSP90 inhibitors resulted in an increased level of firefly luciferase (normalised to renilla signal) indicating activation of the HSE and thus HSF1 activation in the T47D (Figures 28, 29) and MDA-MB-231 (Figures 30, 31). However, although there was a clear increase between the HSP90 inhibitor treated cells and the no treatment control cells, showing a 2-3 fold increase, a concern was that the vehicle control (DMSO) also appeared to be stimulating the HSR to levels similar to that of the HSP90 inhibitors in the T47D and some increase in the MDA-MDA-231 cell line (Figures 28-31). Therefore, before this reporter system could be utilised it was necessary to further investigate the impact of the vehicle control and whether its effects on the reporter cells could be differentiated from the actions of the anticancer drugs on the reporter cells.

Note, cells in this chapter were seeded in 24 well culture plate at 40,000 cells per well,

unless indicated (refer to section 2.4.3 for more detail of the DLR assay).

A

Titration of AUY922 in T47D
Dual HSE Reporter Assay

B

Titration of AUY922 in T47D
Dual HSE Reporter Assay
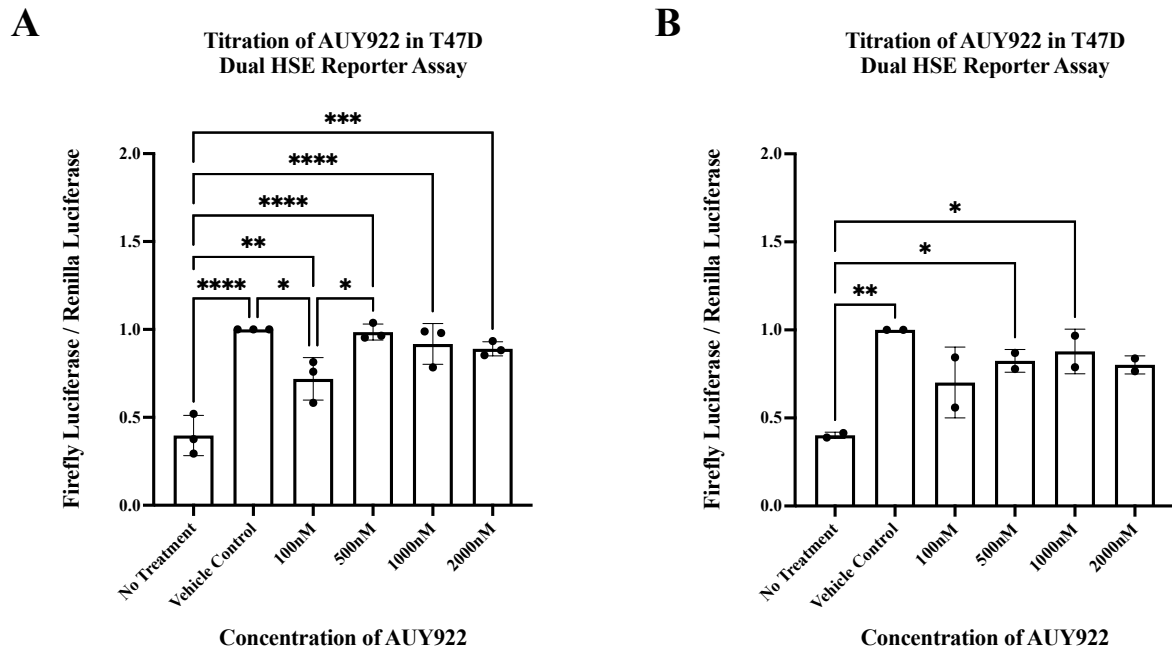
Figure 29 Testing T47D Heat Shock Response (HSE) to AUY922

AUY922 titration on T47D HSE reporter cell lines at **(A)** 40,000 and **(B)** 80,000 cells against no treatment and vehicle control (0.02% v/v DMSO). Expressed as mean $\pm$ SD. n=3.

A

Titration of 17-AAG in T47D
Dual HSE Reporter Assay

B

Titration of 17-AAG in T47D
Dual HSE Reporter Assay
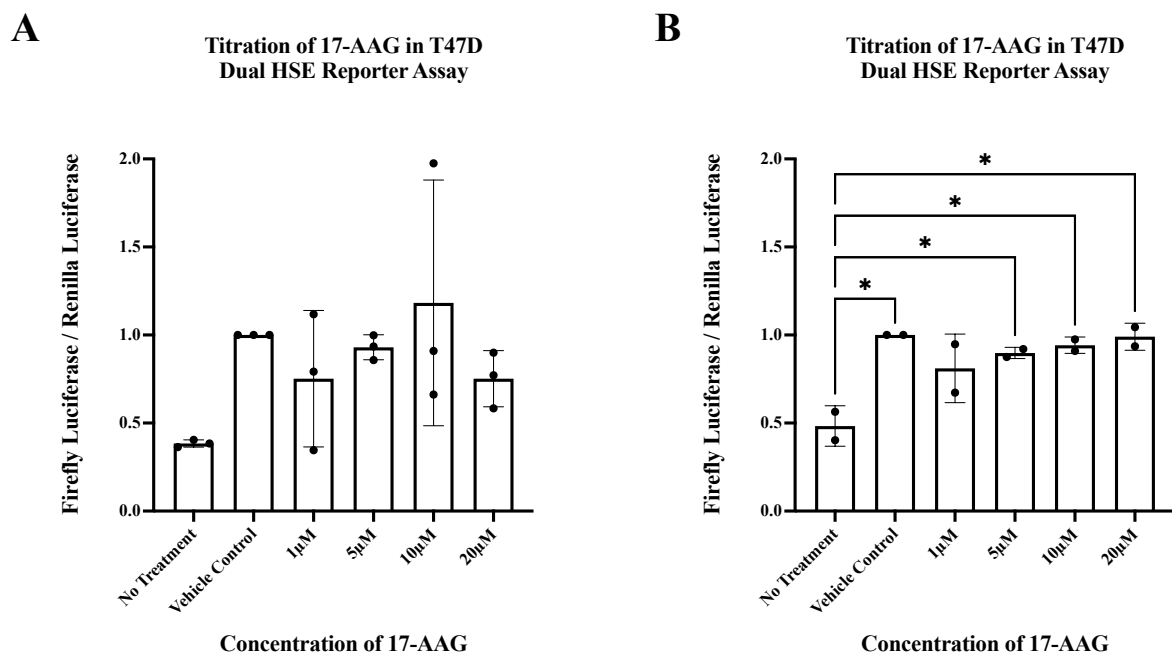
Figure 28 Testing T47D Heat Shock Response (HSE) to 17-AAG

17-AAG titration on T47D HSE reporter cell lines at **(A)** 40,000 and **(B)** 80,000 cells against no treatment and vehicle control (0.02% v/v DMSO). Expressed as mean $\pm$ SD. n=3.

A

Titration of AUY922 in MDA-MB-231 Dual HSE Reporter Assay

B

Titration of 17-AAG in MDA-MB-231 Dual HSE Reporter Assay
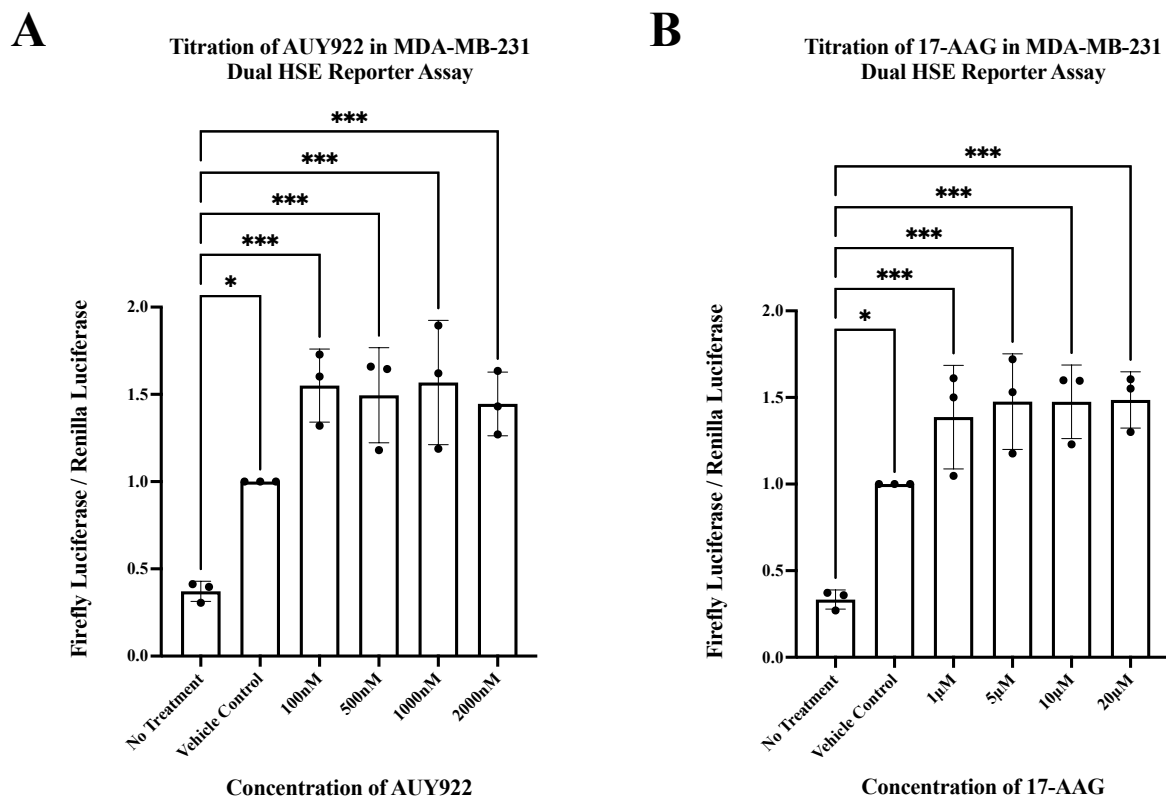
Figure 30 Testing MDA-MB-231 Heat Shock Response (HSE) to HSP90 Inhibitors

AUY922 titration on MDA-MB-231 HSE reporter cell lines against no treatment and vehicle control (0.02% v/v DMSO) **(A)**. 17-AAG titration on MDA-MB-231 HSE reporter cell lines against no treatment and vehicle control (0.02% v/v DMSO) **(B)**. Expressed as mean ± SD. n=3

4.2.3. Investigating the Effect of Common Vehicle Controls on the HSR and Other Factors

To explore the impact of the vehicle control (VC) on the reporter cells that had been previously identified, DMSO was titrated at doubling concentrations of 0, 0.06, 0.125, 0.25, 0.5 and 1% (v/v). This was done to identify whether there was a direct relationship with DMSO concentration and the level of activation of the reporter. Upon the addition of DMSO, regardless of concentration, there was a significant increase in HSE activation when compared to the no treatment controls and represented as much as a threefold increase in the expression of the firefly reporter compared to 0% v/v DMSO (Figures 31, 32).

In addition to the DMSO stored at -80°C, three other DMSO sources that had been stored at room temperatures (RT) were tested. This was to identify whether storage of DMSO at different temperatures or from different sources could alter its property with respect to initiating stress responses. It has been previously reported that DMSO toxicity can increase with increasing temperature (Best, 2015). However, no difference was observed between the differing sources of DMSO, in either the T47D (Figure 31) or MDA-MB-231 (Figure 32) including either between temperature storage or supplier.

Dimethyl sulfoxide (DMSO) Titration in Heat Shock Element Reporter Cell Line, T47D
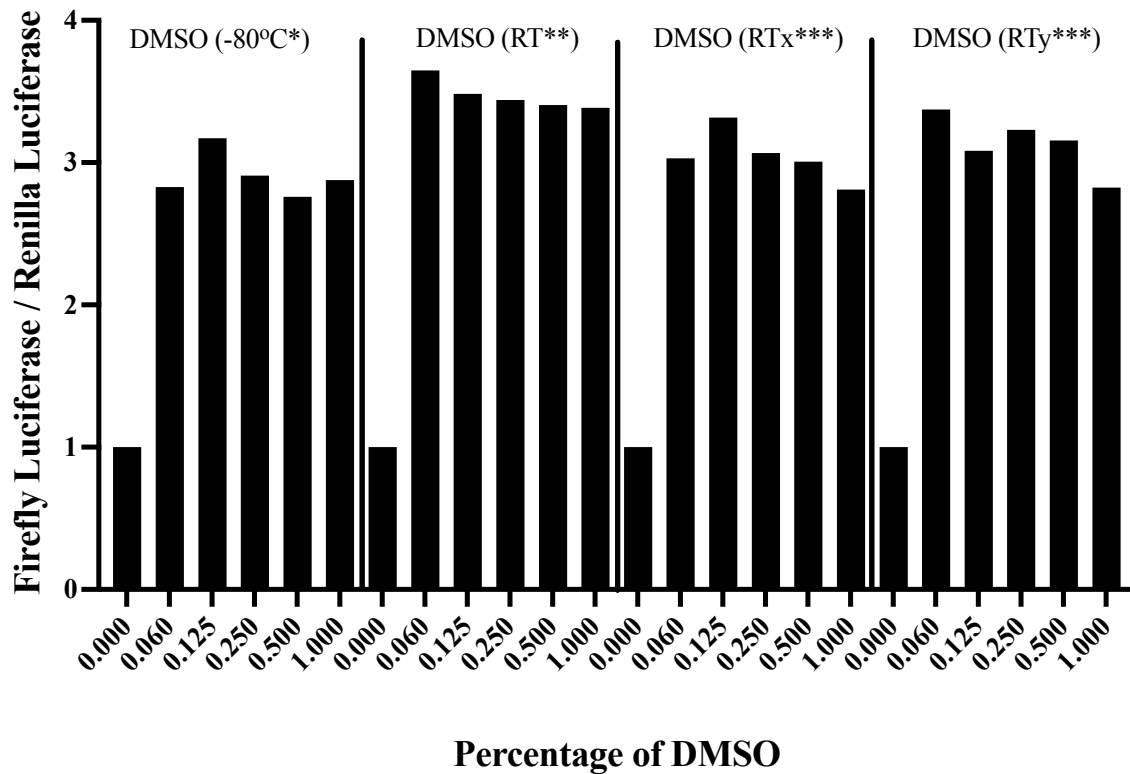
* DMSO stored in -80°C freezer
** DMSO stored at room temperature
*** Different DMSO, also stored at room temperature

Figure 31 Investigating Dimethyl sulfoxide (DMSO) effect on the HSR of T47D

DMSO titration on T47D HSE reporter cell lines for concentrations 0.0, 0.06, 0.125, 0.25, 0.5 and 1% v/v. The four types of DMSO represents DMSO stored at four different conditions or a different supplier. DMSO stored at -80°C. Three different aliquots of DMSO at room temperature (RT): RT**, RTx*** and RTy***).

Dimethyl sulfoxide (DMSO) Titration in Heat Shock Element Reporter Cell Line, MDA-MB-231

DMSO stored in -80°C freezer
DMSO stored at room temperature
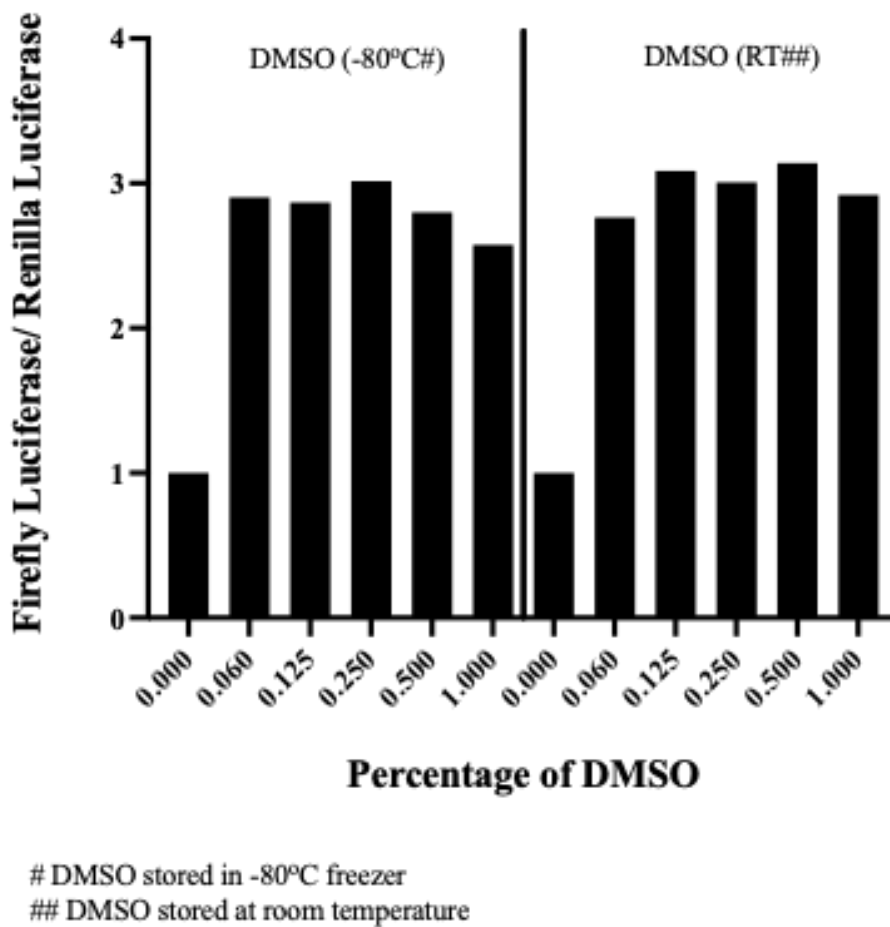
Figure 32 Investigating Dimethyl sulfoxide (DMSO) effect on the HSR of MDA-MB-231

DMSO titration on MDA-MB-231 HSE reporter cell lines for concentrations 0.0, 0.06, 0.125, 0.25, 0.5 and 1% v/v. The two types of DMSO represents DMSO stored at different temperatures, -80°C and at room temperature (RT).

Following the finding of DMSO, the question was posed whether other common solvents used as vehicle controls for the reconstitution of anticancer drugs may have a similar impact upon the reporter cells. DMSO, ethanol and water were initially tested at increasing concentrations between 0.1-10% (v/v). Consistent with previous results, DMSO increased the relative firefly luciferase signal (Figures 33, 34). In addition to that of DMSO, ethanol and surprisingly water also increased the relative level of firefly luciferase when compared to the 0% control (Figures 33, 34). For the highest concentrations of DMSO and ethanol there was a very large level of relative firefly luciferase signal, however, this could be attributed to these concentrations causing significant cell death while maintaining some level of firefly luciferase signal (Figures 33, 34). The amount of cell death was so obvious it was observable by eye and was simply validated looking under the lab bench microscope. Thus, it was unnecessary to quantitively analyse the cell number. As a result, the Renilla reading for higher concentrations cannot be used because of significant cell death. It should be noted that this was not the case for water (Figures 33, 34).
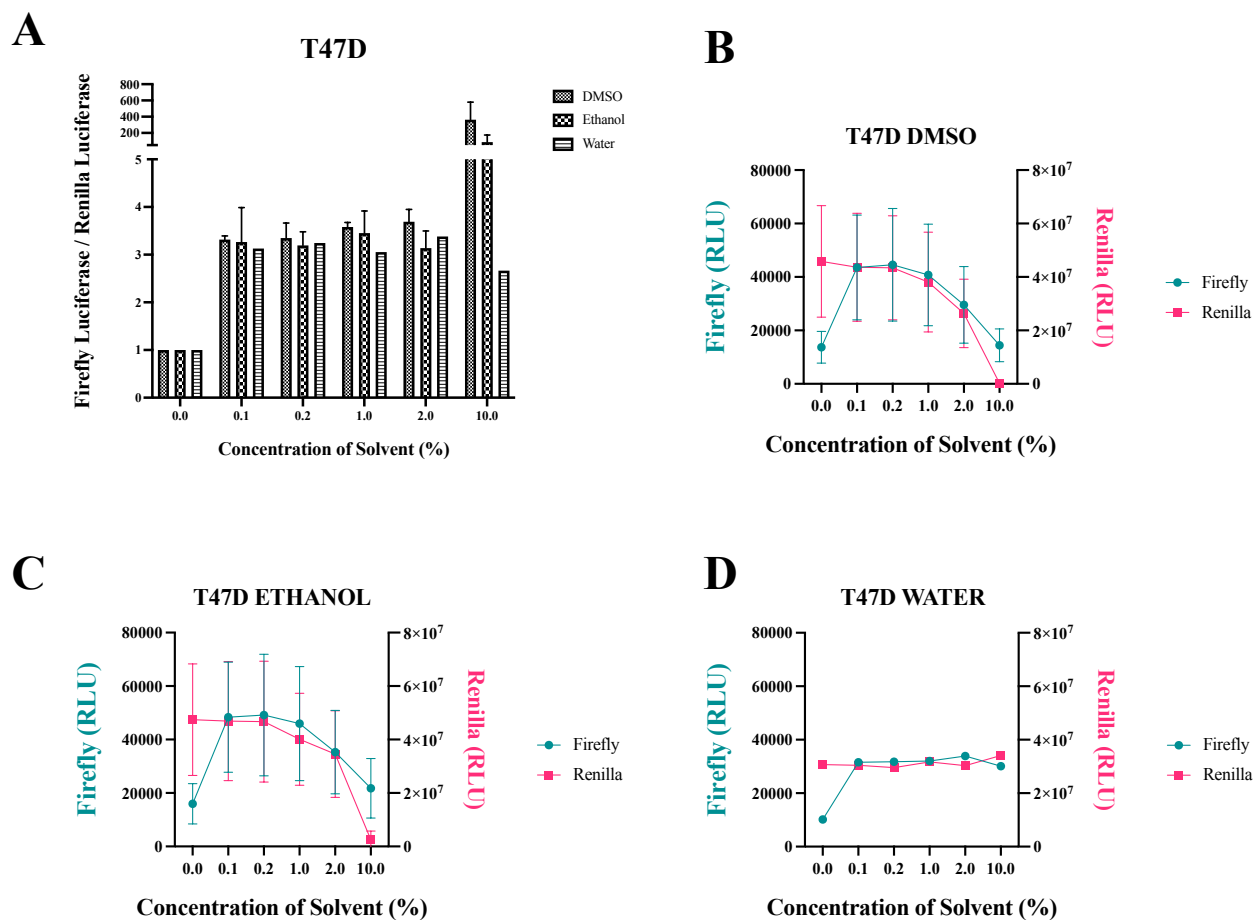
Figure 33 Investigating the effect of common vehicles on the heat shock response (HSR) in T47D cells

Examining the effects of common vehicle controls, DMSO, ethanol and water on the HSR through the transcription of the HSE in T47D HSE reporter cells. Combined graphs of the three common vehicles titrated at concentrations 0.0, 0.1, 0.2, 1.0, 2.0 and 10.0% v/v **(A)**. Individual graphs of each vehicle controls tested looking at their effect on the HSE in T47D; DMSO (n=3), ethanol (n=3) and water (n=1), respectively **(B, C, D)**. Expressed as mean ± SD.
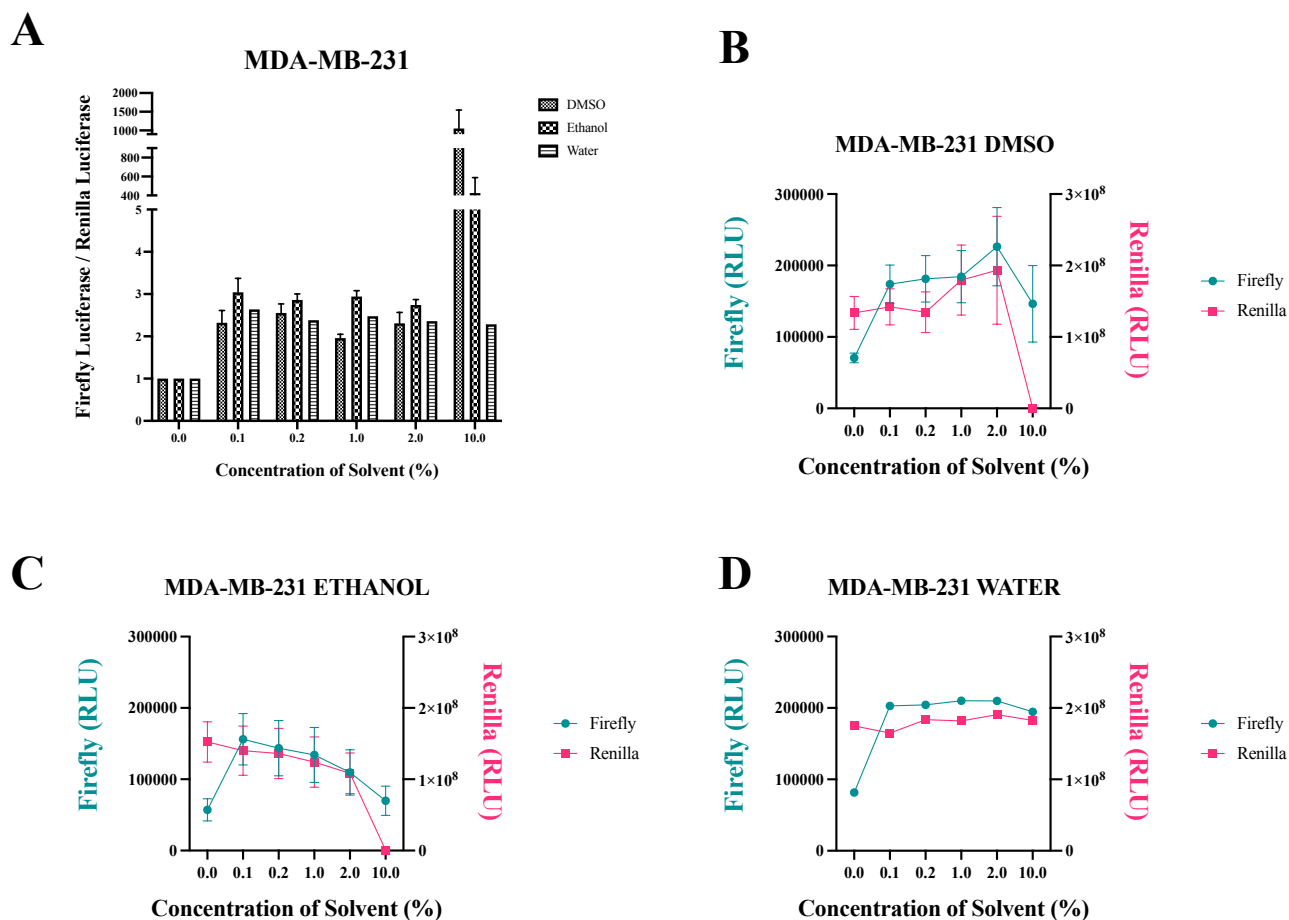
Figure 34 Investigating the effect of common vehicles on the heat shock response (HSR) in MDA-MB-231 cells

Examining the effects of common vehicle controls, DMSO, ethanol and water on the HSR through the transcription of the HSE in MDA-MB-231 HSE reporter cells. Combined graphs of the three common vehicles titrated at concentrations 0.0, 0.1, 0.2, 1.0, 2.0 and 10.0% v/v **(A)**. Individual graphs of each vehicle controls tested looking at their effect on the HSE in MDA-MB-231; DMSO (n=3), ethanol (n=3) and water (n=1), respectively **(B, C, D)**. Expressed as mean ± SD.

The initial investigations that were performed within the reporter cell lines were with incubation periods of 24 hours. To insure that an optimal timepoint had not been overlooked, where the impact of the vehicle control was minimal and the signal generated by the anticancer drug in the reporter cell lines was maximal, four other time points were examined (3, 6, 9 and 12 hours). From this series of experiments, it was determined that there was no difference between the vehicle control group and the AUY922 treatment groups at any of the concentrations tested in either of the reporter cell lines tested (Figure 35).

A

T47D Time Titration: 17-AAG

Firefly Luciferase / Renilla Luciferase (y-axis: 0.0 to 2.0)

Legend:
- 3 Hours
- 6 Hours
- 9 Hours
- 12 Hours

x-axis (Concentration of 17-AAG): No Treatment, Vehicle Control, 1µM, 5µM, 10µM, 20µM

B

MDA-MB-231 Time Titration: 17-AAG

Firefly Luciferase / Renilla Luciferase (y-axis: 0.0 to 2.0)

Legend:
- 3 Hours
- 6 Hours
- 9 Hours
- 12 Hours

x-axis (Concentration of 17-AAG): No Treatment, Vehicle Control, 1µM, 5µM, 10µM, 20µM

Figure 35 Comparing firefly levels in T47D and MDA-MB-231 over time in response to 17-AAG

17-AAG titration on T47D **(A)** and MDA-MB-231 **(B)** HSE reporter cell lines over a time course of 3, 6, 9 and 12 hours. In both low and high metastatic potential cell lines, T47D and MDA-MB-231, respectively, 17-AAG elicited a higher transcription of firefly than no treatment, but no significant difference compared to vehicle control. There is neither a difference between the time points. Expressed as mean ± SD. n=3.

Finally, to examine what was occurring at the protein level, western blot analyses were conducted utilising isolated protein from reporter cell lines that were exposed to increasing concentrations of DMSO and AUY922 over a 24 hour period (Figure 36). Interestingly, although in the luciferase assay, DMSO increased the relative firefly luciferase signal indicating increased activation of HSF1, protein levels of HSPs that should be increased upon HSF1 activation were unaffected (Figure 36A). In contrast to this, AUY922 strongly induced the expression of HSP105, HSP90 and HSP70 in both cell types (Figure 36B). However, the vehicle control, 0.02% v/v DMSO, did not change the expression of HSPs despite increasing the relative firefly luciferase signal in the luciferase assay indicating activation of the HSE (Figure 36B).

A   Concentration of DMSO (%)

HSP105

HSP90α

HSP70

Beta Actin

T47D   MDA-MB-231

B   Concentration of AUY922

HSP105

HSP90α

HSP70

Beta Actin
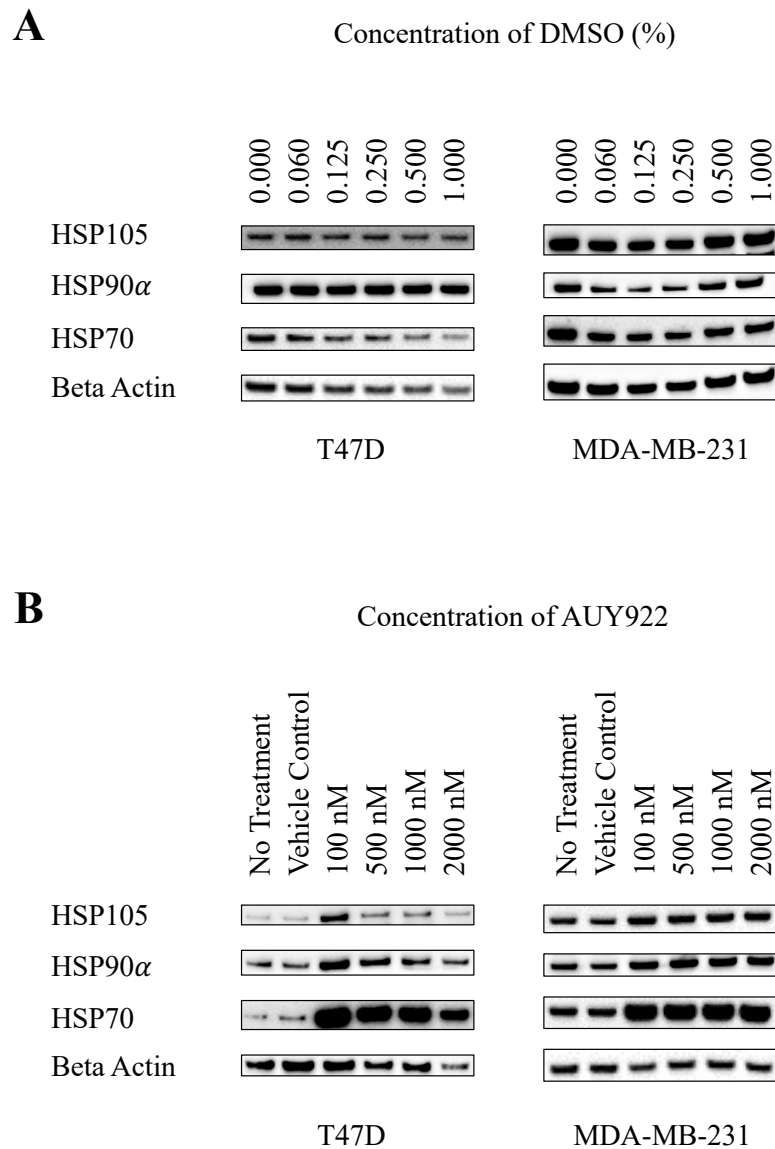
T47D   MDA-MB-231

Figure 36 Western Blots of Heat Shock Proteins for T47D and MDA-MB-231 when treated with different concentrations of DMSO and AUY922

Western blots for proteins from a DMSO titration on T47D and MDA-MB-231 HSE dual-luciferase reporter cells examining HSPs, downstream targets of HSE activation **(A)**. There are no changes between the expression of HSPs between the different concentrations of DMSO and to the 0% DMSO control. Western blots for proteins from the AUY922 titration on T47D and MDA-MB-231 HSE dual-luciferase reporter cells examining HSPs, downstream targets of HSE activation **(B)**. No treatment group refers to cells grown in complete medium. AUY922 upregulated HSPs in both T47D and MDA-MB-231. The vehicle control, 0.02% v/v DMSO, did not affect the expression of HSPs, even when compared to cells in complete medium. n=1.

4.3. Discussion

HSF1 trimers in the nucleus bind to HSE within promoters to enable transcription. However, unlike the conventional HSR in normal cells, tumour cells directly regulate HSF1 activity through oncogenic signals like those named previously (see Chapter 3), and studies have elucidated how HSF1 is regulated and can influence oncogenic signalling in cancer, including some that are involved in anticancer drug resistance (Dai et al., 2007, Tchénio et al., 2006, Wang et al., 2018). Thus, understanding the relationship between available anticancer drugs and the HSR, specifically ones that activate HSF1 activity will inform future treatment regimens for patients. Ultimately, outcomes from an efficient large-scale screen to identify drugs that induce a HSR could form part of a database that provides more informed decisions in relation to the use of anticancer drugs and their combinations.

4.3.1. Generation of HSF1 Activator Screening Model

While there are advances in detection methods and early-stage tumours are more treatable, diagnosis of late stage, particularly metastatic tumours, remains a challenge due to their reduced sensitivity to anticancer drugs. HSF1 is proposed as an attractive target for the sensitisation of cancer cells to anticancer drugs but as postulated in this thesis, this maybe even more so for drugs that activate HSF1.

To identify such anticancer drugs the strategy was to generate a dual-luciferase reporter cell model in two cell lines of which one had a low metastatic potential while the other had a high. These BrCa cells were generated to constitutively expresses renilla luciferase

via pcDNA-RLuc8 as an internal control and pGL4.41[luc2P/HSE/Hygro] vector (Promega Corporation, Madison, WI 53711 USA) that expressed firefly luciferase (luc2P) under the control of a promotor that contains four copies of the canonical HSE sequence. The T47D (low metastatic phenotype) and MDA-MB-231 (high metastatic phenotype) cells were transfected with these vectors and were made stable through antibiotic selection. Compounds that could increase the expression of firefly compared to the no treatment control and being normalised by renilla would be identified as specific HSE transcription promoters, thus HSF1 activators.

4.3.2. Validating dual luciferase HSE reporter cell lines and establishing optimised model for large scale screening of compounds

A specific protocol was developed and optimised for the purpose of this model to automate dual reagent injecting by Varioskan Flash Spectral Scanning Multimode Reader (Thermofisher Scientific, Massachusetts, USA) before assaying. The stable dual luciferase reporter cell lines were first tested for its functionality through examining its renilla- and firefly-luciferase expression levels in unstressed conditions. Each luciferase signal is read continuously twenty-four times and a signal graph was plotted (Figure 27). It was identified that firefly signal was relatively stable after the addition of the first reagent, while renilla signal rose to a peak then plateaued. From this observation, reading number six for firefly and reading number twenty-four for renilla was recognised as the most stable signal and used for signal interpretation moving forward. As expected, luciferase signals for both firefly and renilla increased proportionally to the increase in cell number. Although, at the highest cell number (seeded 160,000 cells per well) there appeared to be a loss of this relationship. One explanation may be that

this is the system's saturation point near that level. If this was the case, then the system may be reaching its maximum range and signals beyond this point will not be detectable. Together, at this point it was believed that both reporter models were optimised and functioning as designed.

To test this model in both cell lines, cells were pre-treated with HSP90 inhibitors, AUY922 and 17-AAG before assaying. HSP90 inhibition was expected to activate HSF1 activity and thus be a positive control for transcriptional activity induced through HSE binding. The intention of a positive control was to set the threshold for HSE activation and test for activators of HSF1 within this dynamic range. The drug concentration for AUY922 and 17-AAG were titrated to 100nM, 500nM, 1000nM and 2000nM or 1μM, 5μM, 10μM and 20μM, respectively. While treatment with AUY922 and 17-AAG showing upregulated HSE binding, when compared to the vehicle control (0.02% v/v DMSO) there was very little difference (Figure 28 – 30). This may be an interesting factor to consider with reference to what we noticed earlier in the discussion where the doubling of firefly signal, thus linear relationship ceased at higher cells numbers. Whether this could be a system limitation of the dynamic range at these higher saturating levels and this is also supported by the disconnect between the firefly signal and HSP expression, to be discussed in section 4.3.3.. Nevertheless, this assay using the two HSP90 inhibitors revealed that the vehicle control, DMSO, used at a concentration of 0.02% v/v increased firefly expression indicating that HSR was stimulated in both the T47D and MDA-MB-231 cells. This is not the first time DMSO has been identified to activate HSF1 activity, in a similar study using luciferase reporters in HEK293 cells treated with ~ 0.7% v/v DMSO control cells also increase the HSR overtime (Kijima et al., 2018a). Although, in their actual methods, it is unclear whether *Kijima et al. (2018)*

had used the appropriate cells as control for DMSO control (Kijima et al., 2018a). Furthermore, in a study by *Bagatell et al. (2000)* looking at activators of HSF1 also demonstrated that in the presence of HSF1, DMSO upregulated HSP72 (Bagatell et al., 2000). This is validated by the fact that in the same experiment, Cisplatin was dissolved in water and under the same conditions did not express HSP72 (Bagatell et al., 2000). Therefore, while maybe overlooked, DMSO appears to have more of an effect on the HSR than previously acknowledged.

4.3.3. Investigating the Effect of Vehicle Control on HSF1 Activity

Previously, concentrations lower than 1% v/v of DMSO were widely accepted as not having an impact in the experimental setting. However, as observed, this as a vehicle control in the BrCa dual-luciferase reporter cells still elicited considerable transcription at the HSE. Initially, we suspected that this was a problem with the DMSO used so we titrated different sources of DMSO stored at different temperatures in both cell models (see Figure 31, 32). It was obvious that there was a difference in firefly signal, thus HSE transcription, between the no DMSO group and the DMSO treated group. This was surprising, both that DMSO at such low concentrations could elicit such a response in cells at a transcriptional level and that there were no proportional changes or any change in the HSF1 activation between the lowest concentration of DMSO at 0.06% v/v and highest concentration at 1% v/v tested. This information supports that DMSO may potentially effect transcription more than previously identified and in a concentration independent manner at concentrations lower than 1% v/v. In a recent study, *Verheijen et al. (2019)* found that DMSO actually induced dramatic changes in human cellular processes *in-vitro* (Verheijen et al., 2019). In fact, at concentration of 0.1% v/v DMSO

they found more than two-thousand differentially expressed genes compared to vehicle control and deregulations of microRNAs in cells (Verheijen et al., 2019). Additionally, DMSO-induced stress was previously identified, and at concentrations of 1%, v/v DMSO can impair cell viability, mitochondrial integrity and glutamate transporter expression of astrocytes (Yuan et al., 2014).

To further understand this, we looked at two other common vehicles, ethanol and water. This time we titrated all three vehicles at concentration 0%, 0.1%, 0.2%, 2% and 10% v/v, again in both cell lines. As seen in Figure 33 and 34, HSE transcription is also sensitive to ethanol and water and effected transcription in a similar way DMSO does. This reiterates the importance of proper vehicle controls as part of good study design and especially in the context of the HSR. Several studies have demonstrated that both DMSO and ethanol can modulate HSF1 activities (Morimoto, 1998, Pignataro, 2019, Muralidharan et al., 2014, Varodayan and Harrison, 2013, Pignataro et al., 2007, Rütgers et al., 2017). Exposure to ethanol increased the expression of Hsp27, HSP40, Hsp70 and Hsp90 *in-vitro* (Pignataro, 2019, Muralidharan et al., 2014). *Pignataro et al. (2019)* also found through immunocytochemistry techniques that there was translocation of HSF1 and induction of HSP mRNAs in acutely intoxicated mice, while an electrophoretic mobility shift assay also showed that ethanol increased the DNA binding ability of HSF1. Moreover, ethanol may also have a role in mediating HSF1 activity. In microarray performed on cultured cortical neurons chronically exposed to ethanol, HSP genes, HSP105, HSP70 and HSP30 were downregulated (Gaspary et al., 1995). Furthermore, loss of HSF1 by either siRNA or dominant-negative HSF1 construct prevented the ethanol induction of the HSPs (Pignataro, 2019). This was also

seen in *Varodayan and Harrison (2013)* with HSF1 knockdown which prevents gene induction by ethanol (Varodayan and Harrison, 2013).

To test whether time played a role in the irregular effect of DMSO as a vehicle control. We titrated 17-AAG at concentrations 1μM, 5μM, 10μM and 20μM over 3, 6, 9 and 12 hours hypothesising that in the original observation at 24 hours post-treatment there was a recovery of the cell, thus the full extent of the HSR was missed (see Figure 35). There was no difference in the response from either cell lines to time between the vehicle control and 17-AAG treated. Confusingly, HSE transcription did not reflect the HSP90 inhibitor's ability to induce HSF1. To validate this, two sets of western blots were analysed with the same proteins used to assay DMSO and AUY922 titration from both cell lines to look at common downstream markers of HSF1 activation including, HSP70, HSP90α, and HSP105. Interestingly, the western blots from the same experiment did not reflect the results seen from the dual-reporter assay. Western blots in Figure 36 showed that DMSO does not influence HSP levels while treatment with AUY922 does and is consistent with HSP90 inhibitors HSR inducing role (Kijima et al., 2018b). Therefore, the issue is that there is a disconnect between the western blots and luciferase assay. In the western blots, showed that the vehicle control was not seen to induce the HSF1 and AUY922 does, and this highlights that the reporter assay failed to differentiate this. Thus, indicating that the reporter cells are not sufficient to accurately monitor the HSR and further investigations will be necessary to explain what is stimulating the low expression of the firefly. One way to examine this would be to use an anti-firefly luciferase antibody to compare expression of firefly protein with the firefly luciferase assay signal. This would narrow down whether there is a technical or biological limitation of the assay.

Interestingly, in a study by *Santagata et al. (2013)* found that HSF1 has the ability to maintain essential support for the malignant state by blocking apoptotic responses and promoting protein synthesis, anabolic energy metabolism, mitogenic signalling pathways, and pathways that facilitate invasion and metastasis is exquisitely sensitive to the activity of the ribosome (Santagata et al., 2013). Cancer cells often coerce highly conserved, adaptive non-oncogene systems for their benefit, HSF1/ ribosome circuit being one of those to support the malignant phenotype (Silvera et al., 2010, Roux and Topisirovic, 2012, Hensen et al., 2012, Peng et al., 2002, Solimini et al., 2007a). Therefore, it is possible that the discrepancy between HSE activation and the translation of HSPs may introduce ideas for the future understanding of the post transcriptional activity in the HSR. While this discovery has impeded the progression of the reporter cell models to identify activators of HSF1, there may be value in exploring HSF1 in relationship to ribosomal activators and valuable insights into to agents that target translation and its upstream regulatory pathways (Solimini et al., 2007b).

Overall, the fact that there are low firefly levels is indicative of low HSE transcription, yet the HSPs remain elevated in the protein analysis suggests there could be altered activity either at post transcription modification to the mRNA or is dependent on ribosomal activities that are not yet understood.

4.4. Conclusion

Ultimately, although this system could enable large-scale screening for HSF1 activators from compound libraries using high-throughput luciferase reading, unfortunately its current dynamic range between vehicle control and sample is problematic. It would be interesting to observe how different levels of elevated HSF1 in two BrCa cell lines with vary metastatic potentials may respond differently to activators of HSF1. This will add to the body of knowledge that others have already demonstrated in relation to inhibitors and activators of HSF1, including similar approaches like use of HSE reporters in other cell lines (Westerheide and Morimoto, 2005, Au et al., 2009, West et al., 2012). At this stage, a possible reason for the unmatched protein expression profile and activation of the HSE may be due to an unknown mechanism along the protein synthesis pathway. Additionally, the fact that DMSO as a vehicle control induced HSE transcription is important for future consideration as many drugs are dissolved in DMSO and thus, may confound results if appropriate controls are not used. Therefore, an understanding of this relationship and the assay's limitation is important before the system can be utilised for screening of activators of HSF1.

CHAPTER 5: FINAL DISCUSSION

5.1. Introduction

Cells initiate stress response pathways to survive stressful conditions that they are naturally and constantly exposed to including biological stressors such as hyperthermia, nutrient deprivation, toxins, and radiation (Swan and Sistonen, 2015). It is normal for healthy cells to be challenged by proteotoxic stressors that can cause unfolded or misfolded proteins but a cellular defensive mechanism called the HSR can buffer against this disruption (Vihervaara and Sistonen, 2014). The HSR is also highly significant in human pathology, particularly in cancer where cells hijack the HSR for tumourigenesis and malignant transformation (Dai and Sampson, 2016).

The main regulator of the HSR is HSF1 (Vihervaara and Sistonen, 2014). In healthy cells, HSF1 is not activated unless there is proteotoxic stress. Under stress, HSF1 monomers will dissociate from chaperone complexes, that normally suppress their function, and undergo multiple steps to achieve activation, including trimerisation, nuclear translocation, phosphorylation and then DNA binding to HSE promoter sites to perform its transcriptional function (Vihervaara and Sistonen, 2014). Moreover, in cancer, HSF1 is believed to act as a pro-oncogenic factor and is regulated by oncogenic and tumour-suppressive signalling pathways (Vydra et al., 2014, Jiang et al., 2015).

Furthermore, evidence is accumulating that HSF1 has involvement in mediating metastasis with highly metastatic tumours having a higher level of activated HSF1 localised in the nucleus (Triandafillou and Drummond, 2016). A study by *Santagata et al. (2011)* identified that HSF1 largely remained in the nucleus of malignant BrCa

compared to healthy breast cells, which is an indication of active HSF1 in these tumours (Santagata et al., 2011a). High levels of nuclear HSF1 are also present in many other types of cancers, including cervical cancer, colon cancer, lung cancer, pancreatic cancer, prostate cancer, and meningioma suggesting favoured HSF1 trimers, relocation to the nucleus and activation in these cancers (Mendillo et al., 2012, Vihervaara and Sistonen, 2014, Jiang et al., 2015, Vydra et al., 2014). Additionally, elevated HSF1 and its activation induce high expression of HSPs which can lead to severe radio/chemoresistance (Frezzato et al., 2019). While, in those patients responding to both traditional chemoimmunotherapy and kinase inhibitors regimens, HSF1 levels are decreased and correlate with responsiveness during treatment course (Frezzato et al., 2019). Chemoresistance is one of the main reasons for the failure of BrCa treatment in many advanced cancers (Yeldag et al., 2018, Han et al., 2019). A major issue with these resilient cancer cells is the complexity and multifactorial nature whereby they continue to evade or adapt to the presence of anticancer drugs (Yeldag et al., 2018). Therefore, HSF1 is not only an important target in the pathology and progression of cancer but may also be a target for sensitising tumours to anticancer therapeutics.

This thesis examined whether the effectiveness of stress-inducing anticancer therapeutics used in the treatment of metastatic BrCa is dependent on the levels of HSF1 and its activity. The study specifically investigated whether HSF1 knockdown in cancer cells sensitised them to these drugs and whether there is a direct link between chemotherapeutic and targeted agents that trigger the HSR. In doing so, the study aimed to firstly, screen whether knockdown of HSF1 in a series of BrCa cells would make them more sensitive to the therapeutic agents identified and secondly, establish a dual

HSE luciferase reporter model for use in different cancer cell lines to perform a large-scale screening looking for activators of HSF1 in cell specific response.

5.2. HSF1 Activity in Cancer is Context Dependent

HSF1 role in cancer broadens to more than just the classical HSR and provides critical relief to the stress experienced by cancer cells (Solimini et al., 2007b). Cancer cells are dependent on HSF1 to facilitate tumourigenesis and progression as a non-oncogenic addiction by regulating several activated oncogenes and mutated tumour suppressors (Solimini et al., 2007b, Mendillo et al., 2012, Xi et al., 2012, Vydra et al., 2014). Therefore, HSF1 is hypothesised as a unique and likely universal therapeutic target to inhibit multiple oncogenic pathways in cancer. Interestingly, both HSF1 activators and inhibitors have been seen in a context specific manner to be an effective anticancer treatment against certain types of tumours (Mun et al., 2020, Velayutham et al., 2018, Dong et al., 2020, Dong et al., 2019).

While HSF1 activation has been shown to promote cancer advancement, drugs activating HSF1 have also been used in cancer treatment regimes. A study by *Santagata et al. (2012)* suggests that over activation of the HSR by HSF1 can heighten stress levels beyond the cells capacity to compensate, where it is no longer beneficial even for cancer cells and thus they will undergo cell death (Santagata et al., 2012). Similarly, hyperthermia (heat therapy) is shown to sensitise cancer cells to some forms of treatment when used conjunction to other forms of cancer therapies such as radiation therapy and chemotherapy (Torigoe et al., 2009). Interestingly, use of some HSP90 inhibitors in clinical trials trigger dissociation of HSF1 from HSP90 complexes and activate the pro-survival HSR. However, this is only a transient induction of HSF1 and will decrease if

HSF1 is not activated through trimerization because HSF1 monomers are less stable and without the binding with HSP90 complexes are susceptible to degradation (Gaspar et al., 2010, Vihervaara and Sistonen, 2014). Furthermore, HSPs are also an important element to tumourigenesis and cancer progression regulated by HSF1 (Vihervaara and Sistonen, 2014, Dai and Sampson, 2016, Calderwood and Ciocca, 2008). However, depletion of HSF1 in normal cells and in cells at an early stage of transformation does not impact on cell growth and survival in the same way that occurs in high-grade cancer cells (Nguyen et al., 2013a). In support if this is a study by *Zaarur et al. (2006)*, suggested that targeting the HSR may facilitate the use of proteasome and Hsp90 inhibitors for cancer treatment (Zaarur et al., 2006). Moreover, a study by *Jin et al. (2011)* also observed in the HSF1-NULL mice that targeting HSF1 did not cause systemic toxicity to normal tissue like the cytotoxic induced by chemotherapeutics (Jin et al., 2011). Thus, targeting HSF1 in combination with other therapies may be preferable with anticancer drugs that are already known to have many side effects. Therefore, combining HSF1 and HSP inhibitors with cytotoxic drugs that elicit a HSR response may have synergistic effects and improve patient outcome.

A major challenge to targeting HSF1 as a combined anticancer strategy is the current lack of specific and approved drugs. Accompanying this is a lack of resources that form a database identifying both the synergistic and antagonistic effects of HSF1 inhibition in combination therapy. This is pivotal considering the diverse role of HSF1 in a context dependent manner. This study provides data that will be beneficial in elucidating the mechanism by which HSF1 interacts with other anticancer drugs used in metastatic BrCa and emphasise the importance of strategic, like cautious combinations with these drugs to avoid adverse or contradictory effects.

In this thesis, we demonstrated that targeting HSF1 activity can be specific to the cancer type and is dependent on the co-targeting pathways. It is interesting that we were able show how the inhibition of HSF1 can have both sensitising and desensitising effects in metastatic BrCa cells. In line with our hypothesis, T47D cells with HSF1 knockdown became significantly sensitive to doxorubicin. As we expected, elevated levels of HSF1 in cancer cells is responsible for HSP chaperoning and aids in cell survival. Thus, with decreased HSF1 activity, we anticipated that the HSP stress response will reduce and cause cell death. However, this was not always true. We also identified how HSF1 knockdown can significantly limit the efficacy of certain drugs like the TKI that targets EGFR like Lapatinib. Knockdown of HSF1 may be interfering with EGFR recycling, such that HSF1 involvement in chaperone-mediated autophagy is impaired and consequently the autophagy-mediated lysosome recycling of the EGFR is loss. Together, in a context dependent manner, activities to either activate or inhibit HSF1's activity may be effective to treat BrCa. For example, KRIBB11 is a more specific HSF1 inhibitor that interferes with co-factors of HSF1 activity rather than inhibiting the broad activity of HSF1 (Yoon et al., 2010, Yoo et al., 2021, Antonietti et al., 2017, Chen and Ott, 2020). *Yallowitz et al. (2018)* used KRIBB11 and lapatinib demonstrated synergised effect in degrading mutant TP53 and EGFR in lapatinib-sensitive BT474 cells while restored mutant TP53 response to lapatinib in BT474 lapatinib resistant cells (Yallowitz et al., 2018). Therefore, HSF1 inhibitors and activators may both have potential therapeutic benefits when considered wisely in the clinic.

5.3. Limitations

While the HSF1 knockdown screen with anticancer drugs for synergistic effects in metastatic BrCa was unable to identify many targets suggested from our labs previous bioinformatic analyses, doxorubicin used combination with HSF1 knockdown did significantly demonstrate a potential for combining chemotherapeutics with an effective HSF1 inhibitor. Moreover, we also highlighted the context dependent and highly specific nature of HSF1 inhibition in cancer cells.

HSF1 knockdown in combination with Lapatinib was significant in reducing cell sensitivity to treatment. Thus, this marks the importance of the selection of anticancer drugs to be used with HSF1 inhibitors in the more aggressive, high-grade cancers.

Furthermore, it is acknowledged that insignificant results using this assay is not enough to reject the relevance of using HSF1 inhibitors in combination with the targeted pathways considered. In fact, the lack of significance can be a limitation of specific sites that the anticancer drugs targeted or the sensitivity and relevance of our assay. Firstly, sensitivity refers to the ability of our assay being able to detect smaller changes in cell death considering the aim of our assay was to look for major differences and with a ten-fold difference between each drug concentrations we could have missed changes that did not fall within this spread. Alternatively, if this assay was to be repeated, instead of a log-10 concentration, it could be adjusted for smaller log differences between each concentration like log-3 to capture changes that maybe have been missed. Of course, it remains necessary to have an assay that will translate into meaningful treatment differences. Therefore, aside from statistical difference, an example of what may have started as changes considered minor in magnitude may have major physiological

consequences is combining recombinant humanized anti-HER2 antibody (Herceptin) and paclitaxel (Baselga et al., 1998). Early studies looking at this combination while showed Herceptin results in an additive effect on the cytotoxicity of paclitaxel, the magnitude of Herceptin-mediated enhancement of the antitumor effects of paclitaxel was only up to 67% in BT-474 cells, 50% in SK-BR-3 cells, and 32% in SK-OV-3 cells (Baselga et al., 1998). However, the combination of Herceptin and paclitaxel is today used clinically as an effective first-line treatment in patients with metastatic HER2 positive BrCa (Guo et al., 2021, Loibl and Gianni, 2017).

Secondly, another possibility is that HSF1 effect in combination with these drugs is highly specific to a sub-population/ phenotype of the cancer cells that are extremely metastatic or resistant as alluded to in prior studies, for example cancer stem cells. Our assay was limited by looking at the effects HSF1 inhibition has on the whole cell population. The sub-populations in cancers are cells with enhanced fitness under harsh environmental pressures encountered during cancer progression (Nguyen et al., 2016). These cells may be harder to treat, more likely to contribute to the cancer initiating cells (CIC) population as they are more resistance to selection pressures of tumourigenesis and anticancer drugs. Therefore, if HSF1 is particularly effective in this situation then it has yet been extensively studied and the assay used needs to tailor this influence of HSF1 on the phenotype, rather than the current focus on enhancing drugs overall kill power.

5.4. Future Direction and Conclusion

In conclusion, criticism for the HSF1 knockdown assay is while it makes me a good screen to get a general idea of drug response and identification of large differences, it

lacks both specificity and sensitivity. Instead, an xCELLigence system may offer a more sensitive way of analysing the percentage of cell death. xCELLigence is a label-free technology that can monitor cell number by changes in impedance on the electrodes in E-plates, but it is expensive and will not be helpful learning about the specific population that HSF1 knockdown may be effective to. Furthermore, while some findings were insignificant this does not necessarily mean that treatment with HSF1 knockdown is ineffective. Instead, maybe HSF1 needs to be combined with two or more drugs that has already been known to have synergistic effect; this advanced multidimensional combination can assess whether HSF1 knockdown further enhances cancer cell sensitivity and potentiates toxicity. This hypothesis comes from the observation of DMSO used at higher concentrations in vehicle control. Alternatively, as discussed it would be interesting to follow up this assay with assays targeting the subpopulation of cancer cells. HSF1 may be ineffective at increasing overall/ mass cell death and cannot be accessed like this, rather due to its specificity may offer efficacy when targeting harder to kills cells (e.g., cancer stem cells or MICS that could in fact be a smaller population). Thus, an overall difference was not observed. Additionally, if the CIC population is identified, there may also be benefits by looking at the role of HSF1 in CIC/ MICS *in-vivo*, as this could give insight into recurrent tumours in a dynamic organism. In terms of the HSE dual-luciferase reporter, the vector used in the study contained four copies of the classical/ canonical HSE and maybe this is less relevant in metastatic BrCa cells. Therefore, it will be interesting to generate a vector that has HSE that are more specific to non-HSP modulation and thus to a non-canonical HSE to compare with the current canonical HSE reporter and provide a different perspective of HSF1 activities in cancer.

REFERENCES

ABO-ZEID, M. A. M., ABO-ELFADL, M. T. & GAMAL-ELDEEN, A. M. 2019. Evaluation of lapatinib cytotoxicity and genotoxicity on MDA-MB-231 breast cancer cell line. *Environ Toxicol Pharmacol,* 71**,** 103207.

AGGARWAL, V., TULI, H. S., VAROL, A., THAKRAL, F., YERER, M. B., SAK, K., VAROL, M., JAIN, A., KHAN, M. A. & SETHI, G. 2019. Role of Reactive Oxygen Species in Cancer Progression: Molecular Mechanisms and Recent Advancements. *Biomolecules,* 9**,** 735.

ALDAPE, K. D., BALLMAN, K., FURTH, A., BUCKNER, J. C., GIANNINI, C., BURGER, P. C., SCHEITHAUER, B. W., JENKINS, R. B. & JAMES, C. D. 2004. Immunohistochemical detection of EGFRvIII in high malignancy grade astrocytomas and evaluation of prognostic significance. *J Neuropathol Exp Neurol,* 63**,** 700-7.

AMICI, C., SISTONEN, L., SANTORO, M. G. & MORIMOTO, R. I. 1992. Antiproliferative prostaglandins activate heat shock transcription factor. *Proc Natl Acad Sci U S A,* 89**,** 6227-31.

AMIN, J., ANANTHAN, J. & VOELLMY, R. 1988. Key features of heat shock regulatory elements. *Molecular and Cellular Biology,* 8**,** 3761.

ANCKAR, J. & SISTONEN, L. 2011. Regulation of HSF1 function in the heat stress response: implications in aging and disease. *Annu Rev Biochem,* 80**,** 1089-115.

ANTONIETTI, P., LINDER, B., HEHLGANS, S., MILDENBERGER, I. C., BURGER, M. C., FULDA, S., STEINBACH, J. P., GESSLER, F., RÖDEL, F., MITTELBRONN, M. & KÖGEL, D. 2017. Interference with the HSF1/HSP70/BAG3 Pathway Primes Glioma Cells to Matrix Detachment and BH3 Mimetic-Induced Apoptosis. *Mol Cancer Ther,* 16**,** 156-168.

ARJONA, D., BELLO, M. J., ALONSO, M. E., AMINOSO, C., ISLA, A., DE CAMPOS, J. M., SARASA, J. L., GUTIERREZ, M., VILLALOBO, A. & REY, J. A. 2005. Molecular analysis of the EGFR gene in astrocytic gliomas: mRNA expression, quantitative-PCR analysis of non-homogeneous gene amplification and DNA sequence alterations. *Neuropathol Appl Neurobiol,* 31**,** 384-94.

ARTEAGA, C. L. & JOHNSON, D. H. 2001. Tyrosine kinase inhibitors-ZD1839 (Iressa). *Curr Opin Oncol,* 13**,** 491-8.

AU, Q., ZHANG, Y., BARBER, J. R., NG, S. C. & ZHANG, B. 2009. Identification of inhibitors of HSF1 functional activity by high-content target-based screening. *J Biomol Screen,* 14**,** 1165-75.

AVRAAMIDES, C. J., GARMY-SUSINI, B. & VARNER, J. A. 2008. Integrins in angiogenesis and lymphangiogenesis. *Nat Rev Cancer,* 8**,** 604-17.

BAGATELL, R., PAINE-MURRIETA, G. D., TAYLOR, C. W., PULCINI, E. J., AKINAGA, S., BENJAMIN, I. J. & WHITESELL, L. 2000. Induction of a heat shock factor 1-dependent stress response alters the cytotoxic activity of hsp90-binding agents. *Clin Cancer Res,* 6**,** 3312-8.

BAGHBAN, R., ROSHANGAR, L., JAHANBAN-ESFAHLAN, R., SEIDI, K., EBRAHIMI-KALAN, A., JAYMAND, M., KOLAHIAN, S., JAVAHERI, T. & ZARE, P. 2020. Tumor microenvironment complexity and therapeutic implications at a glance. *Cell Communication and Signaling,* 18**,** 59.

BARROW-MCGEE, R., KISHI, N., JOFFRE, C., MÉNARD, L., HERVIEU, A., BAKHOUCHE, B. A., NOVAL, A. J., MAI, A., GUZMÁN, C., ROBBEZ-MASSON, L., ITURRIOZ, X., HULIT, J., BRENNAN, C. H., HART, I. R., PARKER, P. J., IVASKA, J. & KERMORGANT, S. 2016. Beta 1-integrin-c-Met cooperation reveals an inside-in survival signalling on autophagy-related endomembranes. *Nat Commun,* 7**,** 11942.

BARTEK, J., BARTKOVA, J. & LUKAS, J. 2007. DNA damage signalling guards against activated oncogenes and tumour progression. *Oncogene,* 26**,** 7773-9.

BASELGA, J., NORTON, L., ALBANELL, J., KIM, Y. M. & MENDELSOHN, J. 1998. Recombinant humanized anti-HER2 antibody (Herceptin) enhances the antitumor activity of paclitaxel and doxorubicin against HER2/neu overexpressing human breast cancer xenografts. *Cancer Res,* 58**,** 2825-31.

BERETTA, G. L., CASSINELLI, G., PENNATI, M., ZUCO, V. & GATTI, L. 2017. Overcoming ABC transporter-mediated multidrug resistance: The dual role of tyrosine kinase inhibitors as multitargeting agents. *European Journal of Medicinal Chemistry,* 142**,** 271-289.

BEST, B. P. 2015. Cryoprotectant Toxicity: Facts, Issues, and Questions. *Rejuvenation research,* 18**,** 422-436.

BETHESDA, M. 2012. *Topoisomerase Inhibitors*, National Institute of Diabetes and Digestive and Kidney Diseases.

BIERNAT, W., HUANG, H., YOKOO, H., KLEIHUES, P. & OHGAKI, H. 2004. Predominant expression of mutant EGFR (EGFRvIII) is rare in primary glioblastomas. *Brain Pathol,* 14**,** 131-6.

BRADY, S. W., ZHANG, J., TSAI, M.-H. & YU, D. 2015. PI3K-independent mTOR activation promotes lapatinib resistance and IAP expression that can be effectively reversed by mTOR and Hsp90 inhibition. *Cancer Biology & Therapy,* 16**,** 402-411.

BRAND, T. M., IIDA, M., LI, C. & WHEELER, D. L. 2011. The nuclear epidermal growth factor receptor signaling network and its role in cancer. *Discov Med,* 12**,** 419-32.

BULL, J. M. C., SCOTT, G. L., STREBEL, F. R., NAGLE, V. L., OLIVER, D., REDWINE, M., ROWE, R. W., AHN, C. W. & KOCH, S. M. 2008. Fever-range whole-body thermal therapy combined with cisplatin, gemcitabine, and daily interferon-α: A description of a phase I-II protocol. *International Journal of Hyperthermia,* 24**,** 649-662.

BUSSE, D., DOUGHTY, R. S., RAMSEY, T. T., RUSSELL, W. E., PRICE, J. O., FLANAGAN, W. M., SHAWVER, L. K. & ARTEAGA, C. L. 2000. Reversible G(1) arrest induced by inhibition of the epidermal growth factor receptor tyrosine kinase requires up-regulation of p27(KIP1) independent of MAPK activity. *J Biol Chem,* 275**,** 6987-95.

CALDERWOOD, S. K. & CIOCCA, D. R. 2008. Heat shock proteins: stress proteins with Janus-like properties in cancer. *Int J Hyperthermia,* 24**,** 31-9.

CALLAGHAN, R., LUK, F. & BEBAWY, M. 2014. Inhibition of the multidrug resistance P-glycoprotein: time for a change of strategy? *Drug metabolism and disposition: the biological fate of chemicals,* 42**,** 623-631.

CARPENTER, R. L., PAW, I., DEWHIRST, M. W. & LO, H. W. 2015. Akt phosphorylates and activates HSF-1 independent of heat shock, leading to Slug overexpression and epithelial-mesenchymal transition (EMT) of HER2-overexpressing breast cancer cells. *Oncogene,* 34**,** 546-557.

CARPENTER, R. L., SIRKISOON, S., ZHU, D., RIMKUS, T., HARRISON, A., ANDERSON, A., PAW, I., QASEM, S., XING, F., LIU, Y., CHAN, M., METHENY-BARLOW, L., PASCHE, B. C.,

DEBINSKI, W., WATABE, K. & LO, H.-W. 2017. Combined inhibition of AKT and HSF1 suppresses breast cancer stem cells and tumor growth. *Oncotarget,* 8**,** 73947-73963.

CHAI, R. C., KOUSPOU, M. M., LANG, B. J., NGUYEN, C. H., VAN DER KRAAN, A. G. J., VIEUSSEUX, J. L., LIM, R. C., GILLESPIE, M. T., BENJAMIN, I. J., QUINN, J. M. W. & PRICE, J. T. 2014. Molecular Stress-inducing Compounds Increase Osteoclast Formation in a Heat Shock Factor 1 Protein-dependent Manner *. *Journal of Biological Chemistry,* 289**,** 13602-13614.

CHANG, M. H., KUO, W. W., CHEN, R. J., LU, M. C., TSAI, F. J., KUO, W. H., CHEN, L. Y., WU, W. J., HUANG, C. Y. & CHU, C. H. 2008. IGF-II/mannose 6-phosphate receptor activation induces metalloproteinase-9 matrix activity and increases plasminogen activator expression in H9c2 cardiomyoblast cells. *J Mol Endocrinol,* 41**,** 65-74.

CHANGAVI, A. A., SHASHIKALA, A. & RAMJI, A. S. 2015. Epidermal Growth Factor Receptor Expression in Triple Negative and Nontriple Negative Breast Carcinomas. *Journal of laboratory physicians,* 7**,** 79-83.

CHAU HOANG, N. 2017. *Investigating the role of the stress-related transcription factor, HSF1, upon breast cancer tumourigenesis and progression.*

CHAVEZ, K. J., GARIMELLA, S. V. & LIPKOWITZ, S. 2011. Triple negative breast cancer cell lines: One tool in the search for better treatment of triple negative breast cancer. *Breast Disease,* 32**,** 35-48.

CHEN, I. P. & OTT, M. 2020. Turning up the heat on HIV-1. *Proc Natl Acad Sci U S A,* 117**,** 16109-16111.

CHEN, R. J., WU, H. C., CHANG, M. H., LAI, C. H., TIEN, Y. C., HWANG, J. M., KUO, W. H., TSAI, F. J., TSAI, C. H., CHEN, L. M., HUANG, C. Y. & CHU, C. H. 2009. Leu27IGF2 plays an opposite role to IGF1 to induce H9c2 cardiomyoblast cell apoptosis via Galphaq signaling. *J Mol Endocrinol,* 43**,** 221-30.

CHEN, Y., CHEN, J., LOO, A., JAEGER, S., BAGDASARIAN, L., YU, J., CHUNG, F., KORN, J., RUDDY, D., GUO, R., MCLAUGHLIN, M. E., FENG, F., ZHU, P., STEGMEIER, F., PAGLIARINI, R., PORTER, D. & ZHOU, W. 2013. Targeting HSF1 sensitizes cancer cells to HSP90 inhibition. *Oncotarget,* 4**,** 816-829.

CHEN, Y., SCULLY, M., PETRALIA, G. & KAKKAR, A. 2014. Binding and inhibition of drug transport proteins by heparin. *Cancer Biology & Therapy,* 15**,** 135-145.

CHEN, Z., GE, Y. & KANG, J. X. 2004. Down-regulation of the M6P/IGF-II receptor increases cell proliferation and reduces apoptosis in neonatal rat cardiac myocytes. *BMC Cell Biol,* 5**,** 15.

CHENG, Y., REN, X., ZHANG, Y., PATEL, R., SHARMA, A., WU, H., ROBERTSON, G. P., YAN, L., RUBIN, E. & YANG, J. M. 2011. eEF-2 kinase dictates cross-talk between autophagy and apoptosis induced by Akt Inhibition, thereby modulating cytotoxicity of novel Akt inhibitor MK-2206. *Cancer Res,* 71**,** 2654-63.

CHOI, C.-H. 2005. ABC transporters as multidrug resistance mechanisms and the development of chemosensitizers for their reversal. *Cancer Cell International,* 5**,** 30.

CHOU, S. D., PRINCE, T., GONG, J. & CALDERWOOD, S. K. 2012. mTOR is essential for the proteotoxic stress response, HSF1 activation and heat shock protein synthesis. *PLoS One,* 7**,** e39679.

CHU, C. H., TZANG, B. S., CHEN, L. M., LIU, C. J., TSAI, F. J., TSAI, C. H., LIN, J. A., KUO, W. W., BAU, D. T., YAO, C. H. & HUANG, C. Y. 2009. Activation of insulin-like growth factor II receptor induces mitochondrial-dependent apoptosis through G(alpha)q and downstream calcineurin signaling in myocardial cells. *Endocrinology,* 150**,** 2723-31.

CIARDIELLO, F., CAPUTO, R., BIANCO, R., DAMIANO, V., POMATICO, G., DE PLACIDO, S., BIANCO, A. R. & TORTORA, G. 2000. Antitumor effect and potentiation of cytotoxic drugs activity in human cancer cells by ZD-1839 (Iressa), an epidermal growth factor receptor-selective tyrosine kinase inhibitor. *Clin Cancer Res,* 6**,** 2053-63.

CIGLIANO, A., WANG, C., PILO, M. G., SZYDLOWSKA, M., BROZZETTI, S., LATTE, G., PES, G. M., PASCALE, R. M., SEDDAIU, M. A., VIDILI, G., RIBBACK, S., DOMBROWSKI, F., EVERT, M., CHEN, X. & CALVISI, D. F. 2017. Inhibition of HSF1 suppresses the growth of hepatocarcinoma cell lines in vitro and AKT-driven hepatocarcinogenesis in mice. *Oncotarget,* 8**,** 54149-54159.

CIOCCA, D. R., FUQUA, S. A., LOCK-LIM, S., TOFT, D. O., WELCH, W. J. & MCGUIRE, W. L. 1992. Response of human breast cancer cells to heat shock and chemotherapeutic drugs. *Cancer Res,* 52**,** 3648-54.

CLEVELAND. 2021a. *How Can We Tell if Chemotherapy is Working? - What is Chemotherapy?* [Online]. Available: http://chemocare.com/chemotherapy/what-is-chemotherapy/how-to-tell-if-chemotherapy-is-working.aspx [Accessed].

CLEVELAND. 2021b. *Types of Chemotherapy - What is Chemotherapy?* [Online]. Available: http://chemocare.com/chemotherapy/what-is-chemotherapy/types-of-chemotherapy.aspx [Accessed].

COTTO, J., FOX, S. & MORIMOTO, R. 1997. HSF1 granules: a novel stress-induced nuclear compartment of human cells. *J Cell Sci,* 110 (Pt 23)**,** 2925-34.

DAI, C. 2018. The heat-shock, or HSF1-mediated proteotoxic stress, response in cancer: from proteomic stability to oncogenesis. *Philos Trans R Soc Lond B Biol Sci,* 373.

DAI, C., DAI, S. & CAO, J. 2012a. Proteotoxic stress of cancer: implication of the heat-shock response in oncogenesis. *J Cell Physiol,* 227**,** 2982-7.

DAI, C. & SAMPSON, S. B. 2016. HSF1: Guardian of Proteostasis in Cancer. *Trends Cell Biol,* 26**,** 17-28.

DAI, C., SANTAGATA, S., TANG, Z., SHI, J., CAO, J., KWON, H., BRONSON, R. T., WHITESELL, L. & LINDQUIST, S. 2012b. Loss of tumor suppressor NF1 activates HSF1 to promote carcinogenesis. *J Clin Invest,* 122**,** 3742-54.

DAI, C., WHITESELL, L., ROGERS, A. B. & LINDQUIST, S. 2007. Heat shock factor 1 is a powerful multifaceted modifier of carcinogenesis. *Cell,* 130**,** 1005-1018.

DAI, W., YE, J., ZHANG, Z., YANG, L., REN, H., WU, H., CHEN, J., MA, J., ZHAI, E., CAI, S. & HE, Y. 2018. Increased expression of heat shock factor 1 (HSF1) is associated with poor survival in gastric cancer patients. *Diagn Pathol,* 13**,** 80.

DAI, X., CHENG, H., BAI, Z. & LI, J. 2017. Breast Cancer Cell Line Classification and Its Relevance with Breast Tumor Subtyping. *Journal of Cancer,* 8**,** 3131-3141.

DAIRKEE, S. H., NICOLAU, M., SAYEED, A., CHAMPION, S., JI, Y., MOORE, D. H., YONG, B., MENG, Z. & JEFFREY, S. S. 2007. Oxidative stress pathways highlighted in tumor cell immortalization: association with breast cancer outcome. *Oncogene,* 26**,** 6269-79.

DAISUKE, U., HITOSHI, K., FUJIYUKI, I., ICHIO, F. & TAKAHIRO, F. 2016. Chemoresistance of Cancer Cells: Oncogenic Mutation of the p53 Tumor Suppressor Gene. *Current Signal Transduction Therapy,* 11**,** 3-8.

DE, P., CARLSON, J., LEYLAND-JONES, B. & DEY, N. 2014. Oncogenic nexus of cancerous inhibitor of protein phosphatase 2A (CIP2A): an oncoprotein with many hands. *Oncotarget,* 5**,** 4581-4602.

DEHGHANKELISHADI, P., SAADAT, E., RAVAR, F., SAFAVI, M., PORDELI, M., GHOLAMI, M. & DORKOOSH, F. A. 2017. In vitro and in vivo evaluation of paclitaxel–lapatinib-loaded F127 pluronic micelles. *Drug Development and Industrial Pharmacy,* 43**,** 390-398.

DESAI, S., LIU, Z., YAO, J., PATEL, N., CHEN, J., WU, Y., AHN, E. E., FODSTAD, O. & TAN, M. 2013. Heat shock factor 1 (HSF1) controls chemoresistance and autophagy through transcriptional regulation of autophagy-related protein 7 (ATG7). *J Biol Chem,* 288**,** 9165-76.

DILLEKÅS, H., ROGERS, M. S. & STRAUME, O. 2019. Are 90% of deaths from cancer caused by metastases? *Cancer medicine,* 8**,** 5574-5576.

DOKLADNY, K., MYERS, O. B. & MOSELEY, P. L. 2015. Heat shock response and autophagy--cooperation and control. *Autophagy,* 11**,** 200-213.

DOKLADNY, K., ZUHL, M. N., MANDELL, M., BHATTACHARYA, D., SCHNEIDER, S., DERETIC, V. & MOSELEY, P. L. 2013. Regulatory coordination between two major intracellular homeostatic systems: heat shock response and autophagy. *J Biol Chem,* 288**,** 14959-72.

DOLADO, I., SWAT, A., AJENJO, N., DE VITA, G., CUADRADO, A. & NEBREDA, A. R. 2007. p38alpha MAP kinase as a sensor of reactive oxygen species in tumorigenesis. *Cancer Cell,* 11**,** 191-205.

DONG, B., JAEGER, A. & THIELE, D. 2019. Inhibiting Heat Shock Factor 1 in Cancer: A Unique Therapeutic Opportunity. *Trends in Pharmacological Sciences,* 40.

DONG, B., JAEGER, A. M., HUGHES, P. F., LOISELLE, D. R., HAUCK, J. S., FU, Y., HAYSTEAD, T. A., HUANG, J. & THIELE, D. J. 2020. Targeting therapy-resistant prostate cancer via a direct

inhibitor of the human heat shock transcription factor 1. *Science Translational Medicine,* 12**,** eabb5647.

DONG, Q. Z., WANG, Y., DONG, X. J., LI, Z. X., TANG, Z. P., CUI, Q. Z. & WANG, E. H. 2011. CIP2A is overexpressed in non-small cell lung cancer and correlates with poor prognosis. *Ann Surg Oncol,* 18**,** 857-65.

DRATKIEWICZ, E., PIETRASZEK-GREMPLEWICZ, K., SIMICZYJEW, A., MAZUR, A. J. & NOWAK, D. 2018. Gefitinib or lapatinib with foretinib synergistically induce a cytotoxic effect in melanoma cell lines. *Oncotarget,* 9**,** 18254-18268.

EKSTRAND, A. J., SUGAWA, N., JAMES, C. D. & COLLINS, V. P. 1992. Amplified and rearranged epidermal growth factor receptor genes in human glioblastomas reveal deletions of sequences encoding portions of the N- and/or C-terminal tails. *Proc Natl Acad Sci U S A,* 89**,** 4309-13.

ENGELMAN, J. A., LUO, J. & CANTLEY, L. C. 2006. The evolution of phosphatidylinositol 3-kinases as regulators of growth and metabolism. *Nat Rev Genet,* 7**,** 606-19.

ESTRELLA, V., CHEN, T., LLOYD, M., WOJTKOWIAK, J., CORNNELL, H. H., IBRAHIM-HASHIM, A., BAILEY, K., BALAGURUNATHAN, Y., ROTHBERG, J. M., SLOANE, B. F., JOHNSON, J., GATENBY, R. A. & GILLIES, R. J. 2013. Acidity Generated by the Tumor Microenvironment Drives Local Invasion. *Cancer Research,* 73**,** 1524.

FAN, Z. & MENDELSOHN, J. 1998. Therapeutic application of anti-growth factor receptor antibodies. *Curr Opin Oncol,* 10**,** 67-73.

FEDERICO, A., MORGILLO, F., TUCCILLO, C., CIARDIELLO, F. & LOGUERCIO, C. 2007. Chronic inflammation and oxidative stress in human carcinogenesis. *Int J Cancer,* 121**,** 2381-6.

FELDKAMP, M. M., LALA, P., LAU, N., RONCARI, L. & GUHA, A. 1999. Expression of activated epidermal growth factor receptors, Ras-guanosine triphosphate, and mitogen-activated protein kinase in human glioblastoma multiforme specimens. *Neurosurgery,* 45**,** 1442-53.

FINGER, E. C. & GIACCIA, A. J. 2010. Hypoxia, inflammation, and the tumor microenvironment in metastatic disease. *Cancer Metastasis Rev,* 29**,** 285-93.

FITZGERALD, D. M., HASTINGS, P. J. & ROSENBERG, S. M. 2017. Stress-Induced Mutagenesis: Implications in Cancer and Drug Resistance. *Annu Rev Cancer Biol,* 1**,** 119-140.

FORTIN, A., RAYBAUD-DIOGÈNE, H., TÊTU, B., DESCHENES, R., HUOT, J. & LANDRY, J. 2000. Overexpression of the 27 KDa heat shock protein is associated with thermoresistance and chemoresistance but not with radioresistance. *Int J Radiat Oncol Biol Phys,* 46**,** 1259-66.

FRAMPTON, J. E. 2013. Crizotinib: a review of its use in the treatment of anaplastic lymphoma kinase-positive, advanced non-small cell lung cancer. *Drugs,* 73**,** 2031-51.

FRASER, J., SIMPSON, J., FONTANA, R., KISHI-ITAKURA, C., KTISTAKIS, N. T. & GAMMOH, N. 2019. Targeting of early endosomes by autophagy facilitates EGFR recycling and signalling. *EMBO Rep,* 20**,** e47734.

FREZZATO, F., RAGGI, F., MARTINI, V., SEVERIN, F., TRIMARCO, V., VISENTIN, A., SCOMAZZON, E., ACCORDI, B., BRESOLIN, S., PIAZZA, F., FACCO, M., BASSO, G., SEMENZATO, G. & TRENTIN, L. 2019. HSP70/HSF1 axis, regulated via a PI3K/AKT pathway, is a druggable target in chronic lymphocytic leukemia. *Int J Cancer,* 145**,** 3089-3100.

FUJIMOTO, M., TAKAKI, E., TAKII, R., TAN, K., PRAKASAM, R., HAYASHIDA, N., IEMURA, S., NATSUME, T. & NAKAI, A. 2012. RPA assists HSF1 access to nucleosomal DNA by recruiting histone chaperone FACT. *Mol Cell,* 48**,** 182-94.

FUNAKOSHI, Y., MUKOHARA, T., TOMIOKA, H., EKYALONGO, R. C., KATAOKA, Y., INUI, Y., KAWAMORI, Y., TOYODA, M., KIYOTA, N., FUJIWARA, Y. & MINAMI, H. 2013. Excessive MET signaling causes acquired resistance and addiction to MET inhibitors in the MKN45 gastric cancer cell line. *Invest New Drugs,* 31**,** 1158-68.

GABAI, V. L., MENG, L., KIM, G., MILLS, T. A., BENJAMIN, I. J. & SHERMAN, M. Y. 2012. Heat shock transcription factor Hsf1 is involved in tumor progression via regulation of hypoxia-inducible factor 1 and RNA-binding protein HuR. *Molecular and cellular biology,* 32**,** 929-940.

GAN, H. K., CVRLJEVIC, A. N. & JOHNS, T. G. 2013. The epidermal growth factor receptor variant III (EGFRvIII): where wild things are altered. *Febs j,* 280**,** 5350-70.

GASPAR, N., SHARP, S. Y., ECCLES, S. A., GOWAN, S., POPOV, S., JONES, C., PEARSON, A., VASSAL, G. & WORKMAN, P. 2010. Mechanistic evaluation of the novel HSP90 inhibitor NVP-AUY922 in adult and pediatric glioblastoma. *Mol Cancer Ther,* 9**,** 1219-33.

GASPARY, H., GRAHAM, S. H., SAGAR, S. M. & SHARP, F. R. 1995. HSP70 heat shock protein induction following global ischemia in the rat. *Molecular Brain Research,* 34**,** 327-332.

GE, H., GONG, X. & TANG, C. K. 2002. Evidence of high incidence of EGFRvIII expression and coexpression with EGFR in human invasive breast cancer by laser capture microdissection and immunohistochemical analysis. *Int J Cancer,* 98**,** 357-61.

GHOSAL, G. & CHEN, J. 2013. DNA damage tolerance: a double-edged sword guarding the genome. *Translational cancer research,* 2**,** 107-129.

GLASER, S., ANASTASSIADIS, K. & STEWART, A. F. 2005. Current issues in mouse genome engineering. *Nat Genet,* 37**,** 1187-93.

GOLDSTEIN, N. S., DECKER, D., SEVERSON, D., SCHELL, S., VICINI, F., MARGOLIS, J. & DEKHNE, N. S. 2007. Molecular classification system identifies invasive breast carcinoma patients who are most likely and those who are least likely to achieve a complete pathologic response after neoadjuvant chemotherapy. *Cancer,* 110**,** 1687-1696.

GOTE, V., NOOKALA, A. R., BOLLA, P. K. & PAL, D. 2021. Drug Resistance in Metastatic Breast Cancer: Tumor Targeted Nanomedicine to the Rescue. *International Journal of Molecular Sciences,* 22.

GRIMMIG, T., MOLL, E. M., KLOOS, K., THUMM, R., MOENCH, R., CALLIES, S., KRECKEL, J., VETTERLEIN, M., PELZ, J., POLAT, B., TRIPATHI, S., REHDER, R., RIBAS, C. M., CHANDRAKER, A., GERMER, C. T., WAAGA-GASSER, A. M. & GASSER, M. 2017. Upregulated Heat Shock Proteins After Hyperthermic Chemotherapy Point to Induced Cell Survival Mechanisms in Affected Tumor Cells From Peritoneal Carcinomatosis. *Cancer Growth Metastasis,* 10**,** 1179064417730559.

GUAN, X. 2015. Cancer metastases: challenges and opportunities. *Acta Pharmaceutica Sinica B,* 5**,** 402-418.

GUO, L., ZHANG, H., LIU, P., MI, T., HA, D., SU, L., HUANG, L., SHI, Y. & ZHANG, J. 2021. Preclinical Assessment of Paclitaxel- and Trastuzumab-Delivering Magnetic Nanoparticles Fe(3)O(4) for Treatment and Imaging of HER2-Positive Breast Cancer. *Frontiers in medicine,* 8**,** 738775-738775.

GUO, W., QIU, W., AO, X., LI, W., HE, X., AO, L., HU, X., LI, Z., ZHU, M., LUO, D., XING, W. & XU, X. 2020. Low-concentration DMSO accelerates skin wound healing by Akt/mTOR-mediated cell proliferation and migration in diabetic mice. *British Journal of Pharmacology,* 177**,** 3327-3341.

GUPTA, P., HAN, S.-Y., HOLGADO-MADRUGA, M., MITRA, S. S., LI, G., NITTA, R. T. & WONG, A. J. 2010. Development of an EGFRvIII specific recombinant antibody. *BMC biotechnology,* 10**,** 72-72.

HAAGENSEN, E. J., KYLE, S., BEALE, G. S., MAXWELL, R. J. & NEWELL, D. R. 2012. The synergistic interaction of MEK and PI3K inhibitors is modulated by mTOR inhibition. *Br J Cancer,* 106**,** 1386-94.

HAN, J., LIM, W., YOU, D., JEONG, Y., KIM, S., LEE, J. E., SHIN, T. H., LEE, G. & PARK, S. 2019. Chemoresistance in the Human Triple-Negative Breast Cancer Cell Line MDA-MB-231 Induced by Doxorubicin Gradient Is Associated with Epigenetic Alterations in Histone Deacetylase. *Journal of Oncology,* 2019**,** 1345026.

HANAHAN, D. & WEINBERG, ROBERT A. 2011. Hallmarks of Cancer: The Next Generation. *Cell,* 144**,** 646-674.

HARGITAI, J., LEWIS, H., BOROS, I., RÁCZ, T., FISER, A., KURUCZ, I., BENJAMIN, I., VÍGH, L., PÉNZES, Z., CSERMELY, P. & LATCHMAN, D. S. 2003. Bimoclomol, a heat shock protein co-inducer, acts by the prolonged activation of heat shock factor-1. *Biochem Biophys Res Commun,* 307**,** 689-95.

HARRIS, A. L. 1985. DNA repair and resistance to chemotherapy. *Cancer Surv,* 4**,** 601-24.

HASHMI, A. A., NAZ, S., HASHMI, S. K., IRFAN, M., HUSSAIN, Z. F., KHAN, E. Y., ASIF, H. & FARIDI, N. 2019. Epidermal growth factor receptor (EGFR) overexpression in triple-negative breast cancer: association with clinicopathologic features and prognostic parameters. *Surgical and Experimental Pathology,* 2**,** 6.

HAY, D. G., SATHASIVAM, K., TOBABEN, S., STAHL, B., MARBER, M., MESTRIL, R., MAHAL, A., SMITH, D. L., WOODMAN, B. & BATES, G. P. 2004. Progressive decrease in chaperone protein levels in a mouse model of Huntington's disease and induction of stress proteins as a therapeutic approach. *Hum Mol Genet,* 13**,** 1389-405.

HAY, N. 2005. The Akt-mTOR tango and its relevance to cancer. *Cancer Cell,* 8**,** 179-83.

HE, H., WU, G., LI, W., CAO, Y. & LIU, Y. 2012. CIP2A is highly expressed in hepatocellular carcinoma and predicts poor prognosis. *Diagn Mol Pathol,* 21**,** 143-9.

HEALTH, A. I. O. & WELFARE 2021. Cancer data in Australia. Canberra: AIHW.

HEIMBERGER, A. B., HLATKY, R., SUKI, D., YANG, D., WEINBERG, J., GILBERT, M., SAWAYA, R. & ALDAPE, K. 2005. Prognostic effect of epidermal growth factor receptor and EGFRvIII in glioblastoma multiforme patients. *Clin Cancer Res,* 11**,** 1462-6.

HEITZ, F., JOHANSSON, T., BAUMGÄRTEL, K., GECAJ, R., PELCZAR, P. & MANSUY, I. 2014. Heritable and inducible gene knockdown in astrocytes or neurons in vivo by a combined lentiviral and RNAi approach. *Frontiers in Cellular Neuroscience,* 8.

HENSEN, S. M. M., HELDENS, L., VAN ENCKEVORT, C. M. W., VAN GENESEN, S. T., PRUIJN, G. J. M. & LUBSEN, N. H. 2012. Heat shock factor 1 is inactivated by amino acid deprivation. *Cell stress & chaperones,* 17**,** 743-755.

HEROLD, M. J., VAN DEN BRANDT, J., SEIBLER, J. & REICHARDT, H. M. 2008. Inducible and reversible gene silencing by stable integration of an shRNA-encoding lentivirus in transgenic rats. *Proceedings of the National Academy of Sciences,* 105**,** 18507.

HETTINGA, J. V., LEMSTRA, W., MEIJER, C., LOS, G., DE VRIES, E. G., KONINGS, A. W. & KAMPINGA, H. H. 1996. Heat-shock protein expression in cisplatin-sensitive and -resistant human tumor cells. *Int J Cancer,* 67**,** 800-7.

HIGHTOWER, L. E. 1980. Cultured animal cells exposed to amino acid analogues or puromycin rapidly synthesize several polypeptides. *J Cell Physiol,* 102**,** 407-27.

HILDENBRAND, R. & SCHAAF, A. 2009. *The urokinase-system in tumor tissue stroma of the breast and breast cancer cell invasion.*

HOLLER, M., GROTTKE, A., MUECK, K., MANES, J., JÜCKER, M., RODEMANN, H. P. & TOULANY, M. 2016. Dual Targeting of Akt and mTORC1 Impairs Repair of DNA Double-Strand Breaks and Increases Radiation Sensitivity of Human Tumor Cells. *PLoS One,* 11**,** e0154745.

HOLMBERG, C. I., ILLMAN, S. A., KALLIO, M., MIKHAILOV, A. & SISTONEN, L. 2000. Formation of nuclear HSF1 granules varies depending on stress stimuli. *Cell Stress Chaperones,* 5**,** 219-28.

HOUGHTON, P. J., GORLICK, R., KOLB, E. A., LOCK, R., CAROL, H., MORTON, C. L., KEIR, S. T., REYNOLDS, C. P., KANG, M. H., PHELPS, D., MARIS, J. M., BILLUPS, C. & SMITH, M. A. 2012. Initial testing (stage 1) of the mTOR kinase inhibitor AZD8055 by the pediatric preclinical testing program. *Pediatr Blood Cancer,* 58**,** 191-9.

HUANG, C. Y., KUO, W. W., LO, J. F., HO, T. J., PAI, P. Y., CHIANG, S. F., CHEN, P. Y., TSAI, F. J., TSAI, C. H. & HUANG, C. Y. 2016. Doxorubicin attenuates CHIP-guarded HSF1 nuclear translocation and protein stability to trigger IGF-IIR-dependent cardiomyocyte death. *Cell Death Dis,* 7**,** e2455.

HUANG, H. S., NAGANE, M., KLINGBEIL, C. K., LIN, H., NISHIKAWA, R., JI, X. D., HUANG, C. M., GILL, G. N., WILEY, H. S. & CAVENEE, W. K. 1997. The enhanced tumorigenic activity of a mutant epidermal growth factor receptor common in human cancers is mediated by threshold levels of constitutive tyrosine phosphorylation and unattenuated signaling. *J Biol Chem,* 272**,** 2927-35.

HUMPHREY, P. A., WONG, A. J., VOGELSTEIN, B., FRIEDMAN, H. S., WERNER, M. H., BIGNER, D. D. & BIGNER, S. H. 1988. Amplification and expression of the epidermal growth factor receptor gene in human glioma xenografts. *Cancer Res,* 48**,** 2231-8.

IM, C. N., YUN, H. H. & LEE, J. H. 2017. Heat Shock Factor 1 Depletion Sensitizes A172 Glioblastoma Cells to Temozolomide via Suppression of Cancer Stem Cell-Like Properties. *Int J Mol Sci,* 18.

JANUS, P., TOMA-JONIK, A., VYDRA, N., MROWIEC, K., KORFANTY, J., CHADALSKI, M., WIDŁAK, P., DUDEK, K., PASZEK, A., RUSIN, M., POLAŃSKA, J. & WIDŁAK, W. 2020. Pro-death signaling of cytoprotective heat shock factor 1: upregulation of NOXA leading to apoptosis in heat-sensitive cells. *Cell Death & Differentiation,* 27**,** 2280-2292.

JIANG, S., TU, K., FU, Q., SCHMITT, D., ZHOU, L., LU, N. & ZHAO, Y. 2015. Multifaceted roles of HSF1 in cancer. *Tumor Biology,* 36.

JIN, X., MOSKOPHIDIS, D. & MIVECHI, N. F. 2011. Heat shock transcription factor 1 is a key determinant of HCC development by regulating hepatic steatosis and metabolic syndrome. *Cell Metab,* 14**,** 91-103.

JODELE, S., CHANTRAIN, C. F., BLAVIER, L., LUTZKO, C., CROOKS, G. M., SHIMADA, H., COUSSENS, L. M. & DECLERCK, Y. A. 2005. The Contribution of Bone Marrow–Derived Cells to the Tumor Vasculature in Neuroblastoma Is Matrix Metalloproteinase-9 Dependent. *Cancer Research,* 65**,** 3200.

JUNGBLUTH, A. A., STOCKERT, E., HUANG, H. J., COLLINS, V. P., COPLAN, K., IVERSEN, K., KOLB, D., JOHNS, T. J., SCOTT, A. M., GULLICK, W. J., RITTER, G., COHEN, L., SCANLAN, M. J., CAVENEE, W. K. & OLD, L. J. 2003. A monoclonal antibody recognizing human cancers with amplification/overexpression of the human epidermal growth factor receptor. *Proc Natl Acad Sci U S A,* 100**,** 639-44.

JURIVICH, D. A., PANGAS, S., QIU, L. & WELK, J. F. 1996. Phospholipase A2 triggers the first phase of the thermal stress response and exhibits cell-type specificity. *J Immunol,* 157**,** 1669-77.

JURIVICH, D. A., SISTONEN, L., KROES, R. A. & MORIMOTO, R. I. 1992. Effect of sodium salicylate on the human heat shock response. *Science,* 255**,** 1243-5.

JURIVICH, D. A., SISTONEN, L., SARGE, K. D. & MORIMOTO, R. I. 1994. Arachidonate is a potent modulator of human heat shock gene transcription. *Proc Natl Acad Sci U S A,* 91**,** 2280-4.

K. ROCHANI, A., BALASUBRAMANIAN, S., RAVINDRAN GIRIJA, A., MAEKAWA, T., KAUSHAL, G. & KUMAR, D. S. 2020. Heat Shock Protein 90 (Hsp90)-Inhibitor-Luminespib-Loaded-Protein-Based Nanoformulation for Cancer Therapy. *Polymers,* 12**,** 1798.

KAMAL, A., THAO, L., SENSINTAFFAR, J., ZHANG, L., BOEHM, M. F., FRITZ, L. C. & BURROWS, F. J. 2003. A high-affinity conformation of Hsp90 confers tumour selectivity on Hsp90 inhibitors. *Nature,* 425**,** 407-10.

KATAYAMA, R., KHAN, T. M., BENES, C., LIFSHITS, E., EBI, H., RIVERA, V. M., SHAKESPEARE, W. C., IAFRATE, A. J., ENGELMAN, J. A. & SHAW, A. T. 2011. Therapeutic strategies to overcome crizotinib resistance in non-small cell lung cancers harboring the fusion oncogene EML4-ALK. *Proc Natl Acad Sci U S A,* 108**,** 7535-40.

KHALEQUE, M. A., BHARTI, A., SAWYER, D., GONG, J., BENJAMIN, I. J., STEVENSON, M. A. & CALDERWOOD, S. K. 2005. Induction of heat shock proteins by heregulin beta1 leads to protection from apoptosis and anchorage-independent growth. *Oncogene,* 24**,** 6564-73.

KHALID, O. A., CLAUDIU, T. S. & LAURENT, S. 2017. The Warburg Effect and the Hallmarks of Cancer. *Anti-Cancer Agents in Medicinal Chemistry,* 17**,** 164-170.

KIERAN, D., KALMAR, B., DICK, J. R., RIDDOCH-CONTRERAS, J., BURNSTOCK, G. & GREENSMITH, L. 2004. Treatment with arimoclomol, a coinducer of heat shock proteins, delays disease progression in ALS mice. *Nat Med,* 10**,** 402-5.

KIJIMA, T., EGUCHI, T., NECKERS, L. & PRINCE, T. L. 2018a. Monitoring of the Heat Shock Response with a Real-Time Luciferase Reporter. *Methods in molecular biology (Clifton, N.J.),* 1709**,** 35-45.

KIJIMA, T., PRINCE, T. L., TIGUE, M. L., YIM, K. H., SCHWARTZ, H., BEEBE, K., LEE, S., BUDZYNSKI, M. A., WILLIAMS, H., TREPEL, J. B., SISTONEN, L., CALDERWOOD, S. & NECKERS, L. 2018b. HSP90 inhibitors disrupt a transient HSP90-HSF1 interaction and identify a noncanonical model of HSP90-mediated HSF1 regulation. *Sci Rep,* 8**,** 6976.

KIM, E. H., LEE, Y. J., BAE, S., LEE, J. S., KIM, J. & LEE, Y. S. 2009. Heat shock factor 1-mediated aneuploidy requires a defective function of p53. *Cancer Res,* 69**,** 9404-12.

KIM, H. R., KANG, H. S. & KIM, H. D. 1999. Geldanamycin induces heat shock protein expression through activation of HSF1 in K562 erythroleukemic cells. *IUBMB Life,* 48**,** 429-33.

KIM, S.-H., YEO, G.-S., LIM, Y.-S., KANG, C.-D., KIM, C.-M. & CHUNG, B.-S. 1998. Suppression of multidrug resistance via inhibition of heat shock factor by quercetin in MDR cells. *Experimental & Molecular Medicine,* 30**,** 87-92.

KIMBRO, K. S. & SIMONS, J. W. 2006. Hypoxia-inducible factor-1 in human breast and prostate cancer. *Endocrine-Related Cancer***,** 739-749.

KIMURA, E. & HOWELL, S. B. 1993. Analysis of the cytotoxic interaction between cisplatin and hyperthermia in a human ovarian carcinoma cell line. *Cancer Chemother Pharmacol,* 32**,** 419-24.

KIOKA, N., YAMANO, Y., KOMANO, T. & UEDA, K. 1992. Heat-shock responsive elements in the induction of the multidrug resistance gene (MDR1). *FEBS Letters,* 301**,** 37-40.

KLAUNIG, J. E. & WANG, Z. 2018. Oxidative stress in carcinogenesis. *Current Opinion in Toxicology,* 7**,** 116-121.

KOAY, Y. C., MCCONNELL, J. R., WANG, Y., KIM, S. J., BUCKTON, L. K., MANSOUR, F. & MCALPINE, S. R. 2014. Chemically accessible hsp90 inhibitor that does not induce a heat shock response. *ACS Med Chem Lett,* 5**,** 771-6.

KOHNO, M. & POUYSSEGUR, J. 2006. Targeting the ERK signaling pathway in cancer therapy. *Ann Med,* 38**,** 200-11.

KRAWCZYK, Z., GOGLER-PIGLOWSKA, A., SOJKA, D. R. & SCIEGLINSKA, D. 2018. The Role of Heat Shock Proteins in Cisplatin Resistance. *Anticancer Agents Med Chem,* 18**,** 2093-2109.

KRISHNAMURTHY, K., VEDAM, K., KANAGASABAI, R., DRUHAN, L. & ILANGOVAN, G. 2012. *Heat shock factor-1 knockout induces multidrug resistance gene, MDR1b, and enhances P-glycoprotein (ABCB1)-based drug extrusion in the heart.*

KRYEZIU, K., BRUUN, J., GUREN, T. K., SVEEN, A. & LOTHE, R. A. 2019. Combination therapies with HSP90 inhibitors against colorectal cancer. *Biochimica et Biophysica Acta (BBA) - Reviews on Cancer,* 1871**,** 240-247.

KUMARASWAMY, E., WENDT, K. L., AUGUSTINE, L. A., STECKLEIN, S. R., SIBALA, E. C., LI, D., GUNEWARDENA, S. & JENSEN, R. A. 2015. BRCA1 regulation of epidermal growth factor receptor (EGFR) expression in human breast cancer cells involves microRNA-146a and is critical for its tumor suppressor function. *Oncogene,* 34**,** 4333-4346.

KUMSTA, C., CHANG, J. T., SCHMALZ, J. & HANSEN, M. 2017. Hormetic heat stress and HSF-1 induce autophagy to improve survival and proteostasis in C. elegans. *Nature Communications,* 8**,** 14337.

KWON, Y.-S., CHUN, S.-Y., NAM, K.-S. & KIM, S. 2015. Lapatinib sensitizes quiescent MDA-MB-231 breast cancer cells to doxorubicin by inhibiting the expression of multidrug resistance-associated protein-1. *Oncol Rep,* 34**,** 884-890.

LALIC, H., LUKINOVIC-SKUDAR, V., BANFIC, H. & VISNJIC, D. 2012. Rapamycin enhances dimethyl sulfoxide-mediated growth arrest in human myelogenous leukemia cells. *Leuk Lymphoma,* 53**,** 2253-61.

LAMPADA, A., O'PREY, J., SZABADKAI, G., RYAN, K. M., HOCHHAUSER, D. & SALOMONI, P. 2017. mTORC1-independent autophagy regulates receptor tyrosine kinase phosphorylation in colorectal cancer cells via an mTORC2-mediated mechanism. *Cell Death Differ,* 24**,** 1045-1062.

LANDER, H. 1997. *An essential role for free radicals and derived species in signal transduction.*

LANSIAUX, A. 2011. Antimetabolites. *Bull Cancer,* 98**,** 1263-74.

LEACH, M. D., BUDGE, S., WALKER, L., MUNRO, C., COWEN, L. E. & BROWN, A. J. P. 2012. Hsp90 Orchestrates Transcriptional Regulation by Hsf1 and Cell Wall Remodelling by MAPK Signalling during Thermal Adaptation in a Pathogenic Yeast. *PLOS Pathogens,* 8**,** e1003069.

LEARN, C. A., HARTZELL, T. L., WIKSTRAND, C. J., ARCHER, G. E., RICH, J. N., FRIEDMAN, A. H., FRIEDMAN, H. S., BIGNER, D. D. & SAMPSON, J. H. 2004. Resistance to Tyrosine Kinase Inhibition by Mutant Epidermal Growth Factor Receptor Variant III Contributes to the Neoplastic Phenotype of Glioblastoma Multiforme. *Clinical Cancer Research,* 10**,** 3216.

LEE, B. S., CHEN, J., ANGELIDIS, C., JURIVICH, D. A. & MORIMOTO, R. I. 1995. Pharmacological modulation of heat shock factor 1 by antiinflammatory drugs results in protection against stress-induced cellular damage. *Proc Natl Acad Sci U S A,* 92**,** 7207-11.

LEE, H. J., SHIN, S., KANG, J., HAN, K. C., KIM, Y. H., BAE, J. W. & PARK, K. H. 2020. HSP90 Inhibitor, 17-DMAG, Alone and in Combination with Lapatinib Attenuates Acquired Lapatinib-Resistance in ER-positive, HER2-Overexpressing Breast Cancer Cell Line. *Cancers (Basel),* 12.

LEE, J. H., SUN, D., CHO, K. J., KIM, M. S., HONG, M. H., KIM, I. K., LEE, J. S. & LEE, J. H. 2007. Overexpression of human 27 kDa heat shock protein in laryngeal cancer cells confers chemoresistance associated with cell growth delay. *J Cancer Res Clin Oncol,* 133**,** 37-46.

LEE, K. H., LEE, J. H., HAN, S. W., IM, S. A., KIM, T. Y., OH, D. Y. & BANG, Y. J. 2011. Antitumor activity of NVP-AUY922, a novel heat shock protein 90 inhibitor, in human gastric cancer cells is mediated through proteasomal degradation of client proteins. *Cancer Sci,* 102**,** 1388-95.

LEE, Y. J. & DEWEY, W. C. 1987. Induction of heat shock proteins in Chinese hamster ovary cells and development of thermotolerance by intermediate concentrations of puromycin. *J Cell Physiol,* 132**,** 1-11.

LEE, Y. J., GALOFORO, S. S., BERNS, C. M., TONG, W. P., KIM, H. R. & CORRY, P. M. 1997. Glucose deprivation-induced cytotoxicity in drug resistant human breast carcinoma MCF-7/ADR cells: role of c-myc and bcl-2 in apoptotic cell death. *Journal of Cell Science,* 110**,** 681.

LEI, N., PENG, B. & ZHANG, J. Y. 2014. CIP2A regulates cell proliferation via the AKT signaling pathway in human lung cancer. *Oncol Rep,* 32**,** 1689-94.

LEWIS, J. S., LANDERS, R. J., UNDERWOOD, J. C. E., HARRIS, A. L. & LEWIS, C. E. 2000. Expression of vascular endothelial growth factor by macrophages is up-regulated in poorly vascularized areas of breast carcinomas. *The Journal of Pathology,* 192**,** 150-158.

LI, D. & MARCHENKO, N. D. 2017. ErbB2 inhibition by lapatinib promotes degradation of mutant p53 protein in cancer cells. *Oncotarget,* 8**,** 5823-5833.

LI, D., YALLOWITZ, A., OZOG, L. & MARCHENKO, N. 2014. A gain-of-function mutant p53-HSF1 feed forward circuit governs adaptation of cancer cells to proteotoxic stress. *Cell Death Dis,* 5**,** e1194.

LI, W., GE, Z., LIU, C., LIU, Z., BJÖRKHOLM, M., JIA, J. & XU, D. 2008. CIP2A is overexpressed in gastric cancer and its depletion leads to impaired clonogenicity, senescence, or differentiation of tumor cells. *Clin Cancer Res,* 14**,** 3722-8.

LIBERTI, M. V. & LOCASALE, J. W. 2016. The Warburg Effect: How Does it Benefit Cancer Cells? *Trends in biochemical sciences,* 41**,** 211-218.

LIN, Y. C., CHEN, K. C., CHEN, C. C., CHENG, A. L. & CHEN, K. F. 2012. CIP2A-mediated Akt activation plays a role in bortezomib-induced apoptosis in head and neck squamous cell carcinoma cells. *Oral Oncol,* 48**,** 585-93.

LIU, C.-Y., HU, M.-H., HSU, C.-J., HUANG, C.-T., WANG, D.-S., TSAI, W.-C., CHEN, Y.-T., LEE, C.-H., CHU, P.-Y., HSU, C.-C., CHEN, M.-H., SHIAU, C.-W., TSENG, L.-M. & CHEN, K.-F. 2016. Lapatinib inhibits CIP2A/PP2A/p-Akt signaling and induces apoptosis in triple negative breast cancer cells. *Oncotarget,* 7**,** 9135-9149.

LIU, T., WANG, X. & ZHANG, L. 2011a. [The correlation between the up-regulation of Hsp90 and drug resistance to cisplatin in lung cancer cell line]. *Zhongguo Fei Ai Za Zhi,* 14**,** 472-7.

LIU, T., YACOUB, R., TALIAFERRO-SMITH, L. D., SUN, S.-Y., GRAHAM, T. R., DOLAN, R., LOBO, C., TIGHIOUART, M., YANG, L., ADAMS, A. & REGAN, R. M. 2011b. Combinatorial Effects of Lapatinib and Rapamycin in Triple-Negative Breast Cancer Cells. *Molecular Cancer Therapeutics,* 10**,** 1460.

LIU, Z., ZHANG, X. S. & ZHANG, S. 2014. Breast tumor subgroups reveal diverse clinical prognostic power. *Sci Rep,* 4**,** 4002.

LOIBL, S. & GIANNI, L. 2017. HER2-positive breast cancer. *Lancet,* 389**,** 2415-2429.

LU, H. P. & CHAO, C. C. 2012. Cancer cells acquire resistance to anticancer drugs: an update. *Biomed J,* 35**,** 464-72.

LU, K. V., ZHU, S., CVRLJEVIC, A., HUANG, T. T., SARKARIA, S., AHKAVAN, D., DANG, J., DINCA, E. B., PLAISIER, S. B., ODERBERG, I., LEE, Y., CHEN, Z., CALDWELL, J. S., XIE, Y., LOO, J. A., SELIGSON, D., CHAKRAVARI, A., LEE, F. Y., WEINMANN, R., CLOUGHESY, T. F., NELSON, S. F., BERGERS, G., GRAEBER, T., FURNARI, F. B., JAMES, C. D., CAVENEE, W. K., JOHNS, T. G. & MISCHEL, P. S. 2009. Fyn and SRC are effectors of oncogenic epidermal growth factor receptor signaling in glioblastoma patients. *Cancer research,* 69**,** 6889-6898.

MARTINEZ-LOPEZ, N., ATHONVARANGKUL, D., MISHALL, P., SAHU, S. & SINGH, R. 2013. Autophagy proteins regulate ERK phosphorylation. *Nat Commun,* 4**,** 2799.

MATSUMOTO, A., HAYASHIDA, T., TAKAHASHI, M., JINNO, H. & KITAGAWA, Y. 2018. Antitumor effect of lapatinib and cytotoxic agents by suppression of E2F1 in HER2-positive breast cancer. *Mol Med Rep,* 18**,** 958-964.

MATSUURA, H. N. & FETT-NETO, A. G. 2017. Plant Alkaloids: Main Features, Toxicity, and Mechanisms of Action. *In:* CARLINI, C. R., LIGABUE-BRAUN, R. & GOPALAKRISHNAKONE, P. (eds.) *Plant Toxins.* Dordrecht: Springer Netherlands.

MCCONNELL, J. R., BUCKTON, L. K. & MCALPINE, S. R. 2015. Regulating the master regulator: Controlling heat shock factor 1 as a chemotherapy approach. *Bioorganic & Medicinal Chemistry Letters,* 25**,** 3409-3414.

MEADOWS, S. A., VEGA, F., KASHISHIAN, A., JOHNSON, D., DIEHL, V., MILLER, L. L., YOUNES, A. & LANNUTTI, B. J. 2012. PI3Kδ inhibitor, GS-1101 (CAL-101), attenuates pathway signaling, induces apoptosis, and overcomes signals from the microenvironment in cellular models of Hodgkin lymphoma. *Blood,* 119**,** 1897-900.

MENDILLO, MARC L., SANTAGATA, S., KOEVA, M., BELL, GEORGE W., HU, R., TAMIMI, RULLA M., FRAENKEL, E., INCE, TAN A., WHITESELL, L. & LINDQUIST, S. 2012. HSF1 Drives a Transcriptional Program Distinct from Heat Shock to Support Highly Malignant Human Cancers. *Cell,* 150**,** 549-562.

MICHAEL COLVIN, M. 2003. *Alkylating Agents*.

MIMNAUGH, E. G., CHAVANY, C. & NECKERS, L. 1996. Polyubiquitination and proteasomal degradation of the p185c-erbB-2 receptor protein-tyrosine kinase induced by geldanamycin. *J Biol Chem,* 271**,** 22796-801.

MIYAJIMA, N., TSUTSUMI, S., SOURBIER, C., BEEBE, K., MOLLAPOUR, M., RIVAS, C., YOSHIDA, S., TREPEL, J. B., HUANG, Y., TATOKORO, M., SHINOHARA, N., NONOMURA, K. & NECKERS, L. 2013. The HSP90 inhibitor ganetespib synergizes with the MET kinase inhibitor crizotinib in both crizotinib-sensitive and -resistant MET-driven tumor models. *Cancer research,* 73**,** 7022-7033.

MODJTAHEDI, H., AFFLECK, K., STUBBERFIELD, C. & DEAN, C. 1998. EGFR blockade by tyrosine kinase inhibitor or monoclonal antibody inhibits growth, directs terminal differentiation and induces apoptosis in the human squamous cell carcinoma HN5. *Int J Oncol,* 13**,** 335-42.

MORIMOTO, R. 2014. Creating a path from the heat shock response to therapeutics of protein-folding diseases: an interview with Rick Morimoto. *Dis Model Mech,* 7**,** 5-8.

MORIMOTO, R. I. 1998. Regulation of the heat shock transcriptional response: cross talk between a family of heat shock factors, molecular chaperones, and negative regulators. *Genes Dev,* 12**,** 3788-96.

MOSCATELLO, D. K., HOLGADO-MADRUGA, M., GODWIN, A. K., RAMIREZ, G., GUNN, G., ZOLTICK, P. W., BIEGEL, J. A., HAYES, R. L. & WONG, A. J. 1995. Frequent expression of a mutant epidermal growth factor receptor in multiple human tumors. *Cancer Res,* 55**,** 5536-9.

MOSSER, D. D. & MORIMOTO, R. I. 2004. Molecular chaperones and the stress of oncogenesis. *Oncogene,* 23**,** 2907-18.

MOYER, J. D., BARBACCI, E. G., IWATA, K. K., ARNOLD, L., BOMAN, B., CUNNINGHAM, A., DIORIO, C., DOTY, J., MORIN, M. J., MOYER, M. P., NEVEU, M., POLLACK, V. A., PUSTILNIK, L. R., REYNOLDS, M. M., SLOAN, D., THELEMAN, A. & MILLER, P. 1997. Induction of Apoptosis and Cell Cycle Arrest by CP-358,774, an Inhibitor of Epidermal Growth Factor Receptor Tyrosine Kinase. *Cancer Research,* 57**,** 4838.

MUN, G.-I., CHOI, E., LEE, Y. & LEE, Y.-S. 2020. Decreased expression of FBXW7 by ERK1/2 activation in drug-resistant cancer cells confers transcriptional activation of MDR1 by suppression of ubiquitin degradation of HSF1. *Cell Death & Disease,* 11**,** 395.

MURALIDHARAN, S., AMBADE, A., FULHAM, M. A., DESHPANDE, J., CATALANO, D. & MANDREKAR, P. 2014. Moderate Alcohol Induces Stress Proteins HSF1 and hsp70 and Inhibits Proinflammatory Cytokines Resulting in Endotoxin Tolerance. *The Journal of Immunology,* 193**,** 1975.

NADIN, S. B., VARGAS-ROIG, L. M., CUELLO-CARRIÓN, F. D. & CIOCCA, D. R. 2003. Deoxyribonucleic acid damage induced by doxorubicin in peripheral blood mononuclear cells: possible roles for the stress response and the deoxyribonucleic acid repair process. *Cell Stress Chaperones,* 8**,** 361-72.

NAKAMURA, Y., FUJIMOTO, M., HAYASHIDA, N., TAKII, R., NAKAI, A. & MUTO, M. 2010. Silencing HSF1 by short hairpin RNA decreases cell proliferation and enhances sensitivity to hyperthermia in human melanoma cell lines. *J Dermatol Sci,* 60**,** 187-92.

NAKATA, Y., TANG, X. & YOKOYAMA, K. K. 1997. Preparation of Competent Cells for High-Efficiency Plasmid Transformation of Escherichia coli. *In:* COWELL, I. G. & AUSTIN, C. A. (eds.) *cDNA Library Protocols.* Totowa, NJ: Humana Press.

NGUYEN, C. H., LANG, B. J., CHAI, R. C., VIEUSSEUX, J. L., KOUSPOU, M. M. & PRICE, J. T. 2013a. Heat-shock factor 1 both positively and negatively affects cellular clonogenic growth depending on p53 status. *Biochem J,* 452**,** 321-9.

NGUYEN, CHAU H., LANG, BENJAMIN J., CHAI, RYAN C. C., VIEUSSEUX, JESSICA L., KOUSPOU, MICHELLE M. & PRICE, JOHN T. 2013b. Heat-shock factor 1 both positively and negatively affects cellular clonogenic growth depending on p53 status. *Biochemical Journal,* 452**,** 321-329.

NIEMELÄ, M., KAUKO, O., SIHTO, H., MPINDI, J. P., NICORICI, D., PERNILÄ, P., KALLIONIEMI, O. P., JOENSUU, H., HAUTANIEMI, S. & WESTERMARCK, J. 2012. CIP2A signature reveals the MYC dependency of CIP2A-regulated phenotypes and its clinical association with breast cancer subtypes. *Oncogene,* 31**,** 4266-78.

NITIKA, BLACKMAN, J. S., KNIGHTON, L. E., TAKAKUWA, J. E., CALDERWOOD, S. K. & TRUMAN, A. W. 2020. Chemogenomic screening identifies the Hsp70 co-chaperone DNAJA1 as a hub for anticancer drug resistance. *Scientific Reports,* 10**,** 13831.

O'CALLAGHAN-SUNOL, C. & SHERMAN, M. Y. 2006. Heat shock transcription factor (HSF1) plays a critical role in cell migration via maintaining MAP kinase signaling. *Cell Cycle,* 5**,** 1431-7.

OHNO, K., FUKUSHIMA, M., FUJIWARA, M. & NARUMIYA, S. 1988. Induction of 68,000-dalton heat shock proteins by cyclopentenone prostaglandins. Its association with prostaglandin-induced G1 block in cell cycle progression. *J Biol Chem,* 263**,** 19764-70.

OLAPADE-OLAOPA, E. O., MOSCATELLO, D. K., MACKAY, E. H., HORSBURGH, T., SANDHU, D. P., TERRY, T. R., WONG, A. J. & HABIB, F. K. 2000. Evidence for the differential expression of a variant EGF receptor protein in human prostate cancer. *Br J Cancer,* 82**,** 186-94.

PADDISON, P. J., CLEARY, M., SILVA, J. M., CHANG, K., SHETH, N., SACHIDANANDAM, R. & HANNON, G. J. 2004. Cloning of short hairpin RNAs for gene knockdown in mammalian cells. *Nature Methods,* 1**,** 163-167.

PANIGRAHI, A. R., PINDER, S. E., CHAN, S. Y., PAISH, E. C., ROBERTSON, J. F. & ELLIS, I. O. 2004. The role of PTEN and its signalling pathways, including AKT, in breast cancer; an assessment of relationships with other prognostic factors and with outcome. *J Pathol,* 204**,** 93-100.

PARK, K.-S., HONG, Y. S., CHOI, J., YOON, S., KANG, J., KIM, D., LEE, K.-P., IM, H.-S., LEE, C. H., SEO, S., KIM, S.-W., LEE, D. H. & PARK, S. R. 2018. HSP90 inhibitor, AUY922, debilitates

intrinsic and acquired lapatinib-resistant HER2-positive gastric cancer cells. *BMB reports,* 51**,** 660-665.

PARK, S., PARK, J. A., JEON, J. H. & LEE, Y. 2019. Traditional and Novel Mechanisms of Heat Shock Protein 90 (HSP90) Inhibition in Cancer Chemotherapy Including HSP90 Cleavage. *Biomol Ther (Seoul)*.

PAVEL, M., RENNA, M., PARK, S. J., MENZIES, F. M., RICKETTS, T., FULLGRABE, J., ASHKENAZI, A., FRAKE, R. A., LOMBARTE, A. C., BENTO, C. F., FRANZE, K. & RUBINSZTEIN, D. C. 2018. Contact inhibition controls cell survival and proliferation via YAP/TAZ-autophagy axis. *Nat Commun,* 9**,** 2961.

PEDERSEN, M. W., MELTORN, M., DAMSTRUP, L. & POULSEN, H. S. 2001. The type III epidermal growth factor receptor mutation. Biological significance and potential target for anti-cancer therapy. *Ann Oncol,* 12**,** 745-60.

PEDERSEN, M. W., PEDERSEN, N., OTTESEN, L. H. & POULSEN, H. S. 2005. Differential response to gefitinib of cells expressing normal EGFR and the mutant EGFRvIII. *Br J Cancer,* 93**,** 915-23.

PEDERSEN, M. W., TKACH, V., PEDERSEN, N., BEREZIN, V. & POULSEN, H. S. 2004. Expression of a naturally occurring constitutively active variant of the epidermal growth factor receptor in mouse fibroblasts increases motility. *International Journal of Cancer,* 108**,** 643-653.

PENG, T., GOLUB, T. R. & SABATINI, D. M. 2002. The immunosuppressant rapamycin mimics a starvation-like signal distinct from amino acid and glucose deprivation. *Molecular and cellular biology,* 22**,** 5575-5584.

PIGNATARO, L. 2019. Alcohol protects the CNS by activating HSF1 and inducing the heat shock proteins. *Neuroscience Letters,* 713**,** 134507.

PIGNATARO, L., MILLER, A. N., MA, L., MIDHA, S., PROTIVA, P., HERRERA, D. G. & HARRISON, N. L. 2007. Alcohol Regulates Gene Expression in Neurons via Activation of Heat Shock Factor 1. *The Journal of Neuroscience,* 27**,** 12957.

POWELL, C. D., PAULLIN, T. R., AOISA, C., MENZIE, C. J., UBALDINI, A. & WESTERHEIDE, S. D. 2016. The Heat Shock Transcription Factor HSF1 Induces Ovarian Cancer Epithelial-Mesenchymal Transition in a 3D Spheroid Growth Model. *PLoS One,* 11**,** e0168389.

POWERS, M. V., CLARKE, P. A. & WORKMAN, P. 2008. Dual targeting of HSC70 and HSP72 inhibits HSP90 function and induces tumor-specific apoptosis. *Cancer Cell,* 14**,** 250-62.

PRICE, J. T., QUINN, J. M., SIMS, N. A., VIEUSSEUX, J., WALDECK, K., DOCHERTY, S. E., MYERS, D., NAKAMURA, A., WALTHAM, M. C., GILLESPIE, M. T. & THOMPSON, E. W. 2005. The heat shock protein 90 inhibitor, 17-allylamino-17-demethoxygeldanamycin, enhances osteoclast formation and potentiates bone metastasis of a human breast cancer cell line. *Cancer Res,* 65**,** 4929-38.

PRINCE, T. L., LANG, B. J., GUERRERO-GIMENEZ, M. E., FERNANDEZ-MUNOZ, J. M., ACKERMAN, A. & CALDERWOOD, S. K. 2020. HSF1: Primary Factor in Molecular Chaperone Expression and a Major Contributor to Cancer Morbidity. *Cells,* 9.

PROIA, D. A., ZHANG, C., SEQUEIRA, M., JIMENEZ, J. P., HE, S., SPECTOR, N., SHAPIRO, G. I., TOLANEY, S., NAGAI, M., ACQUAVIVA, J., SMITH, D. L., SANG, J., BATES, R. C. & EL-HARIRY, I. 2014. Preclinical activity profile and therapeutic efficacy of the HSP90 inhibitor ganetespib in triple-negative breast cancer. *Clin Cancer Res,* 20**,** 413-24.

QI, J., MCTIGUE, M. A., ROGERS, A., LIFSHITS, E., CHRISTENSEN, J. G., JÄNNE, P. A. & ENGELMAN, J. A. 2011. Multiple mutations and bypass mechanisms can contribute to development of acquired resistance to MET inhibitors. *Cancer Res,* 71**,** 1081-91.

RANKIN, E. B. & GIACCIA, A. J. 2016. Hypoxic control of metastasis. *Science (New York, N.Y.),* 352**,** 175-180.

RICHARDS, E., BEGUM, T. & MASTERS, J. 1996. Thermotolerance and sensitivity of human cancer cells to cisplatin and doxorubicin. *Int J Oncol,* 8**,** 1265-71.

RIMAWI, M. F., SHETTY, P. B., WEISS, H. L., SCHIFF, R., OSBORNE, C. K., CHAMNESS, G. C. & ELLEDGE, R. M. 2010. Epidermal growth factor receptor expression in breast cancer association with biologic phenotype and clinical outcomes. *Cancer,* 116**,** 1234-42.

ROSSI, A., CIAFRÈ, S., BALSAMO, M., PIERIMARCHI, P. & SANTORO, M. G. 2006. Targeting the Heat Shock Factor 1 by RNA Interference: A Potent Tool to Enhance Hyperthermochemotherapy Efficacy in Cervical Cancer. *Cancer Research,* 66**,** 7678.

ROSSI, A., ELIA, G. & SANTORO, M. G. 1998. Activation of the heat shock factor 1 by serine protease inhibitors. An effect associated with nuclear factor-kappaB inhibition. *J Biol Chem,* 273**,** 16446-52.

ROUX, P. P. & TOPISIROVIC, I. 2012. Regulation of mRNA translation by signaling pathways. *Cold Spring Harbor perspectives in biology* [Online], 4. [Accessed 2012/11//].

RUSNAK, D. W., LACKEY, K., AFFLECK, K., WOOD, E. R., ALLIGOOD, K. J., RHODES, N., KEITH, B. R., MURRAY, D. M., KNIGHT, W. B., MULLIN, R. J. & GILMER, T. M. 2001. The Effects of the Novel, Reversible Epidermal Growth Factor Receptor/ErbB-2 Tyrosine Kinase Inhibitor, GW2016, on the Growth of Human Normal and Tumor-derived Cell Lines *Molecular Cancer Therapeutics,* 1**,** 85.

RÜTGERS, M., MURANAKA, L., SCHULZ-RAFFELT, M., THOMS, S., SCHURIG, J., WILLMUND, F. & SCHRODA, M. 2017. Not changes in membrane fluidity but proteotoxic stress triggers heat shock protein expression in Chlamydomonas reinhardtii. *Plant, cell & environment,* 40.

RYAN, Q., IBRAHIM, A., COHEN, M. H., JOHNSON, J., KO, C. W., SRIDHARA, R., JUSTICE, R. & PAZDUR, R. 2008. FDA drug approval summary: lapatinib in combination with capecitabine for previously treated metastatic breast cancer that overexpresses HER-2. *Oncologist,* 13**,** 1114-9.

SAIKALI, S., AVRIL, T., COLLET, B., HAMLAT, A., BANSARD, J. Y., DRENOU, B., GUEGAN, Y. & QUILLIEN, V. 2007. Expression of nine tumour antigens in a series of human glioblastoma multiforme: interest of EGFRvIII, IL-13Ralpha2, gp100 and TRP-2 for immunotherapy. *J Neurooncol,* 81**,** 139-48.

SALMAND, P. A., JUNGAS, T., FERNANDEZ, M., CONTER, A. & CHRISTIANS, E. S. 2008. Mouse heat-shock factor 1 (HSF1) is involved in testicular response to genotoxic stress induced by doxorubicin. *Biol Reprod,* 79**,** 1092-101.

SANTAGATA, S., HU, R., LIN, N. U., MENDILLO, M. L., COLLINS, L. C., HANKINSON, S. E., SCHNITT, S. J., WHITESELL, L., TAMIMI, R. M., LINDQUIST, S. & INCE, T. A. 2011a. High levels of nuclear heat-shock factor 1 (HSF1) are associated with poor prognosis in breast cancer. *Proc Natl Acad Sci U S A,* 108**,** 18378-83.

SANTAGATA, S., HU, R., LIN, N. U., MENDILLO, M. L., COLLINS, L. C., HANKINSON, S. E., SCHNITT, S. J., WHITESELL, L., TAMIMI, R. M., LINDQUIST, S. & INCE, T. A. 2011b. High levels of nuclear heat-shock factor 1 (HSF1) are associated with poor prognosis in breast cancer. *Proceedings of the National Academy of Sciences,* 108**,** 18378.

SANTAGATA, S., MENDILLO, M. L., TANG, Y.-C., SUBRAMANIAN, A., PERLEY, C. C., ROCHE, S. P., WONG, B., NARAYAN, R., KWON, H., KOEVA, M., AMON, A., GOLUB, T. R., PORCO, J. A., WHITESELL, L. & LINDQUIST, S. 2013. Tight coordination of protein translation and HSF1 activation supports the anabolic malignant state. *Science (New York, N.Y.),* 341**,** 1238303.

SANTAGATA, S., XU, Y. M., WIJERATNE, E. M., KONTNIK, R., ROONEY, C., PERLEY, C. C., KWON, H., CLARDY, J., KESARI, S., WHITESELL, L., LINDQUIST, S. & GUNATILAKA, A. A. 2012. Using the heat-shock response to discover anticancer compounds that target protein homeostasis. *ACS Chem Biol,* 7**,** 340-9.

SAUNDERS, C. M., JASSAL, S. & LIM, E. 2018. *Breast Cancer*, Oxford University Press, Incorporated.

SEMENZA, G. L. 2010. HIF-1: upstream and downstream of cancer metabolism. *Curr Opin Genet Dev,* 20**,** 51-6.

SHARMA, A., MEENA, A. S. & BHAT, M. K. 2010. Hyperthermia-associated carboplatin resistance: differential role of p53, HSF1 and Hsp70 in hepatoma cells. *Cancer Sci,* 101**,** 1186-93.

SHARMA, C. & SEO, Y. H. 2018. Small Molecule Inhibitors of HSF1-Activated Pathways as Potential Next-Generation Anticancer Therapeutics. *Molecules,* 23.

SHAROM, F. J. 2007. ABC multidrug transporters: structure, function and role in chemoresistance. *Pharmacogenomics,* 9**,** 105-127.

SHIMOMURA, A., YAMAMOTO, N., KONDO, S., FUJIWARA, Y., SUZUKI, S., YANAGITANI, N., HORIIKE, A., KITAZONO, S., OHYANAGI, F., DOI, T., KUBOKI, Y., KAWAZOE, A., SHITARA, K., OHNO, I., BANERJI, U., SUNDAR, R., OHKUBO, S., CALLEJA, E. M. & NISHIO, M. 2019. First-in-Human Phase I Study of an Oral HSP90 Inhibitor, TAS-116, in Patients with Advanced Solid Tumors. *Molecular Cancer Therapeutics,* 18**,** 531.

SHINOJIMA, N., TADA, K., SHIRAISHI, S., KAMIRYO, T., KOCHI, M., NAKAMURA, H., MAKINO, K., SAYA, H., HIRANO, H., KURATSU, J., OKA, K., ISHIMARU, Y. & USHIO, Y. 2003.

Prognostic value of epidermal growth factor receptor in patients with glioblastoma multiforme. *Cancer Res,* 63**,** 6962-70.

SIGISMUND, S., ARGENZIO, E., TOSONI, D., CAVALLARO, E., POLO, S. & DI FIORE, P. P. 2008. Clathrin-mediated internalization is essential for sustained EGFR signaling but dispensable for degradation. *Dev Cell,* 15**,** 209-19.

SILVERA, D., FORMENTI, S. C. & SCHNEIDER, R. J. 2010. Translational control in cancer. *Nature reviews. Cancer,* 10**,** 254-266.

SITTLER, A., LURZ, R., LUEDER, G., PRILLER, J., LEHRACH, H., HAYER-HARTL, M. K., HARTL, F. U. & WANKER, E. E. 2001. Geldanamycin activates a heat shock response and inhibits huntingtin aggregation in a cell culture model of Huntington's disease. *Hum Mol Genet,* 10**,** 1307-15.

SOLIMINI, N. L., LUO, J. & ELLEDGE, S. J. 2007a. Non-oncogene addiction and the stress phenotype of cancer cells. *Cell,* 130**,** 986-988.

SOLIMINI, N. L., LUO, J. & ELLEDGE, S. J. 2007b. Non-oncogene addiction and the stress phenotype of cancer cells. *Cell,* 130**,** 986-8.

SONG, X., LIU, Z. & YU, Z. 2020. EGFR Promotes the Development of Triple Negative Breast Cancer Through JAK/STAT3 Signaling. *Cancer management and research,* 12**,** 703-717.

SONNWEBER, B., DLASKA, M., SKVORTSOV, S., DIRNHOFER, S., SCHMID, T. & HILBE, W. 2006. High predictive value of epidermal growth factor receptor phosphorylation but not of EGFRvIII mutation in resected stage I non-small cell lung cancer (NSCLC). *J Clin Pathol,* 59**,** 255-9.

SØRLIE, T. 2004. Molecular portraits of breast cancer: tumour subtypes as distinct disease entities. *Eur J Cancer,* 40**,** 2667-75.

SPISEK, R. & DHODAPKAR, M. V. 2007. Towards a better way to die with chemotherapy: role of heat shock protein exposure on dying tumor cells. *Cell Cycle,* 6**,** 1962-5.

SREEDHAR, A. S. & CSERMELY, P. 2004. Heat shock proteins in the regulation of apoptosis: new strategies in tumor therapy: a comprehensive review. *Pharmacol Ther,* 101**,** 227-57.

STURLA, L.-M., AMORINO, G., ALEXANDER, M. S., MIKKELSEN, R. B., VALERIE, K. & SCHMIDT-ULLRICHR, R. K. 2005. Requirement of Tyr-992 and Tyr-1173 in Phosphorylation of

the Epidermal Growth Factor Receptor by Ionizing Radiation and Modulation by SHP2 *. *Journal of Biological Chemistry,* 280**,** 14597-14604.

SUGAWA, N., EKSTRAND, A. J., JAMES, C. D. & COLLINS, V. P. 1990. Identical splicing of aberrant epidermal growth factor receptor transcripts from amplified rearranged genes in human glioblastomas. *Proc Natl Acad Sci U S A,* 87**,** 8602-6.

SWAN, C. L. & SISTONEN, L. 2015. Cellular stress response cross talk maintains protein and energy homeostasis. *Embo j,* 34**,** 267-9.

TANG, Z. 2018. *PI3K/AKT Signaling Activates HSF1 to Preserve Proteostasis and Sustain Growth.* Doctor of Philosophy (PhD) Electronic Theses and Dissertations, The University of Maine.

TANG, Z., DAI, S., HE, Y., DOTY, R. A., SHULTZ, L. D., SAMPSON, S. B. & DAI, C. 2015. MEK guards proteome stability and inhibits tumor-suppressive amyloidogenesis via HSF1. *Cell,* 160**,** 729-744.

TCHÉNIO, T., HAVARD, M., MARTINEZ, L. A. & DAUTRY, F. 2006. Heat shock-independent induction of multidrug resistance by heat shock factor 1. *Molecular and cellular biology,* 26**,** 580-591.

TENCONI, E. & RIGALI, S. 2018. Self-resistance mechanisms to DNA-damaging antitumor antibiotics in actinobacteria. *Curr Opin Microbiol,* 45**,** 100-108.

TENG, H. W., YANG, S. H., LIN, J. K., CHEN, W. S., LIN, T. C., JIANG, J. K., YEN, C. C., LI, A. F., CHEN, P. C., LAN, Y. T., LIN, C. C., HSU, Y. N., WANG, H. W. & CHEN, K. F. 2012. CIP2A is a predictor of poor prognosis in colon cancer. *J Gastrointest Surg,* 16**,** 1037-47.

THORN, C. F., OSHIRO, C., MARSH, S., HERNANDEZ-BOUSSARD, T., MCLEOD, H., KLEIN, T. E. & ALTMAN, R. B. 2011. Doxorubicin pathways: pharmacodynamics and adverse effects. *Pharmacogenet Genomics,* 21**,** 440-6.

TILIGADA, E. 2006. Chemotherapy: induction of stress responses. *Endocrine-Related Cancer Endocr Relat Cancer,* 13**,** S115-S124.

TORIGOE, T., TAMURA, Y. & SATO, N. 2009. Heat shock proteins and immunity: application of hyperthermia for immunomodulation. *Int J Hyperthermia,* 25**,** 610-6.

TRIANDAFILLOU, CATHERINE G. & DRUMMOND, D. A. 2016. Heat Shock Factor 1: From Fire Chief to Crowd-Control Specialist. *Molecular Cell,* 63**,** 1-2.

TSUTSUI, S., YASUDA, K., SUZUKI, K., TAHARA, K., HIGASHI, H. & ERA, S. 2005. *Macrophage infiltration and its prognostic implications in breast cancer: The relationship with VEGF expression and microvessel density.*

VAARALA, M. H., VÄISÄNEN, M. R. & RISTIMÄKI, A. 2010. CIP2A expression is increased in prostate cancer. *J Exp Clin Cancer Res,* 29**,** 136.

VALASTYAN, S. & WEINBERG, R. A. 2011. Tumor metastasis: molecular insights and evolving paradigms. *Cell,* 147**,** 275-292.

VALKO, M., RHODES, C. J., MONCOL, J., IZAKOVIC, M. & MAZUR, M. 2006. Free radicals, metals and antioxidants in oxidative stress-induced cancer. *Chemico-Biological Interactions,* 160**,** 1-40.

VARODAYAN, F. P. & HARRISON, N. L. 2013. HSF1 transcriptional activity mediates alcohol induction of Vamp2 expression and GABA release. *Frontiers in integrative neuroscience,* 7**,** 89-89.

VELAYUTHAM, M., CARDOUNEL, A. J., LIU, Z. & ILANGOVAN, G. 2018. Discovering a Reliable Heat-Shock Factor-1 Inhibitor to Treat Human Cancers: Potential Opportunity for Phytochemists. *Front Oncol,* 8**,** 97.

VERHEIJEN, M., LIENHARD, M., SCHROODERS, Y., CLAYTON, O., NUDISCHER, R., BOERNO, S., TIMMERMANN, B., SELEVSEK, N., SCHLAPBACH, R., GMUENDER, H., GOTTA, S., GERAEDTS, J., HERWIG, R., KLEINJANS, J. & CAIMENT, F. 2019. DMSO induces drastic changes in human cellular processes and epigenetic landscape in vitro. *Scientific Reports,* 9**,** 4641.

VIANA-PEREIRA, M., LOPES, J. M., LITTLE, S., MILANEZI, F., BASTO, D., PARDAL, F., JONES, C. & REIS, R. M. 2008. Analysis of EGFR overexpression, EGFR gene amplification and the EGFRvIII mutation in Portuguese high-grade gliomas. *Anticancer Res,* 28**,** 913-20.

VÍGH, L., LITERÁTI, P. N., HORVÁTH, I., TÖRÖK, Z., BALOGH, G., GLATZ, A., KOVÁCS, E., BOROS, I., FERDINÁNDY, P., FARKAS, B., JASZLITS, L., JEDNÁKOVITS, A., KORÁNYI, L. & MARESCA, B. 1997. Bimoclomol: a nontoxic, hydroxylamine derivative with stress protein-inducing activity and cytoprotective effects. *Nat Med,* 3**,** 1150-4.

VIHERVAARA, A. & SISTONEN, L. 2014. HSF1 at a glance. *J Cell Sci,* 127**,** 261-6.

VILABOA, N., BORE, A., MARTIN-SAAVEDRA, F., BAYFORD, M., WINFIELD, N., FIRTH-CLARK, S., KIRTON, S. B. & VOELLMY, R. 2017. New inhibitor targeting human transcription factor HSF1: effects on the heat shock response and tumor cell survival. *Nucleic Acids Res,* 45**,** 5797-5817.

VILABOA, N. E., GALÁN, A., TROYANO, A., DE BLAS, E. & ALLER, P. 2000. Regulation of Multidrug Resistance 1 (MDR1)/P-glycoprotein Gene Expression and Activity by Heat-Shock Transcription Factor 1 (HSF1)*. *Journal of Biological Chemistry,* 275**,** 24970-24976.

VYDRA, N., TOMA, A. & WIDLAK, W. 2014. Pleiotropic role of HSF1 in neoplastic transformation. *Current cancer drug targets,* 14**,** 144-155.

VYDRA, N., TOMA-JONIK, A., GLOWALA-KOSINSKA, M., GOGLER-PIGŁOWSKA, A. & WIDLAK, W. 2013. *Overexpression of Heat Shock Transcription Factor 1 enhances the resistance of melanoma cells to doxorubicin and paclitaxel.*

WANG, J., LV, F.-M., WANG, D.-L., DU, J.-L., GUO, H.-Y., CHEN, H.-N., ZHAO, S.-J., LIU, Z.-P. & LIU, Y. 2020. Synergistic Antitumor Effects on Drug-Resistant Breast Cancer of Paclitaxel/Lapatinib Composite Nanocrystals. *Molecules,* 25.

WANG, K. C., BROOKS, D. A., BOTTING, K. J. & MORRISON, J. L. 2012a. IGF-2R-mediated signaling results in hypertrophy of cultured cardiomyocytes from fetal sheep. *Biol Reprod,* 86**,** 183.

WANG, K. C., BROOKS, D. A., THORNBURG, K. L. & MORRISON, J. L. 2012b. Activation of IGF-2R stimulates cardiomyocyte hypertrophy in the late gestation sheep fetus. *J Physiol,* 590**,** 5425-37.

WANG, K. C., ZHANG, L., MCMILLEN, I. C., BOTTING, K. J., DUFFIELD, J. A., ZHANG, S., SUTER, C. M., BROOKS, D. A. & MORRISON, J. L. 2011. Fetal growth restriction and the programming of heart growth and cardiac insulin-like growth factor 2 expression in the lamb. *J Physiol,* 589**,** 4709-22.

WANG, X., ZHANG, D., CAO, M., BA, J., WU, B., LIU, T. & NIE, C. 2018. A study on the biological function of heat shock factor 1 proteins in breast cancer. *Oncol Lett,* 16**,** 3821-3825.

WATANABE, Y., TSUJIMURA, A., TAGUCHI, K. & TANAKA, M. 2017. HSF1 stress response pathway regulates autophagy receptor SQSTM1/p62-associated proteostasis. *Autophagy,* 13**,** 133-148.

WEI, Y., LI, J., HUANG, J., ZHANG, X., ZHAO, H., CUI, C., LI, Y. & HU, S. 2012. Elevation of IGF-2 receptor and the possible underlying implications in end-stage heart failure patients before and after heart transplantation. *J Cell Mol Med,* 16**,** 1038-46.

WEST, J. D., WANG, Y. & MORANO, K. A. 2012. Small molecule activators of the heat shock response: chemical properties, molecular targets, and therapeutic promise. *Chemical research in toxicology,* 25**,** 2036-2053.

WESTERHEIDE, S. D., BOSMAN, J. D., MBADUGHA, B. N., KAWAHARA, T. L., MATSUMOTO, G., KIM, S., GU, W., DEVLIN, J. P., SILVERMAN, R. B. & MORIMOTO, R. I. 2004. Celastrols as inducers of the heat shock response and cytoprotection. *J Biol Chem,* 279**,** 56053-60.

WESTERHEIDE, S. D. & MORIMOTO, R. I. 2005. Heat shock response modulators as therapeutic tools for diseases of protein conformation. *J Biol Chem,* 280**,** 33097-100.

WIDSCHWENDTER, M. & JONES, P. A. 2002. DNA methylation and breast carcinogenesis. *Oncogene,* 21**,** 5462-5482.

WIKSTRAND, C. J., HALE, L. P., BATRA, S. K., HILL, M. L., HUMPHREY, P. A., KURPAD, S. N., MCLENDON, R. E., MOSCATELLO, D., PEGRAM, C. N., REIST, C. J. & ET AL. 1995. Monoclonal antibodies against EGFRvIII are tumor specific and react with breast and lung carcinomas and malignant gliomas. *Cancer Res,* 55**,** 3140-8.

WONG, A. J., RUPPERT, J. M., BIGNER, S. H., GRZESCHIK, C. H., HUMPHREY, P. A., BIGNER, D. S. & VOGELSTEIN, B. 1992. Structural alterations of the epidermal growth factor receptor gene in human gliomas. *Proceedings of the National Academy of Sciences of the United States of America,* 89**,** 2965-2969.

WOOD, E. R., TRUESDALE, A. T., MCDONALD, O. B., YUAN, D., HASSELL, A., DICKERSON, S. H., ELLIS, B., PENNISI, C., HORNE, E., LACKEY, K., ALLIGOOD, K. J., RUSNAK, D. W., GILMER, T. M. & SHEWCHUK, L. 2004. A unique structure for epidermal growth factor receptor bound to GW572016 (Lapatinib): relationships among protein conformation, inhibitor off-rate, and receptor activity in tumor cells. *Cancer Res,* 64**,** 6652-9.

WORKMAN, P. & VAN MONTFORT, R. 2014. EML4-ALK fusions: propelling cancer but creating exploitable chaperone dependence. *Cancer Discov,* 4**,** 642-5.

WORLD HEALTH, O. 2020. *WHO report on cancer: setting priorities, investing wisely and providing care for all,* Geneva, World Health Organization.

WU, S. & FU, L. 2018. Tyrosine kinase inhibitors enhanced the efficacy of conventional chemotherapeutic agent in multidrug resistant cancer cells. *Mol Cancer,* 17**,** 25.

XI, C., HU, Y., BUCKHAULTS, P., MOSKOPHIDIS, D. & MIVECHI, N. F. 2012. Heat shock factor Hsf1 cooperates with ErbB2 (Her2/Neu) protein to promote mammary tumorigenesis and metastasis. *J Biol Chem,* 287**,** 35646-35657.

XIA, W., LIU, L.-H., HO, P. & SPECTOR, N. L. 2004. Truncated ErbB2 receptor (p95ErbB2) is regulated by heregulin through heterodimer formation with ErbB3 yet remains sensitive to the dual EGFR/ErbB2 kinase inhibitor GW572016. *Oncogene,* 23**,** 646-653.

XU, S., LI, S., GUO, Z., LUO, J., ELLIS, M. J. & MA, C. X. 2013. Combined targeting of mTOR and AKT is an effective strategy for basal-like breast cancer in patient-derived xenograft models. *Mol Cancer Ther,* 12**,** 1665-75.

XU, W., MIMNAUGH, E., ROSSER, M. F., NICCHITTA, C., MARCU, M., YARDEN, Y. & NECKERS, L. 2001. Sensitivity of mature Erbb2 to geldanamycin is conferred by its kinase domain and is mediated by the chaperone protein Hsp90. *J Biol Chem,* 276**,** 3702-8.

XU, Y. M., MARRON, M. T., SEDDON, E., MCLAUGHLIN, S. P., RAY, D. T., WHITESELL, L. & GUNATILAKA, A. A. 2009. 2,3-Dihydrowithaferin A-3beta-O-sulfate, a new potential prodrug of withaferin A from aeroponically grown Withania somnifera. *Bioorg Med Chem,* 17**,** 2210-4.

YALLOWITZ, A., GHALEB, A., GARCIA, L., ALEXANDROVA, E. M. & MARCHENKO, N. 2018. Heat shock factor 1 confers resistance to lapatinib in ERBB2-positive breast cancer cells. *Cell Death & Disease,* 9**,** 621.

YAMAZAKI, H., FUKUI, Y., UEYAMA, Y., TAMAOKI, N., KAWAMOTO, T., TANIGUCHI, S. & SHIBUYA, M. 1988. Amplification of the structurally and functionally altered epidermal growth factor receptor gene (c-erbB) in human brain tumors. *Mol Cell Biol,* 8**,** 1816-20.

YANG, J., NIE, J., MA, X., WEI, Y., PENG, Y. & WEI, X. 2019. Targeting PI3K in cancer: mechanisms and advances in clinical trials. *Molecular Cancer,* 18**,** 26.

YANG, X., WANG, J., ZHOU, Y., WANG, Y., WANG, S. & ZHANG, W. 2012. Hsp70 promotes chemoresistance by blocking Bax mitochondrial translocation in ovarian cancer cells. *Cancer Lett,* 321**,** 137-43.

YAU, C. & BENZ, C. C. 2008. Genes responsive to both oxidant stress and loss of estrogen receptor function identify a poor prognosis group of estrogen receptor positive primary breast cancers. *Breast Cancer Res,* 10**,** R61.

YE, M., HUANG, W., LIU, R., KONG, Y., LIU, Y., CHEN, X. & XU, J. 2021. Synergistic Activity of the HSP90 Inhibitor Ganetespib With Lapatinib Reverses Acquired Lapatinib Resistance in HER2-Positive Breast Cancer Cells. *Frontiers in Pharmacology,* 12.

YELDAG, G., RICE, A. & DEL RÍO HERNÁNDEZ, A. 2018. Chemoresistance and the Self-Maintaining Tumor Microenvironment. *Cancers,* 10**,** 471.

YOO, K., YUN, H. H., JUNG, S. Y. & LEE, J. H. 2021. KRIBB11 Induces Apoptosis in A172 Glioblastoma Cells via MULE-Dependent Degradation of MCL-1. *Molecules,* 26.

YOON, Y., KIM, J., SHIN, K. D., SHIN, D.-S., HAN, Y.-M., LEE, Y., LEE, J., KWON, B.-M. & HAN, D. 2010. KRIBB11 Inhibits HSP70 Synthesis through Inhibition of Heat Shock Factor 1 Function by Impairing the Recruitment of Positive Transcription Elongation Factor b to the hsp70 Promoter. *The Journal of biological chemistry,* 286**,** 1737-47.

YUAN, C., GAO, J., GUO, J., BAI, L., MARSHALL, C., CAI, Z., WANG, L. & XIAO, M. 2014. Dimethyl sulfoxide damages mitochondrial integrity and membrane potential in cultured astrocytes. *PloS one,* 9**,** e107447-e107447.

YUE, J. & LÓPEZ, J. M. 2020. Understanding MAPK Signaling Pathways in Apoptosis. *International journal of molecular sciences,* 21**,** 2346.

ZAARUR, N., GABAI, V. L., PORCO, J. A., JR., CALDERWOOD, S. & SHERMAN, M. Y. 2006. Targeting heat shock response to sensitize cancer cells to proteasome and Hsp90 inhibitors. *Cancer Res,* 66**,** 1783-91.

ZAJDEL, A., NYCZ, J. & WILCZOK, A. 2021. Lapatinib enhances paclitaxel toxicity in MCF-7, T47D, and MDA-MB-321 breast cancer cells. *Toxicology in Vitro,* 75**,** 105200.

ZAJDEL, A., WILCZOK, A., JELONEK, K., MUSIAŁ-KULIK, M., FORYŚ, A., LI, S. & KASPERCZYK, J. 2019. Cytotoxic Effect of Paclitaxel and Lapatinib Co-Delivered in Polylactide-co-Poly(ethylene glycol) Micelles on HER-2-Negative Breast Cancer Cells. *Pharmaceutics,* 11.

ZHANG, N., WU, Y., LYU, X., LI, B., YAN, X., XIONG, H., LI, X., HUANG, G., ZENG, Y., ZHANG, Y., LIAN, J., NI, Z. & HE, F. 2017. HSF1 upregulates ATG4B expression and enhances epirubicin-induced protective autophagy in hepatocellular carcinoma cells. *Cancer Letters,* 409**,** 81-90.

ZHANG, Z., WANG, Y. & LI, Q. 2018. Mechanisms underlying the effects of stress on tumorigenesis and metastasis (Review). *Int J Oncol,* 53**,** 2332-2342.

ZHENG, Y., MA, L. & SUN, Q. 2021. Clinically-Relevant ABC Transporter for Anti-Cancer Drug Resistance. *Frontiers in Pharmacology,* 12.

ZINGONI, A., FIONDA, C., BORRELLI, C., CIPPITELLI, M., SANTONI, A. & SORIANI, A. 2017. Natural Killer Cell Response to Chemotherapy-Stressed Cancer Cells: Role in Tumor Immunosurveillance. *Front Immunol,* 8**,** 1194.

ZOU, H. Y., LI, Q., ENGSTROM, L. D., WEST, M., APPLEMAN, V., WONG, K. A., MCTIGUE, M., DENG, Y. L., LIU, W., BROOUN, A., TIMOFEEVSKI, S., MCDONNELL, S. R., JIANG, P., FALK, M. D., LAPPIN, P. B., AFFOLTER, T., NICHOLS, T., HU, W., LAM, J., JOHNSON, T. W., SMEAL, T., CHAREST, A. & FANTIN, V. R. 2015. PF-06463922 is a potent and selective next-generation ROS1/ALK inhibitor capable of blocking crizotinib-resistant ROS1 mutations. *Proc Natl Acad Sci U S A,* 112**,** 3493-8.

ZOU, J., GUO, Y., GUETTOUCHE, T., SMITH, D. F. & VOELLMY, R. 1998. Repression of Heat Shock Transcription Factor HSF1 Activation by HSP90 (HSP90 Complex) that Forms a Stress-Sensitive Complex with HSF1. *Cell,* 94**,** 471-480.

APPENDIX 1 Extra Time-points and Controls of Tested Drugs

A — 48 hours

B — 24 hours

C — 0 hours

D — Controls (72 hours)
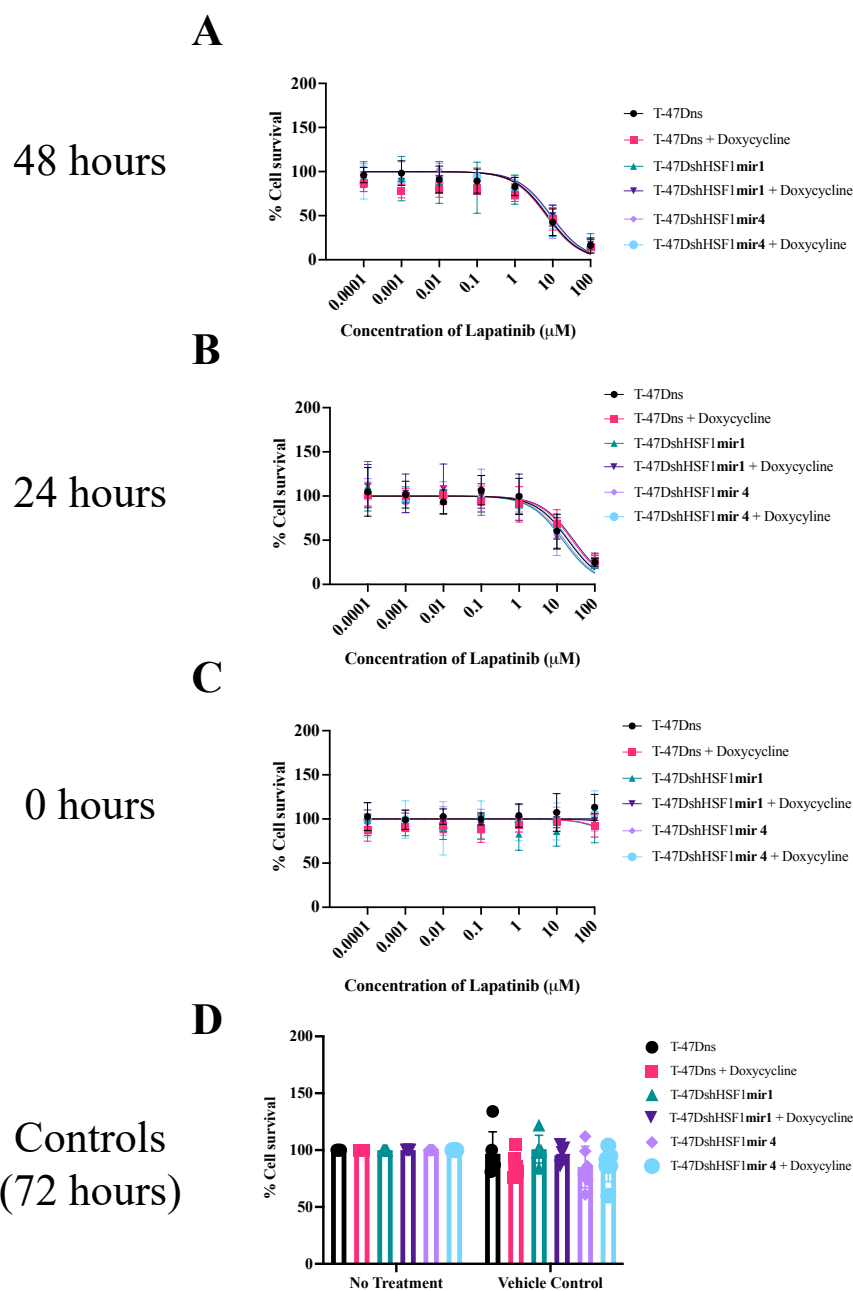
	IC$_{50}$ Cell Survival (μM)	
Cell Line	**T-47D**	
Time (Hours)	**24**	**48**
Non-silencing	20	7
Non-silencing + Doxycycline	25	7
shRNA HSF1 Mir1	14	7
shRNA HSF1 Mir1 + Doxycycline	28	9
shRNA HSF1 Mir4	16	8
shRNA HSF1 Mir4 + Doxycycline	22	9

Figure A1 Additional timepoints and vehicle controls versus no treatment group for T47D inducible HSF1 knockdown cells treated with Lapatinib

Cell survivability graphs for T47D with HSF1 inducible knockdown cells at **(A)** 48 hours **(B)** 24 hours and **(C)** 0 hours cotreated with Lapatinib. **(D)** 72 hours Vehicle Controls (0.2% v/v DMSO) compared to No Treatment (complete medium). Calculated IC50 values are represented in table according to cell conditions: non-silencing (ns), ns + Doxycycline [0.5μg/ ml], shRNA HSF1 Mir1, shRNA HSF1 Mir1 + Doxycycline [0.5μg/ ml], shRNA HSF1 Mir4 and shRNA HSF1 Mir4 + Doxycycline [0.5μg/ ml]. Expressed as mean ± SD. n=6

A

48 hours

B

24 hours

C

0 hours

D

Controls
(72 hours)
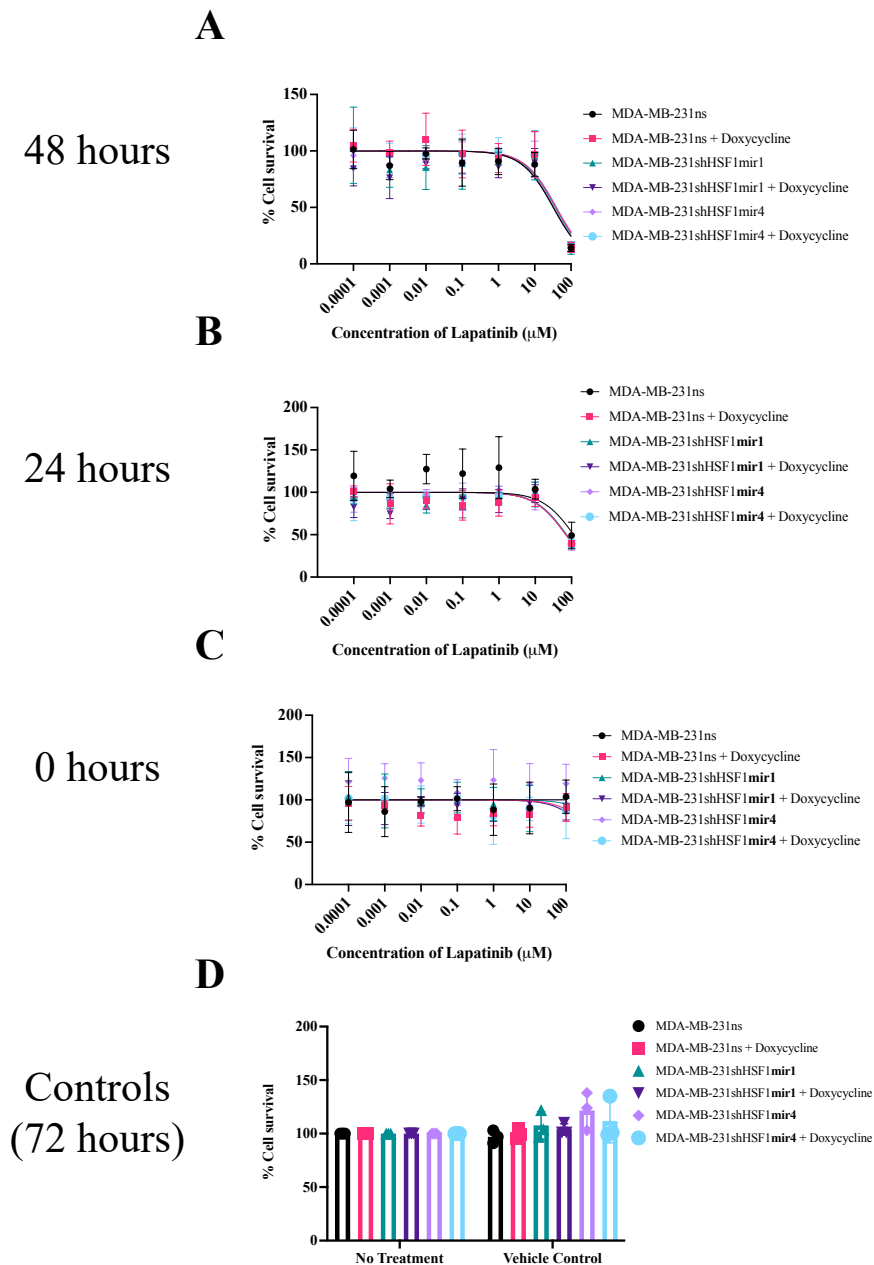
	IC$_{50}$ Cell Survival (μM)	
Cell Line	**MDA-MB-231**	
Time (Hours)	**24**	**48**
Non-silencing	115	32
Non-silencing + Doxycycline	70	39
shRNA HSF1 Mir1	73	37
shRNA HSF1 Mir1 + Doxycycline	70	33
shRNA HSF1 Mir4	70	39
shRNA HSF1 Mir4 + Doxycycline	73	40

Figure A2 Additional timepoints and vehicle controls versus no treatment group for MDA-MB-231 inducible HSF1 knockdown cells treated with Lapatinib

Cell survivability graphs for MDA-MB-231 with HSF1 inducible knockdown cells at **(A)** 48 hours **(B)** 24 hours and **(C)** 0 hours cotreated with Lapatinib. **(D)** 72 hours Vehicle Controls (0.2% v/v DMSO) compared to No Treatment (complete medium). Calculated IC50 values are represented in table according to cell conditions: non-silencing (ns), ns + Doxycycline [0.5μg/ ml], shRNA HSF1 Mir1, shRNA HSF1 Mir1 + Doxycycline [0.5μg/ ml], shRNA HSF1 Mir4 and shRNA HSF1 Mir4 + Doxycycline [0.5μg/ ml]. Expressed as mean ± SD. n=3

A — 48 hours

B — 24 hours

C — 0 hours

D — Controls (72 hours)
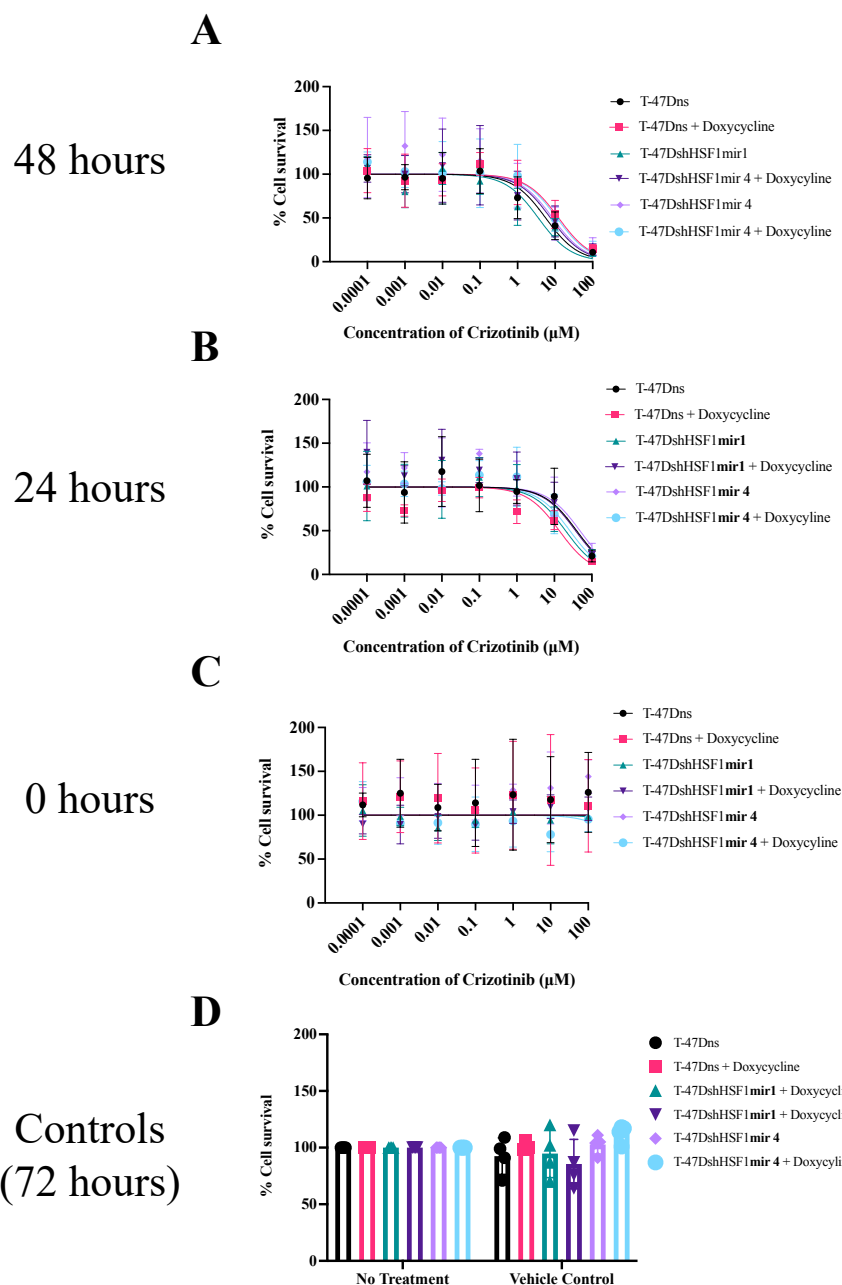
	IC$_{50}$ Cell Survival (μM)	
Cell Line	**T-47D**	
Time (Hours)	**24**	**48**
Non-silencing	39	6
Non-silencing + Doxycycline	14	12
shRNA HSF1 Mir1	20	4
shRNA HSF1 Mir1 + Doxycycline	37	8
shRNA HSF1 Mir4	48	9
shRNA HSF1 Mir4 + Doxycycline	26	11

Figure A3 Additional timepoints and vehicle controls versus no treatment group for T47D inducible HSF1 knockdown cells treated with Crizotinib

Cell survivability graphs for T47D with HSF1 inducible knockdown cells at **(A)** 48 hours **(B)** 24 hours and **(C)** 0 hours cotreated with Crizotinib. **(D)** 72 hours Vehicle Controls (0.2% v/v DMSO) compared to No Treatment (complete medium). Calculated IC$_{50}$ values are represented in table according to cell conditions: non-silencing (ns), ns + Doxycycline [0.5μg/ ml], shRNA HSF1 Mir1, shRNA HSF1 Mir1 + Doxycycline [0.5μg/ ml], shRNA HSF1 Mir4 and shRNA HSF1 Mir4 + Doxycycline [0.5μg/ ml]. Expressed as mean ± SD. n=4

A

48 hours

B

24 hours

C

0 hours

D

Controls
(72 hours)
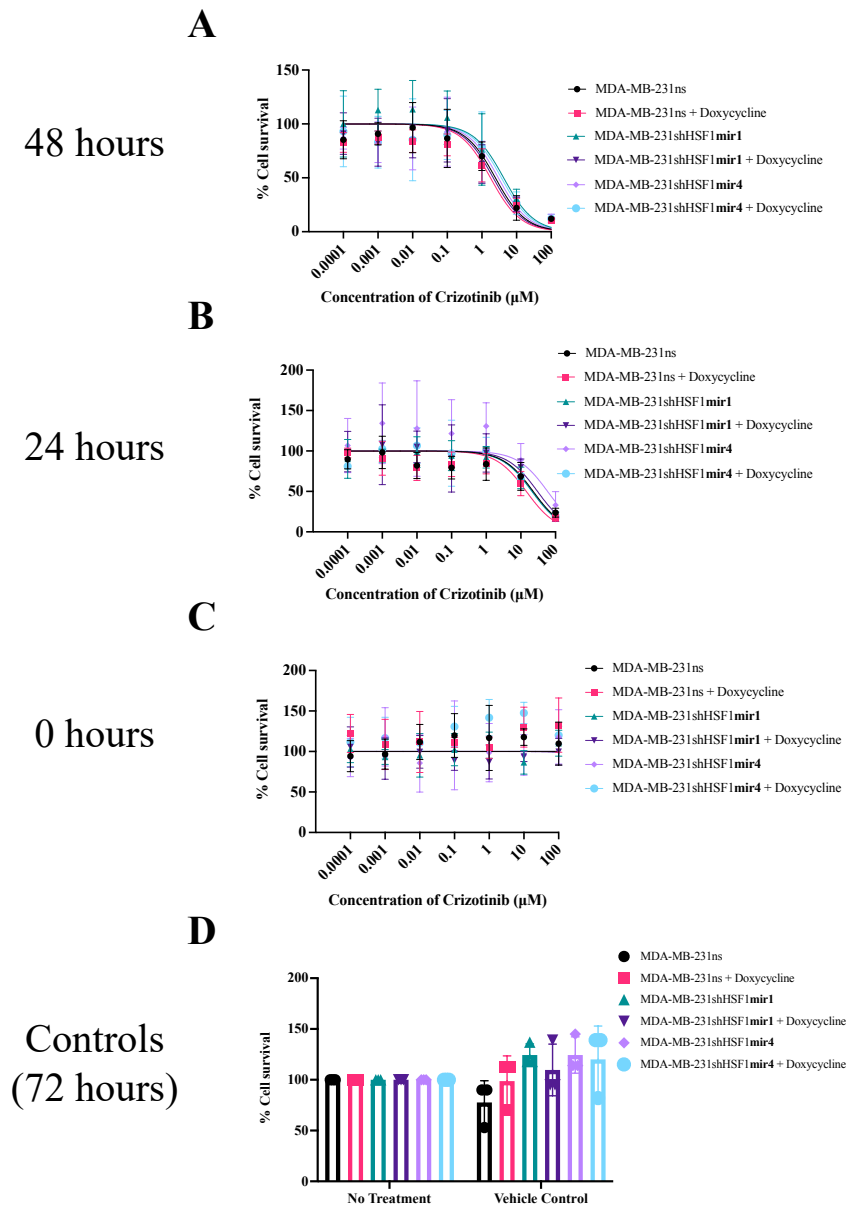
Cell Line	IC_{50} Cell Survival (μM)	
	MDA-MB-231	
Time (Hours)	**24**	**48**
Non-silencing	23	2
Non-silencing + Doxycycline	14	2
shRNA HSF1 Mir1	21	4
shRNA HSF1 Mir1 + Doxycycline	30	2
shRNA HSF1 Mir4	59	3
shRNA HSF1 Mir4 + Doxycycline	21	4

Figure A4 Additional timepoints and vehicle controls versus no treatment group for MDA-MB-231 inducible HSF1 knockdown cells treated with Crizotinib

Cell survivability graphs for MDA-MB-231 with HSF1 inducible knockdown cells at **(A)** 48 hours **(B)** 24 hours and **(C)** 0 hours cotreated with Crizotinib. **(D)** 72 hours Vehicle Controls (0.2% v/v DMSO) compared to No Treatment (complete medium). Calculated IC50 values are represented in table according to cell conditions: non-silencing (ns), ns + Doxycycline [0.5μg/ ml], shRNA HSF1 Mir1, shRNA HSF1 Mir1 + Doxycycline [0.5μg/ ml], shRNA HSF1 Mir4 and shRNA HSF1 Mir4 + Doxycycline [0.5μg/ ml]. Expressed as mean ± SD. n=4

A — 48 hours

B — 24 hours

C — 0 hours

D — Controls (72 hours)
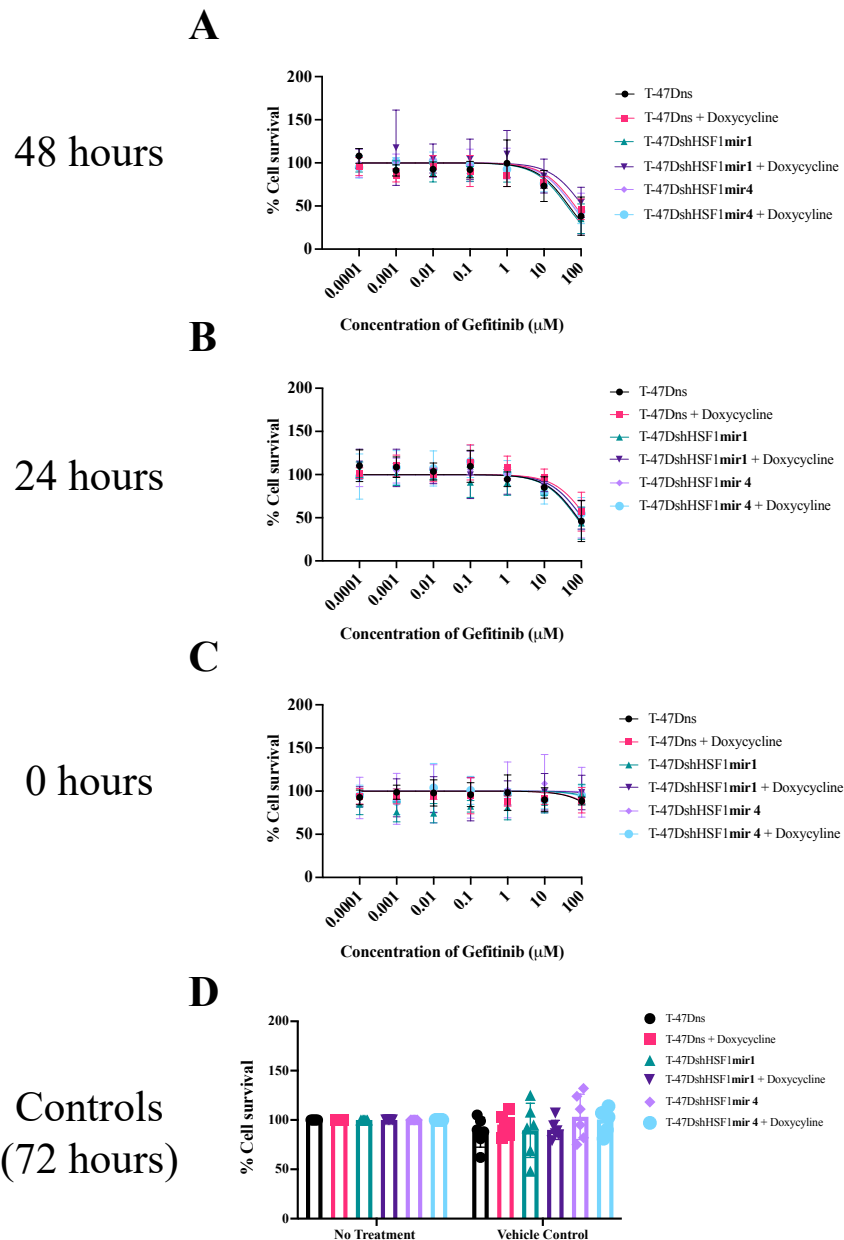
	IC$_{50}$ Cell Survival (μM)	
Cell Line	T-47D	
Time (Hours)	24	48
Non-silencing	80	47
Non-silencing + Doxycycline	138	69
shRNA HSF1 Mir1	75	42
shRNA HSF1 Mir1 + Doxycycline	106	111
shRNA HSF1 Mir4	82	60
shRNA HSF1 Mir4 + Doxycycline	104	61

Figure A5 Additional timepoints and vehicle controls versus no treatment group for T47D inducible HSF1 knockdown cells treated with Gefitinib

Cell survivability graphs for T47D with HSF1 inducible knockdown cells at **(A)** 48 hours **(B)** 24 hours and **(C)** 0 hours cotreated with Gefitinib. **(D)** 72 hours Vehicle Controls (0.2% v/v DMSO) compared to No Treatment (complete medium). Calculated IC50 values are represented in table according to cell conditions: non-silencing (ns), ns + Doxycycline [0.5μg/ ml], shRNA HSF1 Mir1, shRNA HSF1 Mir1 + Doxycycline [0.5μg/ ml], shRNA HSF1 Mir4 and shRNA HSF1 Mir4 + Doxycycline [0.5μg/ ml]. Expressed as mean ± SD. n=6

A   48 hours

B   24 hours

C   0 hours

D   Controls (72 hours)
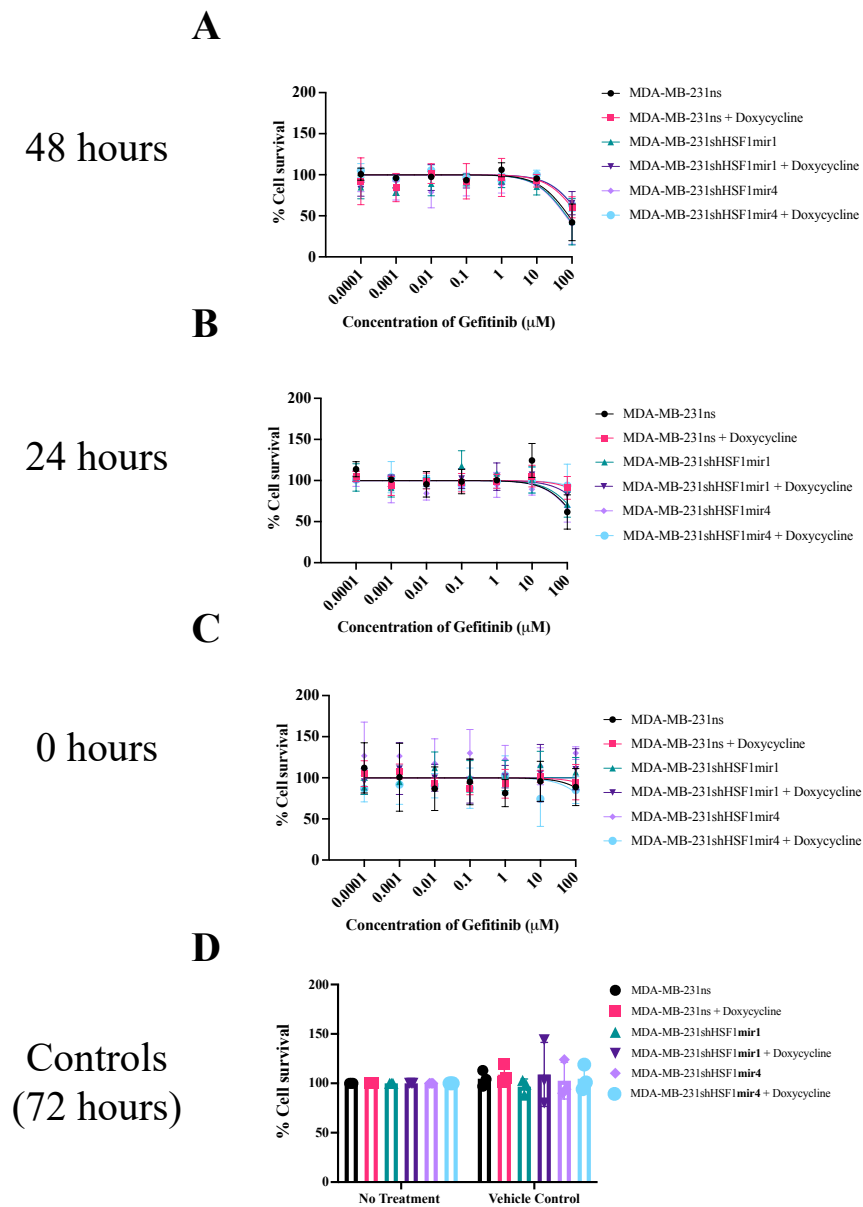
	IC$_{50}$ Cell Survival (μM)	
Cell Line	**MDA-MB-231**	
Time (Hours)	**24**	**48**
Non-silencing	207	81
Non-silencing + Doxycycline	1107	150
shRNA HSF1 Mir1	253	70
shRNA HSF1 Mir1 + Doxycycline	511	174
shRNA HSF1 Mir4	197	66
shRNA HSF1 Mir4 + Doxycycline	1502	180

Figure A6 Additional timepoints and vehicle controls versus no treatment group for MDA-MB-231 inducible HSF1 knockdown cells treated with Gefitinib

Cell survivability graphs for MDA-Mb-231 with HSF1 inducible knockdown cells at **(A)** 48 hours **(B)** 24 hours and **(C)** 0 hours cotreated with Gefitinib. **(D)** 72 hours Vehicle Controls (0.2% v/v DMSO) compared to No Treatment (complete medium). Calculated IC50 values are represented in table according to cell conditions: non-silencing (ns), ns + Doxycycline [0.5μg/ ml], shRNA HSF1 Mir1, shRNA HSF1 Mir1 + Doxycycline [0.5μg/ ml], shRNA HSF1 Mir4 and shRNA HSF1 Mir4 + Doxycycline [0.5μg/ ml]. Expressed as mean ± SD. n=3

A

48 hours

B

24 hours

C

0 hours

D

Controls
(72 hours)
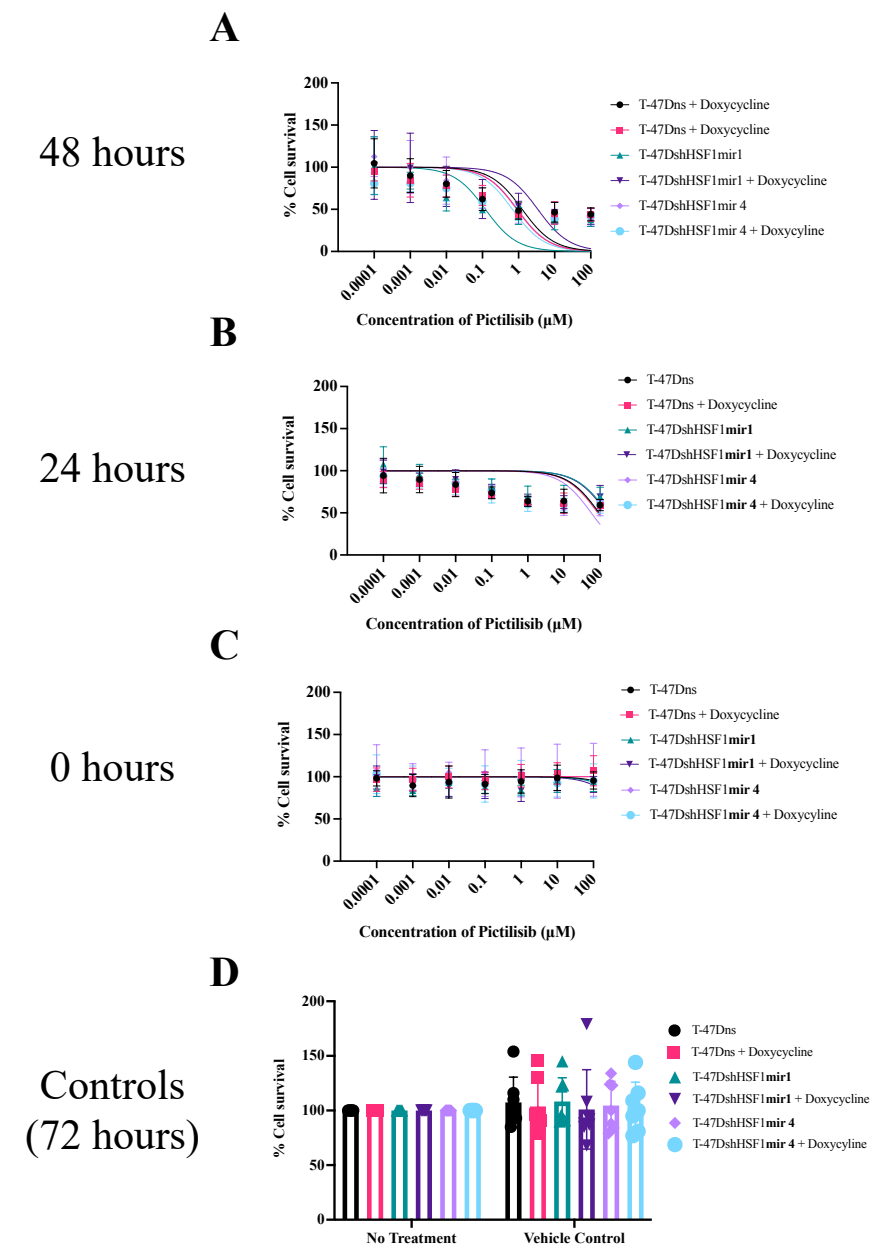
	IC$_{50}$ Cell Survival (μM)	
Cell Line	**T-47D**	
Time (Hours)	**24**	**48**
Non-silencing	94.15	1.26
Non-silencing + Doxycycline	86.78	0.90
shRNA HSF1 Mir1	163.36	0.12
shRNA HSF1 Mir1 + Doxycycline	153.47	3.42
shRNA HSF1 Mir4	57.09	0.94
shRNA HSF1 Mir4 + Doxycycline	94.90	0.68

Figure A7 Additional timepoints and vehicle controls versus no treatment group for T47D inducible HSF1 knockdown cells treated with Pictilisib

Cell survivability graphs for T47D with HSF1 inducible knockdown cells at **(A)** 48 hours **(B)** 24 hours and **(C)** 0 hours cotreated with Pictilisib. **(D)** 72 hours Vehicle Controls (0.2% v/v DMSO) compared to No Treatment (complete medium). Calculated IC50 values are represented in table according to cell conditions: non-silencing (ns), ns + Doxycycline [0.5μg/ ml], shRNA HSF1 Mir1, shRNA HSF1 Mir1 + Doxycycline [0.5μg/ ml], shRNA HSF1 Mir4 and shRNA HSF1 Mir4 + Doxycycline [0.5μg/ ml]. Expressed as mean ± SD. n=7

A

48 hours

% Cell survival

200 150 100 50 0

0.0001 0.001 0.01 0.1 1 10 100

Concentration of Pictilisib (µM)

- MDA-MB-231ns
- MDA-MB-231ns + Doxycycline
- MDA-MB-231shHSF1mir1
- MDA-MB-231shHSF1mir1 + Doxycycline
- MDA-MB-231shHSF1mir4
- MDA-MB-231shHSF1mir4 + Doxycycline

B

24 hours

% Cell survival

200 150 100 50 0

0.0001 0.001 0.01 0.1 1 10 100

Concentration of Pictilisib (µM)

- MDA-MB-231ns
- MDA-MB-231ns + Doxycycline
- MDA-MB-231shHSF1**mir1**
- MDA-MB-231shHSF1**mir1** + Doxycycline
- MDA-MB-231shHSF1**mir4**
- MDA-MB-231shHSF1**mir4** + Doxycycline

C

0 hours

% Cell survival

200 150 100 50 0

0.0001 0.001 0.01 0.1 1 10 100

Concentration of Pictilisib (µM)

- MDA-MB-231ns
- MDA-MB-231ns + Doxycycline
- MDA-MB-231shHSF1**mir1**
- MDA-MB-231shHSF1**mir1** + Doxycycline
- MDA-MB-231shHSF1**mir4**
- MDA-MB-231shHSF1**mir4** + Doxycycline

D

Controls (72 hours)

% Cell survival

200 150 100 50 0

No Treatment   Vehicle Control

- MDA-MB-231ns
- MDA-MB-231ns + Doxycycline
- MDA-MB-231shHSF1**mir1**
- MDA-MB-231shHSF1**mir1** + Doxycycline
- MDA-MB-231shHSF1**mir4**
- MDA-MB-231shHSF1**mir4** + Doxycycline

	IC_{50} Cell Survival (µM)	
Cell Line	**MDA-MB-231**	
Time (Hours)	**24**	**48**
Non-silencing	182.68	48.33
Non-silencing + Doxycycline	157.07	79.81
shRNA HSF1 Mir1	322.79	127.27
shRNA HSF1 Mir1 + Doxycycline	240.95	116.61
shRNA HSF1 Mir4	109.75	96.06
shRNA HSF1 Mir4 + Doxycycline	445.38	144.37

Figure A8 Additional timepoints and vehicle controls versus no treatment group for MDA-MB-231 inducible HSF1 knockdown cells treated with Pictilisib

Cell survivability graphs for MDA-MB-231 with HSF1 inducible knockdown cells at **(A)** 48 hours **(B)** 24 hours and **(C)** 0 hours cotreated with Pictilisib. **(D)** 72 hours Vehicle Controls (0.2% v/v DMSO) compared to No Treatment (complete medium). Calculated IC50 values are represented in table according to cell conditions: non-silencing (ns), ns + Doxycycline [0.5μg/ ml], shRNA HSF1 Mir1, shRNA HSF1 Mir1 + Doxycycline [0.5μg/ ml], shRNA HSF1 Mir4 and shRNA HSF1 Mir4 + Doxycycline [0.5μg/ ml]. Expressed as mean ± SD. n=3

A 48 hours

B 24 hours

C 0 hours

D Controls (72 hours)
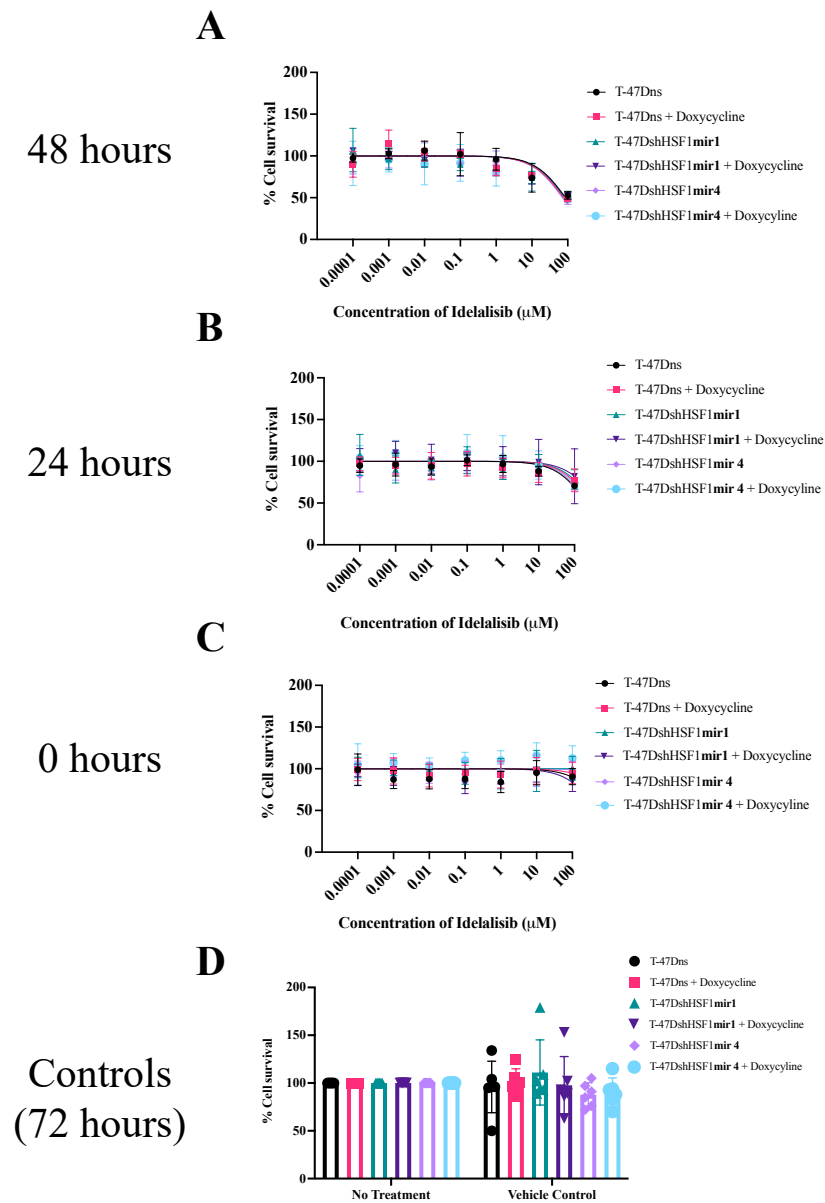
	IC$_{50}$ Cell Survival (μM)	
Cell Line	**T-47D**	
Time (Hours)	**24**	**48**
Non-silencing	222	104
Non-silencing + Doxycycline	307	114
shRNA HSF1 Mir1	352	91
shRNA HSF1 Mir1 + Doxycycline	461	120
shRNA HSF1 Mir4	247	80
shRNA HSF1 Mir4 + Doxycycline	276	108

Figure A9 Additional timepoints and vehicle controls versus no treatment group for T47D inducible HSF1 knockdown cells treated with Idelalisib

Cell survivability graphs for T47D with HSF1 inducible knockdown cells at **(A)** 48 hours **(B)** 24 hours and **(C)** 0 hours cotreated with Idelalisib. **(D)** 72 hours Vehicle Controls (0.2% v/v DMSO) compared to No Treatment (complete medium). Calculated IC$_{50}$ values are represented in table according to cell conditions: non-silencing (ns), ns + Doxycycline [0.5μg/ ml], shRNA HSF1 Mir1, shRNA HSF1 Mir1 + Doxycycline [0.5μg/ ml], shRNA HSF1 Mir4 and shRNA HSF1 Mir4 + Doxycycline [0.5μg/ ml]. Expressed as mean ± SD. n=6

A

48 hours

B

24 hours

C

0 hours

D

Controls
(72 hours)

	IC$_{50}$ Cell Survival (μM)	
Cell Line	**MDA-MB-231**	
Time (Hours)	**24**	**48**
Non-silencing	∞	295
Non-silencing + Doxycycline	588	307
shRNA HSF1 Mir1	3232	352
shRNA HSF1 Mir1 + Doxycycline	135238	260
shRNA HSF1 Mir4	2746	330
shRNA HSF1 Mir4 + Doxycycline	17313	1539

∞ infinite IC$_{50}$ Value/ IC$_{50}$ not determined

Figure A10 Additional timepoints and vehicle controls versus no treatment group for MDA-MB-231 inducible HSF1 knockdown cells treated with Idelalisib
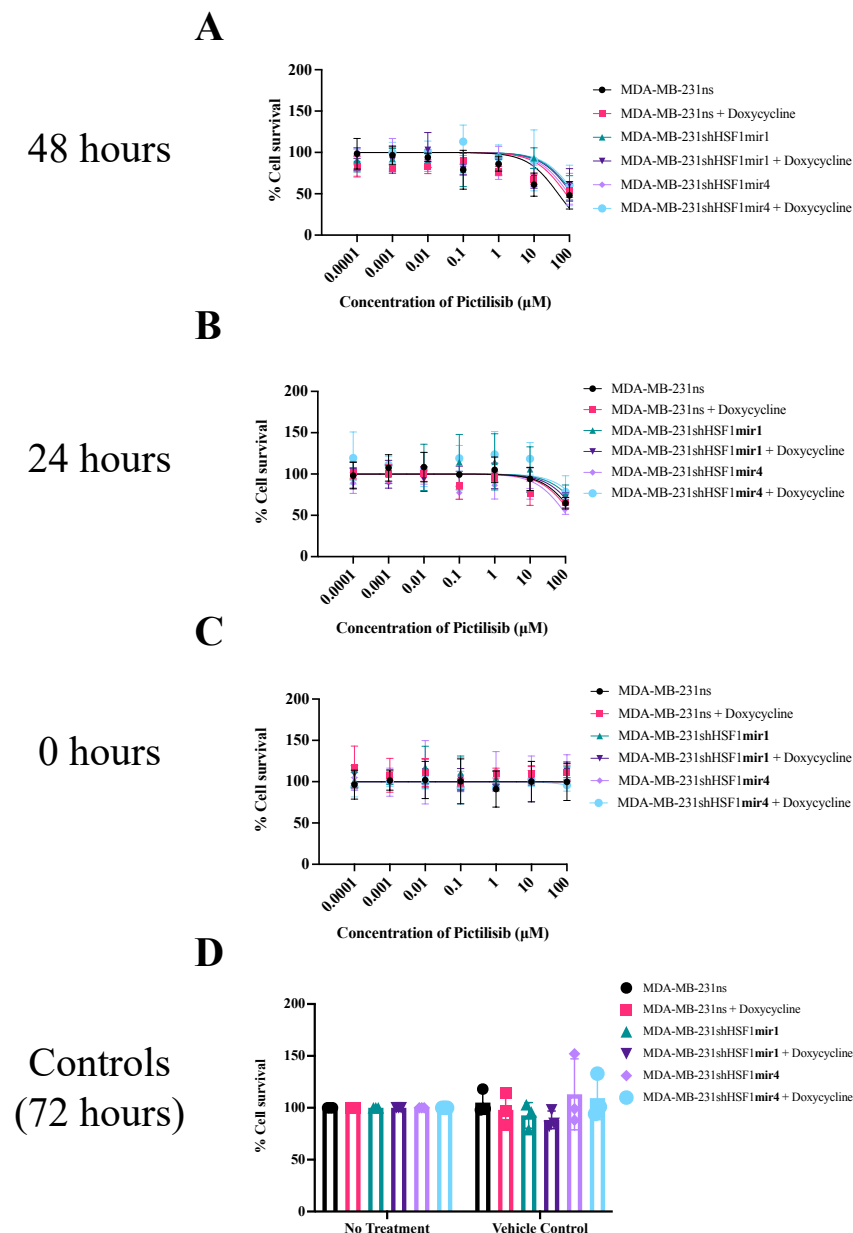
Cell survivability graphs for MDA-MB-231 with HSF1 inducible knockdown cells at **(A)** 48 hours **(B)** 24 hours and **(C)** 0 hours cotreated with Idelalisib. **(D)** 72 hours Vehicle Controls (0.2% v/v DMSO) compared to No Treatment (complete medium). Calculated IC_{50} values are represented in table according to cell conditions: non-silencing (ns), ns + Doxycycline [0.5μg/ ml], shRNA HSF1 Mir1, shRNA HSF1 Mir1 + Doxycycline [0.5μg/ ml], shRNA HSF1 Mir4 and shRNA HSF1 Mir4 + Doxycycline [0.5μg/ ml]. Expressed as mean ± SD. n=3

A

48 hours

% Cell survival

Concentration of Doxorubicin (μM)

- T-47Dns
- T-47Dns + Doxycycline
- T-47DshHSF1mir1
- T-47DshHSF1mir1 + Doxycycline
- T-47DshHSF1mir 4
- T-47DshHSF1mir 4 + Doxycyline

B

24 hours

% Cell survival

Concentration of Doxorubicin (μM)

- T-47Dns
- T-47Dns + Doxycycline
- T-47DshHSF1**mir1**
- T-47DshHSF1**mir1** + Doxycycline
- T-47DshHSF1**mir 4**
- T-47DshHSF1**mir 4** + Doxycyline

C

0 hours

% Cell survival

Concentration of Doxorubicin (μM)

- T-47Dns
- T-47Dns + Doxycycline
- T-47DshHSF1**mir1**
- T-47DshHSF1**mir1** + Doxycycline
- T-47DshHSF1**mir 4**
- T-47DshHSF1**mir 4** + Doxycyline

D

Controls (72 hours)

% Cell survival

No Treatment   Vehicle Control

- T-47Dns
- T-47Dns + Doxycycline
- T-47DshHSF1**mir1**
- T-47DshHSF1**mir1** + Doxycycline
- T-47DshHSF1**mir 4**
- T-47DshHSF1**mir 4** + Doxycyline
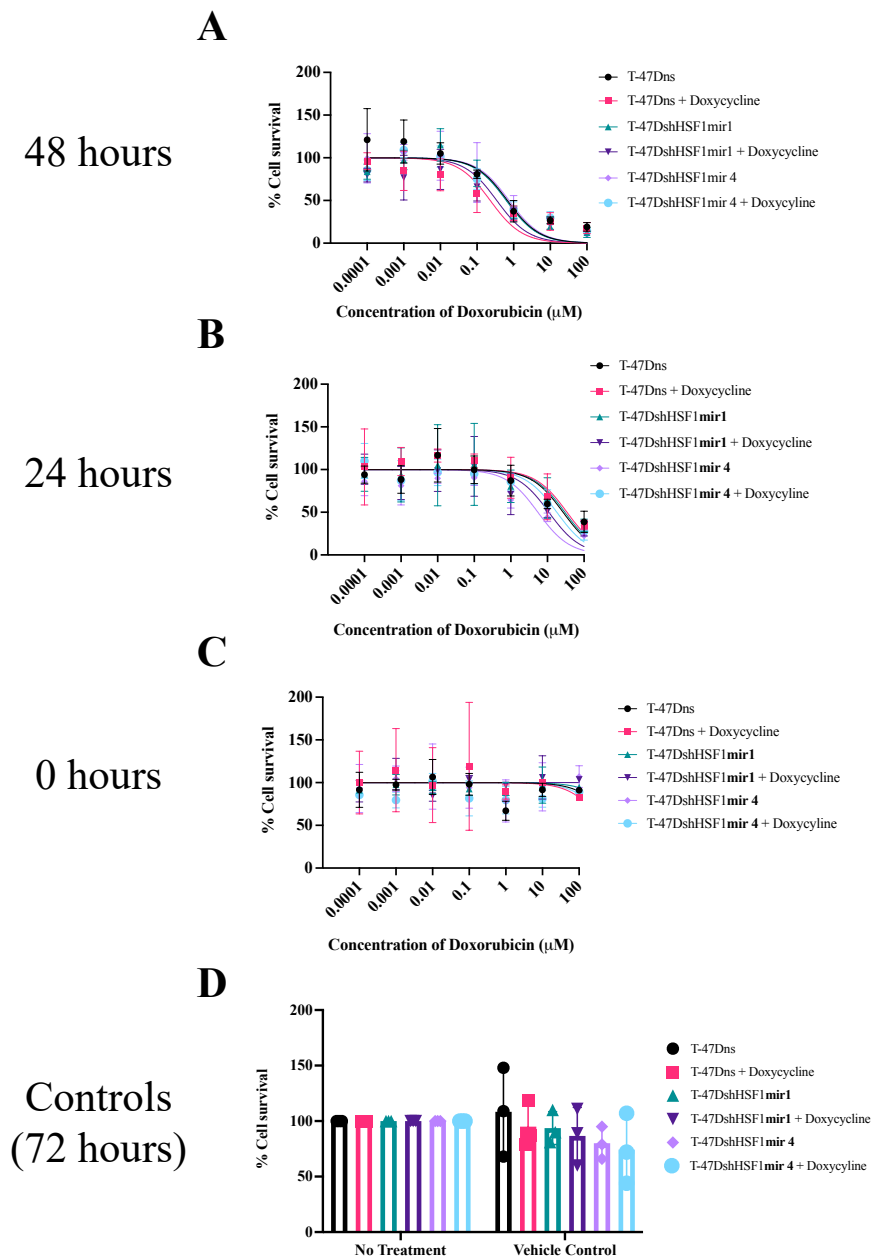
Cell Line	IC_{50} Cell Survival (μM) T-47D	
Time (Hours)	**24**	**48**
Non-silencing	26.78	0.68
Non-silencing + Doxycycline	34.29	0.23
shRNA HSF1 Mir1	30.03	0.63
shRNA HSF1 Mir1 + Doxycycline	10.93	0.35
shRNA HSF1 Mir4	5.49	0.75
shRNA HSF1 Mir4 + Doxycycline	18.07	0.65

Figure A11 Additional timepoints and vehicle controls versus no treatment group for T47D inducible HSF1 knockdown cells treated with Doxorubicin

Cell survivability graphs for T47D with HSF1 inducible knockdown cells at **(A)** 48 hours **(B)** 24 hours and **(C)** 0 hours cotreated with Doxorubicin. **(D)** 72 hours Vehicle Controls (0.2% v/v DMSO) compared to No Treatment (complete medium). Calculated IC50 values are represented in table according to cell conditions: non-silencing (ns), ns + Doxycycline [0.5μg/ ml], shRNA HSF1 Mir1, shRNA HSF1 Mir1 + Doxycycline [0.5μg/ ml], shRNA HSF1 Mir4 and shRNA HSF1 Mir4 + Doxycycline [0.5μg/ ml]. Expressed as mean ± SD. n=3
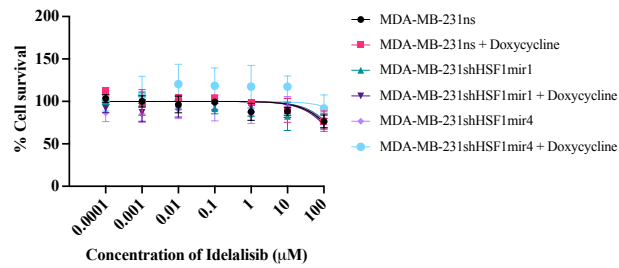
A

48 hours

B

24 hours

C

0 hours

D

Controls
(72 hours)
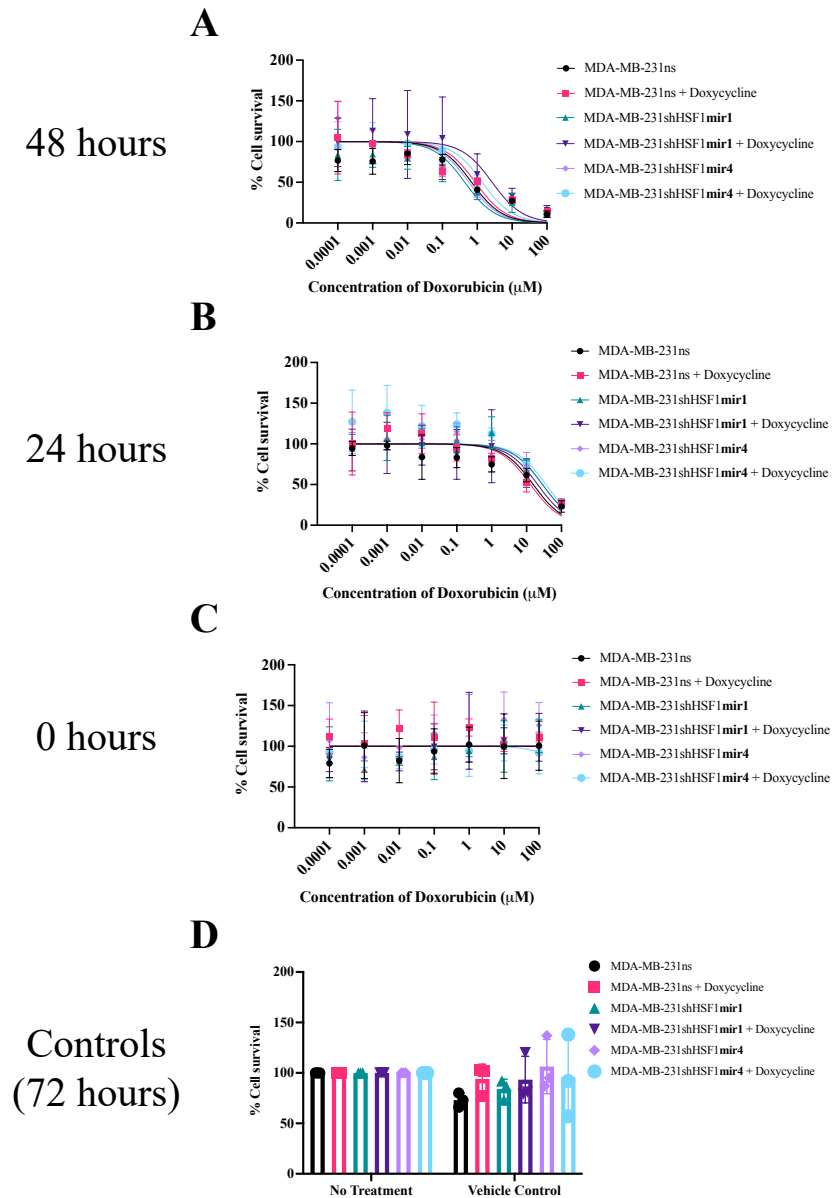
Cell Line	IC_{50} Cell Survival (μM) MDA-MB-231	
Time (Hours)	**24**	**48**
Non-silencing	15.59	0.69
Non-silencing + Doxycycline	12.99	0.88
shRNA HSF1 Mir1	28.77	0.44
shRNA HSF1 Mir1 + Doxycycline	20.82	2.68
shRNA HSF1 Mir4	28.61	0.58
shRNA HSF1 Mir4 + Doxycycline	35.84	1.40

Figure A12 Additional timepoints and vehicle controls versus no treatment group for MDA-MB-231 inducible HSF1 knockdown cells treated with Doxorubicin

Cell survivability graphs for MDA-MB-231 with HSF1 inducible knockdown cells at **(A)** 48 hours **(B)** 24 hours and **(C)** 0 hours cotreated with Doxorubicin. **(D)** 72 hours Vehicle Controls (0.2% v/v DMSO) compared to No Treatment (complete medium). Calculated IC50 values are represented in table according to cell conditions: non-silencing (ns), ns + Doxycycline [0.5μg/ ml], shRNA HSF1 Mir1, shRNA HSF1 Mir1 + Doxycycline [0.5μg/ ml], shRNA HSF1 Mir4 and shRNA HSF1 Mir4 + Doxycycline [0.5μg/ ml]. Expressed as mean ± SD. n=3
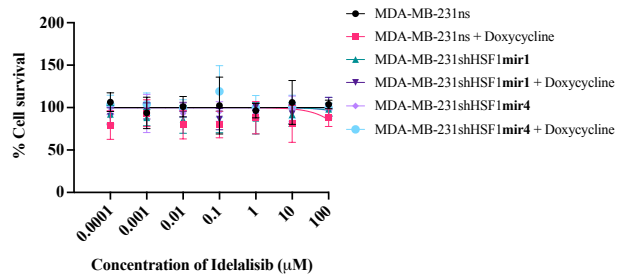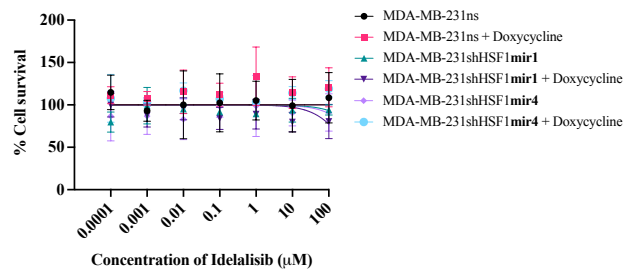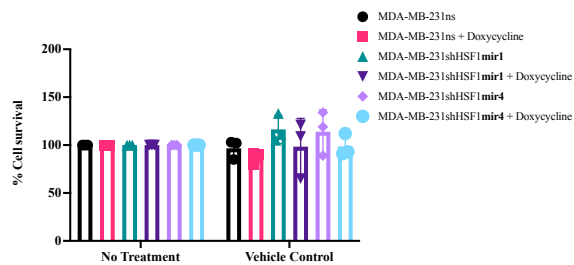
A

72 hours

% Cell survival

200
150
100
50

0.0001 0.001 0.01 0.1 1 10 100

Concentration of AZD8055 (µM)

- T47Dns
- T-47Dns + Doxycycline
- T47DshHSF1**mir1**
- T47DshHSF1**mir1** + Doxycycline
- T-47DshHSF1**mir4**
- T-47DshHSF1**mir4** + Doxycyline

B

0 hours

% Cell survival

200
150
100
50
0

0.0001 0.001 0.01 0.1 1 10 100

Concentration of AZD8055 (µM)

- T47Dns
- T-47Dns + Doxycycline
- T-47DshHSF1**mir1**
- T-47DshHSF1**mir1** + Doxycycline
- T-47DshHSF1**mir 4**
- T-47DshHSF1**mir 4** + Doxycyline

C

Controls
(72 hours)

% Cell survival

200
150
100
50
0

No Treatment   Vehicle Control

- T-47Dns
- T-47Dns + Doxycycline
- T-47DshHSF1**mir1**
- T-47DshHSF1**mir1** + Doxycycline
- T-47DshHSF1**mir 4**
- T-47DshHSF1**mir 4** + Doxycyline

	IC_{50} Cell Survival (µM)
Cell Line	**T-47D**
Time (Hours)	**72**
Non-silencing	0.0081
Non-silencing + Doxycycline	0.0194
shRNA HSF1 Mir1	0.0004
shRNA HSF1 Mir1 + Doxycycline	0.0136
shRNA HSF1 Mir4	0.0072
shRNA HSF1 Mir4 + Doxycycline	0.0414

Figure A13 T47D inducible HSF1 knockdown cells treated with AZD8055

Cell survivability graphs for T47D with HSF1 inducible knockdown cells at **(A)** 72 hours and **(B)** 0 hours cotreated with AZD8055. **(C)** 72 hours Vehicle Controls (0.2% v/v DMSO) compared to No Treatment (complete medium). Hypothesised IC_{50} values are represented in table according to cell conditions: non-silencing (ns), ns + Doxycycline [0.5µg/ ml], shRNA HSF1 Mir1, shRNA HSF1 Mir1 + Doxycycline [0.5µg/ ml], shRNA HSF1 Mir4 and shRNA HSF1 Mir4 + Doxycycline [0.5µg/ ml]. Expressed as mean ± SD. n=2

A

72 hours

B

0 hours

C

Controls
(72 hours)

Cell Line	IC_{50} Cell Survival (μM)
	T-47D
Time (Hours)	**72**
Non-silencing	1.0712
Non-silencing + Doxycycline	0.3384
shRNA HSF1 Mir1	0.1045
shRNA HSF1 Mir1 + Doxycycline	0.1690
shRNA HSF1 Mir4	0.7790
shRNA HSF1 Mir4 + Doxycycline	0.2905

Figure A14 T47D inducible HSF1 knockdown cells treated with MK-2206
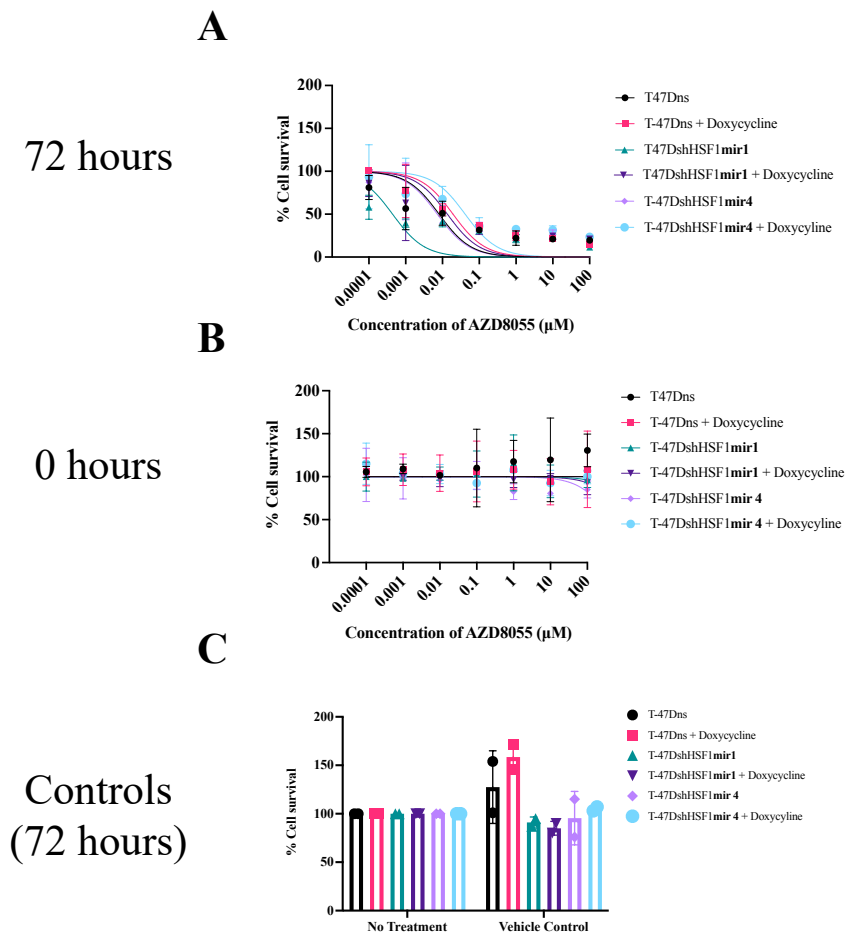
Cell survivability graphs for T47D with HSF1 inducible knockdown cells at **(A)** 72 hours and **(B)** 0 hours cotreated with MK-2206. **(C)** 72 hours Vehicle Controls (0.2% v/v DMSO) compared to No Treatment (complete medium). Hypothesised IC50 values are represented in table according to cell conditions: non-silencing (ns), ns + Doxycycline [0.5μg/ ml], shRNA HSF1 Mir1, shRNA HSF1 Mir1 + Doxycycline [0.5μg/ ml], shRNA HSF1 Mir4 and shRNA HSF1 Mir4 + Doxycycline [0.5μg/ ml]. Expressed as mean ± SD. n=2

A

72 hours

B

0 hours

C

Controls
(72 hours)
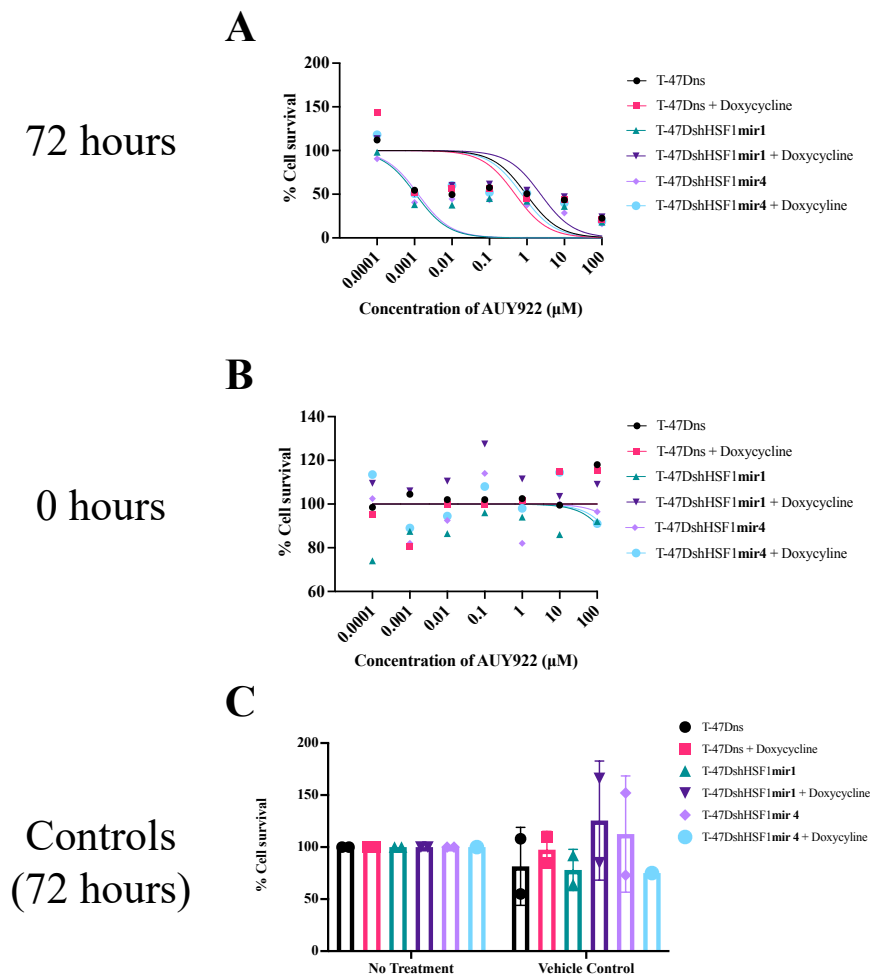
	IC$_{50}$ Cell Survival (μM)
Cell Line	**T-47D**
Time (Hours)	**72**
Non-silencing	0.953
Non-silencing + Doxycycline	0.485
shRNA HSF1 Mir1	0.001
shRNA HSF1 Mir1 + Doxycycline	2.317
shRNA HSF1 Mir4	0.001
shRNA HSF1 Mir4 + Doxycycline	0.727

Figure A15 T47D inducible HSF1 knockdown cells treated with AUY922
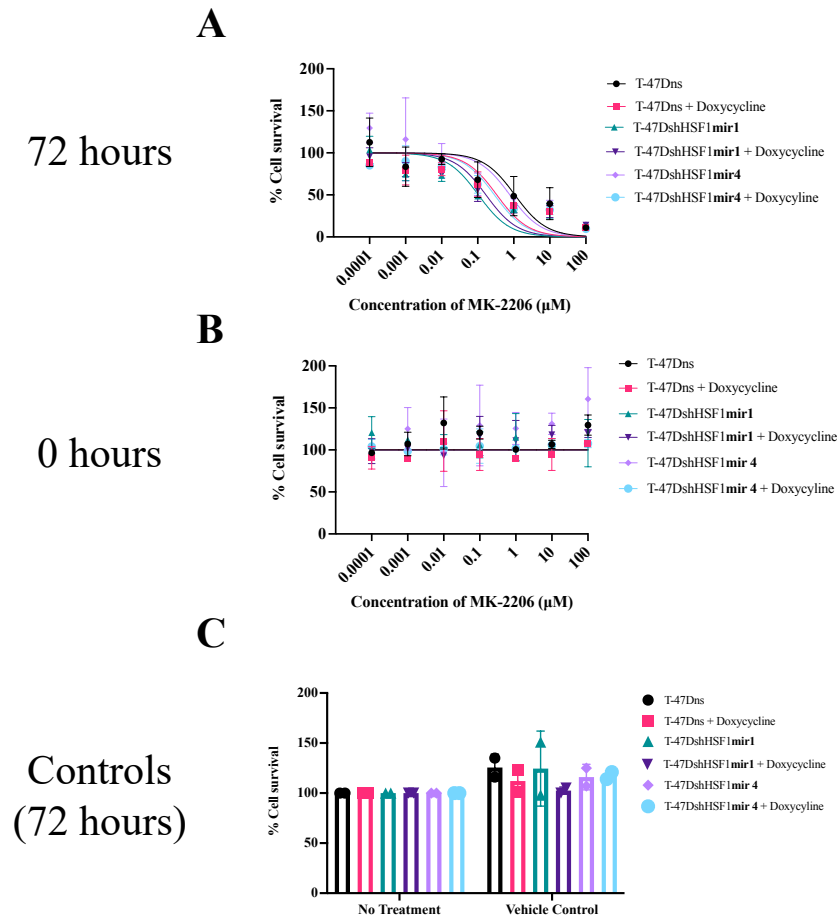
Cell survivability graphs for T47D with HSF1 inducible knockdown cells at **(A)** 72 hours and **(B)** 0 hours cotreated with AUY922. **(C)** 72 hours Vehicle Controls (0.2% v/v DMSO) compared to No Treatment (complete medium). Hypothesised IC50 values are represented in table according to cell conditions: non-silencing (ns), ns + Doxycycline [0.5μg/ ml], shRNA HSF1 Mir1, shRNA HSF1 Mir1 + Doxycycline [0.5μg/ ml], shRNA HSF1 Mir4 and shRNA HSF1 Mir4 + Doxycycline [0.5μg/ ml]. Expressed as mean ± SD. n=2

APPENDIX 2 Tables of Significance for the Anticancer Drugs tested.

Table A1 Doxorubicin

	Cell Line	Tukey's multiple comparisons test / Compared to	T-47D					MDA-MB-231				
			Predicted (LS) mean diff.	95.00% CI of diff.	Below threshold?	Summary	Adjusted P Value	Mean Diff.	95.00% CI of diff.	Below threshold?	Summary	Adjusted P Value
Doxorubicin	Non-silencing	Non-silencing + Doxycycline	8.708	-6.603 to 24.02	No	ns	0.5614	-3.875	-17.26 to 9.505	No	ns	0.9588
		shRNA HSF1 Mir1	2.083	-13.23 to 17.39	No	ns	0.9987	1.708	-11.67 to 15.09	No	ns	0.9991
		shRNA HSF1 Mir1 + Doxycycline	13.67	-3.451 to 30.78	No	ns	0.1939	4.917	-8.464 to 18.30	No	ns	0.8926
		shRNA HSF1 Mir4	0.9167	-16.20 to 18.03	No	ns	>0.9999	4.292	-9.089 to 17.67	No	ns	0.937
		shRNA HSF1 Mir4 + Doxycycline	20.08	4.772 to 35.39	Yes	**	0.0033	6.292	-7.089 to 19.67	No	ns	0.7462
	Non-silencing + Doxycycline	shRNA HSF1 Mir1	-6.625	-21.94 to 8.686	No	ns	0.8037	5.583	-7.797 to 18.96	No	ns	0.8293
		shRNA HSF1 Mir1 + Doxycycline	4.958	-12.16 to 22.08	No	ns	0.9578	8.792	-4.589 to 22.17	No	ns	0.402
		shRNA HSF1 Mir4	-7.792	-24.91 to 9.326	No	ns	0.7681	8.167	-5.214 to 21.55	No	ns	0.4866
		shRNA HSF1 Mir4 + Doxycycline	11.38	-3.936 to 26.69	No	ns	0.2636	10.17	-3.214 to 23.55	No	ns	0.243
	shRNA HSF1 Mir1	shRNA HSF1 Mir1 + Doxycycline	11.58	-5.535 to 28.70	No	ns	0.3652	3.208	-10.17 to 16.59	No	ns	0.9818
		shRNA HSF1 Mir4	-1.167	-18.28 to 15.95	No	ns	>0.9999	2.583	-10.80 to 15.96	No	ns	0.9932
		shRNA HSF1 Mir4 + Doxycycline	18.00	2.689 to 33.31	Yes	*	0.0118	4.583	-8.797 to 17.96	No	ns	0.9181
	shRNA HSF1 Mir1 + Doxycycline	shRNA HSF1 Mir4	-12.75	-31.50 to 6.002	No	ns	0.3598	-0.625	-14.01 to 12.76	No	ns	>0.9999
		shRNA HSF1 Mir4 + Doxycycline	6.417	-10.70 to 23.53	No	ns	0.8822	1.375	-12.01 to 14.76	No	ns	0.9997
	shRNA HSF1 Mir4	shRNA HSF1 Mir4 + Doxycycline	19.17	2.049 to 36.28	Yes	*	0.0191	2	-11.38 to 15.38	No	ns	0.998

Table A2 Crizotinib

	Cell Line	Tukey's multiple comparisons test / Compared to	T-47D					MDA-MB-231				
			Mean Diff.	95.00% CI of diff.	Below threshold?	Summary	Adjusted P Value	Mean Diff.	95.00% CI of diff.	Below threshold?	Summary	Adjusted P Value
Crizotinib	Non-silencing	Non-silencing + Doxycycline	11.44	-2.797 to 25.67	No	ns	0.1925	-3.25	-13.69 to 7.186	No	ns	0.946
		shRNA HSF1 Mir1	3.594	-10.64 to 17.83	No	ns	0.978	0.8438	-9.592 to 11.28	No	ns	>0.9999
		shRNA HSF1 Mir1 + Doxycycline	12	-2.235 to 26.23	No	ns	0.1513	-2.969	-13.40 to 7.467	No	ns	0.9631
		shRNA HSF1 Mir4	21.25	7.015 to 35.48	Yes	***	0.0004	-12.72	-23.15 to -2.283	Yes	**	0.0075
		shRNA HSF1 Mir4 + Doxycycline	9.344	-4.891 to 23.58	No	ns	0.4088	-4.219	-14.65 to 6.217	No	ns	0.8514
	Non-silencing + Doxycycline	shRNA HSF1 Mir1	-7.844	-22.08 to 6.391	No	ns	0.6054	4.094	-6.342 to 14.53	No	ns	0.8668
		shRNA HSF1 Mir1 + Doxycycline	0.5625	-13.67 to 14.80	No	ns	>0.9999	0.2813	-10.15 to 10.72	No	ns	>0.9999
		shRNA HSF1 Mir4	9.813	-4.422 to 24.05	No	ns	0.3525	-9.469	-19.90 to 0.9671	No	ns	0.0989
		shRNA HSF1 Mir4 + Doxycycline	-2.094	-16.33 to 12.14	No	ns	0.9982	-0.9688	-11.40 to 9.467	No	ns	0.9998
	shRNA HSF1 Mir1	shRNA HSF1 Mir1 + Doxycycline	8.406	-5.828 to 22.64	No	ns	0.5303	-3.813	-14.25 to 6.623	No	ns	0.898
		shRNA HSF1 Mir4	17.66	3.422 to 31.89	Yes	**	0.0061	-13.56	-24.00 to -3.127	Yes	**	0.0034
		shRNA HSF1 Mir4 + Doxycycline	5.75	-8.485 to 19.98	No	ns	0.8518	-5.063	-15.50 to 5.373	No	ns	0.7263
	shRNA HSF1 Mir1 + Doxycycline	shRNA HSF1 Mir4	9.25	-4.985 to 23.48	No	ns	0.4205	-9.75	-20.19 to 0.6858	No	ns	0.0817
		shRNA HSF1 Mir4 + Doxycycline	-2.656	-16.89 to 11.58	No	ns	0.9945	-1.25	-11.69 to 9.186	No	ns	0.9993
	shRNA HSF1 Mir4	shRNA HSF1 Mir4 + Doxycycline	-11.91	-26.14 to 2.328	No	ns	0.1576	8.5	-1.936 to 18.94	No	ns	0.1803

Table A3 Gefitinib

	Cell Line	Tukey's multiple comparisons test / Compared to	T-47D					MDA-MB-231				
			Mean Diff.	95.00% CI of diff.	Below threshold?	Summary	Adjusted P Value	Mean Diff.	95.00% CI of diff.	Below threshold?	Summary	Adjusted P Value
Gefitinib	Non-silencing	Non-silencing + Doxycycline	-7.146	-15.69 to 1.402	No	ns	0.1598	-5.333	-19.88 to 9.214	No	ns	0.8935
		shRNA HSF1 Mir1	-4.604	-13.15 to 3.944	No	ns	0.6339	-6.917	-21.46 to 7.630	No	ns	0.7372
		shRNA HSF1 Mir1 + Doxycycline	-1	-9.548 to 7.548	No	ns	0.9994	-6.333	-20.88 to 8.214	No	ns	0.8025
		shRNA HSF1 Mir4	-5.208	-13.76 to 3.340	No	ns	0.4999	0.2917	-14.26 to 14.84	No	ns	>0.9999
		shRNA HSF1 Mir4 + Doxycycline	-2.479	-11.03 to 6.069	No	ns	0.9611	-4	-18.55 to 10.55	No	ns	0.9669
	Non-silencing + Doxycycline	shRNA HSF1 Mir1	2.542	-6.006 to 11.09	No	ns	0.9567	-1.583	-16.13 to 12.96	No	ns	0.9996
		shRNA HSF1 Mir1 + Doxycycline	6.146	-2.402 to 14.69	No	ns	0.309	-1	-15.55 to 13.55	No	ns	>0.9999
		shRNA HSF1 Mir4	1.938	-6.611 to 10.49	No	ns	0.9869	5.625	-8.922 to 20.17	No	ns	0.8701
		shRNA HSF1 Mir4 + Doxycycline	4.667	-3.881 to 13.21	No	ns	0.6202	1.333	-13.21 to 15.88	No	ns	0.9998
	shRNA HSF1 Mir1	shRNA HSF1 Mir1 + Doxycycline	3.604	-4.944 to 12.15	No	ns	0.8311	0.5833	-13.96 to 15.13	No	ns	>0.9999
		shRNA HSF1 Mir4	-0.6042	-9.152 to 7.944	No	ns	>0.9999	7.208	-7.339 to 21.76	No	ns	0.702
		shRNA HSF1 Mir4 + Doxycycline	2.125	-6.423 to 10.67	No	ns	0.9801	2.917	-11.63 to 17.46	No	ns	0.9919
	shRNA HSF1 Mir1 + Doxycycline	shRNA HSF1 Mir4	-4.208	-12.76 to 4.340	No	ns	0.7183	6.625	-7.922 to 21.17	No	ns	0.7708
		shRNA HSF1 Mir4 + Doxycycline	-1.479	-10.03 to 7.069	No	ns	0.9962	2.333	-12.21 to 16.88	No	ns	0.9972
	shRNA HSF1 Mir4	shRNA HSF1 Mir4 + Doxycycline	2.729	-5.819 to 11.28	No	ns	0.9418	-4.292	-18.84 to 10.26	No	ns	0.9554

Table A4 Idelalisib

		T-47D					MDA-MB-231				
	Tukey's multiple comparisons test	Mean Diff.	95.00% CI of diff.	Below threshold?	Summary	Adjusted P Value	Mean Diff.	95.00% CI of diff.	Below threshold?	Summary	Adjusted P Value
Cell Line	Compared to										
Non-silencing	Non-silencing + Doxycycline	-3.700	-13.86 to 6.457	No	ns	0.9007	1.75	-9.031 to 12.53	No	ns	0.997
	shRNA HSF1 Mir1	-6.325	-16.48 to 3.832	No	ns	0.4729	3.167	-7.615 to 13.95	No	ns	0.9562
	shRNA HSF1 Mir1 + Doxycycline	2.025	-8.132 to 12.18	No	ns	0.9926	2.417	-8.365 to 13.20	No	ns	0.9866
	shRNA HSF1 Mir4	-3.725	-13.88 to 6.432	No	ns	0.8981	-3.5	-14.28 to 7.281	No	ns	0.9339
	shRNA HSF1 Mir4 + Doxycycline	-8.925	-19.08 to 1.232	No	ns	0.1207	-4.5	-15.28 to 6.281	No	ns	0.8291
Non-silencing + Doxycycline	shRNA HSF1 Mir1	-2.625	-12.78 to 7.532	No	ns	0.9761	1.417	-9.365 to 12.20	No	ns	0.9989
	shRNA HSF1 Mir1 + Doxycycline	5.725	-4.432 to 15.88	No	ns	0.5846	0.6667	-10.11 to 11.45	No	ns	>0.9999
	shRNA HSF1 Mir4	-0.02500	-10.18 to 10.13	No	ns	>0.9999	-5.25	-16.03 to 5.531	No	ns	0.7172
	shRNA HSF1 Mir4 + Doxycycline	-5.225	-15.38 to 4.932	No	ns	0.6769	-6.25	-17.03 to 4.531	No	ns	0.5445
shRNA HSF1 Mir1	shRNA HSF1 Mir1 + Doxycycline	8.350	-1.807 to 18.51	No	ns	0.1734	-0.75	-11.53 to 10.03	No	ns	>0.9999
	shRNA HSF1 Mir4	2.600	-7.557 to 12.76	No	ns	0.9771	-6.667	-17.45 to 4.115	No	ns	0.4718
	shRNA HSF1 Mir4 + Doxycycline	-2.600	-12.76 to 7.557	No	ns	0.9771	-7.667	-18.45 to 3.115	No	ns	0.3128
shRNA HSF1 Mir1 + Doxycycline	shRNA HSF1 Mir4	-5.750	-15.91 to 4.407	No	ns	0.5800	-5.917	-16.70 to 4.865	No	ns	0.6032
	shRNA HSF1 Mir4 + Doxycycline	-10.95	-21.11 to -0.7931	Yes	*	0.0264	-6.917	-17.70 to 3.865	No	ns	0.4295
shRNA HSF1 Mir4	shRNA HSF1 Mir4 + Doxycycline	-5.200	-15.36 to 4.957	No	ns	0.6814	-1	-11.78 to 9.781	No	ns	0.9998

Table A5 Lapatinib

		T-47D					MDA-MB-231				
	Tukey's multiple comparisons test	Mean Diff.	95.00% CI of diff.	Below threshold?	Summary	Adjusted P Value	Mean Diff.	95.00% CI of diff.	Below threshold?	Summary	Adjusted P Value
Cell Line	Compared to										
Non-silencing	Non-silencing + Doxycycline	-2.229	-9.080 to 4.621	No	ns	0.9371	2.750	-8.387 to 13.89	No	ns	0.9793
	shRNA HSF1 Mir1	1.667	-5.184 to 8.517	No	ns	0.9819	9.542	-1.595 to 20.68	No	ns	0.1369
	shRNA HSF1 Mir1 + Doxycycline	-0.7083	-7.559 to 6.142	No	ns	0.9997	-2.708	-13.85 to 8.429	No	ns	0.9807
	shRNA HSF1 Mir4	-2.521	-9.371 to 4.330	No	ns	0.8977	0.5000	-10.64 to 11.64	No	ns	>0.9999
	shRNA HSF1 Mir4 + Doxycycline	-4.833	-11.68 to 2.017	No	ns	0.3302	-11.79	-22.93 to -0.6545	Yes	*	0.0315
Non-silencing + Doxycycline	shRNA HSF1 Mir1	3.896	-2.955 to 10.75	No	ns	0.577	6.792	-4.345 to 17.93	No	ns	0.4876
	shRNA HSF1 Mir1 + Doxycycline	1.521	-5.330 to 8.371	No	ns	0.988	-5.458	-16.60 to 5.679	No	ns	0.7117
	shRNA HSF1 Mir4	-0.2917	-7.142 to 6.559	No	ns	>0.9999	-2.250	-13.39 to 8.887	No	ns	0.9916
	shRNA HSF1 Mir4 + Doxycycline	-2.604	-9.455 to 4.246	No	ns	0.8842	-14.54	-25.68 to -3.405	Yes	**	0.0034
shRNA HSF1 Mir1	shRNA HSF1 Mir1 + Doxycycline	-2.375	-9.226 to 4.476	No	ns	0.9189	-12.25	-23.39 to -1.113	Yes	*	0.0224
	shRNA HSF1 Mir4	-4.188	-11.04 to 2.663	No	ns	0.4962	-9.042	-20.18 to 2.095	No	ns	0.1807
	shRNA HSF1 Mir4 + Doxycycline	-6.5	-13.35 to 0.3505	No	ns	0.0739	-21.33	-32.47 to -10.20	Yes	****	<0.0001
shRNA HSF1 Mir1 + Doxycycline	shRNA HSF1 Mir4	-1.812	-8.663 to 5.038	No	ns	0.9738	3.208	-7.929 to 14.35	No	ns	0.9597
	shRNA HSF1 Mir4 + Doxycycline	-4.125	-10.98 to 2.726	No	ns	0.5134	-9.083	-20.22 to 2.054	No	ns	0.1767
shRNA HSF1 Mir4	shRNA HSF1 Mir4 + Doxycycline	-2.313	-9.163 to 4.538	No	ns	0.9271	-12.29	-23.43 to -1.155	Yes	*	0.0217

Table A6 Pictilisib

		T-47D					MDA-MB-231				
	Tukey's multiple comparisons test	Mean Diff.	95.00% CI of diff.	Below threshold?	Summary	Adjusted P Value	Mean Diff.	95.00% CI of diff.	Below threshold?	Summary	Adjusted P Value
Cell Line	Compared to										
Non-silencing	Non-silencing + Doxycycline	-0.7321	-6.502 to 5.037	No	ns	0.9992	-1.625	-8.238 to 4.988	No	ns	0.9797
	shRNA HSF1 Mir1	2.446	-3.323 to 8.216	No	ns	0.8286	-0.6667	-7.279 to 5.946	No	ns	0.9997
	shRNA HSF1 Mir1 + Doxycycline	-2.161	-7.930 to 3.609	No	ns	0.8912	3.708	-2.904 to 10.32	No	ns	0.5804
	shRNA HSF1 Mir4	0.6607	-5.109 to 6.430	No	ns	0.9995	2.917	-3.696 to 9.529	No	ns	0.7937
	shRNA HSF1 Mir4 + Doxycycline	-3.161	-8.930 to 2.609	No	ns	0.6179	0.25	-6.363 to 6.863	No	ns	>0.9999
Non-silencing + Doxycycline	shRNA HSF1 Mir1	3.179	-2.591 to 8.948	No	ns	0.612	0.9583	-5.654 to 7.571	No	ns	0.9983
	shRNA HSF1 Mir1 + Doxycycline	-1.429	-7.198 to 4.341	No	ns	0.9806	5.333	-1.279 to 11.95	No	ns	0.1865
	shRNA HSF1 Mir4	1.393	-4.377 to 7.162	No	ns	0.9827	4.542	-2.071 to 11.15	No	ns	0.3515
	shRNA HSF1 Mir4 + Doxycycline	-2.429	-8.198 to 3.341	No	ns	0.8329	1.875	-4.738 to 8.488	No	ns	0.9623
shRNA HSF1 Mir1	shRNA HSF1 Mir1 + Doxycycline	-4.607	-10.38 to 1.162	No	ns	0.2011	4.375	-2.238 to 10.99	No	ns	0.3941
	shRNA HSF1 Mir4	-1.786	-7.555 to 3.984	No	ns	0.9492	3.583	-3.029 to 10.20	No	ns	0.6163
	shRNA HSF1 Mir4 + Doxycycline	-5.607	-11.38 to 0.1625	No	ns	0.0622	0.9167	-5.696 to 7.529	No	ns	0.9986
shRNA HSF1 Mir1 + Doxycycline	shRNA HSF1 Mir4	2.821	-2.948 to 8.591	No	ns	0.7252	-0.7917	-7.404 to 5.821	No	ns	0.9993
	shRNA HSF1 Mir4 + Doxycycline	-1	-6.770 to 4.770	No	ns	0.9962	-3.458	-10.07 to 3.154	No	ns	0.6518
shRNA HSF1 Mir4	shRNA HSF1 Mir4 + Doxycycline	-3.821	-9.591 to 1.948	No	ns	0.4041	-2.667	-9.279 to 3.946	No	ns	0.8487

Table A8 MK-2206

	Cell Line	Tukey's multiple comparisons test / Compared to	T-47D Mean Diff.	95.00% CI of diff.	Below threshold?	Summary	Adjusted P Value
MK-2206	Non-silencing	Non-silencing + Doxycycline	8.188	-5.598 to 21.97	No	ns	0.4987
		shRNA HSF1 Mir1	10	-3.785 to 23.79	No	ns	0.2786
		shRNA HSF1 Mir1 + Doxycycline	9.063	-4.723 to 22.85	No	ns	0.3849
		shRNA HSF1 Mir4	-5.188	-18.97 to 8.598	No	ns	0.872
		shRNA HSF1 Mir4 + Doxycycline	7.5	-6.285 to 21.29	No	ns	0.5931
	Non-silencing + Doxycycline	shRNA HSF1 Mir1	1.813	-11.97 to 15.60	No	ns	0.9988
		shRNA HSF1 Mir1 + Doxycycline	0.875	-12.91 to 14.66	No	ns	>0.9999
		shRNA HSF1 Mir4	-13.38	-27.16 to 0.4103	No	ns	0.0619
		shRNA HSF1 Mir4 + Doxycycline	-0.6875	-14.47 to 13.10	No	ns	>0.9999
	shRNA HSF1 Mir1	shRNA HSF1 Mir1 + Doxycycline	-0.9375	-14.72 to 12.85	No	ns	>0.9999
		shRNA HSF1 Mir4	-15.19	-28.97 to -1.402	Yes	*	0.0231
		shRNA HSF1 Mir4 + Doxycycline	-2.5	-16.29 to 11.29	No	ns	0.9943
	shRNA HSF1 Mir1 + Doxycycline	shRNA HSF1 Mir4	-14.25	-28.04 to -0.4647	Yes	*	0.039
		shRNA HSF1 Mir4 + Doxycycline	-1.563	-15.35 to 12.22	No	ns	0.9994
	shRNA HSF1 Mir4	shRNA HSF1 Mir4 + Doxycycline	12.69	-1.098 to 26.47	No	ns	0.0875

Table A7 AZD8055

	Cell Line	Tukey's multiple comparisons test / Compared to	T-47D Mean Diff.	95.00% CI of diff.	Below threshold?	Summary	Adjusted P Value
AZD8055	Non-silencing	Non-silencing + Doxycycline	-6.125	-20.79 to 8.541	No	ns	0.8153
		shRNA HSF1 Mir1	7.25	-7.416 to 21.92	No	ns	0.6863
		shRNA HSF1 Mir1 + Doxycycline	-2.75	-17.42 to 11.92	No	ns	0.9933
		shRNA HSF1 Mir4	-2.875	-17.54 to 11.79	No	ns	0.9918
		shRNA HSF1 Mir4 + Doxycycline	-9.438	-24.10 to 5.229	No	ns	0.4089
	Non-silencing + Doxycycline	shRNA HSF1 Mir1	13.38	-1.291 to 28.04	No	ns	0.0925
		shRNA HSF1 Mir1 + Doxycycline	3.375	-11.29 to 18.04	No	ns	0.983
		shRNA HSF1 Mir4	3.25	-11.42 to 17.92	No	ns	0.9857
		shRNA HSF1 Mir4 + Doxycycline	-3.313	-17.98 to 11.35	No	ns	0.9844
	shRNA HSF1 Mir1	shRNA HSF1 Mir1 + Doxycycline	-10	-24.67 to 4.666	No	ns	0.3446
		shRNA HSF1 Mir4	-10.13	-24.79 to 4.541	No	ns	0.331
		shRNA HSF1 Mir4 + Doxycycline	-16.69	-31.35 to -2.021	Yes	*	0.0173
	shRNA HSF1 Mir1 + Doxycycline	shRNA HSF1 Mir4	-0.125	-14.79 to 14.54	No	ns	>0.9999
		shRNA HSF1 Mir4 + Doxycycline	-6.688	-21.35 to 7.979	No	ns	0.7539
	shRNA HSF1 Mir4	shRNA HSF1 Mir4 + Doxycycline	-6.563	-21.23 to 8.104	No	ns	0.7682

Table A9 AUY922

	Cell Line	Tukey's multiple comparisons test / Compared to	T-47D Mean Diff.	95.00% CI of diff.	Below threshold?	Summary	Adjusted P Value
AUY922	Non-silencing	Non-silencing + Doxycycline	-3.625	-26.90 to 19.65	No	ns	0.9972
		shRNA HSF1 Mir1	9.438	-13.84 to 32.72	No	ns	0.8331
		shRNA HSF1 Mir1 + Doxycycline	-2.625	-25.90 to 20.65	No	ns	0.9994
		shRNA HSF1 Mir4	11.13	-12.15 to 34.40	No	ns	0.7159
		shRNA HSF1 Mir4 + Doxycycline	-0.0625	-23.34 to 23.22	No	ns	>0.9999
	Non-silencing + Doxycycline	shRNA HSF1 Mir1	13.06	-10.22 to 36.34	No	ns	0.5606
		shRNA HSF1 Mir1 + Doxycycline	1	-22.28 to 24.28	No	ns	>0.9999
		shRNA HSF1 Mir4	14.75	-8.528 to 38.03	No	ns	0.4262
		shRNA HSF1 Mir4 + Doxycycline	3.563	-19.72 to 26.84	No	ns	0.9974
	shRNA HSF1 Mir1	shRNA HSF1 Mir1 + Doxycycline	-12.06	-35.34 to 11.22	No	ns	0.6421
		shRNA HSF1 Mir4	1.688	-21.59 to 24.97	No	ns	>0.9999
		shRNA HSF1 Mir4 + Doxycycline	-9.5	-32.78 to 13.78	No	ns	0.8293
	shRNA HSF1 Mir1 + Doxycycline	shRNA HSF1 Mir4	13.75	-9.528 to 37.03	No	ns	0.5048
		shRNA HSF1 Mir4 + Doxycycline	2.563	-20.72 to 25.84	No	ns	0.9995
	shRNA HSF1 Mir4	shRNA HSF1 Mir4 + Doxycycline	-11.19	-34.47 to 12.09	No	ns	0.7111

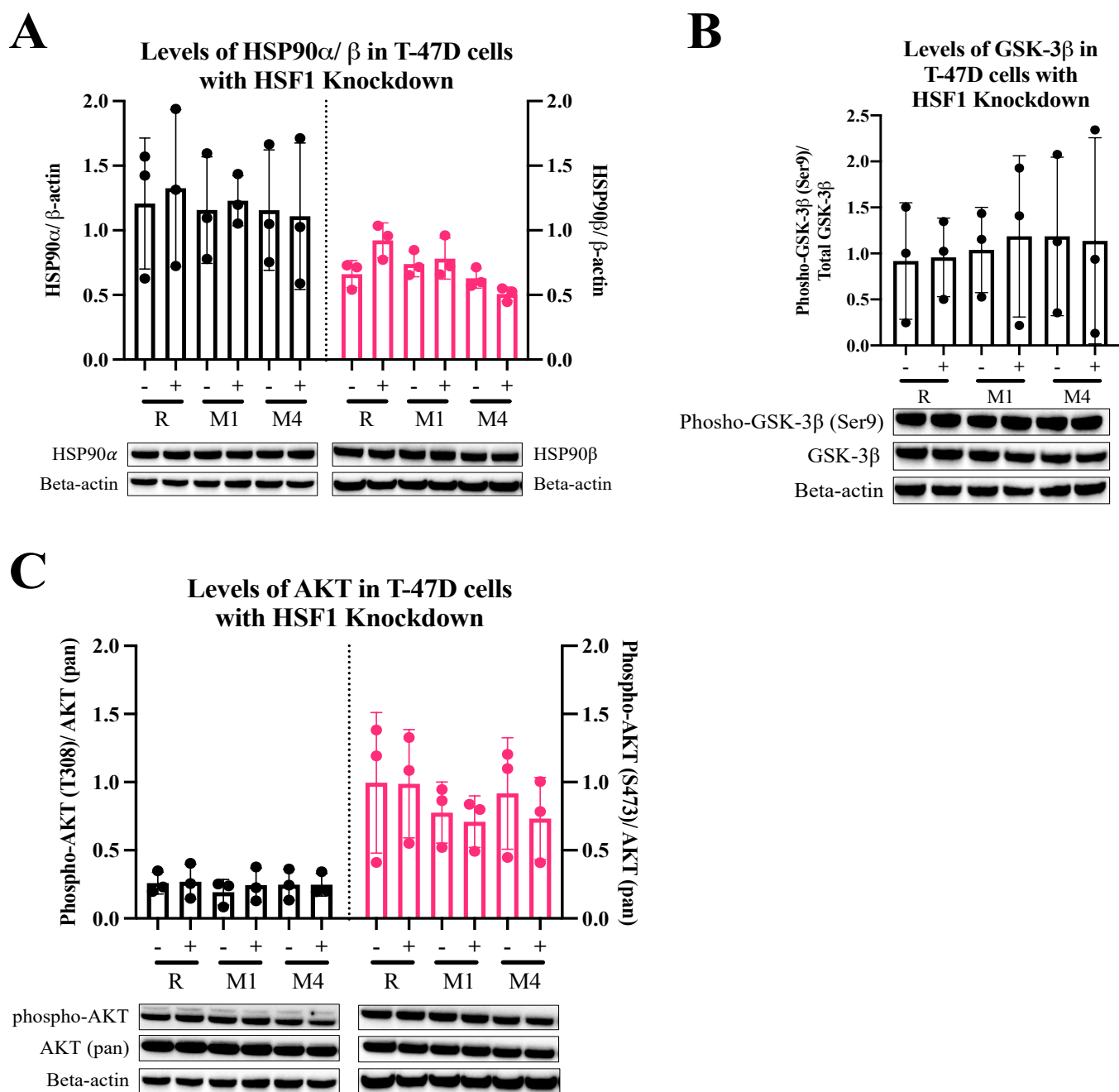**APPENDIX 3** Western blots of mTOR and AKT associated proteins with induced HSF1 knockdown

Figure A16 mTOR and AKT protein levels in T47D cells with HSF1 Knockdown

Western blot for HSP90α, AKT [T308/ pan(total)], P70s6 and GSK3-β, are related markers of mTOR and AKT pathways in inducible HSF1 knockdown T47D cells. Cell conditions: **(R-)** non-silencing (renilla), **(R+)** ns + Doxycycline [0.5μg/ ml], **(M1-)** shRNA HSF1 Mir1, **(M1+)** shRNA HSF1 Mir1 + Doxycycline [0.5μg/ ml], **(M4-)** shRNA HSF1 Mir4 and **(M4+)** shRNA HSF1 Mir4 + Doxycycline [0.5μg/ ml].). n=3.
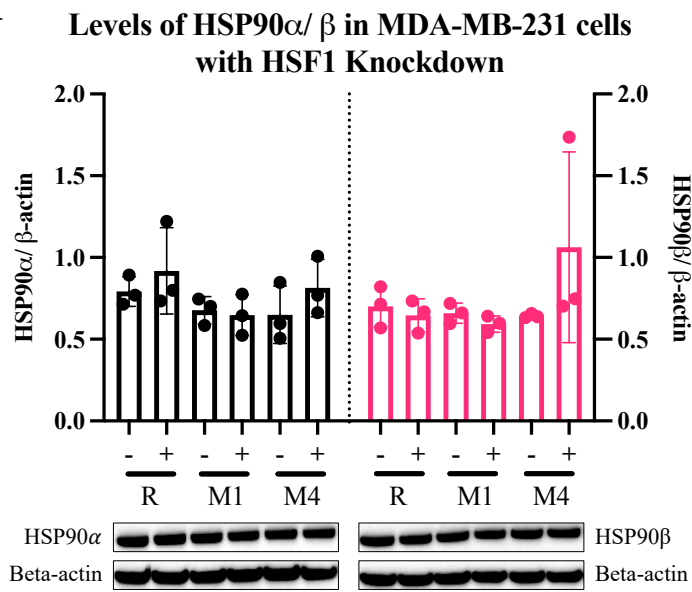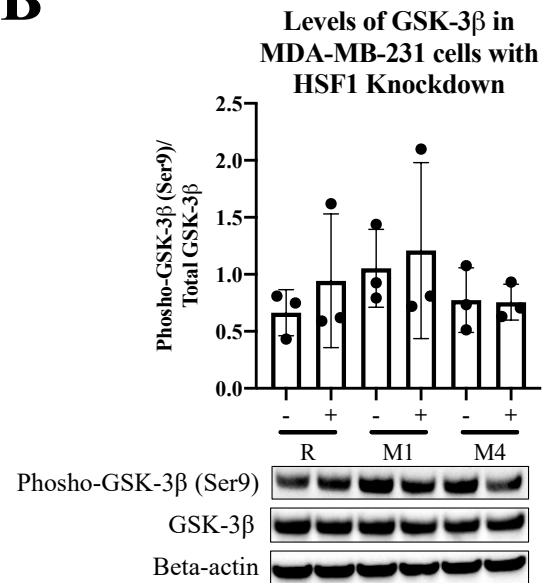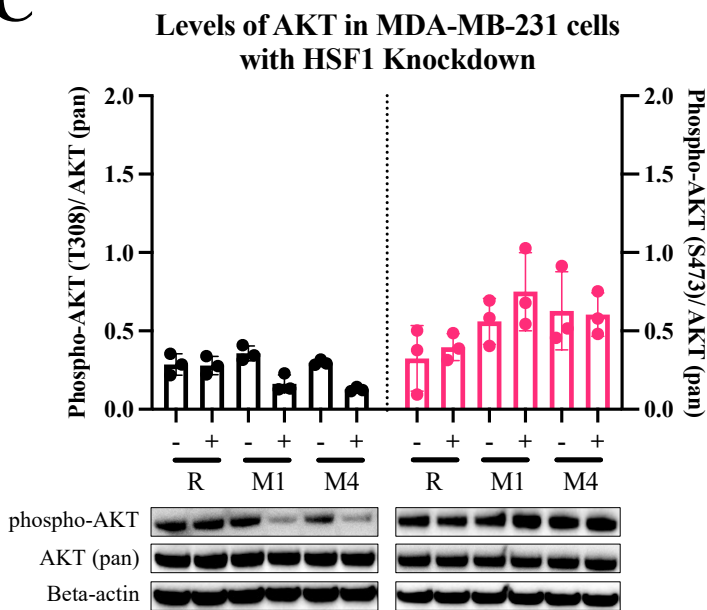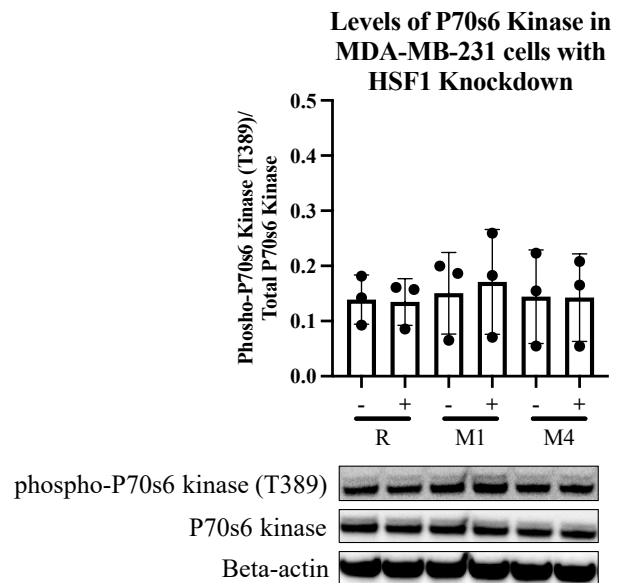
Figure A17 mTOR and AKT protein levels in MDA-MB-231 cells with HSF1 Knockdown

Western blot for HSP90α, AKT [T308/ pan(total)], P70s6 and GSK3-β, are related markers of mTOR and AKT pathways in inducible HSF1 knockdown MDA-MB-231 cells. Cell conditions: **(R-)** non-silencing (renilla), **(R+)** ns + Doxycycline [0.5μg/ ml], **(M1-)** shRNA HSF1 Mir1, **(M1+)** shRNA HSF1 Mir1 + Doxycycline [0.5μg/ ml], **(M4-)** shRNA HSF1 Mir4 and **(M4+)** shRNA HSF1 Mir4 + Doxycycline [0.5μg/ ml].). n=3.